

University of Nottingham

UK | CHINA | MALAYSIA

Investigating how tenascin-C regulates miR-155 expression

Nicole Zordan, MSc

Thesis submitted to the University of Nottingham

for the degree of Doctor of Philosophy

Abstract

Innate immunity is deeply reliant on post-transcriptional gene expression modulators such as microRNAs (miRNAs). miRNAs, such as miR-155, are involved in all levels of immune cell development, function and response, causing excessive inflammation and associating with several diseases when dysregulated.

Tenascin-C is an extracellular matrix (ECM) glycoprotein specifically induced in lipopolysaccharide (LPS)-activated macrophages. It was found that tenascin-C was able to modulate miR-155 expression in bone marrow-derived macrophages (BMDMs) from mouse, consequently regulating pro-inflammatory cytokines, such as TNF-α. However, studies focusing on miRNA expression regulated by the ECM are still in their infancy, and how tenascin-C could regulate miR-155 expression remained unknown.

This work aimed to study the mechanism and form of tenascin-C involved in promoting miR-155 expression, specifically at what stage of miR-155 biogenesis tenascin-C was required and if the ECM-associated tenascin-C was the main actor in miR-155 regulation. Moreover, we aimed to identify the membrane receptor associating with tenascin-C during this regulation.

We demonstrated that tenascin-C was involved in regulating miR-155 specifically by activating receptors located on the plasma membrane of tenascin-C knockout (*tnc-/-*) and *wild type* (*tnc+/+)* macrophages from mice, induced with different pathogenic and sterile inflammation stimuli and measured by qPCR and northern blotting. Furthermore, lack of tenascin-C affected miR-155 expression post-transcriptionally,

reducing precursor miRNA (pre-miR-155) availability in the cytoplasm, possibly influencing deficient Drosha-mediated cleavage of the primary miRNA (pri-miR-155), as determined by qPCR, northern blot and RNA immunoprecipitation.

Additionally, using a murine 3D cell culture model of ECM and inflammation developed by us, we could identify insoluble ECM-assembled tenascin-C as the form required for LPS-induced miR-155 regulation in macrophages. Indeed, ECM-assembled but not soluble tenascin-C was able to rescue miR-155 expression in *tnc*-/- BMDMs.

Finally, we identified a possible novel candidate cell-surface co-receptor or antagonist for tenascin-C that, when silenced enhanced miR-155 expression.

Altogether, this work reveals a novel regulatory mechanism of the inflammatory response to infection and identify a potential therapeutic target that could unveil new ways to control excessive inflammation.

Table of Contents

Abstract *1*

Table of Contents *3*

List of Figures *8*

List of Tables *11*

Acknowledgements *13*

Abbreviations *15*

Chapter 1. Introduction 25

1.1. The Immune System *25*

1.2. The Innate Immune System *26*

1.2.1 Pattern Recognition Receptors 27

1.2.2 Toll-like receptors 32

1.2.3 Toll-like receptors signalling and regulation 35

1.3. microRNAs *42*

1.3.1 Mechanism of action of miRNAs 44

1.3.2 miRNA biogenesis 47

1.3.3 Regulation of miRNA expression 54

1.3.4 miRNAs as key regulators of innate immunity 58

1.4. miR-155 ..... *63*

1.4.1 miR-155 host gene and expression 63

1.4.2 Targets and roles of miR-155 in immunity 66

1.4.3 Controlling miR-155 biogenesis 73

1.5. How the ECM controls miRNA expression in macrophages *80*

1.5.1 Macrophages and the local microenvironment 80

1.5.2 The ECM in the local microenvironment contributes to gene regulation 83

1.6. Tenascin-C as a regulator of miR-155 ..... *86*

1.6.1 Tenascin-C structure and expression 87

1.6.2 Physiological functions of tenascin-C 91

1.6.3 Tenascin-C in inflammation and innate immunity 96

1.6.4 Tenascin-C is a regulator of miR-155 expression 101

1.7. Aims of this study *102*

Chapter 2. Materials and Methods 107

2.1. Reagents *107*

2.1.1 Cell culture reagents 107

2.1.2 Molecular biology reagents 107

2.1.3 Protein chemistry and western blotting reagents and equipment 108

2.2. Buffer Recipes *109*

2.3. Mice *112*

2.3.1 DNA extraction from tail biopsies and mice genotyping 112

2.4. Cell Culture *114*

2.4.1 Preparation of bone marrow-derived macrophages and LPS stimulation 114

2.4.2 RAW 264.7 cells and siRNAs transfection 114

2.4.3 Cell stimulation and membrane receptor inhibition 115

2.4.4 Isolation of mouse skin adult fibroblasts 118

2.4.5 Production of fibroblast-derived matrices 118

2.4.6 Seeding BMDMs on CDMs 120

2.5. Molecular Biology Techniques *121*

2.5.1 Cytoplasmic and nuclear RNA extraction 121

2.5.2 RNA immunoprecipitation (RIP) 122

2.5.3 Total RNA extraction and quantification 123

2.5.4 Agarose gel electrophoresis for RNA quality control 123

2.5.5 Quantitative real-time PCR 124

2.5.6 Northern blot 131

2.6. Protein Analysis 133

2.6.1 Immunocytochemistry 133

2.6.2 Extracellular matrix protein extraction 134

2.6.3 Total, nuclear and cytoplasmic protein extraction 135

2.6.4 Protein extraction from Trizol organic fractions 136

2.6.5 Protein extraction and co-immunoprecipitation (co-IP) 137

2.6.6 Protein quantification 137

2.6.7 Tris-glycine sodium dodecyl sulphate polyacrylamide gel electrophoresis (SDS-PAGE) 138

2.6.8 Brilliant blue G-colloidal staining 139

2.6.9 Western blot 140

2.7. Statistical analysis 142

Chapter 3. Analysis of the effect of tenascin-C on miR-155 expression and biogenesis 145

3.1. Tenascin-C regulates miR-155 expression in macrophages 148

3.1.1 Expression of mature miR-155 in BMDMs 148

3.1.2 Expression of mature miR-155 in RAW 264.7 cells 151

3.2. Analysis of miR-155 transcription 156

3.3. Analysis of miR-155 biogenesis 158

3.3.1 Analysis of miR-155 nuclear processing 162

3.4. Tenascin-C regulation of RBPs involved in miR-155 biogenesis (candidate approach) 166

3.4.1 Investigating tenascin-C-mediated regulation of KH-SRP 169

3.4.2 Investigating tenascin-C-mediated regulation of ZNF-385A 174

3.4.3 Investigating tenascin-C-mediated regulation of ZNF-346 178

3.4.4 Investigating tenascin-C-mediated regulation of TTP 181

3.5. Discussion 187

3.6. Summary 194

Chapter 4. Form versus function: requirements for tenascin-C immune-modulatory function . 197

4.1. Induction of tenascin-C expression in LPS-stimulated macrophages 199

4.1.1 LPS induces tenascin-C expression in RAW 264.7 cells 199

4.1.2 Extracellular localisation of tenascin-C in RAW 264.7 cells 200

4.1.3 LPS induces secretion of soluble tenascin-C by RAW 264.7 cells 204

4.1.4 Not soluble, but cell-associated tenascin-C is involved in the regulation of miR-155 . 205

4.2. Development and characterisation of native ECM 3D culture models to study tenascin-C assembly into ECM from different cell-sources 208

4.2.1 Characterisation of Mouse Embryonic Fibroblast CDMs 208

4.2.2 Comparison of CDMs from adult and embryonic fibroblasts 212

4.3. Analysis of ECM-associated tenascin-C effect on miR-155 modulation 223

4.4. Discussion 227

4.5. Summary 234

Chapter 5. Investigating the cell-surface receptor involved in tenascin-C-mediated regulation of miR-155 237

5.1. Experimentally validated, candidate tenascin-C receptors 243

5.1.1 Toll-like receptor 4 (TLR4) 243

5.1.2 Integrins $\alpha5\beta1$, $\alpha v\beta3$ and $\alpha9\beta1$ 245

5.1.3 Epithelial Growth Factor Receptor (EGFR) 248

5.2. Novel candidate tenascin-C-receptors 249

5.2.1 Macrophage Receptor 1 (MAC-1) 249

5.2.2 Neuropilin-1 (NRP1) 255

5.3. Discussion 258

5.4. Summary 265

Chapter 6. Final Discussion 267

6.1. Concluding Remarks and Future work 276

Chapter 7. Bibliography 279

Appendix 309

List of Figures

Figure 1.1: Cellular localisation of PRRs. 29

Figure 1.2: TLR4 signalling pathway. 38

Figure 1.3 Mechanisms of action of miRNAs 46

Figure 1.4 Canonical miRNA biogenesis pathway 52

Figure 1.5 TLR4 signalling mechanism of auto-regulation through miRNAs 61

Figure 1.6 Human miR-155 host gene and miR-155 sequence 64

Figure 1.7 Human tenascin-C multidomain structure and hexameric oligomerisation 88

Figure 1.8 Tenascin-C ligand binding sites and partners 93

Figure 3.1 Tenascin-C regulates miR-155 expression in BMDMs in response to various signals. ... 149

Figure 3.2 Tenascin-C knock-down in RAW 264.7 cells. 153

Figure 3.3 Tenascin-C regulates expression of miR-155 in RAW 264.7 upon LPS and TNF-α stimulation. 155

Figure 3.4 Tenascin-C does not affect pri-miR-155 transcription. 157

Figure 3.5 Tenascin-C affects pre-miR-155 levels in LPS stimulated BMDMs. 159

Figure 3.6 Tenascin-C affects miR-155 biogenesis of LPS stimulated BMDMs. 160

Figure 3.7 Drosha interacts with total pri-miR-155 during biogenesis. 163

Figure 3.8 Tenascin-C affects Drosha interaction with miR-155 during biogenesis. 164

Figure 3.9 Kinetic of KH-SRP mRNA expression in *tnc+/+* and *tnc-/-* BMDMs. 169

Figure 3.10 KH-SRP protein expression in *tnc+/+* and *tnc-/-* BMDMs. 170

Figure 3.11 KH-SRP nuclear-cytoplasmic distribution in *tnc+/+* and *tnc-/-* BMDMs. 171

Figure 3.12 Drosha interaction with KH-SRP. 173

Figure 3.13 ZNF-385A mRNA expression in *tnc+/+* and *tnc-/-* BMDMs. 174

Figure 3.14 ZNF385A protein expression in *tnc+/+* and *tnc-/-* BMDMs. 175

Figure 3.15 ZNF385A nuclear-cytoplasmic distribution in *tnc+/+* and *tnc-/-* BMDMs. 176

Figure 3.16 Drosha interaction with ZNF-385A. 177

Figure 3.17 ZNF-346 mRNA expression in *tnc+/+* and *tnc-/-* BMDMs. 178

Figure 3.18 ZNF-346 protein expression in *tnc+/+* and *tnc-/-* BMDMs. 179

Figure 3.19 ZNF-346 nuclear-cytoplasmic distribution in *tnc+/+* and *tnc-/-* BMDMs. 180

Figure 3.20 TTP mRNA expression in *tnc+/+* and *tnc-/-* BMDMs. 182

Figure 3.21 TTP protein expression in *tnc+/+* and *tnc-/-* BMDMs. 183

Figure 3.22 TTP nuclear-cytoplasmic distribution in *tnc+/+* and *tnc-/-* BMDMs. 184

Figure 3.23 Microprocessor interaction with TTP. 186

Figure 4.1 LPS induces tenascin-C mRNA expression in RAW 264.7 cells. 199

Figure 4.2 Tenascin-C localisation on the outer cell membrane of RAW 264.7 cells. 201

Figure 4.3 Tenascin-C distribution on the outer side of RAW 264.7 cell membrane. 203

Figure 4.4 Tenascin-C is secreted as a soluble protein in LPS-induced RAW 264.7 cells. 204

Figure 4.5 Insoluble, ECM-assembled tenascin-C is required for its immunomodulatory function. 206

Figure 4.6 Characterisation of ECM deposited by MEFs. 210

Figure 4.7 Collagen-I deposition in CDMs before and after de-cellularisation. 213

Figure 4.8 Deposition of ECM protein collagen-1 in CDMs from *tnc+/+* and *tnc-/-* FBs and MEFs. 215

Figure 4.9 Fibronectin deposition in CDMs before and after de-cellularisation. 217

Figure 4.10 Deposition of ECM protein fibronectin in CDMs from *tnc +/+* and *tnc-/-* FBs and MEFs. 218

Figure 4.11 Tenascin-C deposition in CDMs before and after decellularisation. 220

Figure 4.12 Deposition of extracellular proteins in CDMs from *tnc +/+* and *tnc-/-* FBs and MEFs. 221

Figure 4.13 Seeding of BMDMs on CDMs. 224

Figure 4.14 Rescuing miR-155 in *tnc-/-* BMDMs. 225

Figure 5.1 TLR4 signalling in tenascin-C-mediated regulation of miR-155 expression. 244

Figure 5.2 Investigating integrin signalling regulation of miR-155 expression in BMDMs. 246

Figure 5.3 Investigating integrin signalling regulation of miR-155 in RAW 264.7 cells. 247

Figure 5.4 Investigating EGFR signalling regulation of miR-155 expression in BMDMs. 248

Figure 5.5 Three-dimensional structure of human FBG-γ and tenascin-C FBG domains. 250

Figure 5.6 Homology between FBG-γ and tenascin-C FBG domains in human and mouse. 252

Figure 5.7 Role of Mac-1 in regulating miR-155 expression in BMDMs and RAW 264.7 cells. 254

Figure 5.8 Expression of NRP1 and NRP2 in RAW 264.7 macrophages upon LPS stimulation. 255

Figure 5.9 Expression of miR-155 in RAW 264.7 macrophages is affected by NRP1 knock-down but not by NRP2. 257

Figure 6.1 Summary of discoveries. 275

Figure 7.1 Mouse genotype was confirmed by PCR. 309

Figure 7.2 Amplification efficiency of primers. 310

Figure 7.3 Amplification efficiency of primers. 311

Figure 7.4 Quality of nuclear and cytoplasmic fractionation from BMDMs. 312

Figure 7.5 Ponceau S staining of nitrocellulose membranes before western blot. 313

Figure 7.6 No primary antibody control for CDMs immunofluorescence. 313

Figure 7.7 Decellularisation of CDMs. 314

List of Tables

Table 1: Mammalian TLRs and their ligands. 35

Table 2 Known factors and co-factors involved in miR-155 expression 77

Table 3. Buffer recipes and solutions. 111

Table 4. *Tnc+/-* mice genotyping PCR Reaction mix 112

Table 5. Primers for *tnc*+/- genotyping PCR 113

Table 6. *Tnc+/-* mice genotyping PCR conditions 113

Table 7. List of Dharmacon siRNAs 115

Table 8. Reaction for siRNA transfection 115

Table 9. Macrophage activators and receptor inhibitors 117

Table 10. SYBR green primer sequences 125

Table 11. SYBR green qPCR reaction mix. 126

Table 12. SYBR green qPCR cycles. 126

Table 13. TaqMan® reverse transcription mix. 129

Table 14. TaqMan® reverse transcription cycles 129

Table 15. TaqMan® qPCR reaction mix. 130

Table 16. TaqMan® qPCR cycles 130

Table 17. DIG-labelled DNA probes 132

Table 18. Immunocytochemistry antibodies and staining solutions. 134

Table 19. Composition of solutions and buffers used to prepare separating SDS-PAGE. 139

Table 20 Antibodies for Western Blot and co-IP/RIP 141

Table 21 Experimentally validated, candidate tenascin-C receptors investigated in this study..... 238

Table 22 Novel candidate tenascin-C receptors and co-receptors investigated in this study. 239

Table 23 Identity between FBG-γ and tenascin-C FBG domains in human and mouse. 249

Acknowledgements

"Retrospectively considering my long path, that of my peers and colleagues and of the young recruits who have accompanied us, I think I can affirm that in scientific research, not the intellect nor the ability to perform and conclude exactly the task undertaken, are essential factors to success and personal satisfaction. In both cases, what counts more is complete dedication and closing your eyes despite difficulties: this way, we can face problems that others, more critical and acute, would not face."

Considerando in retrospettiva il mio lungo percorso, quello di coetanei e colleghi e delle giovani reclute che si sono affiancate a noi, credo di poter affermare che nella ricerca scientifica, né il grado di intelligenza né la capacità di eseguire e portare a termine con esattezza il compito intrapreso, siano i fattori essenziali per la riuscita e la soddisfazione personale. Nell'una e nell'altra contano maggiormente la totale dedizione e il chiudere gli occhi davanti alle difficoltà: in tal modo possiamo affrontare problemi che altri, più critici e acuti, non affronterebbero.

Rita Levi-Montalcini – In praise of Imperfection

The experience of doing a DPhil is far from perfect. However, the real value of people's help and affection is much more relevant when there is a little imperfection in life.

I was fortunate enough to encounter and be accompanied by remarkable people, which helped me see through what seemed insurmountable problems, but were definitively not.

First and foremost, I would like to thank my supervisor Dr Anna M. Piccinini. She has given me vital support and is a continuous source of inspiration. Thank you for believing in my potential and pushing me to achieve goals I never thought I could reach.

I would also like to thank Prof David M. Heery, for his invaluable help and reassuring presence and Alessandro for his precious contributions to this work and his friendly smile during my last months in the lab.

Thank you greatly to my most trusted companion and partner in crime, Hannah. I cannot imagine what my experience would have been without her.

The same applies to the fantastic people I was fortunate enough to have on my side at the GRRB laboratory. Exceptional scientists which I feel honoured to call friends. Thank you, Kat,

Poppy, Mitchell, Asta, and everybody else who had crossed my road and made my life a little better.

Thank you to past and present members of our research group and everybody who helped me achieve the goals of my project, including Dr Hilary Collins, Barbara Rampersad and the BSU personnel at QMC.

Lastly, I would like to thank my family. They have been unbelievably supporting during this peculiar year and throughout my PhD. I would not have made this far without my partner, Davide, who gave me strength and was my backbone in the most challenging moments.

Thanks to my parents and my brother, for their encouragement and making sure I was always well fed. It is also thanks to them that I can be proud of what I have achieved. Finally, I will never thank enough my dearest friends – particularly Federica, Alice, Irene, Francesca, Lizzie, Sindhu, Andrea and Emil, always ready to listen to my stories and to support me.

Abbreviations

AGO	Argonaute Protein
AIM2	Absent In Melanoma 2
AML	Acute Myeloid Leukemia
AP-1	Activator Protein 1
APCs	Antigen-Presenting Cells
Aβ	β-Amyloid
BDNF	Brain-derived Neurotrophic Factor
BIC	B-Cell Integration Cluster
BMDC	Bone Marrow-derived Dendritic Cells
BMDM	Bone Marrow Derived Macrophages
BMP	Bone Morphogenetic Protein
Btk	Bruton's Tyrosine Kinase
C/EBP	CCAAT/Enhancer-Binding Protein
CARD	Caspase Recruitment Domain
CDM	Cell-Derived Matrices
cDNA	Complementary DNA
CDS	Cytosolic DNA Sensor
CDS	Coding Sequence
cGAS	Cyclic GMP-AMP Synthase
CLRs	C-Type Lectin Receptors
CMP	Common Myeloid Progenitor
CNPY	Canopy Fibroblast Growth Factor Signalling Regulator

CR3	Complement Receptor 3
c-Scr	Rous Sarcoma Virus Homolog
CSPD	Disodium 3-(4-Methoxyspiro {1,2-Dioxetane-3,2'-(5'-Chloro)Tricyclo [3.3.1.13,7]Decan}-4-Yl)Phenyl Phosphate
DAMPs	Damage-Associated Molecular Patterns
DC	Dendritic Cells
DGCR8	DiGeorge Syndrome Critical Region 8
DMEM	Dulbecco's Modified Eagle Media
dsRBD	dsRNA Binding Domain
dsRNA	Double-Strand RNA
E-BOX	Enhancer Box
ECM	Extracellular Matrix
EDC	1-Ethyl-3-(3-Dimethylaminopropyl)Carbodiimide Hydrochloride
EGF	Epidermal Growth Factor
EGF-L	EGF-Like
eIF	eukaryotic translation Initiation Factor
EVX1	Even-Skipped Homeobox 1
EXP5	Exportin 5
FAK	Focal Adhesion Kinase
FB	Fibroblast
FBG	Fibrinogen-Like Globe
FBS	Fetal Bovine Serum

FGF	Fibroblast Growth Factor
FNIII	Fibronectin Type III
FXR1	Fragile X Mental Retardation-Related Protein 1
gp96	Glucose-regulated Protein 96
GPCRs	G-Protein Coupled Receptors
GPIβα	Platelet glycoprotein Iβα
HGF	Hepatocyte Growth Factor
HLB	Hypotonic Lysis Buffer
HMGB1	High Mobility Group Box 1
HPRT1	Hypoxanthine Phosphoribosyltransferase 1
HSC70	Heat-Shock Cognate 70
HSCs	Hematopoietic Stem Cells
HSP90	Heat-Shock Protein 90
HSPCs	Hematopoietic Stem And Progenitor Cells
HSPGs	Heparan Sulfate Proteoglycans
HuR	Human Antigen R
ICAM 1	Intercellular Adhesion Molecule 1
IGF-BP	Insulin Growth Factor-Binding Protein
IL-1	Interleukin-1
IPS-1	IFN-β Promoter Stimulator 1
IRF	Interferon Regulatory Factor
ISREs	Interferon-Sensitive Response Elements
JNK	JUN N-terminal Kinase

LPS	Lipopolysaccharide
LRR	Leucine-Rich Repeat
Mac-1	Macrophage-1 Antigen
MAPK	Mitogen-Activated Protein Kinase
M-CSF	Macrophage Colony-Stimulating Factor
MDA5	Melanoma Differentiation Associated Protein 5
MDDC	Monocyte-derived Dendritic Cells
MDM	Monocyte-derived Macrophages
MEFs	Mouse Embryonic Fibroblasts
MINCLE	Macrophage-Inducible-C-Type Lectin
miRNA	microRNA
MKP1	MAPK Phosphatase 1
MMP	Matrix Metalloproteinase
MOPS	3-(N-Morpholino)Propanesulfonic Acid
mRNA	Messenger RNA
MS	Multiple Sclerosis
NALP	Nacht LRR Protein
NFI-A	Nuclear Factor I Type A
NF-kB	Nuclear Factor Kappa-Light-Chain-Enhancer of activated B Cells
NLRs	NOD-Like Receptors
NOD	Nucleotide-Binding Oligomerization Domain
NPC	Nuclear Pore Complex

NRP1	Neuropilin 1
NRP2	Neuropilin 2
NT	Neurotrophin
PACT	Protein Activator Of PKR
PAMPs	Pathogen-Associated Molecular Patterns
PBS	Phosphate Buffered Saline
PCR	Polymerase Chain Reaction
pDCs	plasmacytoid Dendritic Cells
PDGF	Platelet Derived Growth Factor
PFA	Paraformaldehyde
PI3K	Phosphatidylinositol-3-Kinase
PIGF	Phosphatidylinositol-Glycan Biosynthesis Class F Protein
PKR	Protein Kinase R
Poly(I:C)	Polyinosinic: Polycytidylic Acid
PP2A	Protein Phosphatase 2A
Pre-miRNA	Precursor miRNA
Pri-miRNA	Primary miRNA
PRRs	Pattern Recognition Receptors
PRRX1	Paired-Related Homeobox 1
PTEN	Phosphatase and Tensin Homolog
qPCR	Quantitative PCR
RA	Rheumatoid Arthritis
RAGE	Receptor for Advanced Glycation Endproducts

RBP	RNA Binding Protein
RIG-I	Retinoic Acid Inducible Gene I
RIIID	RNase III Domains
RISC	RNA-Inducing Silencing Complex
RLRs	RIG-I-Like Receptors
RNA Pol	RNA Polymerase
RNase	RNA Ribonuclease
RPS	RNA Precipitation Solution
RPTPβ/ζ	Receptor Protein-Tyrosine Phosphatase Beta/Zeta
SAP130	Sin3A Associated Protein 130
SDS	Sodium Dodecyl Sulfate
SHIP1	SCR Homology 2 (SH) Domain-Containing Inositol-5'-Phosphatase 1
siRNA	small interfering RNA
SLE	Systemic Lupus Erythematosus
SMAD	Mothers Against Decapentaplegic Homolog
SOCS1	Suppressor Of Cytokine Signalling 1
SRSF3	Serine/Arginine-Rich Splicing Factor 3
SSC	Saline Sodium Citrate
ssRNA	Single-Strand RNA
STAT	Signal Transducer and Activator of Transcription
STING	Stimulator of Interferon Genes
TA	Tenascin Assembly domain

TBE	Tris/Borate/EDTA
TGF-β	Transforming Growth Factor Beta
TIR	Toll/IL-1 Receptor
TLRs	Toll-Like Receptors
TNF-α	Tumour Necrosis Factor Alpha
TRBP	TAR RNA-Binding Protein
TREMs	Triggering Receptor Expressed On Myeloid Cells
TSS	Transcription Start Site
TUTs	Terminal Uridylyl Transferases
UNC93B1	Uncoordinated 93 Homolog B1
UTR	Untranslated Region
VEGF	Vascular Endothelial Growth Factor

Chapter 1

INTRODUCTION

Chapter 1. Introduction

1.1. The Immune System

The ability to adapt to changes determines the success of a species, allowing the survival of individuals and achieving an evolutionary advantage. One of the most advanced and sophisticated survival mechanisms that vertebrates have developed is the immune system. Thanks to it, we can respond to and defeat infectious agents, protecting our organism from offences that could otherwise become life-threatening. The defensive strategy consists of two parts: innate and adaptive immunity, working in combination and sequentially. When the invading organism breaches the physical barriers of the body, the innate immune system is activated. Innate immunity is a very prompt, yet non-specific, defence mechanism that allows rapid clearance of most pathogenic molecules. This initial response, in turn, activates the adaptive immune response, which is slower and involves a precise antigen-specific recognition of the invading pathogen, allowing a more effective reaction and immunological memory to respond faster and more effectively to future exposures to the same agent.

However, without a prompt initial innate immune response, there would not be any adaptive immunity and pathogens would easily spread and overwhelm the host, compromising survival. Thus, innate and adaptive immunity must collaborate in a perfectly interlaced manner to resolve infection.

1.2. The Innate Immune System

A milestone in the history of immunology is Charles Janeway's "Infectious Non-self model" (1989) [1], which opposed to the previous "Self Non-Self model" from Burnet and Fenner (1949), in which antigen-presenting cells were considered to be the leading players in recognising and resolving infections caused by non-self particles. Janeway suggested that immune cells can detect pathogens through pattern recognition receptors (PRRs). Binding of these receptors to conserved patterns in infectious non-self structures leads to the recruitment of immune cells and promotes clearance of the infection. These structures are known as pathogen-associated molecular patterns (PAMPs) and include a wide variety of evolutionarily conserved structures from organisms such as bacteria and viruses. This model, however, failed to explain how the immune system could also react to its self, in occasions such as sterile injury, cell-necrosis, tumour-associated immune responses, transplants or autoimmunity [2, 3]. Polly Matzinger proposed an alternative model in 1994 that complemented Janeway's theory, suggesting that the immune system can distinguish "danger signals" from safe signals [4]. The dangerous self-structures released from the host are known as damage-associated molecular patterns (DAMPs). These include nucleic acids and intracellular proteins released from necrotic cells, extracellular matrix (ECM) fragments and ECM molecules released or overexpressed during infection, tissue damage or cellular stress [5, 6].

Innate immune cells play a major role in activating the immune reaction by sensing microorganisms through PRRs. All immune cells originate from pluripotent hematopoietic stem cells (HSCs) [7] which reside in the bone marrow or, in the

specific case of tissue-resident macrophages, derive from HSCs which are generated in the yolk sack and expanded and differentiated into progenitors in the fetal liver [8]. The progenitor cells differentiating into innate immune cells are part of the myeloid lineage, including monocytes/macrophages and granulocytes (e.g. neutrophils, eosinophils, basophils and mast cells), dendritic cells, and common lymphoid progenitors, precursors of natural killer cells. Macrophages, granulocytes and dendritic cells are also known as phagocytes, for their ability to engulf and kill invading microorganisms.

Macrophages are the most abundant phagocyte population and include tissue-resident macrophages and monocyte-derived macrophages, the latter being recruited to tissues from the circulation during inflammation [9, 10]. Macrophages and dendritic cells are also known as antigen-presenting cells (APCs) as they capture and process antigens, presenting them to T and B lymphocytes. This process switches on the adaptive arm of immunity and is initiated and facilitated by PRR signalling.

1.2.1 Pattern Recognition Receptors

The immune response activation begins when PRR-expressing cells bind to PAMPs and DAMPs, leading to a series of intracellular events involving pro-inflammatory and healing responses. These responses trigger the production of cytokines, type I interferons (IFNs), chemokines, proteases, antimicrobial peptides, immune-receptors and costimulatory molecule up-regulation, resulting in recruitment and activation of phagocytic cells and, ultimately, activation of adaptive immunity [11]. Cells of the innate immune system such as macrophages and dendritic cells are the major contributors to PRR-mediated immune responses. However, non-immune cells such

as epithelial and endothelial cells and fibroblasts also present PRRs and can participate in recognising pathogens and host-derived danger signals. In addition to that, B and T cells of the adaptive immune system can directly be activated by certain DAMPs, such as nucleic acids from dying cells or extracellularly released ADP (adenosine diphosphate) or ATP (adenosine triphosphate) [12, 13].

Five different PRR families have been characterised so far, including C-type lectin receptors (CLRs), RIG-I-like receptors (RLRs), cytosolic DNA sensors (CDS), NOD-like receptors (NLRs) and Toll-like receptors (TLRs) [14-16]. Based on their location, they can be divided into two groups: transmembrane (TLRs and CLRs) and cytosolic (NLRs, RLRs and CDS) PRRs. The range of biochemically different molecules and species that they can recognise is exceptionally vast and, together with specific receptor localisation, it allows an extensive coverage of most pathogenic structures, in an overall specific mechanism. A summary of the main PRRs and their cellular location is reported in Figure 1.1.

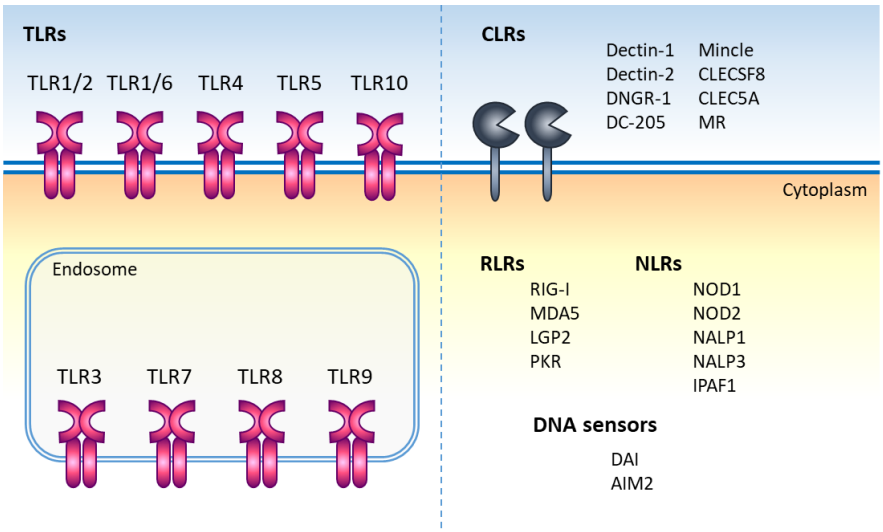


Figure 1.1: Cellular localisation of PRRs.
Transmembrane receptors include TLRs and CLRs, localising on plasma or endosomal membranes. TLRs work as hetero- or homodimers, initiating their intracellular signalling upon ligand binding. Several different kinds of CLRs have been identified, allowing recognition of a wide variety of carbohydrates on pathogens or endogenous molecules. Cytoplasmic receptors include RLRs, NLRs and DNA sensors, each including different subfamily members. These can recognise pathogenic or endogenous molecules entered through the cel membrane, including nucleic acids, or partially degraded pathogenic components. Adapted from [17].

Different PRRs can recognise specific structures and induce activation of different molecular pathways. CLRs are part of a large group of transmembrane receptors binding to carbohydrates, most commonly represented by calcium-dependent carbohydrate recognition domains [18]. They are primarily known for recognising glucan and fucan structures from fungi [19], and other carbohydrates from bacteria and viruses [20, 21]. However, receptors such as macrophage-inducible-C-type lectin (MINCLE) or Dectin-1 have shown to be able to bind also to endogenous molecules, such as Sin3A associated protein 130 (SAP130) [22]. Upon activation, CLRs stimulate proinflammatory cytokine production by signalling through immunoreceptor tyrosine-based activation motif (ITAM)-like domains on their cytoplasmic tails or indirectly through ITAM-harbouring adaptor molecules.

Once in the cytosol, pathogenic molecules and danger signals can be detected by cytosolic PRRs. RLRs are RNA helicases that can recognise viral dsRNA from genomic RNA or from replicating ssRNA of viruses. RLRs retinoic acid-inducible gene I (RIG-I) and melanoma differentiation-associated protein 5 (MDA5) binding to dsRNAs lead to activation of the caspase recruitment domain (CARD) at their N-terminus. Upon dsRNA binding, RIG-I and MDA5 are recruited by adaptor protein IFN-β promoter stimulator 1 (IPS-1) and stimulate type I IFN production, ultimately resulting in antiviral activity [23, 24]. Discrimination between self and pathogenic RNAs occurs by recognition of specific features of the RNA structures. For instance, RIG-I and MDA5 preferentially bind to short RNAs di- or three-phosphorylated at the 5'-end, or blunt-ended RNAs [25]. Moreover, MDA5 can be activated by dsRNAs longer than 300bp. Other RLRs, including LGP2 and dsRNA-activated protein kinase (PKR), have been found to facilitate and contribute to signalling [26, 27].

Different PRRs can recognise cytoplasmic DNA, but recent discoveries identified cytosolic DNA sensors (CDS) that can induce innate immune genes expression, including type I IFN, upon recognition of endogenous and foreign DNA structures. For example, absent in melanoma 2 (AIM2) and cyclic GMP-AMP synthase (cGAS) recognise bacterial and viral DNA molecules inducing innate immune reactions [28, 29]. AIM2 contains a pyrin-domain that activates the inflammasome pathway, inducing secretion of IL-1β and IL-18 [29]. DNA binding to cGAS initiates an enzymatic cascade, leading to activation of adaptor protein stimulator of interferon genes (STING), ultimately promoting pro-inflammatory cytokines and type I IFN expression. CDS can also recognise endogenous DNA and lead to immune reactions in response to DNA damage [30, 31]. Existence of other DNA sensors, such as DNA-dependent

activator of IFN-regulatory factors (DAI) [32], was also suggested, but not independently confirmed.

Other PRRs have shown to be able to detect microbial and viral DNA in the cytosol, as well as bacterial peptidoglycans, flagellin and fungal hyphae. NOD-like receptors (NLRs) are characterised by a central nucleotide-oligomerisation domain and a leucine-rich ligand sensing domain at the C-terminus. At the N-terminus, they generally carry a protein-binding motif, including CARD domains for NOD1 and NOD2, pyrin domains for NALP1 or NALP3 (NAcht LRR protein), or baculovirus inhibitor of apoptosis protein repeat (BIR) domain [11]. NLRs with CARD domains activate NF-κB (nuclear factor-κB) pathways. Pyrin or BIR domains are involved in caspases activation and assembly of the inflammasome, leading to processing and cleavage of precursor cytokines such as pro-IL-1β and pro-IL-18, beginning the process of pro-inflammatory programmed cell-death of pyroptosis [33]. Notably, members of the NLR family of receptors such as NALP3 can additionally detect endogenous signals like ATP, uric acid crystals and β-amyloid (Aβ) [34], involving NLRP3 inflammasome activation. By targeting common ligands, PRR activation can have synergistic effects on the inflammatory response. Non-classical PRRs can sometimes sense the effects and molecules released during these responses. These are non-PRR transmembrane proteins that showed to be able to sense DAMPs, leading to activation of signalling pathways, promoting migration and activation of innate immune cells. These include receptor for advanced glycation end products (RAGE), triggering receptor expressed on myeloid cells (TREMs), G-protein coupled receptors (GPCRs) and ion channels [3].

One important category of PRRs that has not been discussed yet is toll-like receptors (TLRs). TLRs represent the best characterised PRR family, extensively studied for its ability to bind to pathogenic structures, both on the outside of cells and intracellularly within exosomes and lysosomes.

1.2.2 Toll-like receptors

Toll-like receptors (TLRs) are type I integral transmembrane glycoproteins with an extracellular leucine-rich repeat (LRR) ligand-binding domain at the N-terminus, a transmembrane region and a cytoplasmic Toll/interleukin-1 (IL-1) receptor homology (TIR) domain at the C-terminus. Different TLRs can recognise different PAMPs and DAMPs. Currently, 10 TLRs have been characterised in humans (TLR1-10), and 12 in mice (TLR1-9, 11-13). They maintain 20-30% amino acid identity in their TIR domains and share three homology regions, conserved in IL-1R, and fundamental for intracellular signalling. The LRR domain contains β-strands and α-helixes connected by loops, which form an internally concave horseshoe-resembling structure, which is directly involved in ligand recognition [35]. Cell-surface TLRs, including TLR1, 2, 4, 5 and 6, localise on the cell membrane of dendritic cells, macrophages and other immune cells, functioning as sensors of extracellular cues. Intracellular TLR3, 7, 8 and 9 are located on intracellular endosomal membranes detecting cytoplasmic PAMPs or intracellular DAMPs [36]. Interestingly, the cellular localisation of TLRs seems to correlate partially with the type of ligand that they recognise. A summary of TLR locations and their ligands is reported in Table 1.

Toll-like Receptor	Localisation	Ligand	Origin	Ref
TLR1	Plasma membrane	Triacyl lipopeptides	Bacteria	[37]
		Soluble factors	Bacteria	[38]
		β-defensin-3	Host	[39]
TLR2	Plasma membrane	Lipoproteins	Various	[40]
		Peptidoglycans	Bacteria (Gram Pos)	[41, 42]
		Lipoteichoic acid	Bacteria (Gram Pos)	[42]
		Envelope glycoproteins	Viruses	[43]
		Zymosan	Fungi	[44]
		β-glycans	Fungi	[45]
		Several HSPs	Host	[46-48]
		HMGB1	Host	[49-51]
		β-defensin-3	Host	[39]
		Surfactant protein A/D	Host	[52, 53]
		Eosinophil-derived neurotoxin	Host	[54]
		Aβ	Host	[55]
		Decorin	Host	[56]
TLR3	Endolysosome	dsRNA	Viruses	[57]
		mRNA	Host	[58, 59]
TLR4	Plasma membrane	LPS	Bacteria (Gram Neg)	[60]
		Envelope glycoproteins	Viruses	[61]

		Glycoinositolphospholipids	Protozoa	[62]
		Mannan	Fungi	[63]
		HMGB1	Host	[49-51]
		Tenascin-C	Host	[64]
		HSPs	Host	[47, 65]
		Biglycan	Host	[66]
		Decorin	Host	[56]
		Fibrinogen	Host	[67]
		Fibronectin	Host	[68]
		β-defensin-2	Host	[69]
		Surfactant protein A/D	Host	[53, 70]
TLR5	Plasma membrane	Flagellin	Bacteria	[71]
TLR6	Plasma membrane	Dyacil lipopeptides	Bacteria (mycoplasma)	[72]
		Lipoteichoic acid	Bacteria (Gram Neg)	[42]
		Zymosan	Fungi	[73]
TLR7 (human TLR8)	Endolysosome	Imidazoquinoline	Synthetic	[74]
		Loxoribine	Synthetic	[75]
		Bropirimine	Synthetic	[75]
		ssRNA	Viruses, Host	[76-78]
		IgG-ribonucleoprotein complex	Host	[79]
TLR8	Endolysosome	Imidazoquinoline	Synthetic	[74]

		ssRNA	Viruses, Host	[76-78]
TRL9	Endolysosome	CpG-containing DNA	Bacteria, Viruses	[80]
		IgG-chromatin complex	Host	[47, 79]
		mtDNA	Host	[81]
TRL10 (human)	Endolysosome	Unknown	Unknown	

Table 1: Mammalian TLRs and their ligands.
Gram Pos: Gram positive; Gram Neg: Gram negative; HSPs: heat shock protein; HMGB1: high-mobility group box 1 protein; Aβ: β–amyloid; dsRNA: double-strand RNA; mRNA: messenger RNA; LPS: lipopolysaccharide; ssRNA: single-strand RNA; mtDNA: mitochondrial DNA. Adapted from [82], [17], [83] and [3].

Upon activation following ligand-binding, TLRs initiate a signalling cascade involving a series of adaptor proteins and different pathways that promote innate immunity and initiate adaptive immune responses.

1.2.3 Toll-like receptors signalling and regulation

The analysis of the crystal structures of TLRs in complex with their ligands uncovered complex mechanisms for ligand recognition, which sometimes requires co-receptors and accessory proteins [36]. For example, TLR4 requires accessory protein CD14 (cluster of differentiation 14) and co-receptor MD-2 (myeloid differentiation factor 2) to recognise LPS. CD14 binds to monomeric units of LPS [84] and presents it to MD-2, which forms a complex with TLR4 [85]. TLR4-MD-2-LPS complex formation leads to TLR4 activation by inducing its dimerisation [86].

TLR dimerisation following ligand binding is necessary for receptor activation and initiation of inflammatory response. Most TLRs homodimerise, but a few can form

heterodimers, for example, TLR2 with TLR1 and TLR6. Upon dimerisation, TLRs attract adaptor proteins, initiating intracellular signalling. Four main TLR signalling initiating-adaptor proteins have been identified so far: MyD88 (myeloid differentiation primary response 88), TIRAP (TIR-associated protein; also known as Mal (MyD88 adapter-like)), TRIF (TIR-domain-containing adapter-inducing IFN-β) and TRAM (TRIF-related adaptor molecule). TLR signalling can be divided into two main pathways, depending on which adaptor protein is initially involved: the MyD88-dependent pathway, which leads to the production of inflammatory cytokines and chemokines, and the MyD88-independent pathway, which is the primary regulator of IFN-β synthesis and a driver of dendritic cell maturation, but also an inducer of pro-inflammatory cytokine production. Interestingly, only TLR4 uses both pathways, as summarised in Figure 1.2. All TLRs, except TLR3, can activate the MyD88-dependent pathway [87]. It starts when Mal, also referred to as TIRAP, associates with the TIR domain on TLRs or TIR-containing adaptors, bridging MyD88 to the receptor complex for TLR2 and TLR4 signalling [88]. This association leads to recruitment and activation of IRAK (Interleukin-1 receptor-associated kinase) proteins, which are upstream activators of TRAF6 (Tumor necrosis factor receptor-associated factor 6), TAK1 (Transforming growth factor beta-activated kinase 1), TAB1 (TAK1-binding protein 1), TAB2 and TAB3. Active TAK1-TABs complex phosphorylates IKK (IκB kinase) complex, composed of two catalytic subunits, IKK-α and IKK-β, and a regulatory subunit, NEMO (NF-kB essential modulator). IKK complex phosphorylates IκB (inhibitor of NF-κB) leading to its degradation upon polyubiquitination. This event allows NF-κB nuclear translocation and activation as a transcription factor. Also, TAK-1 complex phosphorylates MAP (mitogen-activated protein) kinases, inducing activation of p38,

JNKs (c-Jun N-Terminal kinases) and ERKs (extracellular signal-regulated kinases), which ultimately lead to activation of the transcription factor AP-1 (activator protein 1) [89].

The discovery of a MyD88-independent pathway, also known as TRIF-dependent pathway [90], was made after Akira Shizuo and colleagues showed that MyD88-deficient mice were displaying normal IFN-β levels, when stimulated with endotoxins [91, 92]. This pathway is triggered by TLR3 and internalised TLR4, and involves intracellular recruitment of adaptor protein TRIF, directly interacting with TLR3 or by indirectly binding to TLR4 through TRAM. Activated TRIF associates with TRAF3, inducing activation of IKK-related kinases TBK1 (TANK-binding kinase 1) and IKK-ε. These kinases phosphorylate IRF3 (interferon regulatory factor 3) and IRF7, leading to dimer translocation into the nucleus and induction of type I IFNs and IFN-inducible gene expression. Moreover, TRIF-dependent pathway can induce a late activation of NF-κB and AP-1 through association with TRAF6, or by activation of TAK1 complex through TRADD (TNFR1-associated death domain protein) and RIP (receptor-interacting protein). With TLR4, this happens after internalisation of the receptor, following ligand binding [93].

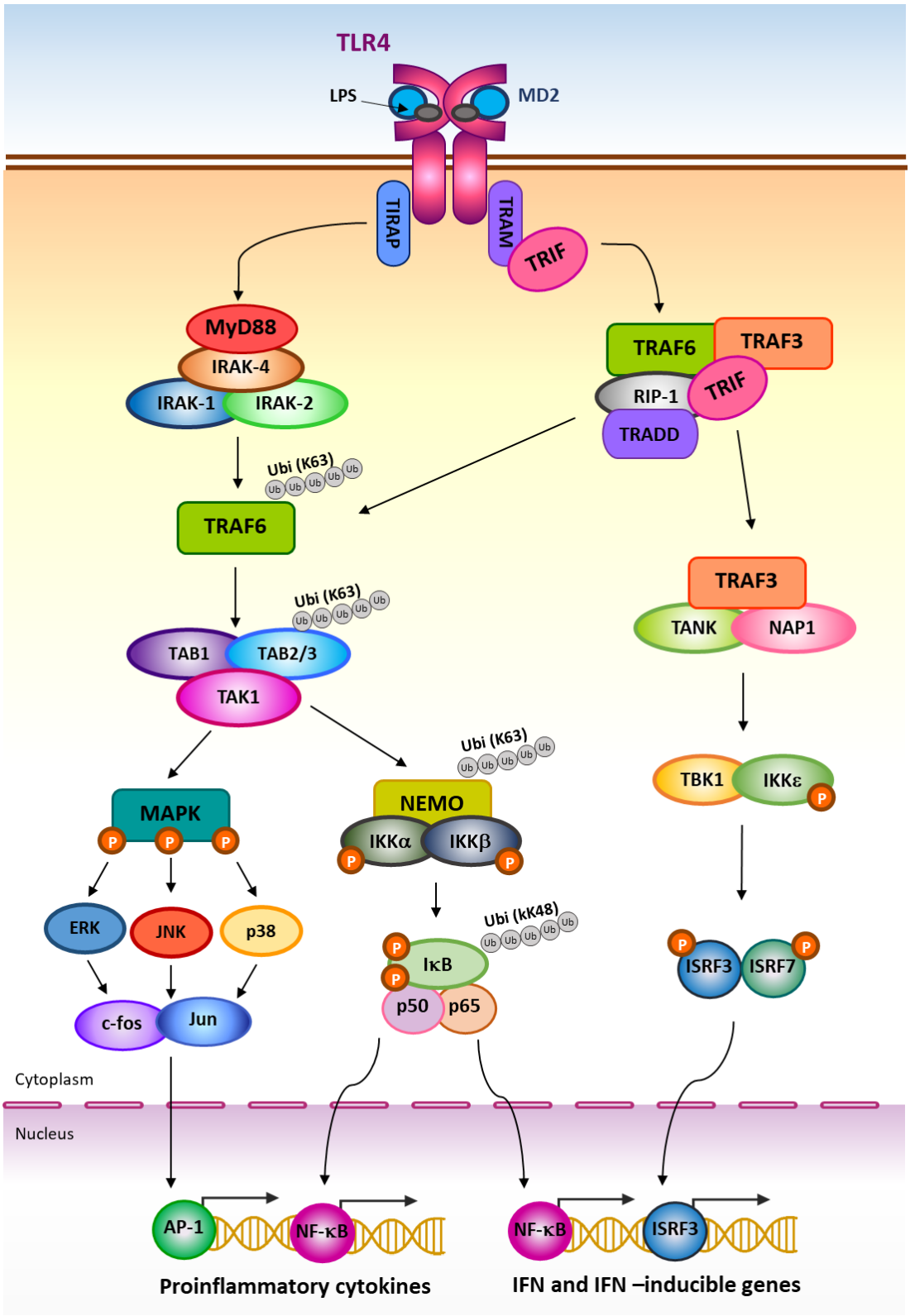


Figure 1.2: TLR4 signalling pathway.

Activation of MD2/TLR4 complex after recognition of LPS can induce both MyD88-dependent and TRIF-dependent (MyD88-independent) pathways. The myD88-dependent pathway is initiated by recruitment of MyD88 to TIRAP on TLR4. MyD88 forms a complex with IRAK proteins, leading to

activation of TRAF6, which, by functioning as E3 ubiquitin, activates the TAK1, TAB1 and TAB2/3 complex. This complex drives phosphorylation of NEMO-IKK complex, and MAP kinases. Phosphorylation and consequent degradation of IκB by IKK complex, and of MAP kinase signalling-cascade events, allow nuclear translocation and activation of transcription factors NF-κB and AP-1, followed by cytokine synthesis. Upon MyD88-independent activation, TLR4 is translocated to the endosomes, where TRAM can activate the TRIF-dependent pathway by recruiting a complex of TRAF6, TRAF3 and RIP1. Following TRAF6-RIP1 activation, NF-κB translocates to the nucleus to induce cytokine expression. TRAF3 leads to activation of ISRF3 and ISRF7, driven by phosphorylation of TBK1/IKKε, through TANK/NAP1. Active nuclear ISF3 and ISF7 induce IFN-β and IFN-inducible gene expression.

1.2.4 Regulation of TLR signalling

Regulation of gene expression during inflammation is tightly controlled by positive and negative modulators that can balance the activation of immune responses and prevent excessive inflammation. When TLR activation is uncontrolled, immune homeostasis is not restored, and aberrant production of inflammatory molecules can lead to inflammatory diseases, including infection-associated sepsis, systemic lupus erythematosus (SLE), rheumatoid arthritis (RA), atherosclerosis and asthma [94-97]. In pathogen-induced sepsis, over-activation of TLRs, specifically TLR2 and TLR4, was found to contribute to overwhelming systemic inflammation and organ injury [96]. In agreement with this, septic shock induced by Gram-negative bacteria did not affect TLR4 knockout mice [98], and TLR2-deficient mice were more protected from polymicrobial-induced sepsis than *wild type* mice [99].

Expression of TLRs is found enhanced in synovial linings and sublining of RA patients [97]. Moreover, monocyte-derived dendritic cells and synovial fluid macrophages from RA patients produce more TNF and IL-6 than healthy control cells, indicating a possible hyper-activation of TLR2 and TLR4 in RA [100, 101].

Several factors can influence signalling and activation of TLRs. Folding and trafficking of TLRs to the cell surface or the endosomal system require several chaperone

proteins, such as gp96 (glucose-regulated protein 96), CNPY3 (canopy fibroblast growth factor signalling regulator 3), CNPY4 and UNC93B1 (uncoordinated 93 homolog B1). For example, trafficking of TLR2 and TLR4 to the cell surface, or TLR7 and TLR9 to endosomes, was compromised in mice with macrophage-specific gp96-deficiency. Lack of gp96 protected the mice from LPS-induced endotoxin shock, but rendered them more susceptible to acute infection by *Listeria monocytogenes (LM)*, indicating that macrophages are the primary source of pro-inflammatory cytokines during endotoxemia and Listeria infections [102].

Proteolytic cleavage is characteristic of nucleic acid-sensing TLRs, following binding to their ligands. It was proposed that proteolysis of TLRs such as TLR9, TLR3, TLR7 and TLR8 is a prerequisite to avoid inappropriate signalling against host DNA/RNA [103, 104], but conflicting evidence suggested that cleavage could be necessary for the signalling instead [105]. Hence, it is not clear yet if cleavage of TLRs exerts a positive or negative effect on TLR signalling.

Moreover, soluble ectodomain forms of TLRs exist that modulate TLR signalling. For example, soluble TLR2 (sTLR2) and sTLR4 are generated through cleavage by metalloproteinases [106] or by alternative splicing of their mRNAs [107]. Soluble variants TLR2 and TLR4 act as negative regulators of membrane-associated TLR2 and TLR4 by competing for ligand and associated protein binding [107, 108]. Associated proteins such as CD14 are involved in stabilisation and ligand binding of TLRs, including LPS binding of TLR4 [109] and poly(I:C)-induced NF-kB activation in mouse bone marrow-derived DCs and *in vivo* [110].

Other mechanisms of TLR signalling regulation include phosphorylation of receptors and downstream accessory proteins. TLR3 can be activated through phosphorylation by several protein kinases, including Btk (Bruton's tyrosine kinase) [111], EGFR (epidermal growth factor receptor), and c-Scr (cellular homolog of the oncogene v-src of Rous sarcoma virus) [112]. LPS binding to TLR4 induces tyrosine phosphorylation, followed by MAPK and NF-kB activation, culminating in cytokine expression [113, 114]. Adapter protein Mal is activated by TLR2 and TLR4 [88]. Btk directly phosphorylates Mal upon TLR2 and TLR4 activation [115] and is required for MyD88 signalling [116]. Phosphatases, such as PP2A (protein phosphatase 2A) and MKP-1 (MAPK phosphatase 1), seem to negatively affect TLR signalling. Increased phosphatase levels have been associated with endotoxin tolerance and are possibly involved in de-phosphorylation of TLRs, Mal, MyD88 and TRIF [117].

TLR signalling can be further affected by alternatively spliced associated proteins, such as MyD88s [118] or TAG, a splice variant of TRAM [119], which negatively influences TLR signalling by inhibiting receptor-adaptor protein interaction. Moreover, ubiquitination inhibitors, like IRAK-M, can contrast events such as TRAF6 ubiquitination promoted by IRAK1 or proteasome-mediated degradation, negatively regulating TLR signalling [120].

Finally, TLR signalling regulation is finely controlled at the transcriptional and post-transcriptional level [121, 122]. Post-transcriptionally, microRNAs have been identified as key regulators of TLR signalling [121, 123].

1.3. microRNAs

The cascade of events that initiates the innate immune response is extremely rapid and requires tight control of gene expression at all levels. Among the post-transcriptional regulators of immunity, we find a class of non-protein coding RNAs known as microRNAs (miRNAs). These are short RNA sequences (18-25 nucleotides) that can regulate gene expression by complementary binding to mRNA transcripts, affecting most biological processes in animals and plants. They were initially discovered studying developmental mechanisms of *Caenorhabditis elegans,* a model in which Ambros and Ruvkun studied the temporal regulation of developmental gene *lin-14*. Previous studies had shown that *lin-4* had negative regulatory functions on *lin-14* [124]. The breakthrough discovery was that *lin-4* was not encoding for a protein, but a short RNA transcript that regulated expression of LIN-14 protein post-transcriptionally, and that the *lin-4* transcript could bind by complementary base pairing to the 3'UTR of *lin-14* mRNA [125, 126]. Other examples were later identified in worms, but it was the discovery that this gene regulation mechanism is shared by most complex organisms, including vertebrate, ascidian, hemichordate, mollusc, annelid and arthropod [127], that revolutionised the world of gene regulation. Nowadays, new miRNAs are constantly discovered and found conserved in different species. More than two thousand microRNAs have been identified and annotated in the human genome, many of which still need to be experimentally validated [128]. Studies demonstrated that newly acquired miRNAs are very rarely lost by following generations, with the consequence that more complex organisms express a higher number of miRNAs, introducing additional layers of control on gene expression [129].

The variety of roles in which miRNAs are involved during gene regulation is well established. Specific temporal and spatial distributions allow miRNAs to participate in most biological processes, including development, cell differentiation and homeostasis. Most miRNAs are ubiquitously expressed in all tissues and cell types. However, tissue-specific miRNAs can have characteristic expression patterns as in neuronal miR-138, which regulates dendritic spine morphogenesis and is post-transcriptionally regulated to be specifically expressed in neurons [130, 131]. Other examples include miR-122, predominantly expressed in the liver [132], or miR-29a, depleted in embryonic tissues, but highly expressed in adult brains [133]. Specific cell types were also reported to have characteristic miRNA signatures. For example, miR-142, miR-144, miR-150, miR-155 and miR-223 are specifically expressed in hematopoietic cells and involved in cell differentiation and function [133, 134].

Additionally, miRNAs could exert different effects depending on their subcellular distribution. The majority of miRNAs are usually found in the cytoplasm [135, 136], but miRNAs were also found in the nucleus [136-139], in mitochondria, RNA granules and endomembranes [140]. Some of the location-specific roles are yet unclear but seem to include non-canonical miRNA functions such as activation or inhibition of transcription [136].

The mode of action of miRNAs is driven by targeted base-pairing with complementary mRNAs, commonly leading to negative regulation of expression. Single miRNAs can target multiple mRNAs [141] and individual mRNAs can be recognised by different miRNAs [142], increasing the complexity and the ability to regulate most of the genes involved in any kind of cellular process. Indeed, miRNAs are involved in the most

diverse processes, from development to differentiation, proliferation and apoptosis. Being involved in so many cellular events, it is no surprise that their homeostasis needs to be strictly controlled and that in several diseases such as cancer and neurological disorders miRNA levels are found to be dysregulated [143, 144]. The mechanism by which miRNAs can regulate gene expression is still under discussion, and new roles and modes of action are still being proposed nowadays.

1.3.1 Mechanism of action of miRNAs

Mature, single-stranded miRNAs need to be incorporated into an RNA-inducing silencing complex (RISC) composed of Argonaute (AGO) proteins. Mammals have four different AGO proteins (AGO 1-4) involved in miRNA binding within the RISC complex. AGO2 is the most abundantly expressed and the only one with endonuclease activity [145]. For their specific targeting, miRNAs use a 2-8 nucleotide long sequence on their 5'-end called "seed" region, which shows high complementarity to target mRNAs. Moreover, binding of an additional sequence at the 3'-end allows specific mRNA selection among miRNAs coming from the same family and having identical seed regions [146]. Perfect miRNA-mRNA complementarity can induce mRNA degradation through the direct endonucleolytic activity of AGO2 [147]. More commonly, mammalian miRNAs show imperfect pairing, with a central mismatch that inhibits AGO2 cleavage, inducing mRNA destabilisation and translational repression [148, 149].

The most common mechanism of action of miRNA induces translation inhibition and target mRNA degradation by targeting the 3'UTR of mRNAs [150, 151], as reported in Figure 1.3a. The mRNA decay function is driven by adaptor protein TNRC6A, known

as GW182 in flies, associated with the AGO proteins and is followed by recruitment of CCR4-NOT complex [149, 152, 153]. Therefore, miRNAs targeting causes an acceleration of mRNA deadenylation and decay, affecting overall levels of mRNAs [154, 155]. It was recently reported how this would prevent the accumulation of short-tailed target mRNA due to a more rapid mRNA degradation of the latter [155].

Other miRNA mechanisms have been reported, as summarized in Figure 1.3b. However, some of these mechanisms are supported by limited proof or are associated with specific developmental or diseased conditions [156]. For example, miRNA targeting on 3'- or 5'UTR or CDS was found to cause translational repression by inhibiting translation initiation factors binding [157] ribosomal complex formation [158] or through inhibition of translation elongation [159]. However, the exact mechanism is still unclear.

In specific cases, miRNAs were found to aid mRNA decay by collaborating with ARE binding proteins such as tristetraprolin (TTP). For example, miR-16 can target tumour necrosis factor-alpha (TNF-α), leading to TTP recruitment and destabilisation and degradation of TNF-α transcript [160].

In specific conditions, miRNAs can act as activators of translation. For example, it was reported in cell-cycle arrest studies by Vasudevan and colleagues that miR-369-3 could promote translation of TNF-α mRNA by recruiting AGO2 and fragile X mental retardation-related protein 1 (FXR1) to the AU-rich element on TNF-α, inducing its translation [161]. Other studies showed similar miRNA behaviour with miR-10a promoting ribosomal protein mRNA translation [162], miR-324-3p inducing

expression of the NF-kB subunit RelA [163], and miR-155 enhancing TNF-α translation via a not fully elucidated molecular mechanism [164].

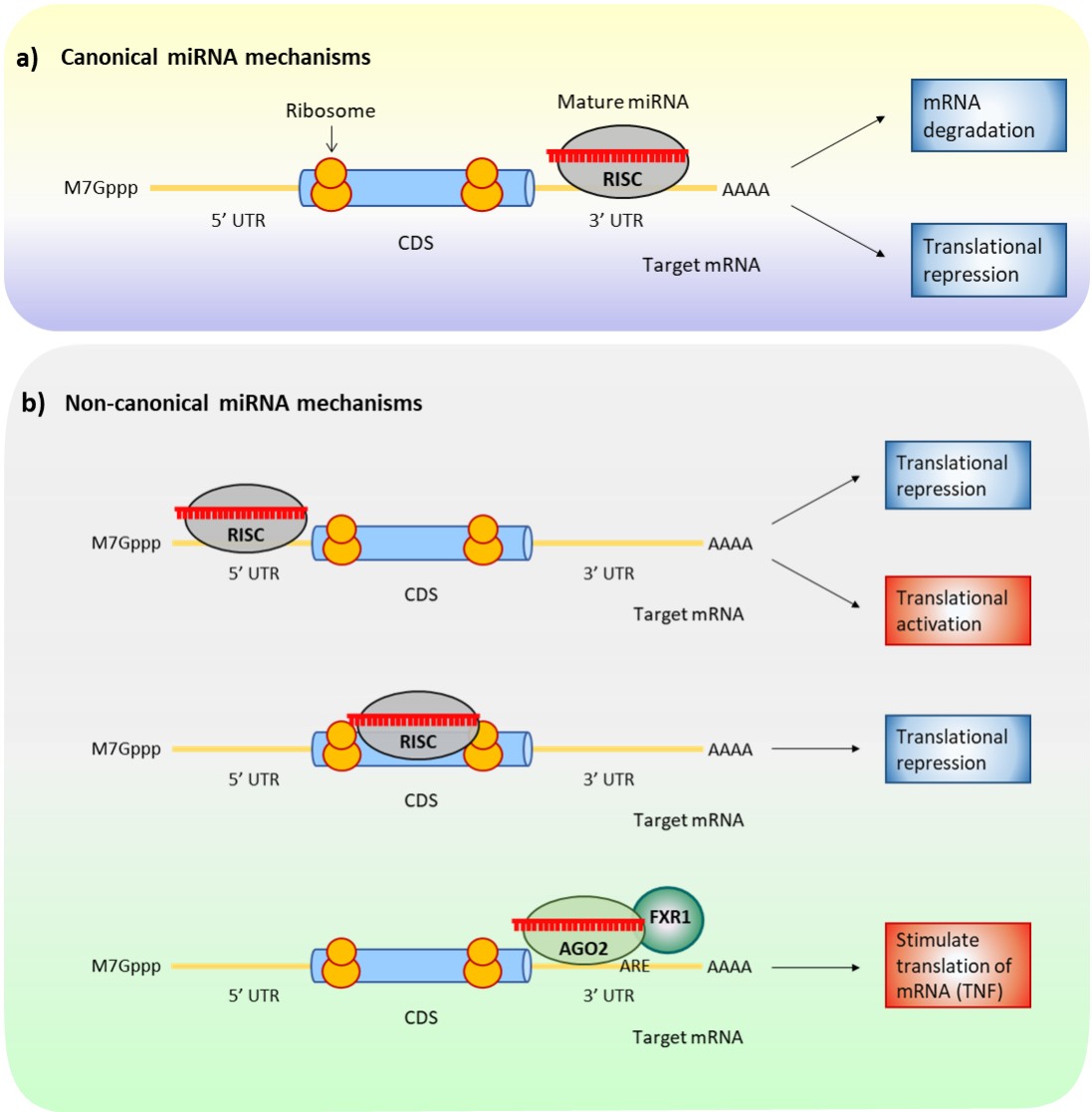


Figure 1.3 Mechanisms of action of miRNAs

a) Generally, miRNAs target 3' UTR to induce mRNA degradation or translational repression. Targeting of mRNAs by miRNAs induces the recruitment of deadenylation complexes, de-stabilising transcripts and driving mRNA decay. Furthermore, translational repression was reported by miRNAs disrupting translational factors recruitment and action. **b)** Rarely, miRNA binding to 5' UTRs or coding sequences (CDS) was found to drive translation inhibition, or, in specific instances, miRNAs can induce activation of translation by binding to promoter regions on 5' UTRs, or by recruiting other regulatory proteins such as AGO2 and fragile X mental retardation-related protein 1 (FXR1) to otherwise unstable regions on the 3' end. Adapted from [156].

Therefore, to maintain homeostatic control on the variety of miRNA-regulated targets and processes, the expression of miRNAs requires to be finely controlled throughout the different steps of their biogenesis. Most miRNAs get to maturity following a common synthesis pathway. However, distinct and specific regulatory mechanisms are in place to control the expression of individual miRNAs. Failure to regulate some of these checkpoints is often involved in uncontrolled miRNA expression and disease, making it very important to understand which regulatory mechanisms can be manipulated to regain equilibrium.

1.3.2 miRNA biogenesis

miRNA genes are found in different locations within genomes, and, due to gene duplication events [129], members of the same family such as miR-125b-1 and miR-125b-2 or miR-125a and miR-125b, respectively, can be found in multiple loci with identical or highly similar sequences and targets. It is common to find clusters of miRNAs known as polycistronic transcription units; these generally reside close to each other and maintain similar sequences or cellular functions [135]. These clusters are usually transcribed together, followed by specific post-transcriptional regulation, as reported for let-7 cluster during embryonic development [165].

The vast majority of miRNA genes are found in intronic regions of non-coding or coding genes. Less commonly, they can be encoded by exonic regions of long non-coding RNAs.

The biogenesis of miRNAs is regulated through a series of steps that ultimately leads to the assembly of a functional mature miRNA-RISC complex that regulates gene

expression. A schematic representation of the miRNA biogenesis pathway is represented in Figure 1.4.

The first step in miRNA biogenesis is transcription. Different transcription factors are involved in the transcription of primary miRNAs (pri-miRNAs). For example, tumour suppressor p53 enhances transcription of miR-34 [166] and activation of transcription factor NF-kB, induced by TLR signalling, has been associated with upregulation of several miRNAs, including miR-146a, miR-155 and miR-21 [121]. Furthermore, negative feedback loops can occur that regulate miRNA transcription. For instance, transcription factor PITX3 induces expression of miR-133b, which in turn negatively regulates PITX3 mRNA [167].

Transcription of miRNAs host genes can be independent of the protein-coding host gene. Indeed, miRNAs can have independent transcription start sites and promoter regions [168, 169] allowing direct control on miRNA transcription [170].

Further transcriptional control mechanisms can involve histone modification or DNA methylation [171]. For example, BRCA1 (breast cancer 1) mutation in breast cancer is associated with increased histone acetylation on the promoter region of miR-155, inducing its transcriptional de-repression [172].

miRNA transcription is catalysed by RNA polymerase II (RNA pol II) [173], which synthesises a long RNA transcript known as primary miRNA (pri-miRNA). Pri-miRNAs contain a central 33-35bp stem-loop structure, connected by a terminal loop at the apical junction, and single-stranded 5'- and 3' ends connected to the stem at the basal junction. The pri-miRNA sequence is processed co-transcriptionally and before any splicing events by the Microprocessor complex [174], which crops the miRNA

transcript into a shorter ~70nt long sequence, known as precursor miRNA (pre-miRNA).

The Microprocessor complex comprises Drosha, a dsRNA-specific nuclear ribonuclease (RNase) III, and DGCR8 (DiGeorge Syndrome Critical Region 8), a dsRNA binding protein that facilitates RNA cleavage by Drosha. Drosha is the catalytic subunit of the complex, harbouring a nuclear localisation signal at the amino-terminus, two tandem RNase III domains (RIIID) and a dsRNA binding domain (dsRBD) at the carboxyl-terminus. Upon binding to pri-miRNA sequences, the two RNase III domains form a dimer, becoming the processing centre. Drosha creates two cuts on 5' and 3' strands of the pri-miRNA sequence, leaving a two-nucleotide long 3' overhang [171]. It was initially thought that Drosha could identify the sequence to cut by "measuring" 11bp from the basal junction and approximately 22bp from the apical junction, thanks to a ~28Å (~11bp) connector helix between the two RIIIDs [175]. Recent studies suggested that the Drosha processing site is determined by its dsRBD recognition of an mGHG motif on the pri-miRNA stem [176]. However, cryoelectron microscopy (cryo-EM) resolution of Microprocessor in complex with pri-miRNA indicated that the processing site is determined through recognition of ssRNA and dsRNA structures by Drosha regions named "Wedge" and "Belt" [177]. Belt, would clump down the basal side of the pri-miRNA, keeping the ssRNA and dsRNA sequences separate, while Wedge could recognise mGHG motif, and, even if researchers observed weak structural evidence for base-specific contacts, it was thought to contribute to cleavage specificity. A second group confirmed these findings by analysing cryo-EM structures of Microprocessor with and without a pri-miRNA [178]. They also showed that large conformational changes follow pri-miRNA

binding, allowing interaction of dsRBDs with dsRNA and ssRNA structures on the basal junction, driving accurate pri-miRNA cleavage.

DGCR8 is necessary for Drosha-substrate interaction and binds to Drosha through its C-terminal domain. Binding of DGCR8 to Drosha is also required for the stability of the complex. However, it was demonstrated that only the C-terminal-Drosha binding domain and part of DGCR8 dsRBDs are essential for functional Drosha-mediated cleavage. Two DGCR8 molecules interact with the pri-miRNA sequence and Drosha. The regions of DGCR8 that are not part of the Microprocessor functional core are still essential for specific pri-miRNA binding and enhance accuracy and efficiency of processing. DGCR8 is composed of a nuclear localisation signal at the N-terminus, a central RNA-binding heme domain (Rhed), two dsRBDs and a C-terminal tail, connecting to Drosha. Importantly, Rhed regions specifically bind to the apical region of pri-miRNAs, recognising a miRNA-specific UGU motif on the terminal loop, and the two dsRBDs enhance processing efficiency, allowing directional loading and specific cleavage of pri-miRNA structures [179, 180]. Drosha is also engaged in orientating the pri-miRNA sequence by recognising the UGU motif at the basal junction [181]. The orientation of pri-miRNA sequence through UG and UGU recognition and, more importantly, Drosha binding to mGHG motif through dsRBD could dictate the pri-miRNA cleavage site with single-nucleotide precision [176]. However, pri-miRNA structural organisation and specific dsRBDs recognition could determine the Drosha cleavage site [177, 178].

After nuclear cleavage, pre-miRNAs are transported to the cytoplasm by the exportin 5-Ran-GTP complex [182-184]. Exportin 5 (EXP5) interacts with the pre-miRNA stem

by recognising a 14bp RNA stem with a short 3' end overhang (1-8 nt) [185, 186]. The pre-miRNA structure is loaded onto a "baseball mitt"-like structure formed by EXP5 and Ran-GTP, and it is translocated through the nuclear pore complex (NPC) by hydrolysis of GTP. Once in the cytoplasm, the transporting complex disassembles and releases the pre-miRNA hairpin, ready for the final steps of processing. EXP5 is the main protein involved in nuclear export of pre-miRNAs and provides nucleolytic protection for the pre-miRNA sequence. Indeed, tests where EXP5 was ablated showed miRNA reduction without accumulating nuclear pre-miRNAs, suggesting their degradation [184].

Cytoplasmic processing is carried out by RNase III endonuclease Dicer, which cleaves the pre-miRNA sequence near its terminal loop, generating a small RNA duplex [187-189]. The catalytic centre of Dicer is composed of two tandem RNase III domains located at the C-terminus that form a dimer to cleave both strands of the stem. At the N-terminus of Dicer resides an ATP-helicase domain that forms a clamp-like structure near the RIIIDs, recognising the pre-miRNA terminal loop and useing ATP to translocate the hairpin into the nuclease core [190]. The helicase is separated from the core by a platform domain and a PAZ domain, which binds to the dsRNA-end through molecular pockets, which selectively bind to phosphorylated 5' end or 2nt 3' overhang. A positively charged connecting helix separates the PAZ domain from RIIIDs. This region is approximately 65Å in length (~25nt) and acts as molecular ruler for Dicer cleavage [191-193]. Dicer can function independently, but several studies reported mammalian Dicer association with TAR RNA-binding protein (TRBP) or protein activator of PKR (PACT), probably affecting the pre-miRNA processing efficiency. However, their exact function is still unknown [194].

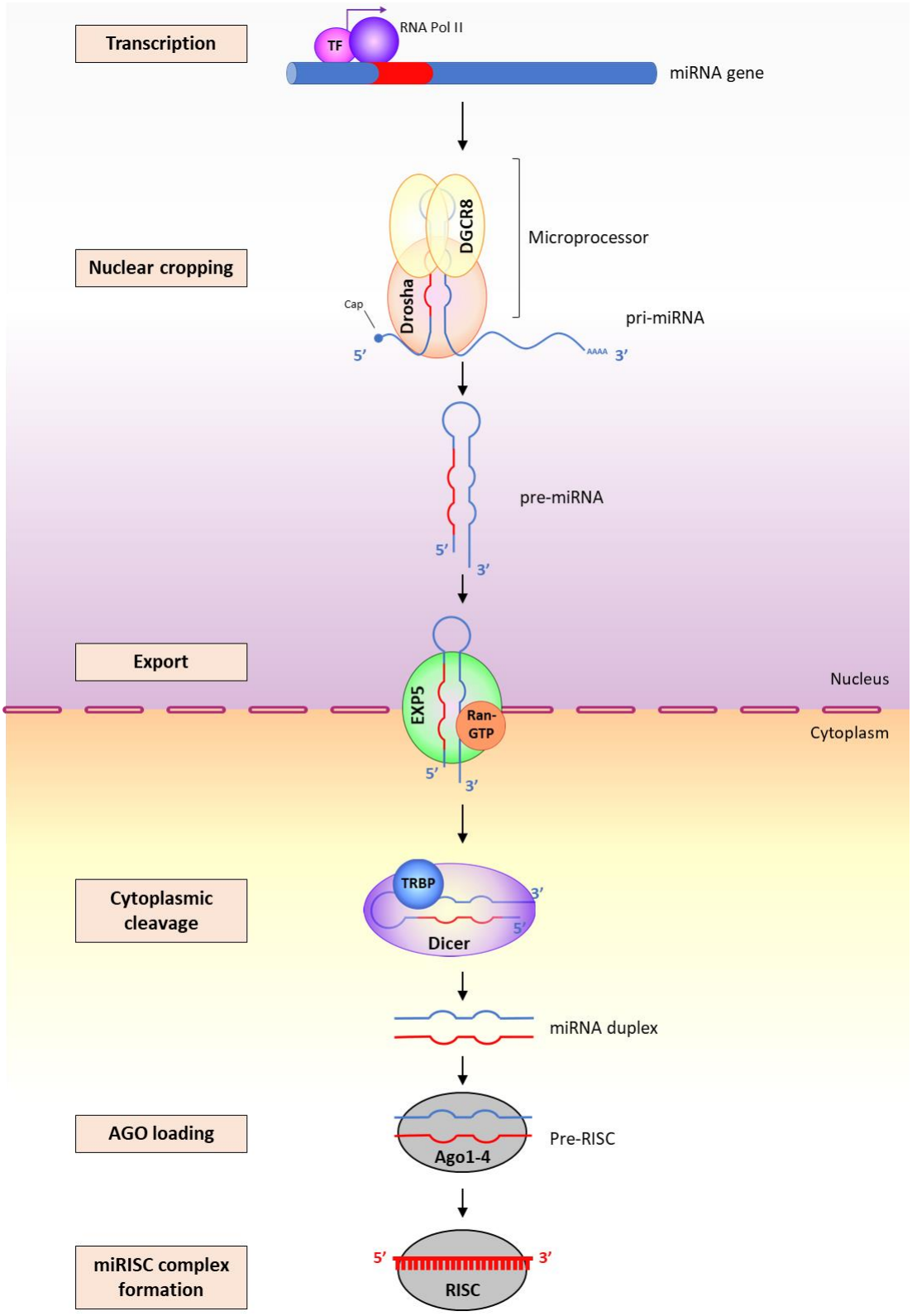


Figure 1.4 Canonical miRNA biogenesis pathway

The synthesis of miRNAs is regulated by several events that lead to the formation of a mature miRNA-RISC complex to modulate gene silencing. RNA polymerase II (RNA Pol II) transcribes miRNA genes and

can be enhanced by transcription factors (TF). A primary miRNA (pri-miRNA) transcript is produced and is recognised by the Microprocessor complex, composed of Drosha and DGCR8, which processes the pri-miRNA into a shorter hairpin: the miRNA precursor (pre-miRNA). Pre-miRNAs are then translocated through the nuclear pore complex into the cytoplasm by the exportin-5 and Ran-GTP complex. In the cytoplasm, pre-miRNAs are cleaved by Dicer, which interacts with TRBP, and are then loaded as a miRNA duplex into Ago proteins, forming the pre-RISC complex. The passenger strand is discarded by the complex, which becomes functional as mature RISC complex.

The miRNA duplex created by Dicer is successively loaded onto AGO proteins to form the pre-RISC complex. Dicer-TRBP or –PACT were suggested to play a role in RISC-assembly [195-197]. Loading of the miRNA duplex onto AGO is catalysed by hydrolysis of ATP mediated by heat shock cognate 70 (HSC70) and heat-shock protein 90 (HSP90). One of the RNA strands of the miRNA duplex is selected based on thermodynamic stability to become the “guide” strand. The other “passenger” strand is removed from the complex by releasing structural tensions created during AGO opening caused by the loading, without using ATP. The passenger strand is quickly degraded and generally found in lower amounts, but it can still be active in silencing [197-201]. Moreover, the selection of the miRNA strand can be context-specific and regulated by RNA modifiers. For example, selection of miR-324-5p or -3p was found to depend on TUT4 (terminal uridylyl transferase 4) and TUT7, leading to alternative Dicer cleavage and arm-switching [202].

About 1% of miRNAs and specific miRNA-like small RNAs follow biogenesis mechanisms considered “non-canonical”. These are mainly divided into “Microprocessor-independent” or “Dicer-independent” pathways. For example, “mirtrons”, which are spliceosome generated introns containing pre-miRNAs [203, 204], can bypass Drosha-cleavage and get processed by Dicer in the cytoplasm. Alternatively, miRNAs such as miR-451 can go through Dicer-independent biogenesis

by exploiting AGO2 endonucleolytic function [205]. Moreover, certain groups of miRNAs, known as group II pre-miRNAs, require monourydilation through terminal uridylyl transferases (TUTs) to extend the 3' end overhang and be recognised by Dicer [206].

Once loaded onto the RISC complex, most miRNAs seem to be stable for days, with variable half-lives [207, 208]. However, the half-lives of certain miRNAs seem to depend on tissue-specific characteristics or transcriptional changes [209, 210].

It is essential to underline that most miRNAs follow the canonical pathway for biogenesis. There are, however, specific mechanisms that are used by the miRNA biogenesis machinery to regulate the expression of specific miRNAs.

1.3.3 Regulation of miRNA expression

The requirement for different types and levels of miRNAs changes swiftly depending on stages of cellular development and differentiation, but also to maintain and restore homeostasis in health and disease. Consequently, mechanisms to regulate expression of individual or classes of miRNAs have evolved to cover all of the steps in miRNA biogenesis.

Transcriptional control is the principal and most effective way to control miRNA levels. A multitude of transcription factors have been identified and are involved in the regulation of miRNA transcription. For example, transcription factors such as MYC and MYCN, often dysregulated in cancer, induce upregulation of miR-17-92 in lymphoma cells [211] and overexpression of miR-9 in neuroblastoma cells [212], leading to pro-tumorigenic outputs. Other miRNAs involved in tumour suppression, including miR-15a, miR-26a, miR-29c, miR-34a, miR-195 and let-7, were found

downregulated by MYC [213]. There are several other examples of oncogenic miRNAs upregulated by transcription factors. For example, miR-21 and miR-155 expression is induced by transcriptional regulator AP-1 in cervical cancer cells and B-cell lymphomas, respectively [214, 215]. Transcription of miR-21 and miR-155 is also induced during inflammation and response to infection, following TLR-mediated NF-kB activation [121].

By promoting the transcription of certain classes of miRNAs, transcription factors can induce specific cell differentiation. For instance, CCAAT/enhancer-binding protein (C/EBP) and PU.1 activate myeloid cell differentiation by promoting miR-223 and miR-142 transcription [216-218]. However, once primary miRNAs are transcribed, several post-transcriptional events can still positively or negatively regulate their expression.

Several events can regulate the Microprocessor function. Drosha and DGCR8 can control each other. For example, DGCR8 showed to enhance the Microprocessor stability and functionality, but the complex can negatively regulate DGCR8 mRNA by prioritising the cleavage of miR-1306, which is embedded in the DGCR8 mRNA sequence [219].

Post-translational protein modifications such as phosphorylation and acetylation can further regulate Drosha and DGCR8 cellular localisation, protein stability and processing efficiency [171]. Characteristic pri-miRNA motifs, including the UGU motif at the terminal loop and the UG and CNNC motifs on the basal segments, can be targeted by processing factors such as serine/arginine-rich splicing factor 3 (SRSF3) or DEAD-box RNA helicase p72 (also called DDX17), influencing Microprocessor cleavage ability [220, 221]. Several accessory proteins, including p72 and p68 (also

known as DDX5), have been found to bind to the Microprocessor, potentially facilitating the loading of certain pri-miRNAs on Drosha [222, 223]. On the one hand, following interaction with Drosha, p68 recruits p53 to the Microprocessor, inducing anti-tumorigenic miR-16, miR-143 and miR-145 expression in response to DNA damage [224]. On the other hand, p72 association with Drosha can enhance the expression of several miRNAs, including miR-9, miR-10a, miR-21 and miR-132 [221, 225]. Stability of AGO2 was reported to be reduced in HeLa cells knocked-down for p72 [226]. However, it seemed to be an indirect consequence of reduced miRNA levels, leading to unloaded AGO2 protein degradation, rather than a direct effect on post-transcriptional regulation as suggested. Indeed, AGO2 levels were stabilised by exogenously added miR-17 mimic [226].

P68 regulates expression of miR-21 during smooth muscle cell differentiation in combination with SMAD proteins. SMADs are signal transducers, activated by Bone Morphogenetic Protein 4 (BMP4) and Transforming Growth Factor-β (TGF-β), which induce their translocation to the nucleus where they can associate with Drosha and p68, promoting processing of pri-miR-21 [227]. RNA binding proteins (RBPs) can induce specific miRNAs expression when these are transcribed as a cluster with other miRNAs. The heterogeneous nuclear ribonucleoprotein A1 (hnRNP A1) can modulate specific processing of pri-miR-18a, part of the miR-17-92 cluster, facilitating Microprocessor processing [228]. RBPs can induce specific sets of miRNAs by directly interacting with the miRNA sequence. For example, KH-type splicing regulatory protein (KHSRP) was shown to induce specific miRNA processing by binding to miRNA terminal loops, enhancing Drosha and Dicer cleavage [229], and indirectly affecting the stability of AGO proteins [226]. However, some of these proteins, such as LIN28A

and LIN28B, can be negative regulators of miRNAs, repressing let-7 processing by Drosha and Dicer [230-232]. Several other RBPs, including Zinc Finger protein 346 (ZNF346 or JAZ) or LIN 41, have been found to interact with miRNA hairpins and could have effects on miRNA biogenesis [233]. However, further studies are necessary to confirm the exact role these RBPs might play in regulating miRNA processing.

Fewer studies have identified mechanisms of regulation of nuclear pre-miRNA export. Notably, it was shown that exportin-5 expression is enhanced during cell-cycle by induction through PI3K (phosphoinositide 3-kinase) [234]. Moreover, nuclear export efficiency of pre-miRNAs by exportin-5 can be enhanced in response to specific stimuli such as the DNA damage response [234, 235]. Genetic mutations can more rarely affect the ability of exportin-5 to translocate pre-miRNAs sequences to the cytoplasm [236].

Cytoplasmic processing can be affected by accessory proteins and de-stabilisation events. It is still unclear what role TRBP and PACT play in Dicer processing; however, they seem to contribute to Dicer specificity and stability [194, 195, 237]. For example, phosphorylation of TRBP induced by MAPK-ERK was shown to upregulate the expression of subsets of miRNAs involved in tumour growth, while reducing expression of anti-tumorigenic let-7 [238]. Moreover, TRBP could help recruit the AGO complex and, in collaboration with Dicer, help miRNA loading and AGO protein stabilisation [195, 239]. AGO phosphorylation and post-transcriptional modifications can affect its cellular translocation to processing bodies (P-bodies) or lead to dissociation from Dicer, repressing miRNA expression [240-242].

Finally, miRNA sequences can go through changes determining their biogenesis. Precursor miRNAs interaction with Dicer or AGO proteins can be affected by mutations of miRNA sequences and enzyme-mediated modifications, such as uridylation by TUTs, RNA methylations, or nucleotide conversion by ADAR proteins. Some of these changes influence miRNA stability, leading to premature degradation [243-245].

Overall, the ability to control miRNA expression through different mechanisms allows prompt and efficient control over the processes that single miRNAs regulate.

Regulation of miRNA biogenesis is a critical component of innate immunity, driving temporal and cellular-specific expression of miRNAs to determine cell-differentiation, maturation, as well as intra- and extracellular responses.

1.3.4 miRNAs as key regulators of innate immunity

The innate immune system is controlled through a series of sophisticated molecular mechanisms balancing haematopoietic cell differentiation and self-renewal, as well as immune cell maturation, mobilisation, propagation and signalling. Among the regulators of innate immune cells, miRNAs are pivotal in supporting balance and control.

By fine-tuning gene expression, miRNAs balance homeostatic self-renewal and differentiation of HSCs. Their action provides expression noise of proteins at molecular checkpoints, allowing or preventing specific cellular events. For example, miR-125 targets pro-apoptotic factors that increase the survival of the stem cell population [246, 247], and miR-29a is involved in self-renewal by targeting an epigenetic regulator and promoting cell-cycle progression [248, 249].

One of the first miRNAs found to be able to regulate granulocytes cell-fate and differentiation was miR-223. Levels of miR-223 increase with the status of granulocytic differentiation and are controlled by a feed-forward regulatory mechanism, involving positive transcription factor C/EBPα and negative nuclear factor 1 A-type (NFI-A), which is itself a target of miR-223 [218, 250]. Further stimulation of granulocyte differentiation is achieved through miR-223 targeting of MEF2C, a transcription factor involved in myeloid progenitor cell proliferation [251], while other miRNAs such as miR-21 and miR-196b can negatively regulate maturation of granulocytes by repressing zinc finger protein GF11 [252].

The activation of the NF-kB pathway, commonly following inflammatory cues activating TLRs, drives macrophage progenitor cells differentiation into mature macrophages. The activation of RNA Pol II induces transcription of pro-inflammatory genes encoding for cytokines, chemokines, and other regulatory molecules, including miRNAs. Two major miRNA players involved in macrophage development are miR-155 and miR-146a, which are generally upregulated in activated immune cells. These miRNAs function as pro- and anti-inflammatory regulators, respectively, by targeting mRNAs with opposite function. Other miRNAs are regulated by TLR activation, for example, miR-21, miR-223, miR-9 and miR-125b. Differences in the expression of these miRNAs are often based on cell type, activated TLR and type and time of stimulation. For example, in mature myeloid cells, miR-125b is downregulated upon LPS stimulation by the kinase AKT, which blocks miRNA-mediated TNF-α synthesis inhibition [164, 253]. Instead, miR-223 was found upregulated in macrophages with developed tolerance to LPS and rheumatoid arthritis synovial fibroblasts [254, 255].

TLR signalling seems to be majorly under the control of three miRNAs: miR-155, miR-146a and miR-21 [256]. Expression of these NF-kB-dependent miRNAs is carefully timed and represents an elegant mechanism of autoregulation of expression, as summarised for TLR4 in Figure 1.5. The first miRNA to be expressed is miR-155, strongly induced within 2 hours of TLR activation. Its role is to promote inflammation rapidly and effectively. In a second phase, miR-146a, followed by miR-21, act as anti-inflammatory regulators, repressing pro-inflammatory molecules to resolve inflammation.

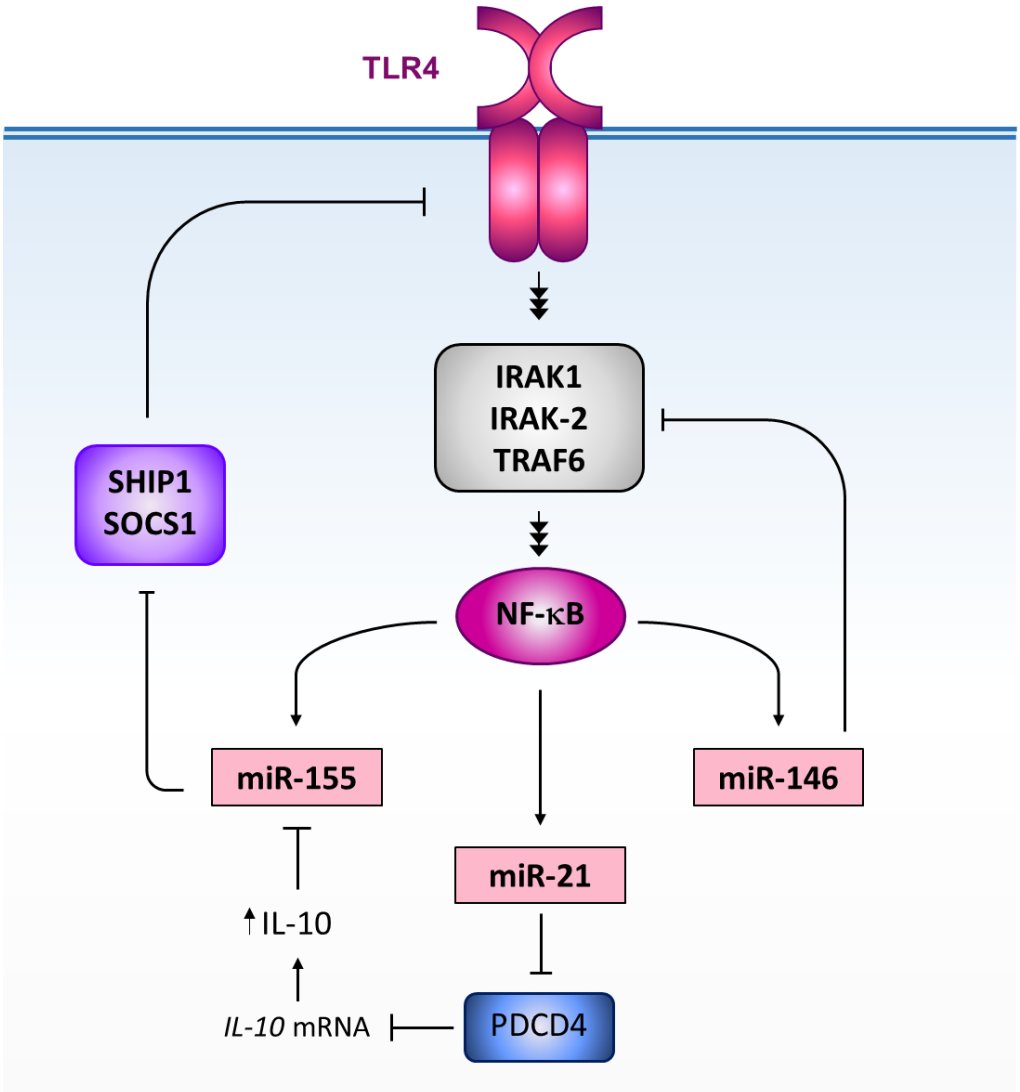


Figure 1.5 TLR4 signalling mechanism of auto-regulation through miRNAs
Activation of TLR4 receptor induces the NF-kB pathway, promoting expression of inflammatory miRNAs, including miR-155, miR-146 and miR-21. Early induction of miR-155 promotes inflammation by inhibiting anti-inflammatory SHIP1 and SOCS1, which represses TLR4 signalling. Later on, miR-146 is induced and its negative regulation of MyD88-dependent proteins IRAK1 and 2, and TRAF6, inhibits the NK-kB pathway and, eventually, the production of pro-inflammatory molecules. Late onset of miR-21 is involved in resolution of inflammation by promoting expression of IL-10, an anti-inflammatory cytokine, which inhibits miR-155 transcription. Adapted from [256, 257].

Targets of miR-155 include anti-inflammatory proteins involved in regulation of TLR signalling such as suppressor of cytokine signalling 1 (SOCS1) and Scr homology 2 (SH2) domain-containing inositol-5'-phosphatase (SHIP1) [258-260]. Additionally, miR-155 directly links to TNF-α production, possibly playing a role in transcript stabilisation [164, 261]. In dendritic cells, miR-155 was found to target pro-inflammatory molecule TAB2 (TAK1-binding protein 2), downstream of TRAF6, involved in MAPK kinases activation [262]. However, specific conditions and abundance of mRNA targets could determine certain events [263]. Induction of miR-146a is not as strong as miR-155, but differences in kinetics and longer stability of miR-146a effectively contribute to the resolution of inflammation [207]. By targeting TRAF6, IRAK1 and IRAK2 mRNAs, miR-146a behaves as a negative regulator of the MyD88-dependent pathway [264, 265]. By engaging in a negative feedback-loop with pro-inflammatory proteins activating NF-kB, miR-146a negatively regulates its and miR-155 transcription, preventing excessive inflammation. Expression of miR-155 is further affected by NF-kB late induction of miR-21. Here, the feedback-loop mechanism involves miR-21 targeting of programmed cell death 4 (PDCD4) [266], which is an inhibitor of transcription initiator factor EIF4F [267, 268]. Increased transcription promotes the expression of IL-10, which is a negative regulator of NF-kB-induced miR-155 transcription [269].

Interestingly, miR-155 is a unique miRNA, mainly acting as a pro-inflammatory molecule, but, in rare instances and depending on target abundance, it was also found to inhibit inflammation [263]. Furthermore, its expression is dysregulated in many inflammatory and autoimmune diseases and several types of cancer [270, 271]. Therefore, understanding the exact mechanism of its regulation is of primary importance.

1.4. miR-155

Before being recognised as a microRNA, miR-155 host gene *bic* (B-cell integration cluster) was identified as a proto-oncogene in chickens. Its transcription was found to be stimulated by integration of retroviral promoter regions in avian leukosis virus (ALV)-induced B-cell lymphomas [272]. Later studies showed that *bic* lacked an open reading frame and functioned as non-coding RNA. *BIC* gene was found conserved in other species, with a 138 nucleotides region showing 78% identity between human, mouse and chicken. Characterisation of the secondary structure within this region showed the formation of an RNA duplex with imperfectly paired stem-loop structures, which was later confirmed to be the miR-155 host gene [273, 274]. Orthologous miR-155 sequences were found in several species, all characterised by a well-organised innate immune system. These included the invertebrate class of ascidian in which *Ciona intestinalis* carries the most evolutionary ancient form of miR-155 [275].

1.4.1 miR-155 host gene and expression

Eis and colleagues confirmed that miR-155 was derived by *BIC* transcription and processing in human B-cell lymphomas. They also showed that miR-155 expression levels were linked to oncogenic activity in B cells and suggested that miR-155 could contribute to cancer by controlling B cell differentiation [270].

BIC (miR-155 host gene) is encoded by three exons in human and mouse, and two exons in chicken. miR-155 resides within the last exon, in the region of highest identity across species. Human BIC is comprised of a 13 kb region on chromosome

21(Hsa21), as shown in Figure 1.6, while in the mouse, *Bic* is located on chromosome 16. The complete or partial extra copy of Hsa21 in Trisomy 21 (Ts21) is believed to induce over-expression of genes like miR-155 encoded by this chromosome and could influence some of the typical features in Down syndrome (Ds). For example, fibroblasts from a monozygotic twin with Ds expressed higher miR-155 levels and decreased expression of its target AGTR1 (Angiotensin II Receptor Type 1) compared to the unaffected twin fibroblasts [276]. Accordingly, Ts21 individuals are less likely to develop coronary disorders, and miR-155 could confer this protection [276].

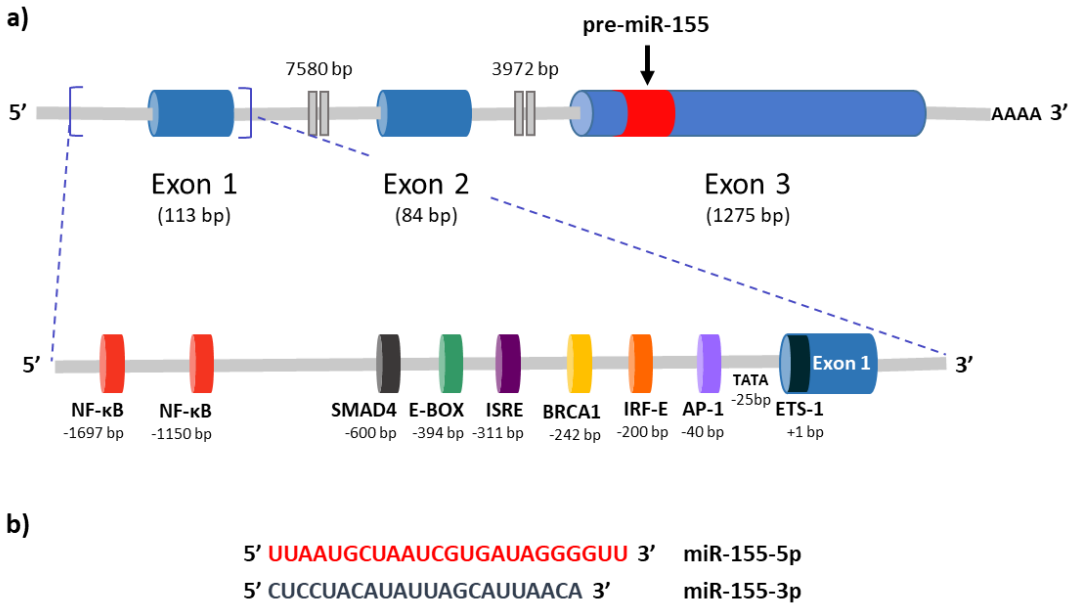


Figure 1.6 Human miR-155 host gene and miR-155 sequence

a) NC_000021.9:25562145-25575168, *Homo sapiens,* chromosome 21, GRCh38.p12. In human, miR-155 is located on exon 3 of the BIC gene. Several transcription factors binding sites have been identified in the promoter region upstream of exon 1, including NF-kB, SMAD4 (mothers against decapentaplegic homolog 4), E-BOX (enhancer box), ISRE (interferon-sensitive response element), BRCA1 (breast cancer 1), IRF-E (interferon regulatory factor E) and AP-1 (activator protein 1), most of which are activated during inflammatory responses. **b)** Mature miR-155 sequences comprise miR-155 guide strand (miR-155-5p, in red) and miR-155 passenger strand (miR-155-3p or miR-155*, in black). Adapted from [277].

Mature miR-155 sequences are highly conserved in human and mouse, differing in only one nucleotide in the non-seed region of miR-155-5p (known as miR-155) and two nucleotides on miR-155-3p (also known as miR-155*). The 5p strand is considered the guide miRNA, expressed 20-200-fold more abundantly than miR-155-3p. However, miR-155-3p is functional and was found to be upregulated at early stages of TLR7 stimulation in plasmacytoid dendritic cells (pDCs), before miR-155-5p induction [278]. The function of miR-155-3p is still not well characterised, but it seems to differ from that of miR-155-5p in TLR7 activated pDCs where miR-155-3p targets IRAK3, a negative regulator of TLR signalling, inducing the production of IFNα/β. Delayed induction of miR-155-5p leads to downregulation of TAB2 mRNA, promoting anti-inflammatory effects by negatively regulating IFNα/β production [278].

Expression of miR-155 is mainly localised in lymphatic organs such as thymus and spleen, but it is also detected in lung, liver, heart and kidney tissues [274, 279, 280]. In these organs, it is an essential component of hematopoietic progenitor and mature immune cells such as monocytes, granulocytes and B and T lymphocytes [133]. Importantly, hematopoietic progenitor cell differentiation and development is influenced by miR-155 during myelopoiesis [281, 282] and erythropoiesis [283], and it is linked to activation and response of B and T cells [284-286].

In 2007 two groups aiming to study the role of miR-155 in the immune response *in vivo*, simultaneously generated the first miR-155 knock-out mice [284, 286]. These were two of the first four miRNA knockout mice and the first to demonstrate the essential role of a miRNA in immunity [287].

It became evident that miR-155 expression is an important link between innate and adaptive immunity, and the roles and targets of this miRNA can vary over time to ensure an effective yet self-contained immune response.

1.4.2 Targets and roles of miR-155 in immunity

To understand the importance of miR-155 in immunity, it is useful to analyse the different mRNA targets that miR-155 regulates in response to signalling events in different cell types.

miR-155 during haematopoiesis

Expression of miR-155 in HSPCs is regulated during development and in adult bone marrow by HOXA9, a homeobox domain protein. In the absence of inflammatory cues, miR-155 is expressed at low levels in immature immune cells, with higher amounts in immature HSCs than more specialised immune progenitors. Changes in miRNA-155 levels in these cells drive specific differentiation. For example, during erythroid differentiation, miR-155 is down-regulated to allow development of mature red blood cells and platelets [283]. By inhibiting transcription factors involved in HSCs homeostasis such as PU.1, C/EBPβ, BACH1 (BRCA1-interacting protein C-terminal helicase 1) and CSF1R (colony-stimulating factor 1), miR-155 can control the molecular switches driving myelopoiesis [281, 288]. Dysregulation of these switches causes loss of homeostatic control and overexpression of miR-155, linked to myelopoietic disorders such as acute myeloid leukaemia (AML) [281, 282].

miR-155 in innate immunity and inflammation

In support of the idea that miR-155 represents a fundamental link between innate and adaptive immunity, activation of TLRs such as TLR3 by synthetic dsRNA poly(I:C)

(Polyinosinic:polycytidylic acid) and TLR4 by LPS, and treatment of macrophages and dendritic cells with TNF-α and IFN-β, were shown to induce strong upregulation of miR-155 [123, 208].

Targeting mRNAs by miR-155 is characterised by context-specific regulation, linked to cell-type and levels of miR-155. Targets with a weaker affinity for miR-155 can only be regulated when miR-155 is present at high levels, or through specific cellular factors [263]. In macrophages and dendritic cells, miR-155 net activity is pro-inflammatory as it preferentially targets mRNAs involved in anti-inflammatory functions, but there are few exceptions.

Well characterised miR-155 targets in macrophages and dendritic cells include SHIP1 and SOCS1 mRNAs. Following miR-155 induction upon LPS stimulation in primary mouse macrophages, SHIP1 is downregulated by direct interaction of miR-155 with SHIP1 3' UTR [259]. SHIP1 is a negative regulator of the kinase AKT, downstream target of the phosphatidylinositol-3-kinase (PI3K) pathway [289]. By downregulating SHIP1, miR-155 enhances activation of AKT, promoting NF-kB signalling [290]. However, AKT is a negative regulator of miR-155 transcription in LPS-activated primary murine macrophages [253], and it was previously found involved in suppressing MAPK/ERK1/2 signalling [291, 292]. AKT-miR-155 negative feedback mechanism could be aimed at regulating LPS endotoxin tolerance. On the other hand, Cheung et al. suggested that AKT could positively affect miR-155 expression. However, the assumption came from a single experiment with a conditionally AKT activated macrophage cell line, and did not further investigate the mechanism that would promote miR-155 expression [293].

SOCS1 promotes resolution of inflammation by negatively regulating type I IFN signalling and controlling the production of cytokines such as IL-2, IL-4 and IL-6. In murine macrophages activated by viral stimuli, expression of SOCS1 was found to be downregulated. This promoted phosphorylation of the JAK/STAT signalling pathway, resulting in the transcription of IFN-stimulated genes [260]. Depletion of miR-155 causes deregulation of cytokine production, leading to changes in T cell development and function. For example, reduced IL-2 in miR-155 deficient T cells caused impaired activation of STAT5 (signal transducer and activator of transcription 5), leading to reduced proliferation of regulatory T cells (Tregs) [294]. Additionally, lack of repression by miR-155 allowed c-Maf to promote production of IL-4, enhancing differentiation of Th2 cells [284].

Another validated target of miR-155 is Bcl6, a negative regulator of NF-kB, transiently expressed in NF-kB-activated macrophages. By targeting Bcl6 in macrophages derived from atherosclerotic lesions, miR-155 can positively enhance inflammation by promoting chemokine CCL2 production and recruitment of monocytes in atherosclerotic plaques [295].

Notably, miR-155 positively correlates with TNF-α production [164, 261, 296]. *In vivo* studies found that transgenic Eμ-miR-155 mice, overexpressing miR-155, challenged by endotoxin shock in response to LPS secreted higher plasma levels of TNF-α, in comparison to wild type mice [164]. Moreover, B-cells from *bic/miR-155-/-* mice produced significantly lower TNF-α levels than controls [286]. An alternative post-transcriptional control was suggested for miR-155-TNF-α regulation. Tili et al. proposed that miR-155 could contribute to TNF-α translation by binding to 3' UTR of

its mRNA to release its self-inhibitory mechanism. However, they tested their hypothesis by microscopy analysis comparing images of HEK-293 cells co-transfected with a GFP positive vector containing the TNF-α 3' UTR sequence with or without miR-155, instead of a more accepted luciferase assay and AGO-RNA immunoprecipitation (AGO-RIP) analysis [164]. Bala et al. proposed that miR-155 could stabilise TNF-α mRNA in Kupffer cells exposed to ethanol and LPS [261]. Nevertheless, confirmation that this mechanism is not associated with the specific cell-type and type of treatment remains to be addressed. Thus, how miR-155 regulates TNF-α remains an open question.

Moreover, miR-155 is involved in inhibiting polarization to a repairing macrophage phenotype, also referred to as M2, by targeting C/EBPβ and MafB or through negative regulation of SMAD2 mRNA, which is involved in the transcription of TGF-β-induced IL-4Rα [297-299].

However, miR-155 is not exclusively acting as a pro-inflammatory regulator. By targeting fundamental signalling molecules in the TLR signalling pathway, miR-155 can also prevent excessive inflammation. For example, miR-155 targets the mRNA of pro-inflammatory TAB2 in dendritic cells and pDCs [262, 263, 278]. Moreover, some studies reported downregulation of MyD88 during *Helicobacter pylori*-induced infection in a human gastric cell line and HEK-293, and in the human monocytic cell line THP1 responding to oxidized low-density lipoprotein, associated with atherosclerosis [300, 301].

miR-155 in adaptive immunity and autoimmunity

Development and differentiation of cells of the adaptive immune system are deeply affected by miR-155. Germinal centre B-cell development, T-cell development and antibody production are positively regulated by miR-155 effect on antigen-receptor signalling [284, 286]. Development of B cells is regulated by miR-155 targeting of SHIP-1 and C/EBPβ, leading to the proliferation of pre-B cells. Overexpression of miR-155 in transgenic Eμ-miR-155 mice during B cell development causes malignant B-cell lymphomas and accumulation of pre-B cells, associated with decreased levels of SHIP-1 and C/EBPβ, which are both involved in anti-inflammatory and anti-proliferative functions in B cells [271, 302]. Upregulated miR-155 was found in B lymphocytes from rheumatoid arthritis (RA) patients, resulting in reduced expression of PU.1. Plasma cell differentiation is controlled through miR-155 modulation of PU.1, leading to immunoglobulin G1 (IgG1) production and mature B cell differentiation [285, 303, 304]. In the collagen-induced arthritis (CIA) mouse model, high miR-155 levels could drive collagen-specific antibody production and develop antigen-specific T cells [305, 306].

Several other studies describe the miR-155 role in B and T cell differentiation. One ground-breaking study analysed the effect of miR-155 on adaptive memory and resolution of infection. The authors demonstrated that mice deficient in miR-155 could not be immunized by vaccination against *Salmonella typhimurium*, and, unlike wild-type mice, most of miR-155-/- mice died when challenged by a second infection. Rodriguez and colleagues found that miR-155 deficient mice displayed lower levels of IgM and antigen-antibody interaction, a sign of impaired B cell function, and that

effector T cells expressed significantly less IFN-γ and IL-2. Because antigen-presenting cells such as dendritic cells are required for appropriate activation and differentiation of adaptive immune cells, they suggested that inefficient activation of B and T lymphocytes was a consequence of impaired DC activation during the innate immune response [284].

Defective development and functioning of T cells were also reported in animal models of multiple sclerosis (MS), in which depletion of miR-155 confers resistance to autoimmune encephalomyelitis, showing reduced levels of T helper 17 (Th17) and Th1 cells. Development of Th17 cells is driven by inflammatory cytokines, including IL-6 and IL-23, which were found downregulated in DCs from miR-155 deficient mice [307].

miR-155 in disease

Aberrant expression of miR-155 was found to be linked to a multitude of autoimmune disorders, including rheumatoid arthritis (RA), systemic lupus erythematosus (SLE), ulcerative colitis and multiple sclerosis (MS) [308].

Levels of miR-155 were found to be higher in synovial tissues and fibroblasts from RA patients, compared to osteoarthritis patients [309]. Upregulated miR-155 in RA synovial macrophages and monocytes associated with decreased SHIP1 levels and increased release of pro-inflammatory cytokines, contributing to chronic inflammation, inducing the development of Th1 and Th17 cells, and production of collagen-specific antibodies [305]. In experimental models of atherosclerosis, a disease often linked to RA, miR-155 was shown to support the development of

atherosclerotic lesions by inducing cytokine production and inflammatory dysregulation [295, 310].

Increased levels of miR-155 were found in human active multiple sclerosis lesions [311]. Upregulated miR-155 expression was also detected in murine models of SLE [311]. miR-155 deficiency correlated with lower autoantibody production and T cell responses in miR-155-/- mouse models of SLE or pristine induced lupus in miR-155-/- mice [312, 313], indicating that miR-155 contributes to immunogenic responses in disease. Furthermore, patients with active ulcerative colitis were found to have upregulated miR-155 expression, with possible links to intestinal inflammation [314].

Sustained overexpression of miR-155 during chronic inflammation can lead to detrimental cellular and tissue damage. A recent analysis from Prinz *et al*. suggested that constant dysregulation of miR-155, a marker of chronic gastric inflammation induced by *H. pylori,* could inhibit expression of anti-tumorigenic molecules such as DNA mismatch repair proteins (e.g. MLH1, MSH2 and MSH6), leading to enhanced carcinogenesis [315].

Due to its upregulation in several cancer types, miR-155 is considered an oncogenic miRNA (or oncomiR). Haematopoietic and myeloid cell lymphomas and leukaemia represent the best-known examples of miR-155 upregulation in cancer. In paediatric Burkitt's lymphoma, Hodgkin lymphoma and diffuse large B cell lymphomas miR-155 contributes to pre-B cell proliferation by targeting SHIP1 and C/EBPβ [302].

However, high levels of miR-155 were also found in solid tumours, including breast, cervical, lung and colon cancers, pancreatic ductal carcinoma and thyroid carcinoma [277]. For example, miR-155 was found to promote the proliferation of breast cancer

by increasing cell proliferation via targeting TP53INP1 (tumour protein 53-induced nuclear protein 1) in the MCF7 cell line [316] or improve energy metabolism by regulating glycolysis factors, such as FOXO3a in breast cancer mouse models [317]. Notably, high levels of miR-155 in tumours are associated with poor prognosis [318, 319]

Additionally, miR-155 is strongly involved in tissue fibrosis [320]. Fibrosis is characteristic of several pathologies, including systemic sclerosis (SSc), rheumatoid arthritis and pulmonary fibrosis, where excessive deposition of collagen and fibrotic scarring severely affects organ functionality. For instance, in SSc miR-155 was found to drive collagen deposition and human fibroblasts proliferation and migration, through targeting of SHIP1 [321].

Regulation of miR-155 levels is therefore pivotal in maintaining homeostasis and appropriate cell signalling during all phases of the immune response, including resolution of inflammation and tissue repair. Understanding what factors are involved in the regulation of miR-155 expression is fundamental to identify the possible mechanism(s) that control inflammation, and what goes wrong when the balance between immune response activation and its resolution is lost.

1.4.3 Controlling miR-155 biogenesis

As discussed in paragraph 1.3.3, expression of miRNAs can be regulated at different levels during their biogenesis. Transcription of miR-155 has been thoroughly investigated and led to the identification of several transcription factors and enhancer of transcription with binding sites located within the *BIC*/*MIR155HG* promoter and transcription start site (TSS) regions (Figure 1.6).

NF-kB activates transcription of miR-155 during TLR signalling [208, 264]. Transcription factor binding sites for NF-kB were identified on miR-155 promoter regions, approximately 1150 and 1697 bps upstream of the TSS. NF-kB proteins were confirmed to induce miR-155 expression and bind to these sites *in vitro* by electrophoresis mobility shift assays and *in vivo* by chromatin immunoprecipitation (ChIP), [322]. More recently, another NF-kB binding site was identified in the proximity of the TSS (~178 bps upstream of *MIR-155HG* TSS) that induces miR-155 expression upon LPS stimulation [323].

Activation of TLR signalling induces transcriptional activation also through AP-1 transcription factor. O'Connell and colleagues identified an AP-1 consensus sequence upstream of TSS and showed how blocking c-Jun N-terminal kinase (JNK), an upstream activator of AP-1, could inhibit expression of miR-155 [123]. Binding of AP-1 onto consensus sites on *MIR155HG* was later confirmed to activate B cells through JunB and FosB recruitment [215]. JunB and FosB were established to drive upregulation of miR-155 following LPS stimulation in THP1 cells, which was partially abrogated by resveratrol activation of miR-663, targeting JunB [324]. Furthermore, McCoy and colleagues reported that LPS activated RAW 264.7 cells require a functional AP-1 binding site to be able to induce miR-155 expression [269].

Transcription of miR-155 can be negatively affected by anti-inflammatory cytokines such as IL-10. Specifically, the presence of IL-10 in immortalised bone marrow-derived macrophages (BMDMs) and human peripheral blood mononuclear cells (hPBMCs) was shown to downregulate miR-155 expression, through a mechanism involving STAT3 and dependent on Ets1 transcription factor binding site [269].

Other transcriptional regulators have been found to affect miR-155 expression in association with tumours. For example, BRCA1 (breast cancer 1) mutation is associated with miR-155 overexpression. Putative BRCA1 binding sites were identified on miR-155 promoter region, suggesting that BRCA1 could control epigenetic regulation of *MIR155HG* by inhibiting acetylation of H2A and H3 [172]. Increased expression of miR-155 in malignant carcinomas was also found to be associated with increased cell proliferation and differentiation following TGF-β activation. Exogenous TGF-β promotes metastasis and tumour invasion by activating SMAD proteins. Smad4 can bind to the promoter region of *MIR155HG* and promote miR-155 expression through TGF-β signalling [325, 326]. A list of transcription factors and transcriptional regulators of miR-155 is reported in Table 2 and includes IRF (interferon regulatory factors), ISRE (interferon-sensitive responsive element), E-BOX elements and FOXP3 binding sites [277].

Although transcriptional control plays a pivotal role in the regulation of miRNA expression, specific regulatory proteins can also control the expression of certain miRNAs by aiding or interfering with each step of their biogenesis. Therefore cells can modulate miRNA maturation in response to specific molecular cues and in a time-specific manner. Several studies began to identify miRNA-specific RNA binding proteins (RBPs) that are involved in miRNA-155 biogenesis.

KH-SRP was found to promote pri- and pre-miRNAs cleavage through specific recognition of terminal loop regions on miRNA subsets and association with Microprocessor and Dicer [229, 327]. KH-SRP was identified as a post-transcriptional regulator of miR-155 expression that enhanced Drosha and Dicer-mediated cleavage

efficiency of pri- and pre-miR-155, respectively, in LPS-induced BMDMs and RAW 264.7 cells [328]. KH-SRP was also found to be activated by type I interferon in pDCs following stimulation of TLR7. Activation of KH-SRP could control the temporal expression of miR-155, preferentially enhancing miR-155-5p levels and interfering with miR-155-3p expression [278]. Selective strand selection was proposed as a possible KH-SRP regulatory mechanism, but, it was not further investigated.

Another study suggested that STAT3 and SHIP1 could negatively control miR-155 expression post-transcriptionally through an additive response to IL-10 [293]. According to the researchers, STAT3 could not inhibit miR-155 transcription, as previously reported [269], because RAW 264.7 cells induced with LPS and IL-10 showed no BIC promoter activation in a luciferase assay experiment. However, the BIC promoter failed to be activated by LPS alone, contrary to many other reports [269, 277, 323]. They also proposed that IL-10 could inhibit miR-155 expression through SHIP1. They showed reduced downregulation of miR-155 in LPS and IL-10 stimulated SHIP1-/- peritoneal macrophages and SHIP1 siRNA transduced RAW 264.7 cells, and suggested that SHIP1 may inhibit AKT activation, consequently suppressing miR-155. However, unclear treatment times, lack of confirming experiments and valid literature support makes the proposed mechanism less trustworthy [293].

miR-155 biogenesis event	Location	Factor/co-factor	Reference
Transcription	Nucleus	NF-kB	[322, 323]
		AP-1	[123, 215, 269]
		ETS-1	[269, 277]
		BRCA1	[172]
		SMAD4	[325, 326]
		FOXP3	[277]
		ISRE	[277]
		E-BOX	[277]
		IRF-E	[277]
Microprocessor-mediated cleavage	Nucleus	KH-SRP	[278, 328, 329]
		ZNF-385A (HZF)	[233, 330, 331]
EXP-5-mediated nuclear export	NPC	ZNF-346 (JAZ)	[233, 332]
Dicer-mediated cleavage	Cytoplasm	KH-SRP	[278, 328, 329]
		TTP	[329, 333]
miRNA stability/decay	Cytoplasm	N/A	[207, 208]

Table 2 Known factors and co-factors involved in miR-155 expression

Transcription and biogenesis of miR-155 can be mediated by different transcription factors, enhancer and repressor of transcription and accessory proteins, promoting or inhibiting expression of miR-155. AP-1: activator protein 1; BRCA1: breast cancer 1; SMAD4: mothers against decapentaplegic homolog 4; FOXP3: forkhead box protein P3; ISRE: interferon-sensitive responsive element; IRF-E: interferon regulatory factor E; KH-SRP: KH type-splicing regulatory protein; ZNF-385A: zinc finger protein 385A; ZNF346: zinc finger protein 346; TTP: tristetraprolin.

A recent study by Treiber et al. identified novel RNA-binding proteins potentially involved in miRNA biogenesis via interaction with miRNA precursors on their loop or stem structures. Notably, pre-miR-155 was shown to bind to RBPs, including ZNF346 (zinc finger 346, or JAZ), ZNF385A (zinc finger 385A or HZF), SF1 (splicing factor 1)

and ADARB1 (double-stranded RNA-specific editase 1), in 13 different human cancer cell lines, including Burkitt's lymphoma and acute T cell leukemia cells [233]. Many of these proteins are associated with RNA binding, processing and stabilisation of transcripts or translocation, but they had not yet been associated with miRNA biogenesis. Nevertheless, ZNF346 was previously found to shuttle to the cytoplasm with Exportin-5 [332], and ZNF385A was found to promote targeting of cell cycle arrest genes over pro-apoptotic genes, in association with p53/TP53 [330]. Oncogenic mutation of p53 is associated with upregulation of miR-155. It was suggested that mutant p53 would inactivate p63, leading to aberrant expression of miR-155 in breast cancer. ChIP experiments in a non-malignant breast epithelial cell line demonstrated that p63 and p53 recruitment to *MIR155HG* leads to repression of transcription [331].

The anti-inflammatory RBP tristetraprolin (TTP), well known for its post-transcriptional regulatory activity on mRNAs such as TNF-α and IL-6, containing AU-rich elements leading to their degradation, has also been implicated in miRNA biogenesis. Specifically, TTP has been recently shown to bind to Dicer and positively contribute to miR-145 expression. Dysregulated phosphorylation of TTP by p70 S6 kinase ($p70^{S6K}$), downstream of PI3K/Akt, was associated with decreased miR-145 expression in ovarian cancer [333]. Dicer and TTP were found to immunoprecipitate together, and TTP knock-down in ovarian cancer cell line was associated with decreased expression of miR-145. However, TTP is generally associated with destabilisation of mRNA transcripts, and its role in association with Dicer is not clear.

A different mechanism was suggested to drive post-transcriptional regulation of miR-155 by TTP in cystic fibrosis cells where TTP would control the expression of miR-1, indirectly inducing downregulation of miR-155 [329]. How TTP is involved in miR-1 expression and how miR-1 could induce downregulation of miR-155 expression was not addressed, overall providing little mechanistic insight into the potential role of TTP in miRNA biogenesis.

Finally, stability and half-life kinetics of miR-155 need to be controlled in a timely manner in order for cells to be able to resolve inflammatory responses after the infection has been cleared. It was previously discussed in paragraph 1.3.4 how the anti-inflammatory miRNAs miR-146a and miR-21 are stable for a long time and can negatively regulate miR-155 at late stages of inflammation [207, 208]. Mann *et al.* demonstrated that when miR-146 does not control the expression of miR-155, levels of miR-155 increase more rapidly and remain high for longer. Persistent high miR-155 levels correlate with chronic activation of macrophages and inflammatory response. Nevertheless, the mechanism controlling miR-155 stability and rate of degradation has not yet been clarified.

Mechanisms regulating miR-155 expression are complex and involve different molecules of the immune system, including intracellular and extracellular signals. Extracellular microenvironmental changes are communicated to cells not only by soluble factors such as cytokines and growth factors, but also insoluble molecules of the extracellular matrix (ECM). These signals are transmitted from cell surface receptors to a range of intracellular targets, making up a sophisticated system where cells, ECM and signalling molecules are interconnected.

1.5. How the ECM controls miRNA expression in macrophages

1.5.1 Macrophages and the local microenvironment

Sentinels of the innate immune system, macrophages are the most plastic cells of the hematopoietic system [334]. They origin from the myeloid lineage and are professional phagocytic cells, able to respond to environmental changes and signals. Classification of macrophages is still under discussion, but it is known that in adult human tissues and organs, macrophages derive from three different sources: the yolk sac, fetal liver and adult hematopoietic stem cells [8]. Yolk sac and fetal liver provide the initial tissue-resident macrophages maintained throughout adult life [335, 336]. Tissue-resident macrophages are characterised by a variety of morphologies and phenotypes specific to each tissue such as brain microglia, Kupffer cells in the liver and cardiac macrophages. After birth, blood monocytes originating from adult bone marrow HSCs replenish tissue macrophages, particularly in organs with high macrophage turnover and in response to increased demand. Therefore, several tissues are constituted by a mixture of embryo and marrow-derived macrophages, expressing heterogeneous markers [337].

In mice, circulating monocytes are characterised by surface marker combinations that can identify them as “classical”, previously known as inflammatory macrophages, expressing $Ly6C^{hi}CX3CR1^{int}CCR2^{+}CD62L^{+}CD43^{Low}$, or “non-classical” $Ly6C^{low}CX3CR1^{hi}CCR2^{low}CD62L^{-}CD43^{+}$ [338, 339]. Human blood monocytes are classified according to a combination of CD14 and CD16 markers, which include “classical” monocytes ($CD14^{+}CD16^{-}$), and the less abundant “intermediate” ($CD14^{+}CD16^{+}$) and “non-classical” ($CD14^{low}CD16^{+}$) monocytes [338, 340]. Classical

monocytes are generally recruited to tissues during inflammatory responses, where they differentiate into mature macrophages [334]. Non-classical monocytes, instead, patrol the vasculature system to clear damaged endothelial cells [341].

Macrophages are fundamental mediators of development, homeostasis and immune response [334, 342]. For example, during development microglia are involved in pruning synapses to remodel neural circuits of the post-natal brain [343, 344]. In the spleen, iron homeostasis is maintained by red pulp macrophages, which phagocytose erythrocytes and recycle heme groups [345, 346]. Macrophages are particularly essential for initiating and resolving inflammation in response to pathogens and sterile tissue injury [334]. They can induce inflammation by producing molecules such as cytokines, chemokines, extracellular matrix-degrading enzymes and reactive oxygen species. Through communication with the extracellular environment, macrophages can switch to a reparative phenotype and start releasing healing and tissue repair molecules, including matrix proteins such as fibronectin and growth factors such as platelet-derived growth factor (PDGF) [347].

Macrophage phenotypic spectrum *in vivo* is complex, with no clear boundaries between pro- and anti-inflammatory macrophages [348]. *In vitro,* macrophages can be driven towards specific phenotypes through stimulation with activators such as LPS, IL-4, or IFN-γ. However, other conditions, including growth medium and types of plastic used, also need to be considered, because they can affect cell growth and activation [347].

Notably, the composition of the extracellular microenvironment can completely re-program macrophages, an event that is particularly relevant in conditions such as

chronic inflammatory diseases, tissue fibrosis and cancer, where macrophages can become pathogenic and contribute to disease progression [349, 350]. In particular, the tumour microenvironment is rich in tumour-associated macrophages (TAMs), which can contribute to tumour growth, metastasis and immunosuppression [334, 351].

In diseases such as autoimmune RA, persistent expression of pro-inflammatory cytokines and matrix-degrading molecules in the extracellular space promotes tissue damage, including the synthesis and release of DAMPs, causing persistent activation of pro-inflammatory macrophages [352]. Aberrant wound healing can follow this non-resolving activation, leading to tissue fibrosis [353]. Appropriate cell-cell and cell-extracellular matrix (ECM) communication and switch to anti-inflammatory phenotypes are essential to overcome these conditions.

Signature epigenetic features and gene expression patterns characterise tissue-resident macrophages, exhibiting lineage and tissue-specific expression, including transcription factors like *Sall1* in microglia, *Gata6* in peritoneal macrophages and *Spi-c* in red pulp macrophages [354, 355]. The local microenvironment plays a fundamental role in conditioning gene expression, modulating and reprogramming macrophages according to changes in the environment and the ECM [354, 356].

However, it is yet unclear how the ECM can regulate gene expression through transcriptional and post-transcriptional regulators such as miRNAs.

1.5.2 The ECM in the local microenvironment contributes to gene regulation

The ECM is a complex and highly dynamic three-dimensional network of extracellular macromolecules present within all tissues and organs. It fills the spaces between cells and connects cells and tissues. For a long time, it was thought that the ECM was solely giving structural and physical support to cells, facilitating cell migration. It is now well established that the ECM is, in fact, an essential component of the cellular signalling machinery, in all physiological conditions [357].

The biochemical composition and architecture of the ECM differ in and within each tissue [358]. The main components of the ECM include structural elements such as collagens, laminins and proteoglycans (PGs), and modulatory glycoproteins such as fibronectins and tenascins that are directly involved in cell signalling and adhesion. ECM glycoproteins can bind to growth factors (e.g. VEGF and FGF), cytokines (e.g. TNF, IFNγ and TGF-β) and cell transmembrane receptors such as integrins and PRRs [64, 359].

Continuous physiological remodelling of the ECM ensures maintenance of tissue homeostasis. The ECM composition can rapidly change in response to perturbations to cellular processes and noxious stimuli, leading to inflammation and disease. These changes are mediated by molecules released by the cells, including proteases such as metalloproteinases (MMPs), which lead to degradation of the ECM [360], and wound healing induced cytokines such as TGF-β, which promotes ECM synthesis [361].

Importantly, synthesis and degradation of the ECM must be stringently regulated as changes in the mechanical and biochemical properties of the ECM can potently modulate gene expression of most cells, including macrophages [354]. For instance,

the extracellular microenvironment of the lung, with the ECM as its primary component, can completely re-program differentiated peritoneal macrophages by changing its genome to adopt a lung-specific gene signature with upregulation of lung-specific genes (e.g. transcription factor *Pparg*) and downregulation of peritoneal-specific genes (e.g. *Gata6*) [354].

Notably, the ECM can regulate miRNA expression as well. Increased ECM stiffness of human breast cancer tissue has been a clinical feature with diagnostic value in mammography screenings for a long time, yet the molecular mechanism linking ECM stiffness and cancer pathogenesis was unknown. It was recently demonstrated that increased ECM stiffness, due to excessive deposition of collagen, can modulate the expression of miR-18a, a miRNA involved in tumour progression through repression of the tumour suppressive gene PTEN (phosphatase and tensin homolog) [362]. ECM stiffness triggered β-catenin signalling and MYC-induced miR-18a expression, following clustering and increased activation of integrin receptors.

Furthermore, cell density activation of Hippo signalling was found to regulate miRNA biogenesis. Under low cell density, the Hippo signalling transducer YAP (yes-associated protein 1) was shown to be translocated to the nucleus, leading to reduced Microprocessor activity and lower levels of a subset of miRNAs such as miR-125b [221]. According to the authors, lower cell-densities would recapitulate tumour microenvironments in which miRNA expression is reduced. However, miR-125b, which they found down-regulated in mouse models of skin and hepatocellular carcinomas [221], is upregulated in hematopoietic and brain tumours, as well as

other cancers [363]. Tissue- and localisation-dependent miRNA regulation could indicate specific activation of membrane receptors by ECM components.

In this fashion, activation of integrin $\alpha 6\beta 4$ was found to downregulate the expression of miR-29a in breast cancer cell lines. Reduced miR-29a levels caused increased expression of ECM-associated protein SPARC (Secreted Protein Acidic And Cysteine Rich), facilitating carcinoma invasion and ECM remodelling [364].

While the impact of the ECM on gene expression continues to be a central subject of cancer research, fewer studies have investigated the role of the ECM in regulating miRNA expression during inflammation. Decorin, a small leucine-rich proteoglycan of the ECM, was found to negatively regulate miR-21 expression in LPS-stimulated mouse peritoneal macrophages and *in vivo* in septic mice. This involved decorin inhibition of TGF-β signalling [56]. TGF-β was found to induce pri-miR-21 processing through SMAD signalling [227]. However, the mechanism by which decorin would block TGF-β was not investigated. Later, Piccinini *et al*. demonstrated that tenascin-C, a multimeric glycoprotein of the ECM, modulates inflammatory cytokine production by regulating miR-155 expression in bone marrow-derived macrophages and *in vivo*, during systemic inflammation caused by LPS [296]. This study implicated tenascin-C as an important component of innate immunity that modulates the strength and duration of inflammatory responses.

1.6. Tenascin-C as a regulator of miR-155

Tenascin-C is specifically induced upon tissue injury and infection, where it triggers innate immune responses through activation of TLR4 [64, 365-370] and α9 integrin [371-373], but it is generally absent or expressed at low levels at specific sites in healthy adults (e.g. tendons, spleen and lymph nodes) [374]. Its multidomain structure and tightly controlled gene expression pattern confer to tenascin-C the ability to contribute to a wide range of cellular functions, many of which are still partially unknown.

Tenascin-C, previously known as myotendinous antigen, GMEM or cytotactin, is one of four tenascin family members. The tenascin family of ECM glycoproteins is highly conserved in tetrapods (mammals, birds, reptiles and amphibians) and includes tenascin-R (restricitin, janusin), tenascin-X (gene X, tenascin-Y in chicken) and tenascin-W (tenascin-N) [375]. Their roles are context-specific, varying from cell adhesion and migration during development to tissue homeostasis in response to activating stimuli in adulthood (reviewed in [375-377]). While they are all involved in interactions with cell receptors, ECM components and growth factors, each tenascin family member is characterised by distinctive tissue distribution patterns and features.

Tenascins are generally expressed in connective tissues. Tenascin-X is the most common tenascin, expressed in developing and adult loose connective tissues, including dermis, epimysium and blood vessels. Its mutation was found to cause a recessive form of Ehlers-Danlos syndrome [378, 379]. Tenascin-R is expressed in embryonic and adult central nervous systems and peripheral nerves [380, 381], while

tenascin-W is mainly found in bones and stroma of certain tumours [382-384]. Overall, tenascins share a similar molecular architecture and assembly in complex oligomeric structures in the ECM.

Founding member of the family, tenascin-C was discovered in the 1980s by independent groups studying brain cancer in glioma and glioblastoma cell lines [385], morphogenesis of muscles and tendons in chicks (myotendinous junction) [386] and embryonic development of the nervous system [387, 388]. It was later discovered that pathological conditions, such as infection, tissue damage and tumorigenic environment, triggered specific expression of tenascin-C (reviewed in [389] and [376]).

1.6.1 Tenascin-C structure and expression

Tenascin-C structure

Tenascin-C is composed of a large series of repeats and domains, creating extended molecules with the ability to oligomerise into more complex structures. Oligomerisation is supported at the N-terminus by a tenascin assembly domain (TA), allowing the formation of a hexameric structure. Proceeding from the TA-domain, tenascin-C is composed of heptad repeats, epidermal growth factor-like (EGF-like) repeats, fibronectin type III-like (FNIII-like) repeats and a C-terminal fibrinogen-like globe (FBG) (Figure 1.7).

The human tenascin-C gene is located on chromosome 9 and is composed of a total of 30 exons [390, 391]. In mouse, tenascin-C locates on chromosome 4 and is structurally similar to human tenascin-C. Both orthologs contain 14.5 EGF-like repeats and 8 constitutively expressed FNIII-like repeats. However, the number of

alternatively spliced FNIII-like repeats is different, with 9 expressed in humans and 6 in mice [392].

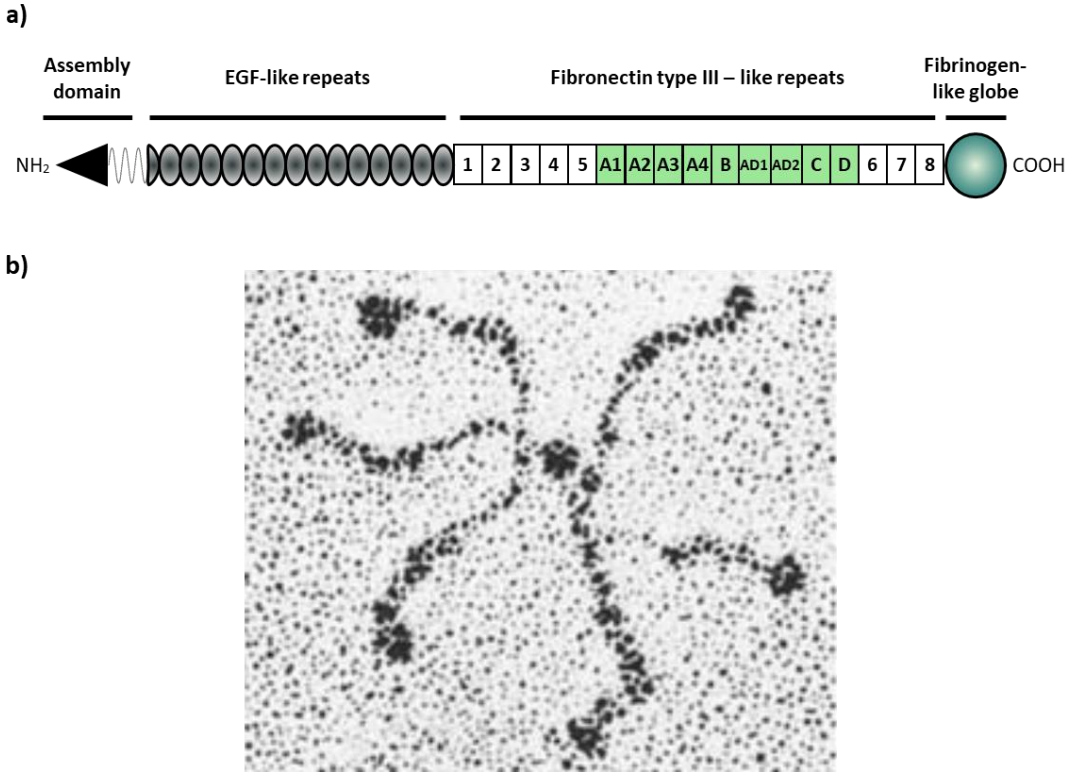


Figure 1.7 Human tenascin-C multidomain structure and hexameric oligomerisation
a) Representation of tenascin-C subunit structural domains, composed of an N-terminal tenascin-C assembly domain (TA), 14.5 epidermal growth factor-like (EGF-like) repeats, up to 17 fibronectin type III-like (FNIII-like) repeats and a C-terminal fibrinogen-like globe (FBG). In the FNIII region 8 domains are constitutively expressed (white boxes), and 9 are alternatively spliced (green boxes). **b)** Electron micrograph of tenascin-C hexabrachion structure, composed of 6 tenascin-C subunits branching out from the central assembly domain. Image from [393].

Human tenascin-C is known to express 9 protein-coding isoforms, with certain FNIII-like domains generally splicing together [392].

The preferential expression for specific splice variants seems to correlate with certain conditions such as carcinogenesis. For example, exon AD1 was found in human

glioblastoma, neuroblastoma and osteosarcoma, but otherwise absent in healthy human cells [394].

Expression of longer or shorter isoforms was also studied during inflammatory responses known to up-regulate tenascin-C expression in keratinocytes. Short tenascin-C isoforms (5800nt) were shown to be induced by pro-inflammatory TNF-α, while IFN-γ was preferentially inducing longer tenascin-C transcripts (7500nt) [395].

Tenascin-C transcriptional and post-transcriptional regulation

Tenascin-C expression is transcriptionally controlled by several transcription factor binding sites identified on its promoter region (reviewed in [396]).

Tenascin-C expression is induced during embryogenesis and development. Its transcription can be controlled by homeobox transcription factors, such as PRRX1 (paired-related homeobox 1), involved in morphogenesis of limbs and craniofacial structures [397]. Another example of TF enhancing tenascin-C transcription is EVX1 (even-skipped homeobox 1), involved in embryonic and neuronal development [398].

In adults, tenascin-C expression is maintained at low levels but is rapidly and transiently induced in response to infection and during inflammation. Several pro- and anti-inflammatory cytokines, including IL-1α and IL-1β [399, 400], IL-4 and IL-13 [401, 402] can upregulate tenascin-C, initiating intracellular signalling pathways such as PI3K/Akt/NF-kB [365]. Another known regulator of tenascin-C is TGF-β, involved in tissue development and repair [403]. Direct transcriptional regulation by TGF-β was reported in mammary epithelial cells (HC11) and mouse embryonic fibroblasts [404]. Moreover, induction of TGFβ1 was found to upregulate TNC gene expression during axonal regeneration in rat astrocytes [405]. TGFβ signalling works through activation

of SMAD proteins. Two potential SMAD2/3 binding sites were identified on tenascin-C promoter region in human dermal fibroblasts [406].

Additionally, tenascin-C expression in bone marrow stromal cells was found downregulated by glucocorticoids [407]. Glucocorticoids are anti-inflammatory steroid hormones involved in myelopoiesis [408], which can downregulate pro-inflammatory factors like AP-1 and NF-kB [409]. Several NF-kB putative binding sites were identified within the human tenascin-C gene, leading to enhanced tenascin-C expression in human myeloid cells [365].

Tenascin-C post-transcriptional regulation is primarily controlled by alternative splicing. Besides, miRNAs can regulate tenascin-C expression. For example, miR-335 was suggested to target *TNC* and transcription factor *SOX4* mRNAs. MiR-335 is downregulated in metastatic cancers, possibly leading to enhanced expression of tenascin-C and increased cell proliferation [410]. Moreover, miR-494 can directly target tenascin-C in macrophages. Upon LPS activation, miR-494 levels are decreased, allowing tenascin-C induction, which engages in a positive feedback mechanism with NF-kB [411].

Tenascin-C post-translational regulation

Post-translational modification and processing by proteolytic molecules can further regulate tenascin-C. Tenascin-C has several predicted sites for glycosylation [392, 412, 413] and citrullination [414], which can modify the apparent molecular weight of the protein on reducing gels. Glycosylation was shown to modulate cell-adherence and binding to proteins [415, 416]. It could also confer protection against proteolytic degradation in isoforms with a higher number of glycosylated sites [417].

Matrix metalloproteinases (MMPs) such as MMP-1, -2, -3 and -7 can target splice variants of tenascin-C. Larger tenascin-C isoforms display additional MMPs target sites on FNIII alternatively spliced region, making them more susceptible to MMPs degradation than smaller isoforms [418]. Cleavage of tenascin-C is a way to control tissue protein levels and transient expression. However, fragments released by proteolysis can uncover hidden binding sites for cell adhesion receptors [418, 419].

The complex structural organisation and protein processing events contribute to the wide range of tenascin-C roles. However, what has been discovered so far about this protein seems to be only the tip of the iceberg.

1.6.2 Physiological functions of tenascin-C

Early studies identified high levels of tenascin-C in developing organs and tissues, such as neural crest cells and peripheral nerves (Schwann cells precursors) [420, 421], muscles, bones and ligaments [386, 422]. It was also found induced in organ morphogenesis, during the formation of mammary glands [423, 424], kidneys [425] and lungs [426], to mention but a few. In healthy adult tissues, tenascin-C expression is confined to a few connective tissues subject to tensile forces [427], some epithelial cells [425] and certain stem cell niches, including bone marrow, intestine and hair follicles [428]. Tenascin-C is linked to events involving rapid transformation and cellular motility, such as pathological and mechanical stress. During these events, tenascin-C is transiently induced and rapidly down-regulated upon resolution of inflammation and tissue repair [389].

In vivo function of tenascin-C was initially analysed by Saga et al. and Forseberg et al. They independently generated tenascin-C knockout (*tnc-/-)* mouse strains and,

surprisingly, found that *tnc-/-*mice developed normally. Mice presented no evident abnormalities and were fertile [429, 430]. Nevertheless, later studies demonstrated that *tnc-/-*mice were hyper-locomotive and were characterised by abnormal circadian rhythm [431, 432]. Moreover, mice lacking tenascin-C displayed phenotypic differences when challenged by disease or injury. For example, in models of myocardial injury and infarction, *tnc-/-*mice had slower myofibroblast infiltration to granulation tissues and were more prone to left ventricular remodelling and cardiac failure, compared to their wild-type counterparts [433, 434]. In tumour transplantation models, absence of tenascin-C correlated with smaller tumours, reduced VEGF (vascular endothelial growth factor) expression and angiogenesis [435]. In inflammatory arthritis models, *tnc-/-*mice were found protected from chronic inflammation of the joint, with reduced cell infiltration and proteoglycan loss. Contrary to wild-type mice, *tnc-/-* showed no articular cartilage destruction or bone erosion [64].

However, the role of tenascin-C in these conditions is not easy to define. Complexity is added by its multidomain structure, which confers the ability to interact with a multitude of molecules, promoting different outcomes. Tenascin-C binding partners include ECM molecules, including fibronectin, collagen and proteoglycans, cellular membrane receptors such as integrins, EGF receptor and TLR4, and growth factors like TGF-β and VEGF (reviewed in [436]).

Tenascin-C binding partners interact with specific regions on tenascin-C domains, as summarised in Figure 1.8. Binding of tenascin-C to different molecules can induce

changes on structural organisation and adhesive properties of the ECM, and influence cell signalling, activation, differentiation, proliferation and migration [374].

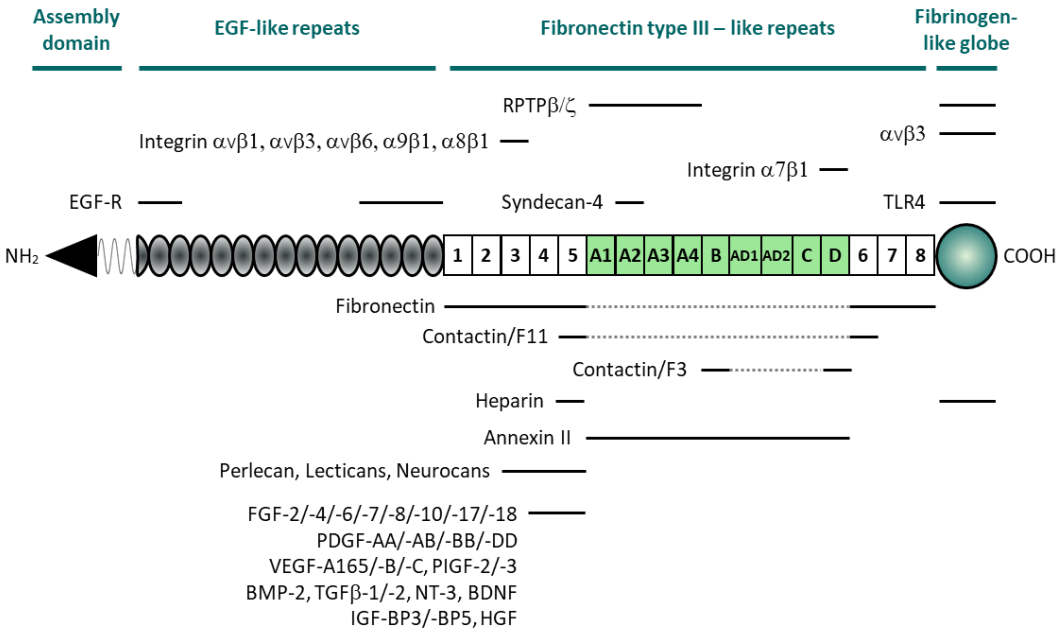


Figure 1.8 Tenascin-C ligand binding sites and partners

Schematic representation of tenascin-C domains depicts N-terminal tenascin assembly (TA) domain, epidermal growth factor (EGF)-like repeats, fibronectin type III (FNIII)-like repeats and C-terminal fibrinogen (FBG)-like domain. Binding sites of tenascin-C ligands are represented above and below tenascin-C subunit. EGF-receptor (EGF-R) can bind to EGF-like repeats [437, 438]. Integrins αvβ1, αvβ3, αvβ6, α8β1 and α7β1 connect to different sites on FNIII domain [439, 440]. αvβ3 integrin has an additional binding site on FBG domain, where tenascin-C can also bind to TLR4 [64, 441]. Receptor protein-tyrosine phosphatase β/ζ (RPTPβ/ζ), mainly expressed in neural cells, binds to FNIII A1-A4 [442] and FBG [443], while syndecan-4 binds to an alternatively spliced sequence on FNIII-A2 [419]. Fibronectin mainly binds to full-length constitutively expressed FNIII domains of tenascin-C [444]. Modulators of neuronal cell adhesion, contactin/F11 and contactin/F3 interact with small splice variants of tenascin-C, on contiguous FNIII 5-6 or contiguous FNIII B-D, respectively [445, 446]. Two heparin-binding sites are located on FNIII-5 and FBG [447, 448], while Annexin II binds to the FNIII alternatively spliced segment [449]. Perlecans and lecticans bind to FNIII 3-5, neurocans recognise FNII4-5 [393]. Finally, on FNIII 4-5, promiscuous growth factors binding sites include fibroblast growth factor (FGF)-2/-4/-6/-7/-8/-10/-17/-18; platelet derived growth factor (PDGF)-AA/-AB/-BB/-DD; vascular endothelial growth factor (VEGF)-A165/-B/-C; phosphatidylinositol-glycan biosynthesis class F protein (PIGF)-2/-3; bone morphogenetic protein (BMP)-2; transforming growth factor beta (TGFβ)-1/-2; neurotrophin (NT)-3; brain derived neurotrophic factor (BDNF); insulin-like growth factor-binding protein (IGF-BP)3/-5; hepatocyte growth factor (HGF) [450].

Binding of tenascin-C to ECM components, such as fibronectin, or proteoglycan receptors such as syndecan-4, leads to decreased cell-adhesion and down-regulation of focal adhesion [451-453]. Known binding sites for ECM molecules are, for example, constitutively expressed FNIII repeats for fibronectin and FNIII 3-5 for proteoglycan families of lecticans and perlecans [454]. However, for other tenascin-C ligands such as collagen, periostin and fibrillin-2, binding sites are still unknown [374].

Tenascin-C can manipulate cell adhesion and migration by inhibiting other ECM protein signalling. It can inhibit T-lymphocyte migration by blocking fibronectin interaction with integrin $\alpha5\beta1$ [455]. It can otherwise prevent co-activation and signal amplification of syndecan-4 and $\alpha5\beta1$ by preventing fibronectin binding to syndecan-4 [452].

Tenascin-C can also directly control cellular behaviour and signalling by binding to integrins. At least five integrins can interact with the third FNIII domain: $\alpha v\beta1$, $\alpha v\beta3$, $\alpha v\beta6$, $\alpha9\beta1$ and $\alpha8\beta1$. $\alpha7\beta1$ binds to the alternatively spliced FNIII D domain, and $\alpha v\beta3$ has a second binding site on the FBG domain (reviewed in [439, 440]).

Tenascin-C activation of integrin signalling can contribute to several cellular events, including inflammation and tissue repair. For example, activation of $\alpha9$ integrin by tenascin-C increased cytokine production in experimental rheumatoid arthritis [371], while activation of $\alpha v\beta3$ integrin in cardiac fibrosis induced macrophage migration and NF-kB-dependent cytokine expression [456]. Additionally, binding of $\alpha v\beta3$ integrin to tenascin-C FBG domain can induce neovascularization of wounded tissues and endothelial sprouting, favouring tissue repair phenotypes [457, 458].

Studies of tenascin-C in inflammation found that three epitopes on the C-terminal FBG domain are required to bind and activate TLR4 [441]. Tenascin-C-mediated activation of TLR4 induced NF-kB signalling and expression of pro-inflammatory cytokines such as TNF-α, IL-6 and IL-8 [64, 356, 441], but also tissue rebuilding molecules, including matrix proteins such as type I collagen [356].

Several other ligands can contribute to cellular signalling. For example, tenascin-C can bind to EGF-receptor (EGF-R) on its EGF-L repeats, promoting receptor phosphorylation and activating MAPK/ERK cascade [437, 438]. It can also bind to growth factors such as platelet-derived growth factor (PDGF), fibroblast growth factor (FGF) or TGF-β via its FNIII repeats 4-5. Binding extends growth factors half-lives, increasing their local concentration and induces conformational changes, modulating cell signalling [450, 459].

Tenascin-C signalling can be amplified by co-activation of different growth factor receptors and integrins. For example, tenascin-C-mediated activation of $\alpha v\beta 3$ integrin mediates focal adhesion formation, which clusters with activated EGF-R, promoting cell growth [460]. Similarly, tenascin-C-mediated phosphorylation of PDGF receptor beta in smooth muscle cells was found associated with clustering of $\alpha v\beta 3$, activation of focal adhesion kinase (FAK) and cell proliferation [461].

Transient expression of tenascin-C is vital for tissue repair and in situations of pathological stress. However, a persistent tenascin-C expression is associated with chronic inflammatory diseases, underlining an important role for tenascin-C in immunity.

1.6.3 Tenascin-C in inflammation and innate immunity

In adult tissues, expression of tenascin-C is transiently induced at sites of inflammation during pathogenic infection or sterile injury. Tenascin-C contributes to inflammatory responses by activating partner receptors TLR4 and integrins $\alpha9\beta1$ and $\alpha v\beta3$. However, the involvement of further ligands cannot be excluded. Tenascin-C pro-inflammatory action could also be achieved through synergistic or antagonistic effect with multiple ligands.

Tenascin-C was initially found to drive TLR4 activation in primary human macrophages and synovial fibroblasts [64]. Midwood and colleagues demonstrated that tenascin-C could promote expression of pro-inflammatory cytokines IL-6, IL-8 and TNF-α in macrophages, and IL-6 in fibroblasts in a MyD88-dependent manner. Binding of the FBG domain was found to be TLR4 specific and recognition of the tenascin-C FBG domain was independent of classical LPS co-receptors MD-2 and CD14 [64]. A later study found three distinct epitopes on tenascin-C FBG domain collaborate in the binding with TLR4 [441].

Tenascin-C activation of TLR4 confirmed to induce cytokine expression in human and mouse macrophages [64, 296, 441, 462], dendritic cells [365, 369, 463], fibroblasts [64, 464] and chondrocytes [367].

Constant expression of tenascin-C is one of the hallmarks of chronic inflammatory diseases such as rheumatoid arthritis, ulcerative colitis and systemic lupus erythematosus.

In certain types of cancer, such as breast, ovarian and lung cancer, or colorectal and hepatocellular carcinoma, tenascin-C levels correlate with the stage of the disease

and can be used as a biomarker (reviewed in [389] and [465]). Tenascin-C seems to be associated with cancer progression and the development of metastasis. Indeed, high tenascin-C levels are associated with poor prognosis and reduced survival [465]. However, the exact role of tenascin-C in cancer is still under investigation. It was recently discovered that TAMs from ovarian carcinoma could secrete tenascin-C and transforming growth factor beta-induced (TGFBI). These could promote metastatic propagation and cell migration, exacerbating cancer progression. Importantly, IL-10 stimulated monocyte-derived macrophages (m2c-MDMs) matched TAMs phenotype, with similar tenascin-C and TGFBI expression and increased migratory effects. On the other side, LPS and IFNγ stimulated MDMs (m1c-MDMs) expressed comparatively less tenascin-C and TGBI and displayed less migratory potential [466].

High levels of tenascin-C contribute to detrimental tissue remodelling, cell damage and death. In addition to upregulation of pro-inflammatory molecules, tenascin-C is involved in inflammasome driven pyroptosis and fibrotic tissue deposition. Specifically, tenascin-C was recently found involved in inflammasome formation and IL-1β synthesis after myocardial infarction [467]. Moreover, tenascin-C induction of cytokines such as IL-1α, IL-1β, IL-6 and IL-17 in dendritic cells was linked to polarization of Th17 cells [369, 463], drivers of pathogenesis in autoimmune diseases such as rheumatoid arthritis [468]. Specifically, IL-6 expression in DCs was fundamental for the differentiation of Th17 cells and the induction of IL-17 [369]. Furthermore, tenascin-C was found to stimulate prostaglandin E2 and cytokine release in chondrocytes, also involved in Th17 polarization [367].

IL-6 upregulation, following tenascin-C activation of TLR4, was also found responsible for collagen I and alpha-smooth muscle actin (αSMA) expression, driving persistence of fibrosis in models of systemic sclerosis (SSc) [370].

In addition to TLR4, integrins α9β1 and αvβ3 are linked to the pro-inflammatory activity of tenascin-C. Interaction between tenascin-C and α9 integrin induced expression of cytokines IL-1α, IL-6 and chemokines CCL2, CCL4 and CXCL5 in mice synovial macrophages and fibroblasts [371]. In DCs, a synergistic effect of TLR4 and α9 integrin signalling mediated by tenascin-C could drive Th17 cell differentiation by regulating IL-6 and IL-23 levels [372].

The ability of tenascin-C to drive pro-inflammatory cytokine expression was further demonstrated through activation of αvβ3 integrin. In peritoneal macrophages, tenascin-C could drive IL-6, IL-1β and TNF-α expression in an NF-kB-dependent manner. Increased cytokine expression was associated with higher collagen I levels and cardiac fibrosis [456].

In most of the literature, tenascin-C is depicted with a preponderant pro-inflammatory function, associated with long-term negative effects. However, tenascin-C is involved in mechanisms of resolution of inflammation as well.

By activating EGFR and its downstream MAP kinase signalling pathway in NR6 fibroblasts and myofibroblasts, tenascin-C can promote mitogenesis and cell-survival, [437, 438, 469]. Moreover, tenascin-C activation of transmembrane receptors, such as integrin αvβ3, can lead to activation of EGFR by mediating focal adhesion formation and inducing cell growth in smooth muscle cells from rats [460].

Moreover, through binding to TGF-β, a key factor in the resolution of inflammation and tissue repair, tenascin-C seems to actively participate in the healing process [403, 450]. Indeed, tenascin-C knockout mice are characterised by defective repair mechanisms following corneal and myocardial injuries, presenting reduced macrophage infiltration, lower TGF-β levels and reduced fibronectin and collagen synthesis [433, 470, 471]. However, the uncontrolled expression of tenascin-C and upregulation of TGF-β can ultimately lead to tissue fibrosis and excessive collagen deposition [370, 472].

Tenascin-C-mediated inflammation resolution is further achieved through its immunosuppressive functions on lymphocytes, halting T-cell activation [473, 474] and inhibiting myeloid cell migration [475].

These examples indicate how tenascin-C function can vary depending on the context and temporal expression. Nonetheless, tenascin-C-mediated activation of TLR4 in macrophages promoted distinct signalling outcomes and cell behaviour than activation with LPS. Tenascin-C binding to TLR4 induced IL-6 as efficiently as LPS and significantly higher levels of IL-8. However, it promoted significantly lower levels of TNF-α and could not induce IL-23 and IL-12 synthesis. Moreover, in contrast to LPS-induced synthesis of macrophage collagenases, tenascin-C stimulated macrophages to synthesize and phosphorylate collagen molecules, promoting tissue repair via a moderate inflammatory response and synthesis of ECM molecules [356].

Tenascin-C expression is transiently induced in human myeloid cells during acute inflammation. Induction of tenascin-C can be driven by different TLR/PAMP interactions, including TLR4/LPS, TLR1/2/LTA (5,6-oxido-7,9,11,14-eicosatetraenoic

acid), TLR2/6/PAM3 and TLR5/flagellin. Other TLRs, such as TLR3 or TLR7/8 activated by poly(I:C) and R848 respectively, did not induce tenascin-C expression. Goh and colleagues confirmed that induction of tenascin-C is mediated by PI3K/AKT and NF/kB pathway activation, shared by all involved TLRs [365].

Tenascin-C expression is induced early during inflammation by pathogenic components. It had previously been detected in plasma from septic patients [476], and in patients with *Staphylococcus aureus* and other infections [477, 478]. Piccinini *et al*. investigated the role of tenascin-C in the innate immune response to LPS-induced sepsis [296]. They confirmed that tenascin-C is rapidly induced in plasma of mice injected with a sub-lethal dose of LPS. When subject to LPS, *tnc-/-* mice showed less severe symptoms and reduced neutrophil infiltration into lungs and liver than *tnc+/+* mice. *Tnc-/-* mice produced significantly lower levels of circulating cytokines IL-6 and TNF-α, indicating that tenascin-C is required for the pro-inflammatory response *in vivo*. Allogenic bone marrow transplantation of *tnc+/+* bone marrow into *tnc-/-* irradiated mice could replenish TNF-α levels.

Tenascin-C expression was confirmed to be transiently induced by LPS in bone marrow-derived macrophages (BMDMs). ELISA-detectable levels of tenascin-C protein were found in cell lysates from as early as 1.5 hours, peaking at 8 hours after LPS stimulation. Soluble tenascin-C was then found secreted in the medium, significantly increasing after 24 hours of LPS induction.

Analysis of cytokines and chemokines found lower levels of pro-inflammatory TNF-α, IL-6 and CXCL1 and higher anti-inflammatory IL-10 in *tnc-/-* compared to wild type cells. However, mRNA levels of the same molecules showed no differences linked to

the presence or absence of tenascin-C. The mechanism of regulation of cytokines by tenascin-C was likely mediated at the post-transcriptional level.

1.6.4 Tenascin-C is a regulator of miR-155 expression

The expression of 375 miRNAs was analysed by microarray analysis, comparing LPS-activated BMDMs from *tnc+/+* and *tnc -/-* mice. Among miRNAs involved in immune responses, miR-155 was significantly downregulated in *tnc-/-* BMDMs compared to *tnc+/+* cells. Reduced miR-155 levels were confirmed *in vivo*, comparing miR-155 expression in spleen from *tnc+/+* and *tnc-/-* septic mice. Notably, the expression of LPS-induced TNF-α was rescued in *tnc-/-* BMDMs by over-expression of miR-155, indicating that tenascin-C could drive miR-155 expression to control cytokine production. However, how tenascin-C can regulate LPS-induced miR-155 expression is still unknown.

1.7. Aims of this study

The ECM glycoprotein tenascin-C was found to contribute to an effective immune response by regulating miR-155 levels in macrophages activated by LPS [296]. However, the molecular mechanism behind this regulation remains unknown.

This project aimed to unveil the mechanism by which tenascin-C regulates miR-155 expression in mouse macrophages. Specifically, we intended to identify the stage of miR-155 biogenesis that tenascin-C is influencing, study what form tenascin-C requires to achieve its regulatory power, and identify the membrane receptor tenascin-C associates with to regulate miR-155.

The specific objectives addressing this aim were:

1) To study the intracellular events triggered by tenascin-C to regulate miR-155 expression. This was achieved by:
    a. Studying the specificity of tenascin-C effect on miR-155 expression by using different macrophage activators and gene expression analysis techniques, including quantitative PCR (qPCR) and Northern blot;
    b. Analysing different steps of miR-155 biogenesis utilising gene expression analysis (qPCR) and cellular fractionation techniques;
    c. Pinpointing the event of miR-155 biogenesis in which tenascin-C is involved by RNA-immunoprecipitation and qPCR;
    d. Analysing RBPs potentially involved in tenascin-C-mediated regulation of miR-155, using gene and protein analysis techniques, including qPCR, Western blot and protein co-immunoprecipitation.

2) To determine which form (soluble versus ECM-assembled) of tenascin-C is involved in regulating miR-155 expression by:
    a. Studying the expression and form of tenascin-C in LPS-activated macrophages by using gene and protein detection assays, including immunofluorescence cell imaging and Western blot;
    b. Optimizing and characterizing a 3D cell culture model to study the role of ECM-assembled tenascin-C, combining immunofluorescence microscopy and Western blot analyses;
    c. Applying the model mentioned above to analyse the role of matrix-assembled tenascin-C in miR-155 expression by qPCR analysis.
3) To identify the cell membrane receptor and/or co-receptor involved in miR-155 regulation, together with tenascin-C, by:
    a. Selecting experimentally validated candidate tenascin-C receptors based on their involvement in immune responses and expression by macrophages;
    b. Determining the effect of candidate receptors selected above on miR-155 expression by qPCR following receptor blockade or silencing;
    c. Identifying novel candidate tenascin-C receptors/co-receptors by combining literature search with *in silico* prediction of candidate receptors binding to tenascin-C;
    d. Determining the effect of candidate receptors identified above on miR-155 expression by qPCR following receptor blockade or silencing.

Chapter 2

MATERIALS AND METHODS

Chapter 2. Materials and Methods

2.1. Reagents

Reagents were purchased from the following sources:

2.1.1 Cell culture reagents

HBSS without calcium and magnesium, DMEM with L-Glutamine and Na-Piruvate, Optimem and trypsin Versene (EDTA) were from Lonza. Fetal Bovine Serum (FBS), β-Mercaptoethanol and cell dissociation buffer were from Gibco and antibiotic-antimycotic solution from GE Healthcare. M-CSF was from Peprotech. Red Blood Cell Lysis Buffer, L-ascorbic acid, NH_4OH, Dulbecco's phosphate-buffered saline with calcium chloride and magnesium chloride, Penicillin-Streptomycin, gelatin, Trypan blue and Poly(I:C) were from Sigma-Aldrich. LPS (*E. coli,* Serotype EH100 (Ra)) was from Enzo Life Sciences. Recombinant Mouse TNF-alpha (aa 80-235) Protein was from R&D Systems. Cyclo (RGDfC), avb3 Integrin Binding Cyclic RGD Peptide was from AnaSpec. Tlr-cli095, TLR4 inhibitor was from Invivogen. DNase I and Liberase™ TL Research Grade were from Roche. Lipofectamin® RNAiMAX reagent was purchased from Invitrogen. ON-TARGETplus SMARTpool siRNAs were purchased from Dharmacon.

2.1.2 Molecular biology reagents

TRIzol® reagent was from Invitrogen. QuantiTect Reverse Transcription Kit was from Qiagen. GoTaq® qPCR Master mix was from Promega. SYBR green primers for qPCR and GenElute™ Mammalian Genomic DNA Miniprep Kit from Sigma-Aldrich. PCRBIO

Taq DNA Polymerase was from PCR Biosystems. TaqMan™ MicroRNA Reverse Transcription Kit, MicroRNA Assays, Universal PCR Master Mix, no AmpErase™ UNG and UltraHyb ultrasensitive Hybridisation buffer were from Applied Biosystems. DIG luminescent detection kit was from Roche and miRCURY LNA Detection probes from Exiqon. DIG-labelled Blue Colour Marker for Small RNA was from BioDynamics Lab. RiboLock RNase inhibitor was from Thermo Scientific and Quick-Load® Purple 1 kb DNA Ladder was from NEB.

2.1.3 Protein chemistry and western blotting reagents and equipment

PageRuler™ Plus Pre-stained protein ladder (10 to 250 kDa) was from Thermo Scientific. SDS-PAGE electrophoresis apparatus, wet transfer apparatus and 0.45 µm nitrocellulose membranes were all from Bio-Rad. Amersham ECL Western blotting Detection Reagents™ were from GE Healthcare Life Science. DTT solution was from VWR. Re-Blot Plus stripping solution was from Millipore. Brilliant Blue G-Colloidal, protease inhibitor cocktail, phosphatase inhibitors and other reagents used for buffers preparation were from Sigma-Aldrich.

2.2. Buffer Recipes

Buffers and solutions	Recipes
1% agarose gel	0.5 g agarose, 1mL of TAE or TBE buffer 50X, 5µl ethidium bromide in 49mL of H_2O.
4X Tris-Cl/SDS, pH 6.8	0.5M Tris-Cl (pH 6.8) and 0.4% SDS
4X Tris-Cl/SDS, pH 8.8	1.5M Tris-Cl (pH 8.8) and 0.4% SDS
Blocking solution for immunocytochemistry	5% (v/v) Goat serum, 3% (w/v) Bovine Serum Albumin (BSA) in 1XTBS
Blocking solution for Northern Blot 1X	10X Blocking solution (Roche) in Maleic Acid Buffer
Decellularization buffer	20mM NH_4OH and 0.5 % Triton X-100 in PBS
Detection buffer for Northern Blot	0.1M Tris-Cl, 0.1M NaCl, pH 9.5
EDC solution	9ml RNase free H_2O, 254µl I-methylmidazole (12.5M, pH 8.0), 0.753g EDC (1-ethyl-3-(3-dimethylaminopropyl)carbodiimide hydrochloride), to a final volume of 24ml RNase free H_2O
Fixing Solution	7% Glacial acetic acid (v/v), 40% methanol (v/v)
Hypotonic Lysis Buffer (HLB)	10mM Tris-Cl (pH 7.5), 10mM NaCl, 3mM $MgCl_2$, 0.3% NP40 (v/v), 10% Glycerol (v/v), Protease inhibitor cocktail (1:1000), Phosphatase inhibitors (1:1000)
Maleic Acid Buffer	0.1M Maleic Acid, 0.15M NaCl, pH 7.5
Modified RIPA Buffer	0.1% SDS (w/v), 0.25% Na-deoxycholate (w/v), Protease inhibitor cocktail (1:1000), EDTA 1mM in PBS, pH 7.4
Modified RIPA lysis buffer (co-IP)	20mM Tris-Cl (pH 8.0), 50mM NaCl, 1% Triton X-100 (v/v), 0.5% Na-deoxycholate (w/v), Protease inhibitor cocktail (1:1000), Phosphatase inhibitors (1:1000)
MOPS 50X	1M MOPS pH7.0
Nuclear Lysis Buffer	20 mM Tris HCl (pH 7.5), 150mM KCl, 3mM MgCl2, 0.3% NP40 (v/v), 10% Glycerol (v/v), Protease inhibitor cocktail (1:1000), Phosphatase inhibitors (1:1000)

Polysome Lysis Buffer 10X	1000mM KCl, 50mM $MgCl_2$, 100mM HEPES pH 7.0, 5% NP-40
Polysome Lysis Buffer 1X	10X PLB, 1mM Dithiothreitol (DTT), Protease inhibitor cocktail (1:1000), Phosphatase inhibitors (1:1000), RNase inhibitors (100U/ml)
Ponceau S staining solution	0.5% Ponceau S (w/v), 1% Acetic acid
Protein Loading Buffer 10X	20% SDS, 80% Glycerol and bromophenol blue, 50mM β-mercaptoethanol, to be added to diluted sample
Protein Wash Solution	0.3M guanidine hydrochloride, 95% ethanol (v/v)
RNA loading dye	95% formamide, 500mM RNase–free EDTA, bromophenol blue
RNA Precipitation Solution (RPS)	5% 3M Sodium Acetate (pH5.5), 95% Ethanol (99.9%)
SDS Sample Buffer 6X	0.375M Tris-Cl (pH 6.8), 12% SDS (w/v), 60% Glycerol, bromophenol blue, 300mM β-mercaptoethanol (added just before use)
Solubilisation Buffer 2X	100 mM Tris-Cl (pH 6.8), 200mM DTT, 4% SDS (w/v), bromophenol blue
SSC 20X	3M NaCl, 0.3M Sodium citrate, pH 7.0, autoclave
Staining Solution	75% 1X Brilliant Blue G-colloidal (v/v), 25% methanol (v/v)
Stripping Buffer (for DIG-labelled RNA probes)	50% (v/v) Deionized formamide, 5% (v/v) SDS, 50mM Tris-Cl, pH7.5
TAE 50X	50mM EDTA (pH 8.0), 2.5M Tris-acetate
TBE 10X	1M Tris-b Base, 1M Boric acid, 20mM EDTA (pH 8.0)
TBS 10X	100ml 1M Tris-Cl (pH 7.5), 87.7g NaCl, H_2O to 1L
TBS-T 1X	10X TBS, 0.1% Tween-20
Total Lysis Buffer	1% NP-40, 150 mM NaCl, 20 mM Tris-Cl (pH 7.5), 10 mM EDTA, 10 mM EGTA, Protease inhibitor cocktail (1:1000), Phosphatase inhibitors (1:1000)
Transfer Buffer for Western Blot 10X	15g Tris-base, 72g Glycine, H_2O to 1L

Transfer Buffer for Western Blot 1X	100ml 10X Transfer Buffer, 200ml Methanol, H_2O to 1L
Tris-Glycine Running Buffer 10X	30g Tris-base, 144g Glycine, 1% SDS (w/v), H_2O to 1L
Urea Lysis Buffer	5M Urea, 2M Thiourea, 50mM DTT, 0.1% (w/v) SDS in PBS, pH 7.4
Washing buffer for Northern Blot	Maleic acid buffer, 0.3% (v/v) Tween-20

Table 3. Buffer recipes and solutions.

2.3. Mice

Homozygous littermate *tnc+/+* and *tnc-/-* mice, kindly gifted by Prof Kim Midwood (Oxford), were female and male aged 9 weeks and on a 129/SvJ background [429]. They were used to isolate bone marrow from femurs and tibias and subsequent generation of bone-marrow derived macrophages, and skin fibroblasts. Breeding and humane killing of animals were approved by the UK Home Office.

2.3.1 DNA extraction from tail biopsies and mice genotyping

Genomic DNA was extracted from *tnc+/+* and *tnc-/-* tail biopsies from mice with GenElute™ Mammalian Genomic DNA Miniprep Kit, according to manufacturer instructions. Genotyping PCR was performed with PCRBIO Taq DNA polymerase, and reactions were set up as described in the table below:

Component	Final Concentration	Volume
5XPCRBio Reaction Buffer	1X	5µl
10µM Forward Primer	200nM	0.5µl
10µM Reverse Primer	200nM	0.5µl
PCRBIO Taq DNA Polymerase	5U/µl	0.125µl
Genomic DNA	100ng	Variable
Nuclease-free water	To a final volume of 25µl	

Table 4. *Tnc+/-* mice genotyping PCR Reaction mix

Reactions were prepared with different combinations of primers (Table 5): the forward primer was 3'TN (mTNC FW) for *tnc+/+* and *lacZ* (LacZ FW) for *tnc-/-* and the

reverse primer was 5'TN G1-2 (mTNC&LacZ RV) for both genotypes, as described in detail by Saga et al. [429].

PCR Tnc Genotyping	Sequence (5'-3')
mTNC&LacZ RV	GAAGTCACTAGAAACTAGTGGACAACTC
mTNC FW	AAGATGCCTGGCAGTAGCCAGGTCAC
LacZ FW	CTCCATGCTTGGAACAACGAGCGCAGC

Table 5. Primers for *tnc+/-* genotyping PCR

PCR reaction was set as follows:

Step	Temperature	Duration	Cycle
Initial denaturation	95°C	5 minutes	Hold
Denaturation	95°C	1 minute	x35
Annealing	63°C	2 minutes	
Extension	68°C	2 minutes	
Final extension	68°C	10 minutes	Hold

Table 6. *Tnc+/-* mice genotyping PCR conditions

After PCR amplification, samples were run on 1% agarose gels in 1X Tris/Acetate/EDTA (TAE) buffer and stained with Ethidium Bromide (1:10,000).

2.4. Cell Culture

All cells were cultured in a humidified incubator at 37°C, in 5% CO_2 atmosphere.

2.4.1 Preparation of bone marrow-derived macrophages and LPS stimulation

For the generation of bone marrow-derived macrophages (BMDMs), bone marrow was flushed from femurs and tibias of *tnc+/+* and *tnc-/-* mice with DMEM. Cells were pelleted and erythrocytes lysed for 5 min with Red Blood Cell Lysis Buffer at room temperature. Cells were washed 3 times in DMEM and finally resuspended in 1ml culture medium. Viable cells were counted using trypan blue and 5 x 10^6 cells were seeded in 10 cm Petri dishes and cultured in DMEM supplemented with 20% (v/v) FBS, 1% (v/v) antibiotic-antimycotic solution, 50 µM β–Mercaptoethanol and 100ng/ml recombinant human M-CSF. On day 7, adherent cells were washed in 1x PBS and directly used for experiments, or detached with cell dissociation buffer and replated in 12-well or 6-well plates in complete DMEM medium with 10% (v/v) FBS and 1% (v/v) penicillin/streptomycin before experiments.

2.4.2 RAW 264.7 cells and siRNAs transfection

RAW 264.7 cells (ATCC® TIB-71™) were maintained in DMEM with 10% (v/v) FBS and 1% (v/v) penicillin/streptomycin. Cells were used for experiments between passage 4 and 20 and passaged when 70-80% confluent.

Cells at 60-65% confluence were used for knockdown experiments of target mRNAs by transfecting them with Lipofectamine RNAiMAX reagent and siRNAs (Table 7).

Dharmacon siRNA – ON-TARGETplus SMARTpool	Cat no
Mouse Tnc	L-046798-01-0005
Mouse Nrp1	L-040787-00-0005
Mouse Nrp2	L-040423-00-0005
Non-targeting Pool	D-001810-10-05

Table 7. List of Dharmacon siRNAs

Macrophages were seeded on 24-well ($7.5x10^4$cells/well), 12-well ($1.5x10^5$cells/well), or 10cm plates ($2.5x10^6$) and left to rest overnight.

For a 24 well plate, the transfection reaction was prepared as follows:

siRNA mix		Lipofectamine RNAiMAX mix	
Opti-MEM	To 25µl	**Opti-MEM**	25µl
siRNA (10uM stock)	2µl (0.2 µM)	**RNAiMAX**	1.5µl

Table 8. Reaction for siRNA transfection

Lipofectamine and siRNA reactions were thoroughly mixed and incubated at room temperature for 5 minutes. Cells were refreshed with 450µl new media, and 50 µl of transfection solution was added to the cells in a drop-wise manner, followed by a gentle swirl to distribute the solution to the cells. After 24 hours medium was replaced. Cells were maintained in culture for a total of 48 or 72 hours after transfection. Twenty-four hours before collection, cells were either stimulated with LPS or with TNF-α, as described in paragraph 2.4.3

2.4.3 Cell stimulation and membrane receptor inhibition

BMDMs and RAW macrophages were treated with 100ng/ml LPS, 10ng/ml TNF-α, or 20µg/ml Poly(I:C) for BMDMs (kindly gifted by Dr Madeleine King, Nottingham) for the duration indicated in the text.

Small molecule inhibitors or function blocking antibodies (Table 9) were used to block membrane receptors before activating the macrophages. Function blocking antibodies were used at a concentration of 25μg/ml and incubated with BMDMs for 30 minutes: CD-29 (Integrin β1), EGFR, Integrin α5β1 and CD11b. αvβ3 Integrin Binding Cyclic RGD Peptide was used at a concentration of 100μg/ml and incubated for 30 minutes with the cells before stimulation with LPS. In the case of Cli095-TLR4 inhibitor, cells were incubated for 6 hours with 1μg/ml inhibitor or 0.1% DMSO as control prior to stimulation with TNF-α. RAW 264.7 cells were treated with 10μg/ml CD11b antibody overnight prior to LPS stimulation.

Treatment	Name	Source	Final concentration
TLR4 activation	LPS from *E. coli Serotype EH100 (Ra))*	Enzo Life Sciences	100ng/ml
TNFR activation	Recombinant Mouse TNF-alpha (aa 80-235) Protein	R&D Systems 410-MT	10ng/ml
TLR3 activation	Polyinosinic–polycytidylic acid sodium salt (Poly(I:C))	Sigma-Aldrich P1530	20μg/ml
Integrin beta1 blocking	Anti-CD29 (Integrin beta1) antibody	Thermo-Fisher 16-0291-85	25μg/ml
EGFR blocking	Anti-EGFR antibody	Abcam ab231	25μg/ml
Integrin alpha5 beta1 blocking	Anti-Integrin $\alpha 5\beta 1$ antibody	NovusBio NBP2-29788	25μg/ml
Integrin alphaM blocking	Ultra-LEAF Anti-CD11b antibody	Biolegend 101248	10 or 25μg/ml
Rat IgG2b isotype control	Ultra-LEAF Purified Rat IgG2b, κ Isotype Control antibody (Clone RTK4530)	Biolegend 400643	10μg/ml
Integrin alphaV beta3 blocking	Cyclo (RGDfC), avb3 Integrin Binding Cyclic RGD Peptide	Anaspec AS-63785-1	100μg/ml
TLR4 signalling inhibitor	Cli-095 (also TAK 242)	Invivogen tlrl-cli95	1μg/ml

Table 9. Macrophage activators and receptor inhibitors

2.4.4 Isolation of mouse skin adult fibroblasts

Skin samples from underarms of *tnc+/+* and *-/-* mice were prepared as reported by Seluanov et al. [479]. Tissue samples were cut into 1mm pieces and digested in DMEM containing 0.14 Wunsch units/ml Liberase™ TL Research Grade, 10μg/ml DNase I and 1% (v/v) penicillin/streptomycin for 30-90 minutes at 37°C. Enzymatic digestion was blocked by adding DMEM medium with 15% (v/v) FBS and 1% (v/v) penicillin/streptomycin, and samples were centrifuged at 524xg for 5 minutes. Pellets were resuspended and spun as before, for a total of three washes. After the final wash, the pellets were resuspended in complete DMEM culture media, supplemented with 15% FBS (v/v) and 1% penicillin/streptomycin (v/v) and plated on 10 cm cell-culture plates. Skin tissues were maintained in culture until fibroblasts crawled out of fragments and covered the plates. Cells were then harvested and replated at a density of 5×10^5 on new 10 cm plates in EMEM with 10% FBS (v/v) and 1% pen/strep. Fibroblasts were used for the production of cell-derived matrices (CDMs) between passages 1 and 2.

2.4.5 Production of fibroblast-derived matrices

Primary mouse embryonic fibroblasts (MEFs) were kindly gifted by Prof Kim Midwood (Oxford). MEFs and adult skin fibroblasts, isolated as explained in paragraph 2.4.4, were used for the production of cell-derived matrices (CDMs) and were tested for the deposition of ECM and expression of tenascin-C.

Fibroblasts were cultured in 10cm, gelatin-coated tissue culture dishes in complete medium (DMEM supplemented with 10% FBS and 1% penicillin/streptomycin). Cell-culture dishes were coated with 1% sterile gelatin at 37°C for 1 hour. Excess gelatin

was aspirated and gelatin was cross-linked by exposing plates to UV light for 20 minutes. Plates were washed three times with PBS. Gelatin-coated dishes were incubated in serum-free culture media for 30 minutes at 37°C before seeding fibroblasts. The same procedure was followed when seeding cells on coverslips for immunocytochemical analysis or 6-well plates for other experiments.

MEFs and adults skin fibroblasts (FBs) were seeded at high density (2 x 10^6 cells/10cm dish, 3.2 x 10^5 cells/6-well and 1.6 x 10^5 cells/12-well) in order to be at 100% confluence throughout the generation of the ECM. Cells were maintained in culture for ten days in complete media supplemented with 50 µg/ml L-ascorbic acid, replaced every other day.

After ten days, matrices were either decellularised or directly used for characterisation.

Cells were rinsed twice in PBS, and 10cm dishes were incubated with 5 ml of decellularisation buffer for 2-4 minutes at 37°C. The gentle extraction buffer was used to eliminate cells and debris while maintaining an intact ECM. Cell lysis was checked under a light microscope. The extraction buffer was partially aspirated, and matrices were carefully washed three times with PBS with Mg^{2+} and Ca^{2+}. Finally, residual DNA was digested with 10µg/ml DNase I in PBS with Mg^{2+} and Ca^{2+} for 30 minutes at 37°C. Matrices were washed twice with PBS with Mg^{2+} and Ca^{2+}. CDMs were either analysed for their protein content after fixation in 4% PFA/PBS by immunocytochemistry or by Western blot after protein extraction (Section 3.6). After testing the protein composition, CDMs were used as a three-dimensional substrate for seeding of BMDMs, as described below.

2.4.6 Seeding BMDMs on CDMs

Cell-denuded CDMs deposited on 6-well plates were used as a substrate for BMDMs seeding and tenascin-C rescue experiments. Differentiated BMDMs, obtained as described in Section 2.4.1were seeded on de-cellularised CDMs from MEFs or adult mice skin fibroblasts at a density of 2 x 10^6 cells/6-well. Cells were left to rest overnight before LPS treatment and RNA extraction.

2.5. Molecular Biology Techniques

2.5.1 Cytoplasmic and nuclear RNA extraction

Cell fractionation and cytoplasmic and nuclear RNA extraction was conducted as described by Gagnon et al. [480] with minor adjustments to the protocol. BMDMs stimulated with LPS were washed with PBS and directly lysed on 10cm culture dishes in 500µl Hypotonic Lysis Buffer (HLB) supplemented with 100U RNase inhibitor. Cell lysates were lifted with a cell scraper and transferred to a microcentrifuge tube. The mixture was incubated on ice for 10 minutes. After vortexing, lysates were centrifuged at 1000x*g* at 4°C for 3 min, and the supernatants (~80%) were transferred to new chilled tubes. Supernatants contain the cytoplasmic fractions, and the pellets contain the nuclear fractions. 1ml of RNA precipitation solution (RPS) was added to the cytoplasmic fractions, which were then incubated for at least 1 hour at -20°C. In the meantime, nuclear pellets were washed three times with ice-cold HLB and centrifuged at 200x*g* at 4°C for 2 min. After the final wash, pellets were lysed in 500 µl TRIzol® Reagent. After incubation, cytoplasmic fractions were vortexed for 30 seconds and centrifuged at 14000x*g* at 4°C for 15min. The resulting pellets were washed by vortexing in ice-cold 70% ethanol and then centrifuged at 14000x*g* at 4°C for 5 min. Pellets were left to partially air dry and finally lysed in 1 ml TRIzol® Reagent. In order to avoid RNA degradation, pellets and supernatants were kept on ice throughout the whole procedure. Recipes for buffers used for fractionation are reported in Table 3.

2.5.2 RNA immunoprecipitation (RIP)

RAW 264.7 cells were seeded on 10 cm plates and transfected with siRNA for tenascin-C or controls, as described in Section 2.4.2. Macrophages were maintained in culture until 70-80% confluent and were then treated with LPS for 2 hours, as described in Section 2.4.3. After cell stimulation, plates were washed in 10ml ice-cold PBS, lifted with a cell scraper in 500µl PBS and moved to 1.5ml tubes. Cells were pelleted at 2000x*g* for 3 minutes at 4°C and supernatants were removed. The cell pellets were lysed in 500µl of 1X PLB buffer, prepared as described in Table 3. Cell lysis was completed by gentle rotation at 4°C for 30 minutes. Samples were then centrifuged at 14000x*g* for 15 minutes at 4°C to remove cell debris.

Protein-RNA immunocomplexes were immunoprecipitated using the Dynabeads Protein G Immunoprecipitation kit, following manufacturer instruction with minor adjustments for RIP, as recommended by Gagliardi and Matarazzo [481].

After beads preparation, each 500µl sample was pre-cleared by incubation with 10µl of magnetic beads on rotation for 30 minutes at 4°C. This passage allows reduction of aspecific binding of immunocomplexes to beads. In the meantime, for each sample 50µl of Dynabeads were incubated for 30 minutes at room temperature with 4µg of antibody binding to Drosha or IgG isotype control, diluted in 200µl of antibody binding and washing buffer. Antibodies used for RIP are listed in Table 20.

50µl of pre-cleared samples were kept as Input control. The remaining sample volumes were equally divided between Drosha and IgG control antibody-beads complexes (475µl of pre-cleared lysate for each antibody).

To immunoprecipitate RNA-immunocomplexes, sample lysates were incubated with antibody-beads complexes under gentle rotation at 4°C overnight. On the following day, supernatants were transferred to new tubes, kept as unbound controls. Magnetic beads bound to antibody-RNA immunocomplexes were washed three times in 200µl washing buffer. After the final wash, beads were resuspended in 100µl of fresh washing buffer and moved to new 1.5ml tubes. After removal of washing buffer, RNA-immunocomplexes associated with beads were resuspended in 500µl of Trizol. RNA extraction was performed as described below.

2.5.3 Total RNA extraction and quantification

Total and fractionated RNA was extracted from BMDMs using TRIzol® reagent, following manufacturer's instructions. RNA quantification and purity were checked using a NanoDrop® (Thermo Scientific). RNA concentration is calculated through the Modified Beer-Lambert Equation, using sample absorbance at 260nm, and purity is analysed by measurement of the 260/280 and 260/230 ratios, which are indicative of protein and phenolic contaminations, respectively, and are expected to be ~2.0-2.2.

2.5.4 Agarose gel electrophoresis for RNA quality control

RNA samples were run on an agarose gel to test for their integrity. Agarose gel was prepared by dissolving 1% agarose in 1X Tris/Borate/EDTA (TBE) in a mini-autoclave. The molten gel was poured in a clean and RNase free gel tray, after addition of 1:10,000 Ethidium Bromide. 1 µg of RNA sample was mixed with 10 µl of RNA loading dye and heated for 3 minutes at 70°C. Gel was immersed in 0.5X TBE buffer. RNA samples were loaded in the gel alongside with 5 µl of 1Kb Quick load purple DNA

ladder. Gel was run at 80V for ~1-2 hours. RNA bands were visualised on a UV transilluminator.

2.5.5 Quantitative real-time PCR

Relative quantification of mRNA and miRNA expression was measured by quantitative real-time PCR (qPCR) using two different techniques: TaqMan and SYBR green qPCR. TaqMan uses a forward and a reverse primer and a sequence-specific probe. Probes contain a fluorophore (FAM) at their 5'end and a quencher (NFQ) at their 3'end and emit fluorescence once hybridised to a complementary sequence. Taq polymerase extends the cDNA sequence from the probe binding site and degrades the 3'end of the probe, allowing the separation of the fluorophore from the quencher, thus increasing the fluorescent signal that can be measured. SYBR green qPCR uses a forward and a reverse primer and non-specific fluorescent dyes that intercalate into double-stranded DNA, generating a fluorescent signal that can be measured. The specificity of primer amplification can be addressed at the end of the PCR cycles by detection of a single and narrow peak on the dissociation/melting curve. QPCRs were run on a Qiagen Rotor-Gene Q machine and data obtained were analysed with the $\Delta\Delta$Ct method, using hypoxanthine phosphoribosyltransferase 1 (HPRT1) for SYBR-green qPCR and U6 snRNA for TaqMan® qPCR as housekeeping genes.

Reverse Transcription and SYBR-green qPCR

500 ng of RNA was reverse transcribed with QuantiTect Reverse Transcription Kit into cDNA, following manufacturer's instructions. Samples were incubated for 2 minutes at 42°C in genomic DNA elimination buffer. The reverse transcription mix was added

to the samples, which were incubated for 15 minutes at 42°C. The Reverse Transcriptase was then deactivated by incubating the samples for 3 minutes at 95°C.

mRNA expression was quantified by SYBR green qPCR using GoTaq® qPCR Master mix and specific primers (Table 10). Expression of genes of interest was normalised to the housekeeping gene HPRT1.

Gene	*Forward Sequence (5'-3')*	*Reverse Sequence*
HPRT1	*CAGTCCCAGCGTCGTGATTA*	*TGGCCTCCCATCTCCTTCAT*
pre-miR155	*TGCTAATTGTGATAGGGGTTTTG*	*TGCTAACAGGTAGGAGTCAGTCA*
pri-miR155	*CCCTGCTGGATGAACGTAGA*	*TGTGGGCTTGAAGTTGAGATGT*
pri-miR-155 (unspliced)	*AAGCTGAAGTCTACCTTGCCT*	*CTTCCTGGTTTGCAGCACCT*
TN-C	*ACCATGCTGAGATAGATGTTCCAAA*	*CTTGACAGCAGAAACACCAATCC*
7SRNA1	*ATCGGGTGTCCGCACTAAGTT*	*CAGCACGGGAGTTTTGACCT*
KHSRP	*CAAGAAGCAAGCACAAGTGGC*	*CTGGGGTCTGTCCGTAGTAAGC*
TTP	*CCATCTACGAGAGCCTCCAGTC*	*AAAGGTGCAAAACCAGGGGG*
ZFP346	*GACTCAGATCAGAAGAGCAGCA*	*AAGGCTGCCCCCTTAGT*
ZFP385A	*GTAGCCCCTCGTCCAGTTTC*	*CCTTGGTTACACCCTGTCCC*
NRP1	*TACTGGGCTGTGAAGTGGAAG*	*TGTCGGGAACTCTGATTGGATG*
NRP2	*TGACTGGACAGACTCAAAGCC*	*CACCCAACCACAGGTCTCTT*

Table 10. SYBR green primer sequences

cDNA was diluted 1:3 with nuclease-free water, and the PCR reaction was prepared as described in the table below.

Component	Volume
GoTaq® qPCR Master Mix, 2X	5.0 µl
0,4 µM Forward Primer	0.4 µl
0,4 µM Reverse Primer	0.4 µl
cDNA	3.0 µl
Nuclease-free water	1.2 µl
Total	10.0 µl

Table 11. SYBR green qPCR reaction mix.

Settings for qPCR run were programmed as follows:

Step	Temperature	Duration	Cycle
Enzyme activation	95°C	2 minutes	Hold
Denaturation	95°C	5 seconds	x40
Annealing	62°C	30 seconds	
Extension	68°C	15 seconds	
Data acquisition			
Melting			

Table 12. SYBR green qPCR cycles.

SYBR-green primers validation

Primers for SYBR green qPCR were tested for amplification efficiency and target specificity as recommended by the MIQE guidelines [482]. Primers amplification efficiency was estimated for all the primers listed in Table 9. Standard-calibration curves were created by 10-fold serial dilutions of cDNA templates, starting from 25ng to 2.5pg. PCR amplification efficiency was calculated by the Rotor Gene-Q software. The amplification efficiency indicates the rate at which a PCR amplicon is generated. With optimal primer amplification, the amplicon is duplicated in each cycle, resulting in an M value, corresponding to the slope of a standard curve, equal to -3.322. The slope is calculated as the change in Ct divided by the change in log input (e.g. concentration or copy number). The reaction efficiency is calculated from M using the following formula:

$$Reaction\ efficiency = \left[10^{(-\frac{1}{M})}\right] - 1$$

A reaction efficiency equal to 1 corresponds to 100% efficient amplification of the PCR product.

Additionally, melting curves were analysed for the presence of a single and narrow peak in melting curve graphs, indicating specificity of amplification.

Reverse Transcription and TaqMan® qPCR

miR-155 was quantified by qPCR using TaqMan® MicroRNA Assay (mmu-miR-155) in combination with TaqMan® MicroRNA Reverse Transcription kit and TaqMan® Universal PCR Master mix, no AmpErase™ UNG. miRNA expression levels were normalised to the endogenous invariant control small nuclear RNA U6.

miRNA expression was quantified through a two-step quantitative RT-PCR:

1) **REVERSE TRANSCRIPTION (RT)**: cDNA is reverse transcribed from total RNA using specific stem-loop RT primers that contain a highly stable stem-loop structure that lengthens the cDNA;
2) **qPCR AMPLIFICATION**: PCR products are amplified from cDNA samples, using specific TaqMan® primers and probes.

RT master mix was prepared as explained in Table 13, using 200ng of total RNA for each reaction.

Component	Initial Concentration	Volume
dNTPs (with dTTP)	100mM	0.15 µl
Multiscribe™ Reverse Transcriptase	50 U/µl	1.00 µl
Reverse Transcription Buffer	10X	1.50 µl
RNase inhibitor	20 U/µl	0.19 µl
TaqMan® MicroRNA RT Primer	5X	3.0 µl
Total RNA sample	20ng/µl	1.0 µl
Nuclease-free water		8.16 µl
Total		15.0 µl

Table 13. TaqMan® reverse transcription mix.

The protocol used for the RT is described below:

Step	Temperature	Duration (min)
Hold	16°C	30
Hold	42°C	30
Hold	85°C	5
Hold	4°C	∞

Table 14. TaqMan® reverse transcription cycles.

cDNA obtained from RT was diluted 1:3 with nuclease-free water.

The reaction for qPCR amplification was prepared as described below:

Component	Volume
TaqMan® 2X Universal PCR Master Mix (No AmpErase® UNG)	5.0 µl
Nuclease-free water	2.5 µl
TaqMan® MicroRNA Assays 20X	0.5 µl
cDNA	2.0 µl
Total	10.0 µl

Table 15. TaqMan® qPCR reaction mix.

Samples were measured in triplicate with the PCR cycling conditions shown in Table 16.

Step	Temperature	Duration	Cycle
Enzyme activation	95°C	10 minutes	Hold
Denaturation	95°C	15 seconds	
Annealing/Extension	60°C	60 seconds	x40
Data acquisition			

Table 16. TaqMan® qPCR cycles

2.5.6 Northern blot

A non-radioactive Northern blot technique was optimised for the analysis of pre-miR-155 and miR-155. This technique allows the detection of RNA molecules through the hybridisation of specific digoxigenin (DIG)-labelled probes to nucleic acids.

12 µg of total RNA extracted from *tnc+/+* BMDMs ± LPS and 5 µl DIG-labelled Blue Colour Marker for Small RNA were loaded and resolved on a 15% denaturing polyacrylamide gel, containing 7M urea in 1X MOPS buffer. Before loading, RNA samples were denatured at 75°C for 10 minutes and then ran in 1X MOPS running buffer at 15-20 W, until the loading dye reached the bottom of the gel. RNA was then transferred onto Hybond N+ membrane for 1 hour at 4°C at 10 V. The membrane was cross-linked for 1 hour at 60°C in EDC solution, pre-hybridised in UltraHyb ultrasensitive Hybridisation buffer and incubated overnight at 42°C with slow rotation. Before hybridisation, DIG-labelled probes (3'- or 3'- and 5'- end-DIG, Table 17) were denatured at 95°C for 1 minute and a final concentration of 0.5nM was added to the hybridisation buffer. After hybridisation, membrane was washed at 37°C for 30 minutes in 2 x SSC (Saline Sodium Citrate)/0.5 % SDS and rinsed in washing buffer (Table 3). Membrane was incubated in blocking solution and then antibody solution (1:10,000 Anti-Digoxigenin-AP in blocking solution), each incubation performed for 30 minutes at room temperature. Finally, the membrane was washed twice in washing buffer for 15 minutes and incubated in detection buffer (Table 3) for 2-5 minutes. The chemiluminescent substrate for alkaline phosphatase CSPD solution was distributed on the membrane on a development folder, which was then sealed and incubated for 5-15 minutes at 37°C. Finally, chemiluminescence was detected

using the ImageQuant™ LAS 4000 system (GE Heathcare) and images analysed with ImageJ 1.50i.

Northern blot probes	Sequence (5'-3')
U6 DIG PROBE	CACGAATTTGCGTGTCATCCTT
Mmu-miR-155 DIG PROBE	TATCACAATTAGCATTA

Table 17. DIG-labelled DNA probes

2.6. Protein Analysis

2.6.1 Immunocytochemistry

Immunocytochemistry analyses were performed on fibroblast-derived matrices and RAW 264.7 macrophages.

RAW 264.7 cells, untreated or LPS-stimulated (section 2.4.3), and CDMs deposited on 18 mm glass coverslips (section 2.4.5), were fixed in 4% PFA for 15 minutes at 4°C and stored at 4°C in 1X PBS supplemented with 0.2% sodium azide until immunocytochemical analysis was performed.

CDMs were either de-cellularised or non-de-cellularised and were analysed for the presence of the ECM proteins collagen type I, fibronectin and tenascin-C. RAW 264.7 cells were analysed for the extracellular expression of tenascin-C.

Coverslips were placed onto 150 µl drops of blocking solution (Table 3) and incubated overnight at 4°C. Samples were then incubated with primary antibody (Table 18), diluted 1:200 in blocking solution, for 1 hour at room temperature for CDMs or overnight at 4°C for RAW 264.7 cells. Coverslips were washed 4 times in 1X TBS (Table 3) and subsequently incubated with secondary antibody (Table 18), diluted 1:500 in blocking solution, for 1 hour at room temperature in the dark. Samples were washed 4 times in 1X TBS and finally incubated with 3nM DAPI staining or 1µM DRAQ5 dye in blocking solution, for 20 minutes at room temperature in the dark. Coverslips were washed 4 times in 1X TBS and transferred to microscope slides onto 10 µl drops of Prolong Gold antifade agent, sealed and kept in the dark at 4°C before fluorescence microscopy analysis. No primary antibody controls were also included.

Images were captured by fluorescence microscopy with Evos FL Cell Imaging System, Leica DM2000 microscope or Zeiss LSM-510 Confocal System, as indicated in the text.

Primary antibodies and probes	Dilution	Source	Secondary antibody (1:500; Invitrogen)
Anti-fibronectin (F3648)	1:200	Sigma-Aldrich	Anti-Rb Alexa-fluor 546 (A-11012)
Anti-collagen I (NB600 408.1)	1:200	Novusbio	Anti-Rb Alexa-fluor 546 (A-11012)
Anti-collagen III (NB600-594)	1:200	Novusbio	Anti-Rb Alexa-fluor 546 (A-11012)
Anti-tenascin C (T3413)	1:200	Sigma-Aldrich	Anti-Rat Alexa-fluor 488 (A-21210)
DAPI staining	3nM	Invitrogen	
DRAQ5 staining	1µM	Thermo Scientific	

Table 18. Immunocytochemistry antibodies and staining solutions.

2.6.2 Extracellular matrix protein extraction

After de-cellularisation of MEF-derived matrices (2.6.2) protein were extracted in two-steps to obtain the soluble and insoluble matrix components. Each 10cm tissue culture dish was incubated on a rocker for 5 minutes at room temperature with 1ml of modified RIPA buffer before protein extracts collection. Remaining insoluble proteins were extracted from the plates with 1 ml urea lysis buffer and incubated at room temperature on a rocker for 5 minutes. Insoluble proteins were collected by scraping the plates. Both samples were dialysed against 1X PBS (three buffer changes

each with at least 500 times the volume of the sample) at 4°C using Slide-A-Lyzer G2 Dialysis Cassettes (Thermo Scientific) with a 2K molecular weight cut off in order to remove unwanted compounds such as SDS and urea and make the protein samples compatible with downstream applications.

2.6.3 Total, nuclear and cytoplasmic protein extraction

Proteins were extracted from total, cytoplasmic and nuclear fractions of BMDMs after treatment with LPS, as described in 2.4.3

Proteins were extracted from differentiated macrophages seeded on 6-well plates. Cells were washed twice in PBS, and, on their final wash, they were gently detached with a cell-lifter. Cells were spun down at 1500rpm for 5 minutes at 4°C and supernatant was eliminated.

For the total protein lysates, cell pellets were resuspended in ice-cold 50µl total lysis buffer (Table 3). Protein lysates were incubated 15 minutes on ice to complete cell-disruption, before being centrifuged at 12000x*g* at 4°C for 15 minutes. Supernatants containing protein extracts were moved to new 1.5ml tubes for protein quantification and protein expression analysis.

For nuclear and cytoplasmic proteins, two different lysis buffers were used in sequence, as described by Gagnon et al. [480]. The first buffer disrupts only the outer cell membrane, leaving intact the nuclear membrane, while the second is used for nuclear protein extraction. Cells pellets were lysed in 350µl ice-cold Hypotonic Lysis Buffer (HLB, Table 3). After 10 minutes incubation on ice, samples were briefly vortexed and centrifuged at 800x*g* at 4°C for 8 minutes. The supernatant,

corresponding to the cytoplasmic fraction, was transferred to a pre-chilled 1.5ml tube, while the pellet corresponding to the nuclear fraction was kept on ice.

NaCl was added to cytoplasmic protein lysates to a final concentration of 150mM, and mixed by gentle inversion. Nuclei pellet were washed four times with HLB buffer. After each wash, nuclei fraction were spun at 100x*g* at 4°C for 2 min, and supernatants were removed. Nuclei pellet were then lysed in 150µl of ice-cold Nuclear Lysis Buffer (NLB, Table 3) and incubated on ice for 15 minutes, with regular vortexing.

Finally, cytoplasmic and nuclear extracts were centrifuged at 12000x*g* at 4°C for 15 minutes, before moving supernatants into fresh tubes for downstream analysis.

2.6.4 Protein extraction from Trizol organic fractions

After TRIzol® RNA extraction from cytoplasmic and nuclear fractions of BMDMs, proteins were isolated from the phenol-chloroform layer saved from the phase separation step. DNA was precipitated in 100% ethanol and pelleted at 3000x*g* for 5 minutes at 4°C. The supernatant was moved to a fresh tube for protein precipitation in 900 µl of isopropanol. Tubes were inverted several times and incubated at room temperature for at least 30 minutes. Proteins were pelleted at 12000x*g* for 10 minutes at 4°C before discarding supernatants. The protein pellet was washed twice in protein wash solution (Table 3) and once in 95% ethanol. Each wash was followed by 20 minutes incubation at room temperature and 10 minutes centrifugation at 12000x*g* at 4°C. The purified pellet was dissolved in 100µl 2X solubilisation buffer (Table 3) by incubating it at 45°C for 1 hour.

2.6.5 Protein extraction and co-immunoprecipitation (co-IP)

RAW 264.7 cells were seeded on 10 cm plates and maintained in culture until 70-80% confluent. Macrophages were then treated with LPS for one hour. After cell stimulation, plates were washed in 10ml ice-cold PBS, before being scraped with 500µl PBS. Cells were spun at 2000x*g* for 3 minutes at 4°C. After removal of supernatants, macrophages were lysed in 500µl of ice-cold modified RIPA lysis buffer for co-IP (Table 3). Cell lysis was completed by gentle rotation at 4°C for 30 minutes. Samples were centrifuged at 14000x*g* for 15 minutes at 4°C, and supernatants were transferred into fresh tubes.

Co-immunoprecipitation of protein complexes was performed as previously described for RIP (Section 2.5.2), following the Dynabeads Protein G Immunoprecipitation kit instructions. Protein concentration was measured as described below, in Section 2.6.6, and 1mg of protein was used as starting material for each immunoprecipitation. 100µg of pre-cleared protein lysates was kept as input control. Each immuno-complex was pulled-down with 4µg of antibody, as indicated in Table 20.

Finally, after the removal of the washing buffer, samples were eluted in denaturing conditions, in 20µl elution buffer from the kit and 6X SDS Sample Buffer (Table 3). Co-IP immunocomplexes and input samples were immediately run on SDS-gels, as described in Section 2.6.7.

2.6.6 Protein quantification

Protein concentration was determined by Bradford assay using a Bio-Rad protein assay. Standard-calibration curves were created by a five-point 2-fold serial dilutions

of BSA, from 0.50mg/ml to 0.032mg/ml. Both standards and samples were diluted with 1X PBS to a final volume of 10µl and transferred to a 96 well microplate to which 200µl/well of diluted dye reagent was added. The absorbance of protein extracts was measured in triplicates at 595nm with the Biotek Synergy HTX plate reader. Protein concentrations were calculated by plotting standard curves absorbance values against their concentration, which was then fit for linear regression. The equation obtained was used to estimate the unknown protein samples concentration.

2.6.7 Tris-glycine sodium dodecyl sulphate polyacrylamide gel electrophoresis (SDS-PAGE)

Protein extracts from experiments were resolved on SDS-PAGE gels, prepared according to Table 19, together with 5 µl of PAGE-ruler plus pre-stained protein marker. 10µg of total proteins from BMDMs total, cytoplasmic and nuclear fractions were prepared with 6X Loading Buffer. Cell supernatants were prepared by mixing 10% of the volume collected from wells (e.g. 50µl loaded sample for 500µl collected), with 10X loading buffer. 120µl of soluble and insoluble MEF-CDMs and 30µl of decellularised CDMs from MEFs and adult skin fibroblasts were prepared as above with 10X loading buffer. For co-IP, 50-100µg of INPUT extracts was prepared with 6X Loading Buffer and loaded with 30µl of resuspended beads-bound immunocomplexes, prepared as explained in Section 2.6.5

All samples were boiled for 15 minutes at 100°C, before loading. Samples were run in 1 X Tris-glycine running buffer at 10mA/gel for 20 minutes and at 20mA/gel for 3 to 4 hours, using a BIO-RAD PowerPac Universal.

	Separating gel			Stacking gel
Component	**5%**	**8%**	**12%**	**3.9%**
30% acrylamide/0.8% bisacrylamide	1.25 ml	2 ml	3 ml	0.32 ml
4X Tris-Cl/SDS, pH 8.8	1.875 ml	1.875 ml	1.875 ml	-
4X Tris-Cl/SDS, pH 6.8	-	-	-	0.62 ml
H_2O	4.375 ml	3.625 ml	2.625 ml	1.525 ml
10% (w/v) ammonium persulfate (APS)	25 µl	25 µl	25 µl	12.5 µl
TEMED	5 µl	5 µl	5 µl	2.5 µl

Table 19. Composition of solutions and buffers used to prepare separating SDS-PAGE.

2.6.8 Brilliant blue G-colloidal staining

Total MEF-derived matrix proteins were separated on 8% SDS-PAGE gels, fixed for 30 minutes in fixing solution and stained in staining solution for 2 hours (Table 3). After that, the gel was de-stained for 60 seconds in 10% acetic acid in 25% (v/v) methanol and rinsed in 25% methanol, until protein bands were visible above the background. Gels were scanned with ImageQuant™ LAS 4000 system.

2.6.9 Western blot

After SDS-PAGE, proteins were wet-transferred onto nitrocellulose membranes by electroblotting. The membrane was firstly hydrated in water and then equilibrated in ice-cold 1X transfer buffer for 10 minutes with shaking. Protein transfer was carried out using a PowerPac Universal from BIO RAD, at 350 mA for 60-90 minutes in ice-cold 1X transfer buffer. Protein transfer was confirmed by visualisation of the pre-stained protein ladder and by visualisation of protein with Ponceau S staining solution. After de-staining of membranes in distilled H_2O, they were blocked overnight at 4°C on rotation in 5% BSA in PBS and 0.05% tween-20 (PBST) or 5% dry milk/PBST, depending on the antibody used (see Table 20). Membranes were then incubated with primary antibody at 4°C on rotation overnight. On the following day, membranes were washed 3 times in TBS-T and incubated with secondary antibody for 1 hour at room temperature. Membranes were then washed 3 times in TBS-T, before protein detection. Protein bands were visualised using ECL and chemiluminescence was detected on ImageQuant™ LAS 4000 system. After detection, antibodies were stripped from the membranes with Re-blot Plus stripping solution and re-probed with different antibodies.

Recipes for buffers used for Western Blotting are reported in Table 3.

Antibodies	Western Blot dilution	Co-IP/RIP	Source
Alpha Tubulin	1:5000 in 2%milk/TBST (w/v)		Abcam (Ab52866, Rabbit)
Collagen-I	1:5000 in 2%milk/TBST (w/v)		NovusBio (NB600 408.1, Rabbit)
DGCR8	1:1000 in 5%BSA/TBST (w/v)	4µg	Proteintech (25835-1-AP, Rabbit)
Drosha	1:1000 in 5%BSA/TBST (w/v)	4µg	Abcam (Ab12286, Rabbit)
Fibronectin	1:1000 in 10%milk/TBST (w/v)		Sigma (F3648, Rabbit)
Histone H2A	1:1000 in 2%milk/TBST (w/v)		Abcam (Ab18255, Rabbit)
KH-SRP	1:1000 in 2%BSA/TBST (w/v)	4µg	Abcam (Ab150393, Rabbit)
Lamin A/C	1:1000 in 2%milk/TBST (w/v)		NovusBio (NB100-56649SS, Rabbit)
Tenascin-C	1:1000 in 2%BSA/TBST (w/v)		Sigma (T3413, Rat)
TTP	1:1000 in 5%BSA/TBST (w/v)	4µg	Millipore (ABE285, Rabbit)
ZNF346	1:1000 in 5%milk/TBST (w/v)		CaltagMedsystems (PSI-6209, Rabbit)
ZNF385A	1:1000 in 5%milk/TBST (w/v)		Proteintech (26288-1-AP, Rabbit)
Anti-Rat (secondary)	1:5000 in 5%milk/TBST (w/v)		Millipore (AP136P, Goat)
Anti-Rabbit (secondary)	1:5000 in 5%milk/TBST (w/v)		Dako (P0217, Pig)

Table 20 Antibodies for Western Blot and co-IP/RIP

2.7. Statistical analysis

Mean, standard deviation (SD) and standard error of the mean (SEM) were calculated using GraphPad Prism version 7.02 (GraphPad Software, Inc.). Statistical significance was assessed using two-way ANOVA with Sidak's posthoc-test.

Chapter 3

ANALYSIS OF THE EFFECT OF TENASCIN-C ON miR-155 EXPRESSION AND BIOGENESIS

Chapter 3. Analysis of the effect of tenascin-C on miR-155 expression and biogenesis

An effective innate immune response against pathogens is composed of three finely-tuned phases: a proinflammatory phase aimed at eliminating the threat, a reparative phase to resolve inflammation and a final readjustment to homeostasis. Levels of inflammatory regulators, such as cytokines, chemokines and other soluble factors, control the molecular checkpoints leading from one phase to another. Regulation of these factors is managed through an elegantly organised mechanism, including fundamental post-transcriptional regulators, such as miR-155. Thus, maintaining control over miRNA levels at all stages of inflammation is essential to achieve a strong, effective, but self-contained immune response.

When Piccinini *et al*. discovered that tenascin-C could control TNF-α levels through regulation of miR-155 expression [296], a novel mechanism of miRNA regulation through the ECM was uncovered. However, many new questions arose from that discovery.

First of all, is it possible to reproduce the results relative to the regulation of miR-155 expression and can they be confirmed by different techniques? Second, if so, is this mechanism of regulation specific to bacterial activation of TLR4, or do other activated immune receptors share it?

Previously, the involvement of tenascin-C in regulating miR-155 expression was only tested in LPS-activated bone marrow-derived macrophages (BMDMs) by qPCR.

In this chapter, we will extensively analyse the expression of miR-155. First, we will confirm published results by reproducing the experiments in BMDMs and testing miR-155 by qPCR. Then, we will test miR-155 expression by Northern blotting for the first time, consolidating the previous findings even further. Furthermore, with this work, we will introduce an additional macrophage model: RAW 264.7 cells.

Additionally, we will show for the first time that the tenascin-C-miR-155 mechanism of regulation is not limited to LPS-stimulation but involves other macrophage miR-155-inducing stimuli.

Another crucial point to be clarified here is how tenascin-C regulates miR-155 levels. For example, does it regulate miR-155 expression at the transcriptional level, or does it induce miRNA biogenesis at the post-transcriptional level? Systematic dissection and analysis of the specific stages of miR-155 synthesis will identify which event is regulated by tenascin-C.

Preliminary data from Piccinini *et al*. (2012) suggested that transcription of miR-155 is not regulated by tenascin-C [296]. Here, we will use alternative technologies to analyse transcriptional regulation to validate and expand these results. Moreover, we will endeavour in investigating miR-155 processing, revealing a novel role for tenascin-C in miRNA processing.

Specific RNA-binding proteins have been found to associate with the miRNA biogenesis machinery and contribute to the maturation of specific miRNAs [227, 229, 233, 328]. Therefore, expression of tenascin-C could be linked to miR-155 levels through regulation of accessory proteins of the miRNA biogenesis machinery. Here,

analysis of carefully selected candidate proteins will investigate their possible role in tenascin-C-induced regulation of miR-155.

Overall, the work reported in this chapter found that tenascin-C is involved in regulating miR-155 expression following LPS- and TNF-α activation in macrophages. Indeed, lack of tenascin-C negatively regulates miR-155 levels during miRNA biogenesis and after transcription. Specifically, it demonstrated that tenascin-C regulates Drosha-mediated cleavage of pri-miR-155.

3.1. Tenascin-C regulates miR-155 expression in macrophages

3.1.1 Expression of mature miR-155 in BMDMs

Tenascin-C role in regulating miR-155 expression was investigated by measuring miR-155 levels via qPCR and Northern blot in BMDMs from tnc+/+ and tnc-/- mice (Figure 3.1 a and b). Total RNA, including small RNAs, was extracted after treatment with LPS for 1 to 24 hours (0, 1, 2, 4, 8 and 24 hours) for Northern blot and for 4 to 24 hours (0, 4, 8 and 24 hours) for qPCR analyses.

Previously, Piccinini *et al.* measured miR-155 levels solely by qPCR and found tnc+/+ BMDMs expression miR-155 to peak around 35- and 40-folds at 8 and 24 hours from LPS-induction, respectively, while miR-155 levels in tnc-/- BMDM increased maximum to 15- to 20-fold at the same time points [296].

By reproducing the same conditions in our lab, we obtained a stronger miR-155 induction, peaking up to 400-folds in tnc+/+ BMDMs stimulated 24 hours with LPS, but we confirmed a similar trend between tnc+/+ and tnc-/- BMDMs. Indeed, miR-155 levels were found between two to three times lower in tnc-/- BMDMs, than tnc+/+ cells, and this difference was statistically significant at 24 hours after LPS activation.

Additionally, Northern blot analysis of miR-155 levels in BMDMs was first introduced here to confirm that absence of tenascin-C affects miR-155 levels. Similarly to what seen with qPCR, miR-155 levels were reduced in tnc-/- BMDMs, starting from 4 hours after LPS stimulation, compared to tnc+/+ BMDMs. These results allowed us to consolidate the findings that tenascin-C plays a role in regulating miR-155 expression.

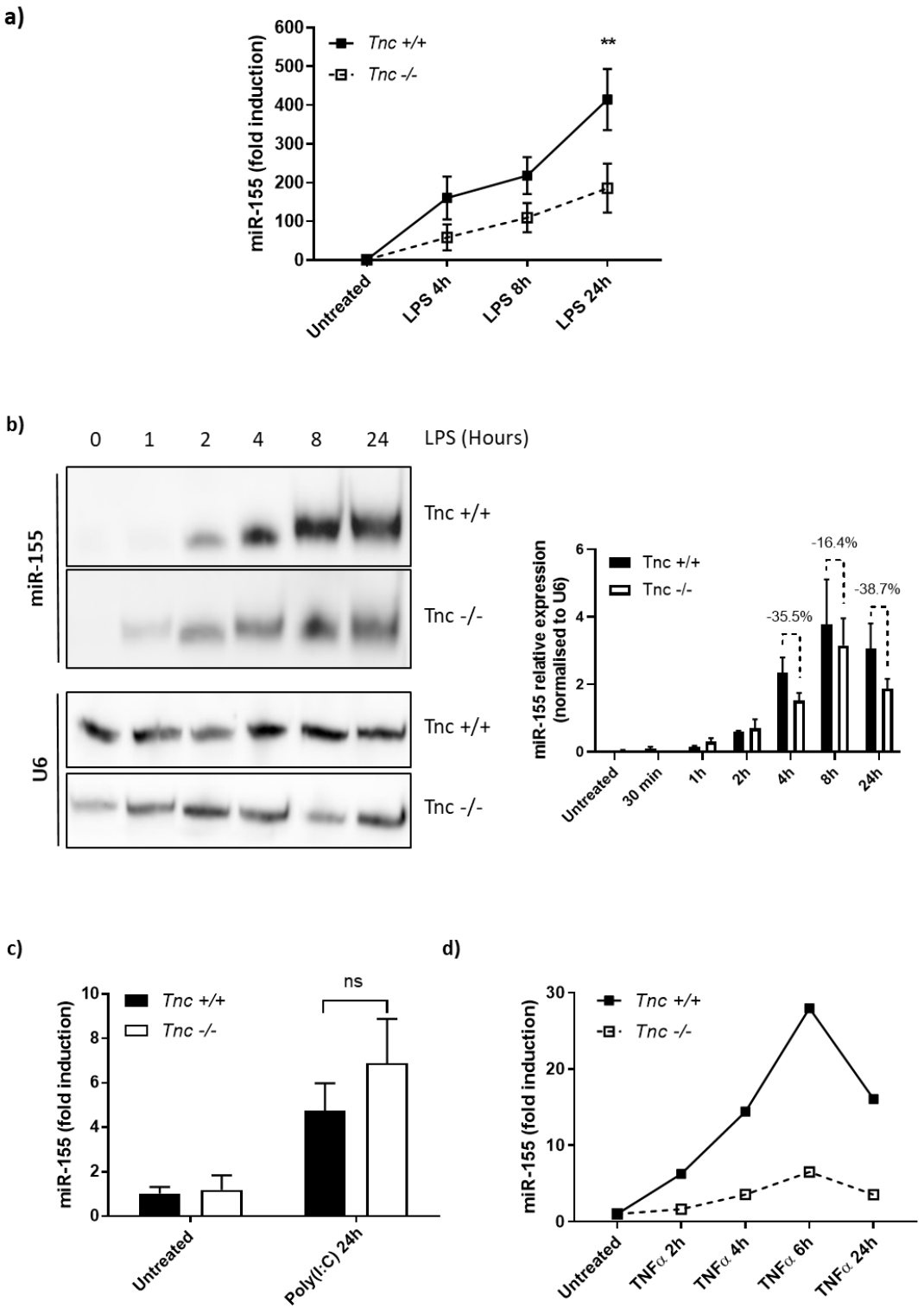


Figure 3.1 Tenascin-C regulates miR-155 expression in BMDMs in response to various signals.
Total RNA was extracted from tnc+/+ and tnc-/- BMDMs after stimulation with 100ng/ml LPS **(a** and **b)**, 20µg/ml Poly(I:C) **(c)** or 10ng/ml recombinant TNF-α **(d)** for the indicated times. **a)** Expression levels of mature miR-155 were measured by qPCR. snU6 was used as endogenous housekeeping gene and untreated samples as calibrator (ΔΔCt method). qPCR data are presented as mean fold induction relative to untreated tnc+/+ and tnc-/- BMDMs ± SEM (n≥5 mice per genotype). **b)** 30 µg of RNA sample was loaded on each well and miR-155 expression of was analysed by Northern blot. U6 small

nuclear RNA (snU6) was used as endogenous control. Data are representative of 6 independent experiments (left). Quantification of mature miR-155 normalised to snU6 by densitometric analysis (right). **c)** Expression levels of mature miR-155 were measured by qPCR as in **(a)**. qPCR data are presented as mean fold induction relative to untreated tnc+/+ and tnc-/- BMDMs ± SEM (n=3 mice per genotype) **d)** Expression levels of mature miR-155 were measured by qPCR as in **(a).** TNF-α data represent a single experiment (n=1 mouse per genotype) and is shown as fold induction relative to untreated tnc+/+ and tnc-/- BMDMs.** = $p<0.01$; two-way Anova with Sidak's post-hoc test.

However, it was still unclear if tenascin-C is specifically acting through LPS-TLR4 signalling to regulate the miR-155 expression or if other exogenous and endogenous stimuli could be involved [123].

TLR3 signalling was activated with synthetic dsRNA Poly(I:C) (Polyinosinic:polycytidylic acid) to simulate virus-induced inflammation, while endogenous cytokine signalling was replicated by activation of TNF receptor with recombinant TNF-α protein. Induction of miR-155 by Poly(I:C) was measured by qPCR after 24 hours of treatment (Figure 3.1 c). Activation of TLR3 promoted miR-155 expression at similar levels in both *tnc+/+* and *tnc-/-* cells. On the other hand, preliminary results from one experiment on *tnc+/+* and *tnc-/-* BMDMs activated with TNF-α showed that miR-155 was expressed at remarkably lower levels in tenascin-C knock-out cells compared to wild-type macrophages. Notably, a difference in miR-155 expression was detected across the entire duration of TNF-α kinetic expression (Figure 3.1 d).

3.1.2 Expression of mature miR-155 in RAW 264.7 cells

Tenascin-C-mediated regulation of miR-155 was characterised for the first time in RAW 264.7 cells, a murine macrophage-like cell line derived from leukaemia. This cell line represented an independent model to confirm data obtained from BMDMs and could reduce the number of animals used for experiments and technique optimisation. RAW 264.7 cells were also chosen for their suitability for transfection, hence used in tenascin-C siRNA knock-down experiments. Cell-specific knock-down of tenascin-C could underline the role of tenascin-C in mature and developed macrophages, excluding possible effects due to defective macrophage development and tissue environment affecting *tnc-/-* mice.

Optimisation of TNC siRNA in RAW 264.7 cells

Optimal conditions for tenascin-C knock-down were preliminarily tested in single experiments in RAW 264.7 cells transfected for 48 and 72 hours. Before RNA extraction, cells were treated with LPS for 24 hours or with recombinant TNF-α for 3, 6 and 24 hours (TNF-α experiment performed by Alessandro Nunziata, an MSc student I trained and task-supervised). Non-targeting siRNA (siCTRL) was used as a reference control.

Tenascin-C protein is hardly detectable in macrophage cell-lysates by western blot but is abundantly found secreted in the conditioned medium upon stimulation with LPS. Levels of secreted tenascin-C from LPS-stimulated and unstimulated RAW 264.7 cells were analysed by western blotting 48 hours after transfection (Figure 3.2 a). Transfection with tenascin-C siRNA showed an evident reduction of tenascin-C (TN-C) protein in LPS stimulated macrophages, compared to siCTRL transfected and non-

transfected cells. Serum-derived tenascin-C was not detectable by western blot in non-stimulated samples.

The efficiency of tenascin-C knock-down was further quantified via qPCR. 48 hours after transfection, tenascin-C mRNA levels were markedly reduced in all siTn-C transfected samples compared to controls. Reduction ranged from 69.2% to 97.8% in untreated or LPS/TNF-α treated RAW 264.7 cells (Figure 3.2 b and c). 72-hour transfection was also tested, confirming tenascin-C mRNA reductions up to 96% in LPS stimulated macrophages (Figure 3.2 d). Although data shows single experiments, transfection efficiency for tenascin-C was tested for different experiments and macrophage treatments, outlining consistent knock-down.

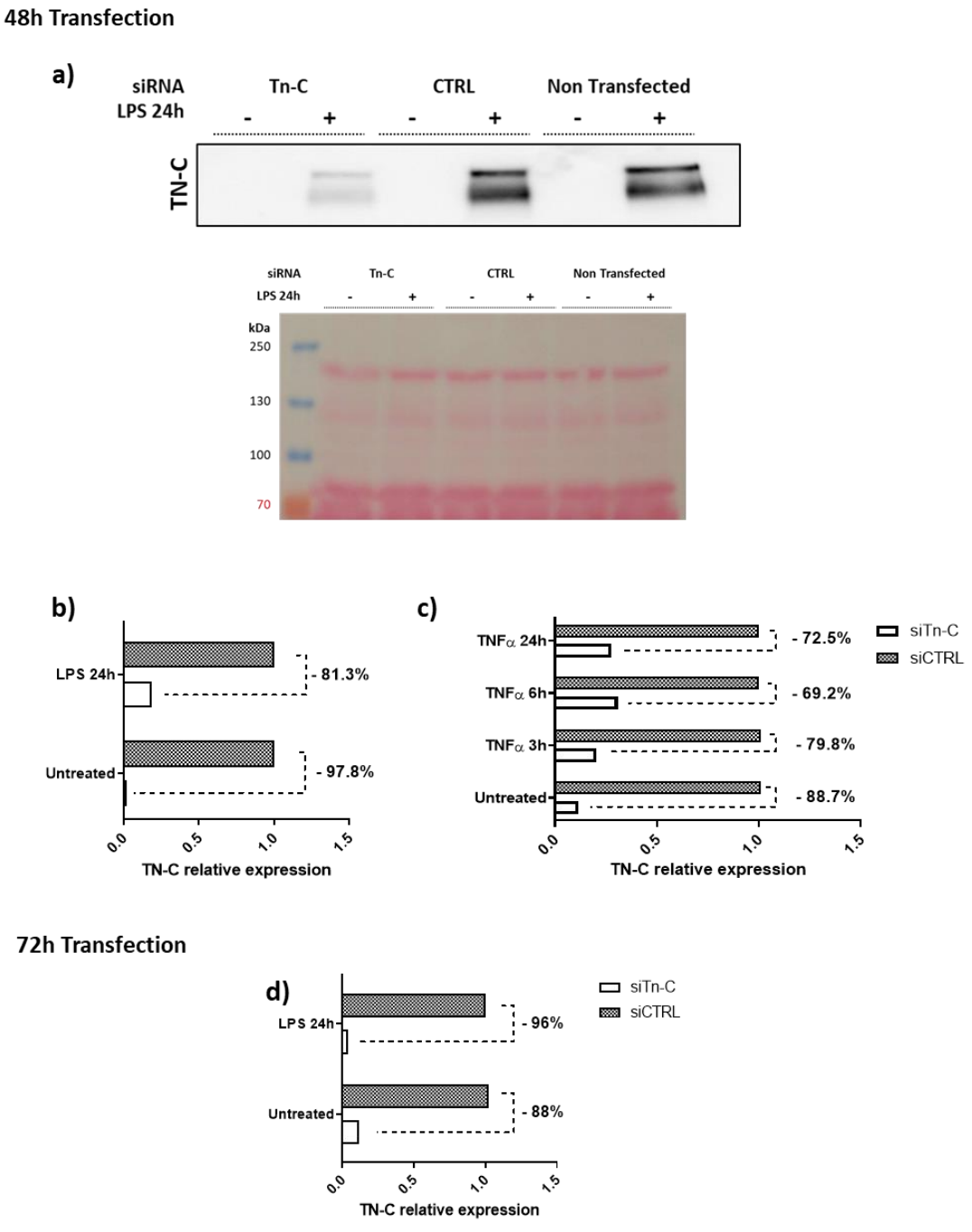


Figure 3.2 Tenascin-C knock-down in RAW 264.7 cells.

RAW 264.7 were transfected for 48 or 72 hours with non-targeting control or Tn-C siRNAs, and stimulated with LPS or TNF-α for the indicated times before collection of cell-supernatants and RNA extraction. **a)** 50µl of supernatants from 48 hours transfected RAW 264.7 cells were tested for expression of TN-C by Western blot analysis. Loading of supernatants was tested by Ponceau S staining before incubating with antibodies (below). **b-d)** Expression levels of Tn-C transcript were measured by qPCR using HPRT1 as endogenous housekeeping gene. Data are from a single experiments and are represented as relative expression of Tn-C, calculated using siCTRL as calibrator (ΔΔCt method).

Expression of miR-155 in siTn-C RAW 264.7 cells

RNA extracts from RAW 264.7 cells tested above for tenascin-C knock-down were analysed for miR-155 expression by qPCR. These preliminary data showed that knock-down of tenascin-C in LPS-activated macrophages for 48 or 72 hours reduced induction of miR-155 levels by 41.5% and 26.2%, respectively, compared to siCTRL cells (Figure 3.3 a).

Additionally, in agreement with previous data on BMDMs, knock-down of tenascin-C in RAW 264.7 macrophages treated with recombinant TNF-α protein showed a pronounced reduction in miR-155 expression compared to control. Lower levels of miR-155 in siTn-C cells could be detected 6 hours after TNFR activation and stayed significantly lower until 24 hours after stimulation (Figure 3.3 b; experiment performed by Alessandro Nunziata).

Importantly, these data represent preliminary results from single experiments. However, taken together with previous analysis on miR-155 expression in BMDMs, they indicate that the presence of tenascin-C is essential for an optimal expression of miR-155 in activated macrophages.

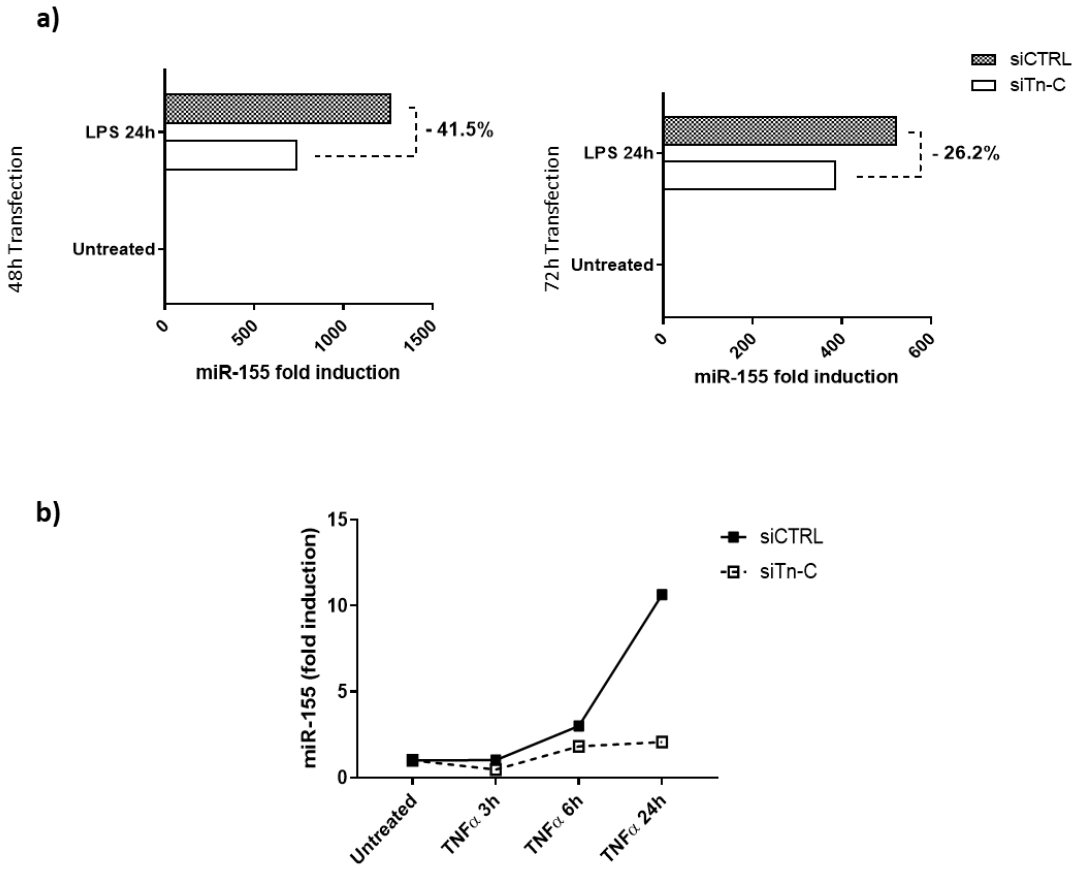


Figure 3.3 Tenascin-C regulates expression of miR-155 in RAW 264.7 upon LPS and TNF-α stimulation.

RAW 264.7 were treated with non-targeting control or Tn-C siRNAs and stimulated with LPS or TNF-α for the indicated times, before RNA extraction. **a-b)** Mature miR-155 measured by qPCR. snU6 was used as endogenous housekeeping gene and untreated samples as calibrator (ΔΔCt method). Data are from a single experiment and are represented as fold induction relative to siCTRL untreated RAW 264.7.

3.2. Analysis of miR-155 transcription

Transcription represents the first level of regulation of miRNA expression. To address if tenascin-C is involved in transcriptional regulation of miR-155, primers for SYBR-green qPCR were designed to amplify total and unspliced transcripts from mouse pri-miR-155 (*Bic* mRNA). Specifically, primers were designed to bind outside the Drosha cleavage site on the pri-miR-155 sequence (Figure 3.4 a). The efficiency of amplification of primers was tested (see Appendix Figure 7.2), and melting curves were checked for target specificity, according to MIQE guidelines [482].

Levels of total and unspliced pri-miR-155 were measured by qPCR from total RNA extracted from *tnc+/+* and *tnc-/-* BMDMs. Cells were stimulated with LPS for 1 to 24 hours (Figure 3.4 b and c). Levels of pri-miR-155 rapidly increased upon LPS activation of BMDMs and stayed high until 4 hours after stimulation. After 8 hours, pri-miR-155 levels started to decrease and returned to basal levels after 24 hours. Pri-miR-155 expression remained similar for both total and unspliced forms in *tnc+/+* and *tnc-/-* BMDMs and was not statistically significant.

To confirm that transcriptional control of miR-155 is not affected by tenascin-C, RNA was extracted from cellular nuclear fractions and expression of total pri-miR-155 was quantified (Figure 3.4 d). Firstly, the quality of nuclear fractionation was analysed by western blotting, qPCR and RNA gel electrophoresis (see Appendix Figure 7.4).

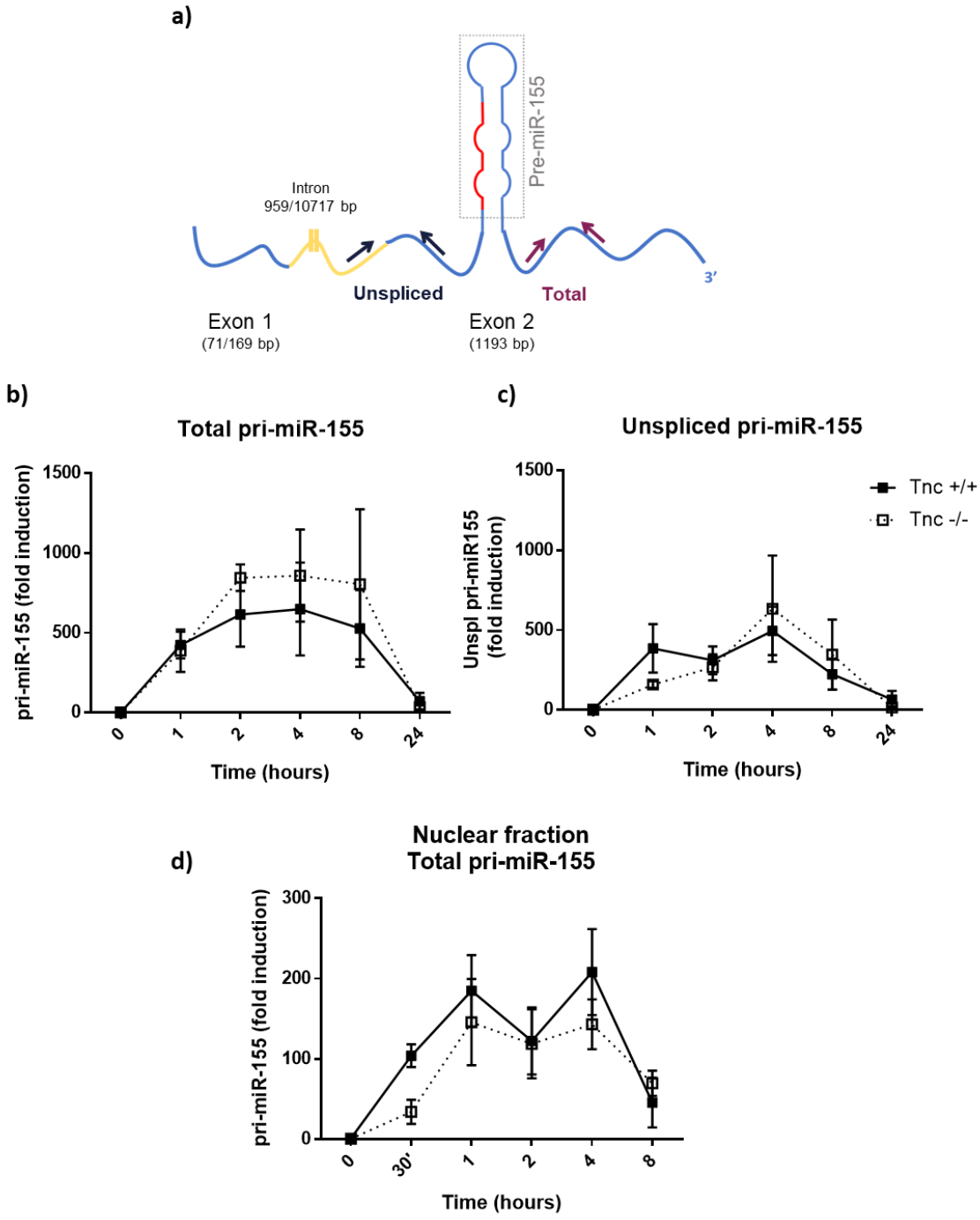


Figure 3.4 Tenascin-C does not affect pri-miR-155 transcription.

a) Schematic representation of primary miR-155 transcript (*BIC*), pre-miR-155 (grey box) and primers binding sites for unspliced pri-miR-155 (blue arrows) and total pri-miR-155 (purple arrows). **b and c)** Total RNA was extracted from *tnc+/+* and *tnc-/-* BMDMs after stimulation with 100 ng/ml of LPS for the indicated durations. Expression levels of total pri-miR-155 **(b)** and unspliced pri-miR-155 **(c)** were measured by qPCR. HPRT1 was used as endogenous housekeeping gene and untreated samples as calibrator (ΔΔCt method). **(d)** RNA was extracted from nuclear fractions of *tnc+/+* and *tnc-/-* BMDMs stimulated with LPS as above. Levels of total pri-miR-155 transcript were measured by qPCR as in **(b)**. Data are presented as mean fold induction relative to untreated *tnc+/+* and *tnc-/-* BMDMs ± SEM; n≥4 mice per genotype; two-way Anova with Sidak's post-hoc test.

Similarly to total RNA, nuclear pri-miR-155 was strongly induced as early as 30 minutes and sharply decreased 8 hours after LPS stimulation. Overall, total pri-miR-155 was found expressed at comparable levels between the two genotypes, except around 30 minutes after LPS-induction, when tnc-/- BMDMs levels resulted lower than tnc+/+. However, this timepoint was only tested in nuclear fractions with no statistically significant differences in *tnc+/+* and *tnc-/-* BMDMs during the whole course of LPS-induction.

Altogether, these data indicated that miR-155 expression is regulated by tenascin-C at the post-transcriptional level.

3.3. Analysis of miR-155 biogenesis

De-regulation of miR-155 levels in *tnc-/-* BMDMs seemed to happen after transcription, during subsequent events of miRNA biogenesis. To confirm this hypothesis, expression levels of pre-miR-155 were analysed by Northern blot of RNA samples from LPS stimulated *tnc+/+* and *tnc-/-* BMDMs. LPS time-course treatment ranged from 1 to 24 hours (0, 1, 2, 4, 8 and 24 hours). Pre-miR-155 was detectable in *tnc+/+* samples starting at 2 hours after LPS stimulation, until 8 hours. Levels decreased at 24 hours (Figure 3.5). Pre-miR-155 in *tnc-/-* BMDMs was expressed at lower levels, compared to *tnc+/+*, and hard to detect.

These results linked tenascin-C to the regulation of miR-155 biogenesis, prompting further investigation on which event of miR-155 biogenesis could be controlled by tenascin-C.

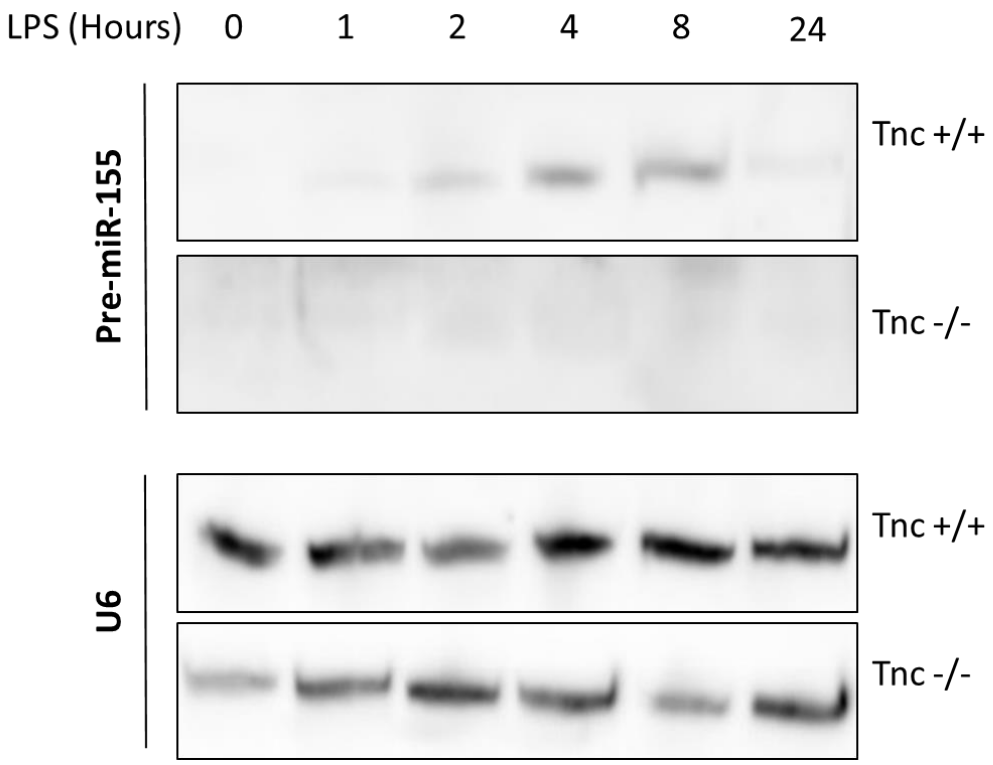


Figure 3.5 Tenascin-C affects pre-miR-155 levels in LPS stimulated BMDMs.
Total RNA was extracted from *tnc+/+* and *tnc-/-* BMDMs untreated or stimulated with LPS for the indicated times. 30 µg of RNA sample was loaded on each well and pre-miR-155 expression was analysed by Northern blot. snU6 was used as endogenous control. Data are representative of 6 independent experiments.

Pre-miR-155 levels were tested by qPCR in nuclear and cytoplasmic fractions from LPS stimulated *tnc+/+* and *tnc-/-* BMDMs. Quality of nuclear and cytoplasmic fractionation was tested and deemed appropriate (see Appendix Figure 7.4).

Pre-miR-155 in nuclear fractions showed patterns of expression similar to pri-miR-155 in total and nuclear fractions (Figure 3.4). Increasing levels of pre-miR-155 peaked at 4 hours after LPS stimulation and decreased after 8 hours (Figure 3.6 a). In nuclei of *tnc+/+* and *tnc-/-* BMDMs, pre-miR-155 was found expressed at similar levels.

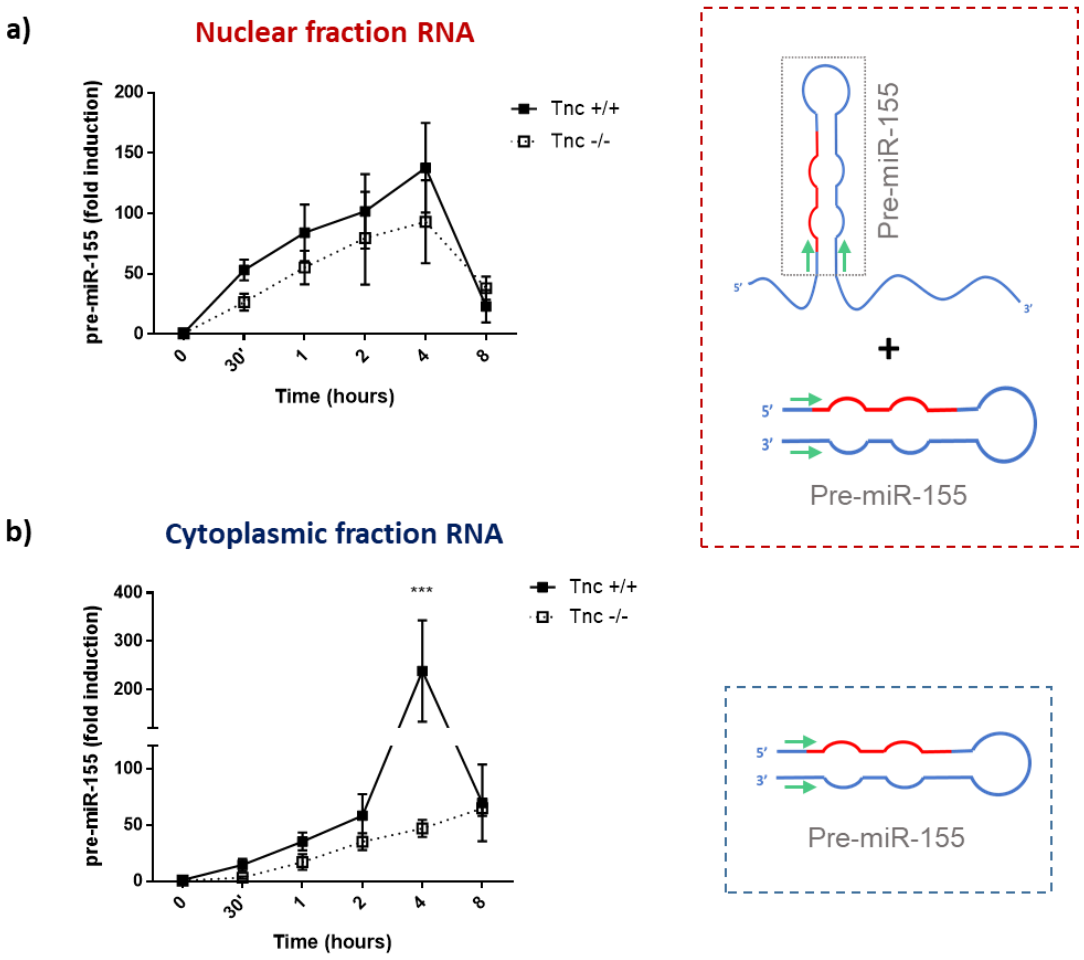


Figure 3.6 Tenascin-C affects miR-155 biogenesis of LPS stimulated BMDMs.

RNA was extracted from nuclear and cytoplasmic fractions of *tnc*+/+ and *tnc*-/- BMDMs untreated or stimulated with 100ng/ml of LPS for the indicated times. **a)** On the left, nuclear pre-miR-155 expression was measured by qPCR. HPRT1 was used as endogenous housekeeping gene for pre-miR-155, and untreated samples were used as calibrator (ΔΔCt method). On the right, schematic representation of pre-miR-155 primers binding sites on nuclear miR-155 transcript (*BIC*) and nuclear Drosha-cleaved pre-miR-155. **b)** On the left, cytoplasmic pre-miR-155 (top) and mature miR-155 (bottom) were measured by qPCR. Analysis was performed as explained above, using HPRT1 as housekeeping gene. On the right, representation of amplified cytoplasmic pre-miR-155 and mature miR-155. Data are represented as mean fold induction relative to untreated *tnc*+/+ and *tnc*-/- BMDMs ± SEM; n≥3 mice per genotype; *** = $p<0.001$; two-way Anova with Sidak's post-hoc test.

However, because primers amplifying pre-miR-155 can also bind to uncleaved pri-miR-155 transcript in the nucleus (as shown in Figure 3.6 a, right panel), it is not possible to distinguish pri-miR-155 from pre-miR-155 with this technique.

To further analyse if tenascin-C could affect pre-miR-155 levels, cytoplasmic fractions from the same BMDMs samples were tested. Cytoplasmic pre-miR-155 levels increased rapidly in both genotypes upon LPS stimulation, but *tnc+/+* BMDMs showed a much stronger and statistically significant induction at 4 hours after LPS treatment, before decreasing at levels similar to *tnc-/-* BMDMs after 8 hours (Figure 3.6 b).

Taken together, these results showed that lack of tenascin-C corresponds to impaired pre-miR-155 levels in the cytoplasm that are likely causing impaired levels of mature miR-155 in *tnc-/-* BMDMs. Nevertheless, these results could not clarify whether tenascin-C is affecting the Microprocessor-dependent processing in the nucleus, the pre-miRNA nuclear-cytoplasmic translocation or multiple events.

To start to address this question, analysis of miR-155 processing in the nucleus was carried out.

3.3.1 Analysis of miR-155 nuclear processing

To understand if Microprocessor cleavage of pri-miR-155 is affected by the lack of tenascin-C, RNA sequences physically interacting with Drosha were analysed by RNA immunoprecipitation (RIP), followed by qPCR.

Optimisation and experiments were carried out using RAW 264.7 cells. LPS-induction of pri-miR-155 and miR-155 expression patterns are similar in RAW 264.7 macrophages and BMDMs [229], and, equally, miR-155 showed to be affected by tenascin-C regulation in both cell types (paragraph 3.1.2).

During technique optimisation, total lysates from RAW 264.7 cells treated for 1 hour with LPS were immunoprecipitated with Drosha antibody or IgG isotype control. RNA purified from immunocomplexes was analysed by qPCR using primers amplifying unspliced pri-miR-155, total pri-miR-155 or pre-miR-155 sequences, as summarised in Figure 3.4 a.

Pri-miR-155 was found to interact with Drosha using total pri-miR-155 primers (Figure 3.7). This was comparable to published results, using similar pri-miR-155 primer sets in KH-SRP RIP from RAW 264.7 cell lysates [229]. Pre-miR-155 did not show enrichment of amplification, in comparison to IgG control. This is expected since once cleaved precursor miRNAs are released by the Microprocessor to continue with processing. Finally, unspliced pri-miR-155 showed inconsistent results, suggesting a lack of interaction with Drosha. Unspliced primers were designed to bind outside of Drosha binding region, on the part of the RNA sequence that is not supposed to interact with Drosha. As a consequence, total pri-miR-155 primers were selected for experimentation.

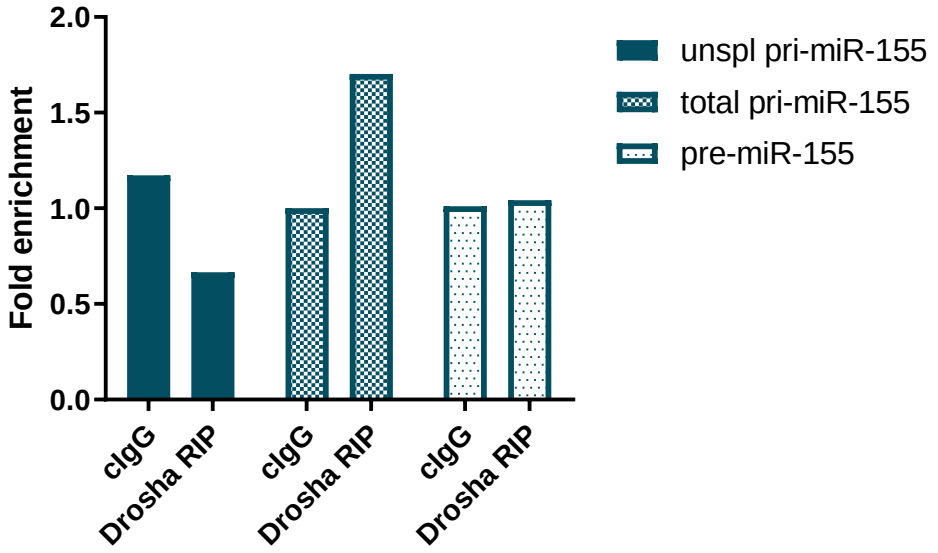


Figure 3.7 Drosha interacts with total pri-miR-155 during biogenesis.
Total cell extracts from RAW 264.7 cells stimulated with 100ng/ml LPS for 1 hour were immunoprecipitated with anti-Drosha antibody or IgG control. Enrichment for unspliced or total primary and precursor miR-155 was analysed by qPCR. Data are from a single experiment and are represented as fold enrichment relative to IgG control.

RAW 264.7 cells were transfected with Tn-C or CTRL siRNAs to analyse if tenascin-C affects pri-miR-155 interaction with Microprocessor catalytic component Drosha. After siRNA knock-down, RAW 264.7 cells were treated with LPS for 2 hours instead of 1 hour. This decision was taken after considering miR-155 kinetics from previous experiments, indicating a stronger induction at later timepoints and better aligned with the literature [229]. Total cell lysates were immunoprecipitated with Drosha antibody or IgG isotype control before RNA extraction and purification. Pri-miR-155 interaction with Drosha was analysed as described by Gagliardi and Matarazzo [481]. IP values were initially normalised based on the percentage of the input used for the IP (10%) to account for differences in sample preparation. Results are presented as relative quantifications, where total pri-miR-155 levels are either reported in comparison to the initial input amount (Figure 3.8 a) or as fold enrichment (Figure 3.8

b), where the adjusted Drosha RIP fractions are further normalised to the background or negative control (cIgG RIP).

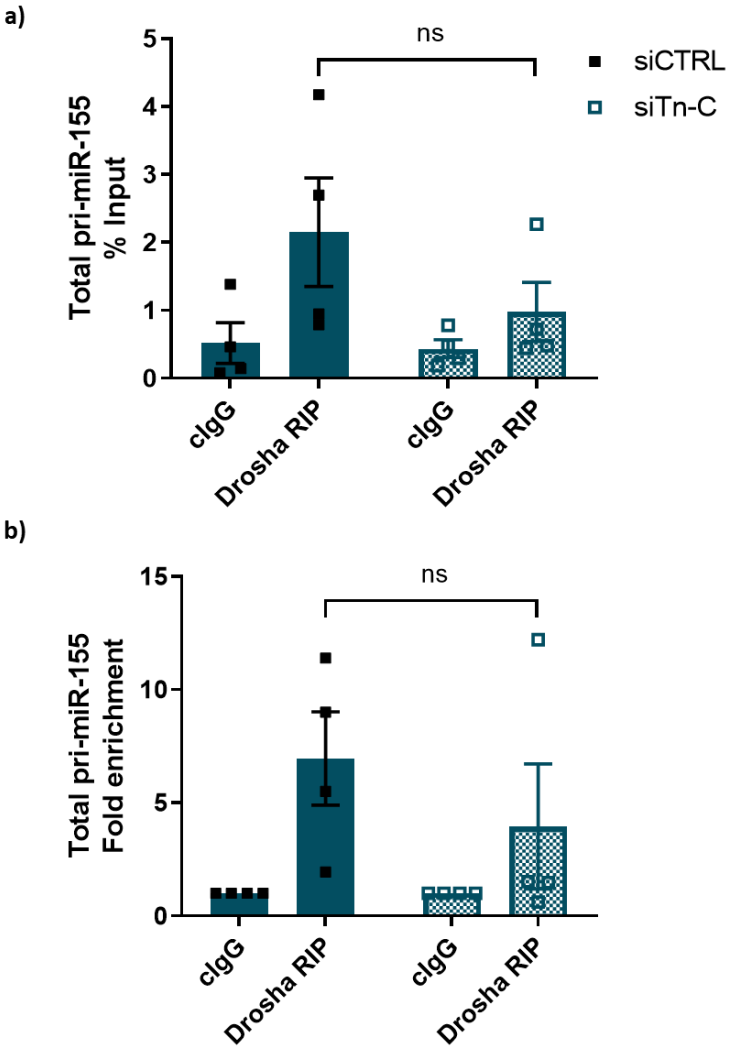


Figure 3.8 Tenascin-C affects Drosha interaction with miR-155 during biogenesis.

RAW 264.7 cells were treated with non-target control or Tn-C siRNAs for 48 hours and stimulated with LPS for 2 hours before immunoprecipitation with anti-Drosha antibody or IgG control. **a)** Percentage of pri-miR-155 in comparison with the input was analysed by qPCR. Data from 4 independent experiments are represented as mean % of input, calculated on normalised RIP Δct ± SEM. **b)** Enrichment in total pri-miR-155 was analysed by qPCR. Data from 4 independent experiments are represented as mean fold enrichment relative to IgG control ± SEM. Two-way Anova with Sidak's post-hoc test.

Comparison of Drosha immunoprecipitated siTn-C and siCTRL samples showed a clear trend, possibly indicating a more stable interaction between pri-miR-155 and Drosha when tenascin-C is expressed (siCTRL), compared to macrophages where tenascin-C is knocked-down (siTn-C) (Figure 3.8 a and b). Nevertheless, the difference between siTn-C and siCTRL macrophages did not reach significant levels.

These data indicated that tenascin-C regulation of miR-155 expression could operate at the Microprocessor level, affecting pri-miR-155 processing.

Notably, previous microarray analysis indicated that miRNAs are not globally affected by tenascin-C, which seemed to be involved in regulating only specific miRNA subsets [296]. Therefore, accessory protein(s) specifically involved in the regulation of miR-155 may act as intermediaries between the signal induced by the extracellular protein tenascin-C and pri-miR-155 processing.

In the following section, candidate RNA binding proteins (RBPs) known to regulate miR-155 expression specifically during its biogenesis will be investigated.

3.4. Tenascin-C regulation of RBPs involved in miR-155 biogenesis (candidate approach)

RBPs interacting with specific miRNA subsets can contribute to miRNA biogenesis by collaborating with or inhibiting the miRNA processing machinery. This mechanism is often driven by targeting RNA features or sequences that allow targeted recognition of miRNA groups [229, 233, 328].

RBPs previously associated with miR-155 regulation were identified by carefully scanning the literature, and candidate RBPs for experimental analysis were also selected considering their potential links with tenascin-C. As a result, four principal candidates could be linked to miR-155 regulation at different stages of biogenesis and had been implicated in immunity. These were: KH-SRP (KH-type splicing regulatory protein), ZNF385A (Zinc Finger Protein 385A), ZNF346 (also known as JAZ) and TTP (tristetraprolin).

KH-SRP was found associated with nuclear Drosha and DGCR8, and cytoplasmic Dicer, contributing to miRNA processing [229]. Additionally, KH-SRP was found to bind to pri-miR-155 and promote the miRNA processing in macrophages activated with LPS [328]. Besides miR-155, KH-SRP was found to regulate other miRNAs, such as miR-15a and b, miR-16, miR-21 and miR-27b [229, 327-329].

Treiber *et al.* performed *in vitro* pull-down experiments and mass-spec for several RBPs and found miR-155 associated with ZNF385A and ZNF346, in addition to miR-19b, miR-9, miR-15a, among others [233]. The role of these RBPs in miRNA biogenesis is yet to be defined. ZNF346 was found to translocate with exportin-5 into the

cytoplasm, possibly linking it to miRNA nuclear export [332]. ZNF385A association with the miRNA biogenesis machinery remains elusive. However, its activation was found to be controlled by the tenascin-C FBG domain, which promoted its phosphorylation in human peripheral blood monocyte-derived macrophages [356].

Tristetraprolin (TTP) is an RBP well known for its role in the degradation of ARE-containing mRNAs [483]. Targets of TTP include inflammatory molecules, such as TNF mRNA [484, 485], IL-6 mRNA [486] and IL-10 mRNA [487]. Its function in miRNA regulation is not yet clear. However, it may promote Dicer processing of miR-145 in an ovarian cancer cell line [333] or inhibit miR-155 processing in cystic fibrosis through an unclear mechanism involving miR-1 [329].

Importantly, TTP and miRNAs seem to be often linked through their post-transcriptional regulatory roles. Indeed, miR-16 and TTP were found to collaborate to destabilise ARE containing mRNAs, including TNF-α mRNA [160]. Alternatively, TTP and miRNAs can compete for the same mRNA sequences. For example, miR-466l was found to extend IL-10 mRNA half-life by preventing TTP-induced degradation [488]. Additionally, miRNAs such as miR-29a, b and c have been found to target TTP, affecting the expression of inflammatory cytokines in diabetic nephropathy and simian immunodeficiency virus infection [489, 490]. TTP was consequentially included in the analysis for its essential role in inflammation and the possible link to miRNA regulation.

The following section analysed if tenascin-C could be involved in the expression and cellular localisation of the candidate RBPs. Additionally, through co-

immunoprecipitation experiments, we analysed potential interaction between Drosha and KH-SRP, ZNF385A and TTP.

3.4.1 Investigating tenascin-C-mediated regulation of KH-SRP

Levels of KH-SRP mRNA were quantified by qPCR in LPS-stimulated *tnc+/+* and *tnc-/-* BMDMs to verify that KH-SRP expression is not altered in the knock-out mouse. KH-SRP transcript was equally induced in both genotypes up to 8 hours after LPS treatment (Figure 3.9). At 24 hours, KH-SRP mRNA progressively decreased in *tnc-/-* BMDMs, while *tnc+/+* levels remained more stable. However, the difference between the two genotypes was not significant.

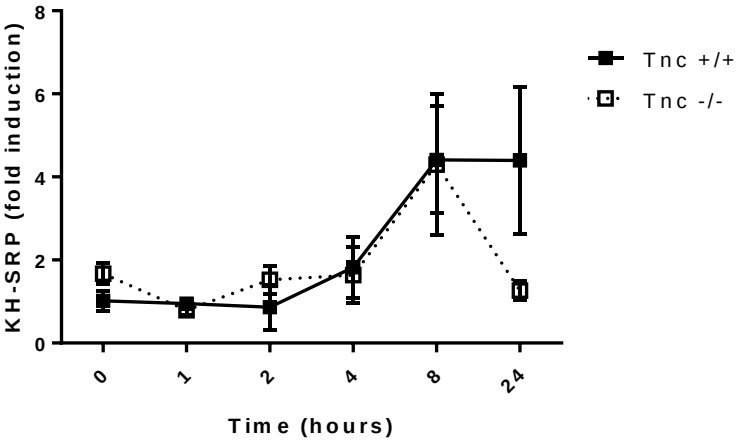


Figure 3.9 Kinetic of KH-SRP mRNA expression in *tnc+/+* and *tnc-/-* BMDMs.
Total RNA was extracted from *tnc+/+* and *tnc-/-* BMDMs untreated or stimulated with 100ng/ml LPS for the indicated duration. Expression levels of KH-SRP transcript were measured by qPCR. HPRT1 was used as housekeeping gene and untreated samples were used as calibrator ($\Delta\Delta$Ct method). Data are represented as mean fold induction relative to untreated *tnc+/+* and *tnc-/-* BMDMs ± SEM; n=3 mice per genotype, measured in triplicate.

Levels of translated protein were measured early in the innate immune response when miR-155 biogenesis was found to be affected by tenascin-C. Total protein lysates from *tnc+/+* and *tnc-/-* BMDMs untreated or stimulated with LPS for 1 and 4 hours were analysed by western blot. KH-SRP protein levels were detected and

quantified by densitometric analysis (Figure 3.10 a and b). Loading control α-tubulin was used for normalisation.

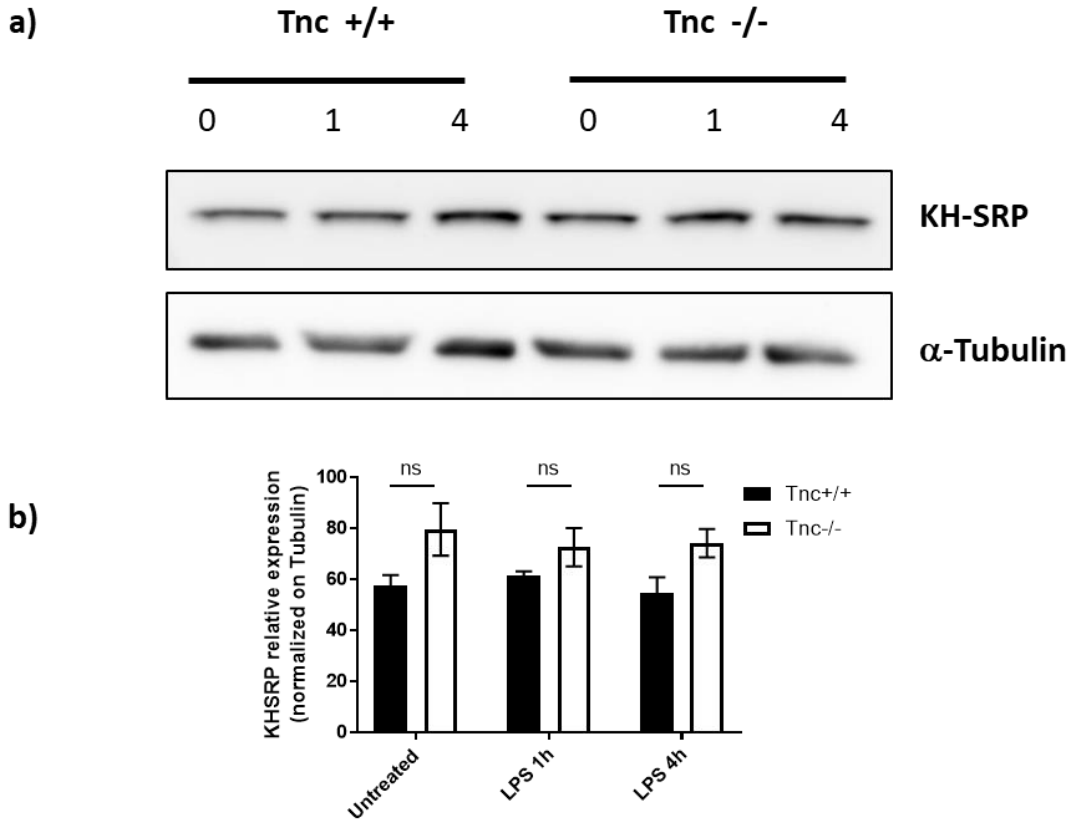


Figure 3.10 KH-SRP protein expression in *tnc+/+* and *tnc-/-* BMDMs.
a) Total protein was extracted from *tnc+/+* and *tnc-/-* BMDMs at the indicated time points after stimulation with LPS and 10 µg of each sample was loaded on each well. α-Tubulin was used as loading control. Representative of 3 biological replicates **b)** Quantification of KH-SRP normalised to α-tubulin by densitometric analysis. Data are means ± SEM of three experiments.

LPS stimulation did not enhance protein levels in BMDMs compared to untreated controls. Moreover, protein expression remained similar within the two genotypes for the entire duration of the treatment. It was then investigated if tenascin-C could influence protein localisation and distribution between cytoplasmic and nuclear fractions of BMDMs. Nuclear and cytoplasmic protein fractions from *tnc+/+* and *tnc-/-* BMDMs, stimulated with LPS as above, were used to detect KH-SRP in the different

locations. α-tubulin was used as loading and quality control for the cytoplasmic fraction, while lamin A/C was used for the nuclear fraction. As seen for total protein fractions (Figure 3.10), levels of KH-SRP did not change in response to LPS in the cytoplasm nor the nucleus. Similarly, lack of tenascin-C did not affect the cellular translocation of KH-SRP in BMDMs (Figure 3.11). Low variability present in nuclear fractions matched variable levels in loading control (lamin A/C) and was considered not noteworthy.

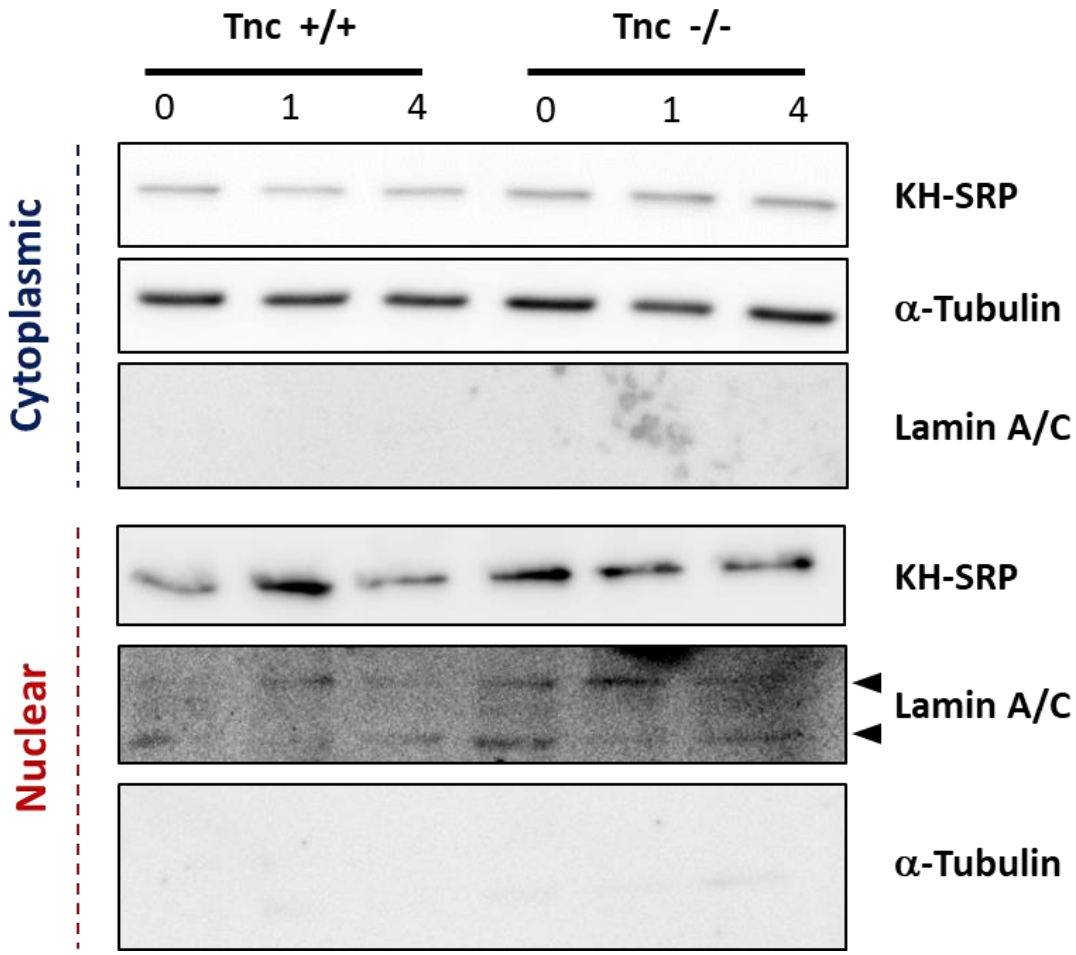


Figure 3.11 KH-SRP nuclear-cytoplasmic distribution in *tnc+/+* and *tnc-/-* BMDMs.
Protein extracted from cytoplasmic and nuclear fractions of *tnc+/+* and *tnc-/-* BMDMs at the indicated time points after stimulation with LPS and 10 µg of each sample was loaded on each well.. α-Tubulin or Lamin A/C were used as loading controls for cytoplasmic and nuclear fractions, respectively. Representative of 2 independent experiments with cells from two mice per genotype in total.

Overall, expression of KH-SRP did not vary with or without tenascin-C, or LPS stimulation. However, post-translational modification events, such as phosphorylation or SUMOylation can affect the activation status of KH-SRP [327, 491]. Drosha and KH-SRP were co-immunoprecipitated (co-IP) in preliminary experiments to begin to analyse the role of KH-SRP in Drosha-mediated cleavage of miR-155 in macrophages, as previously reported by Ruggiero et al. [328]. Total protein from RAW 264.7 cells was extracted after LPS stimulation for 1 hour. Samples were resolved on SDS-page gels after immunoprecipitation with Drosha, KH-SRP or isotype control antibodies. Microprocessor component DGCR8 was confirmed to bind to Drosha, but not to IgG isotype control (Figure 3.12 a). However, KH-SRP could not be detected in Drosha pull-down from three independent experiments (Figure 3.12 b and c), while KH-SRP pull-down from two independent experiments showed unclear results for Drosha (Figure 3.12 b). Therefore, more optimisation is necessary to draw any conclusion on Drosha interaction with KH-SRP in BMDMs.

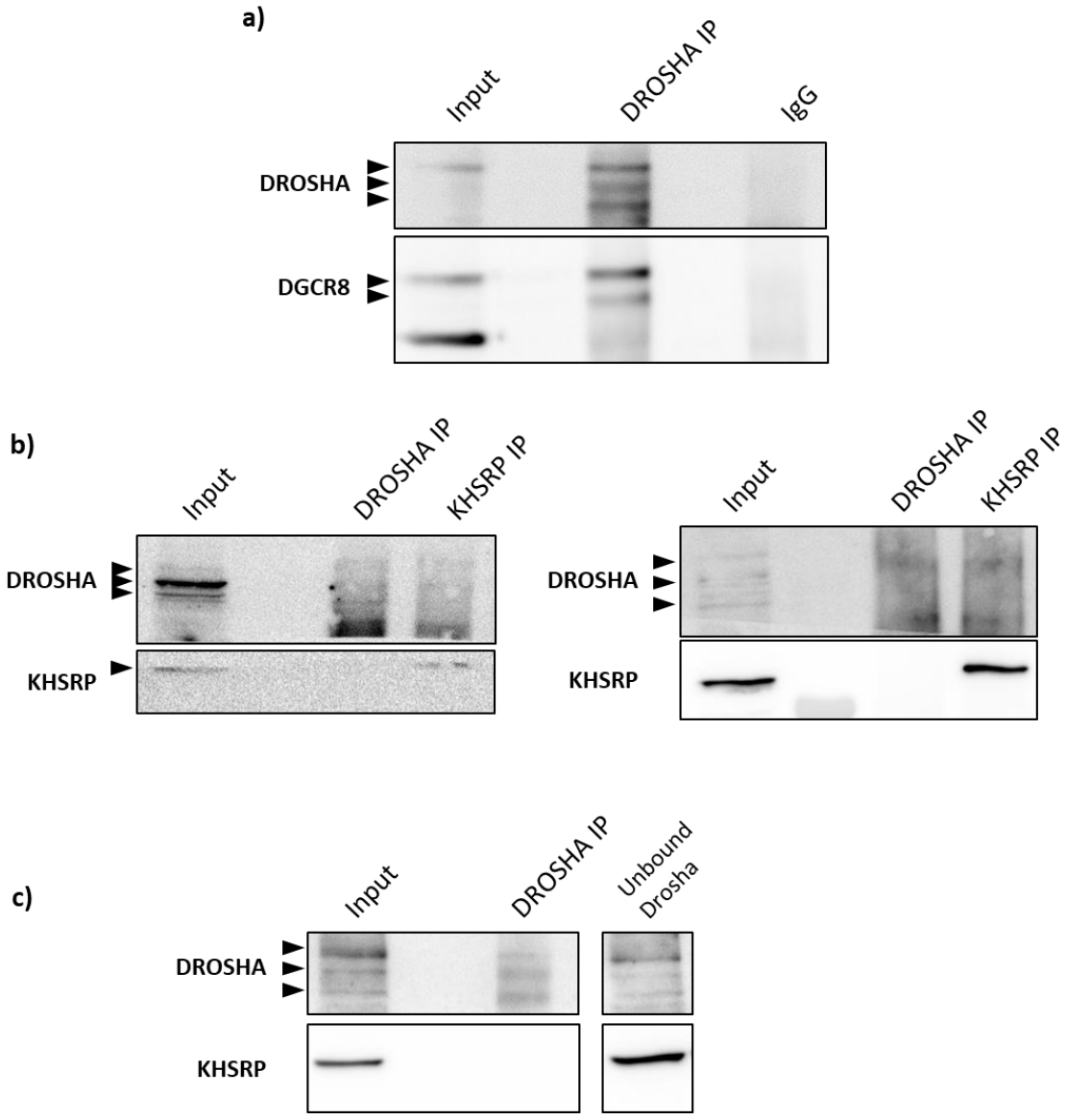


Figure 3.12 Drosha interaction with KH-SRP.

Total cell extracts from RAW 264.7 cells stimulated with 100ng/ml LPS for 1 hour were immunoprecipitated with anti-Drosha, anti-KH-SRP or IgG isotype control. Expression analysis of Drosha, DGCR8 and KH-SRP were analysed by Western blot. **a)** Drosha and IgG control IP samples were tested for Drosha and DGCR8 expression. **b)** Drosha and KH-SRP IP samples were tested for Drosha and KH-SRP expression. **c)** Drosha IP and unbound Drosha IP samples were tested for Drosha and KH-SRP expression. 100 µg input samples and 30µl of IP samples were loaded on each well. Data represents single independent experiments.

3.4.2 Investigating tenascin-C-mediated regulation of ZNF-385A

Treiber et al. [233] were the first to report a link between ZNF-385Aand miRNA biogenesis. However, Piccinini *et al*. (2016) previously found that phosphorylated ZNF-385A is enriched in human macrophages stimulated with tenascin-C. ZNF-385A expression in relation to tenascin-C and LPS stimulation was therefore investigated, beginning with qPCR analysis of ZNF-385A transcript.

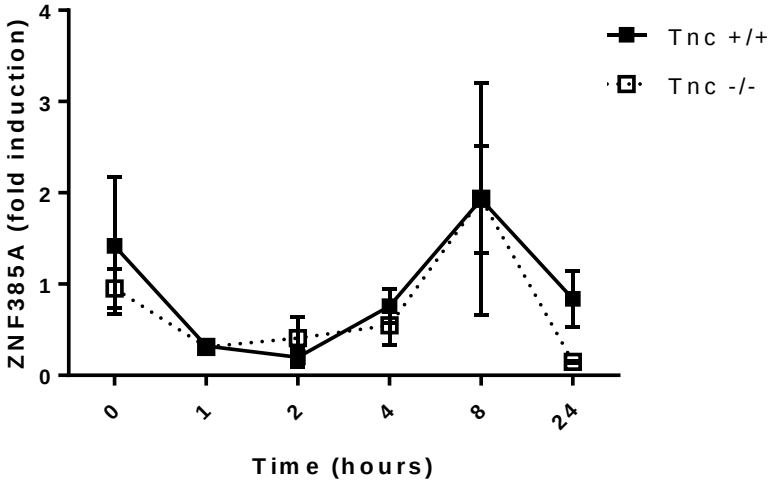


Figure 3.13 ZNF-385A mRNA expression in *tnc+/+* and *tnc-/-* BMDMs.
Total RNA was extracted from *tnc*+/+ and *tnc*-/- BMDMs untreated or stimulated with 100ng/ml LPS for the indicated duration. Expression levels of ZNF-385A transcript were measured by qPCR. HPRT1 was used as housekeeping gene and untreated samples were used as calibrator ($\Delta\Delta$Ct method). Data are represented as mean fold induction relative to untreated *tnc*+/+ and *tnc*-/- BMDMs ± SEM; n=3 mice per genotype, measured in triplicate.

BMDMs from *tnc+/+* and *tnc-/-* mice were stimulated with LPS for a time-course ranging from 1 to 24 hours. Levels of ZNF-385A mRNA showed an initial decrease up to 4 hours after LPS-induction (Figure 3.13). At 8 hours after LPS treatment, ZNF-385A mRNA was partially induced and returned to lower levels at 24 hours. Overall, both *tnc+/+* and tnc-/- BMDMs showed similar patterns of ZNF-385A expression.

In parallel, ZNF-385A protein levels were analysed by western blot in total or cytoplasmic and nuclear protein fractions from *tnc+/+* and *tnc-/-* BMDMs stimulated with LPS for 1 and 4 hours (Figure 3.14 and Figure 3.15).

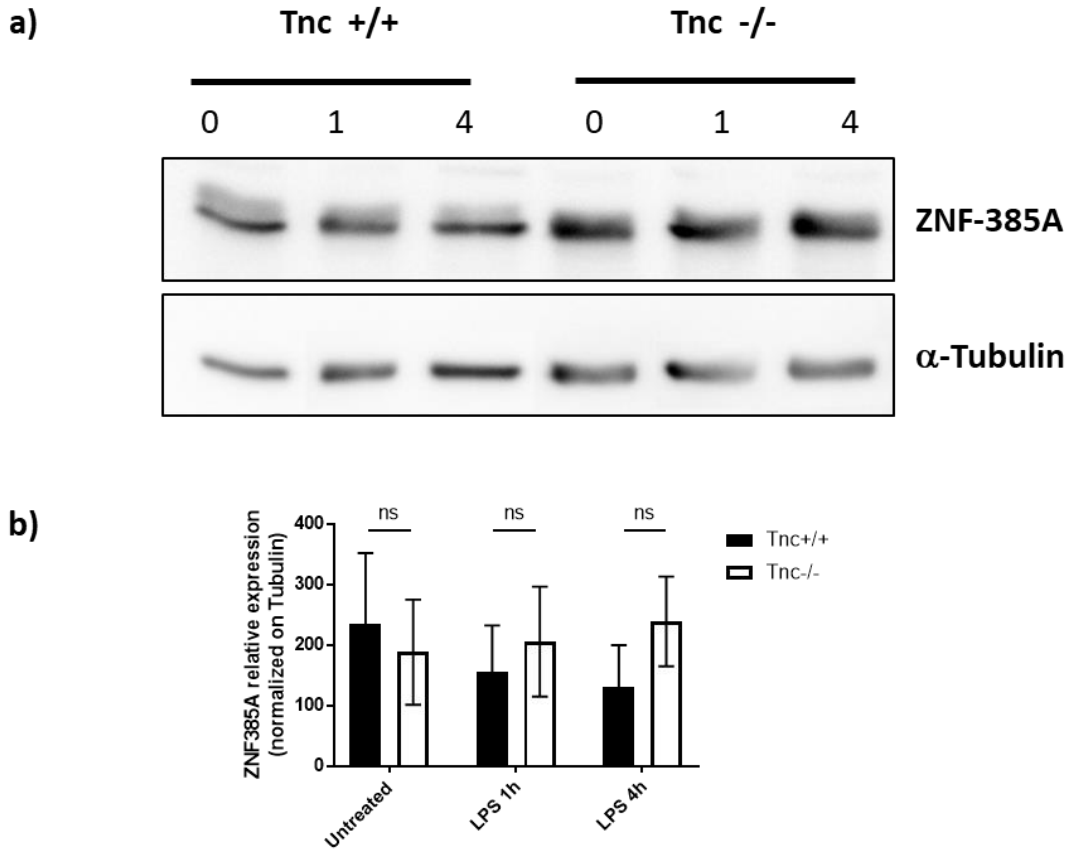


Figure 3.14 ZNF385A protein expression in *tnc+/+* and *tnc-/-* BMDMs.
a) Total protein was extracted from *tnc+/+* and *tnc-/-* BMDMs at the indicated time points after stimulation with LPS and 10 µg of each sample was loaded on each well. α-tubulin was used as loading control. Representative of 3 biological replicates. **b)** Quantification of ZNF-385A normalised to α-tubulin by densitometric analysis. Data are means ± SEM of three experiments.

LPS-activated BMDMs did not show changes in levels of ZNF-385A in total protein extracts from *tnc+/+* and *tnc-/-* cells, and were similar for the two genotypes (Figure 3.14). Quantification of ZNF-385A by densitometric analysis confirmed that depletion of tenascin-C did not affect total protein expression in BMDMs.

Analysis of cytoplasmic and nuclear protein fractions showed similar results, with stable expression and subcellular distribution within all conditions and different genotypes (Figure 3.15).

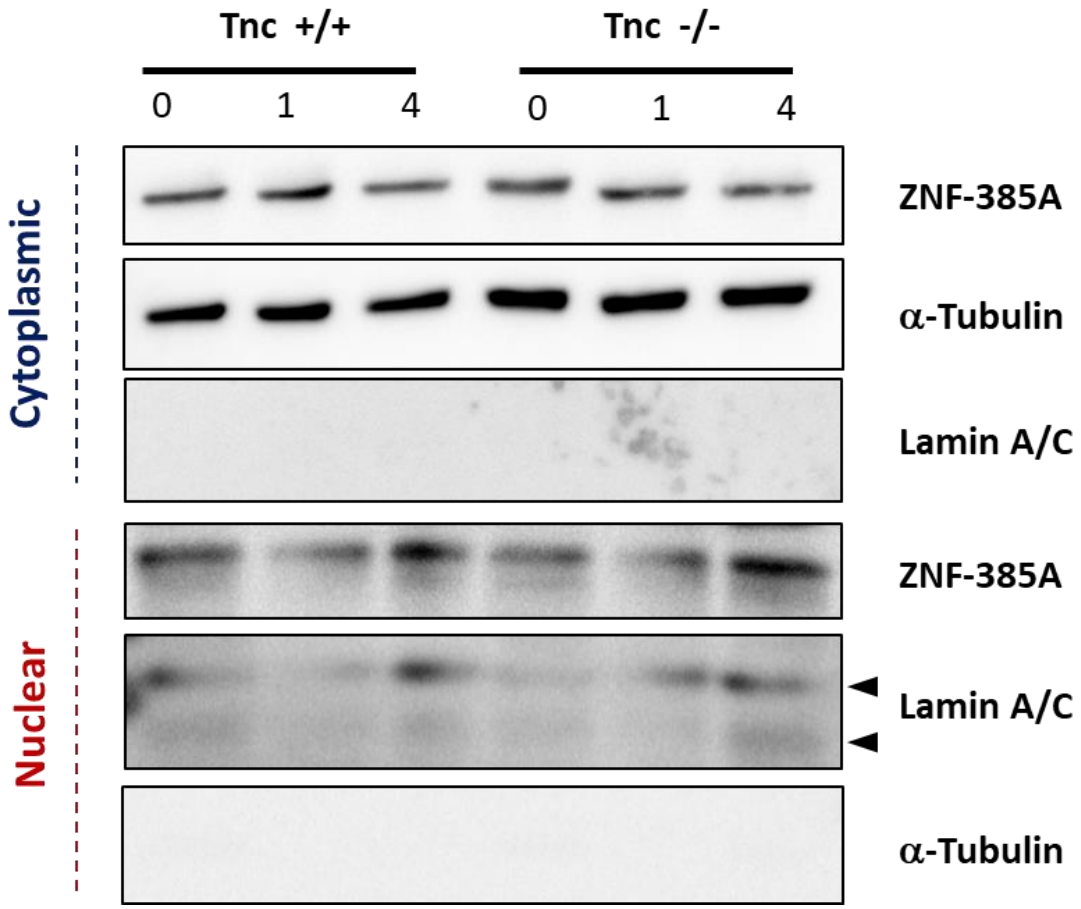


Figure 3.15 ZNF385A nuclear-cytoplasmic distribution in *tnc+/+* and *tnc-/-* BMDMs.
Protein extracted from cytoplasmic and nuclear fractions of *tnc+/+* and *tnc-/-* BMDMs at the indicated time points after stimulation with LPS and 10 µg of each sample was loaded on each well. α-Tubulin or Lamin A/C were used as loading controls for cytoplasmic and nuclear fractions, respectively. Representative of 2 independent experiments.

Expression of ZNF-385A did not seem to be affected by tenascin-C in response to LPS. However, differences in protein activation status could not be excluded, but could

not be tested as anti-phospho-ZNF-385A antibodies were not available when the experiments were conducted.

Preliminary co-immunoprecipitation experiments on RAW 264.7 cells stimulated with LPS for 1 hour were performed to determine if ZNF-385A could interact with Drosha upon LPS stimulation.

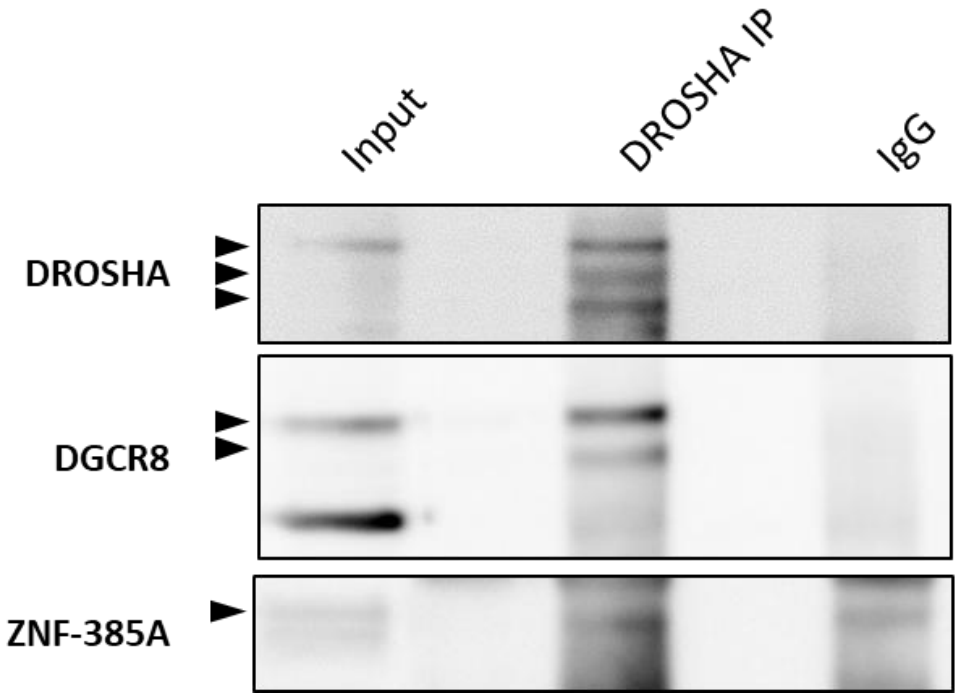


Figure 3.16 Drosha interaction with ZNF-385A.
Total cell extracts from RAW 264.7 cells stimulated with 100ng/ml LPS for 1 hour were immunoprecipitated with anti-Drosha or IgG isotype control. Expression analysis of Drosha, DGCR8 and ZNF-385A were analysed by Western blot. 100 µg input samples and 30µl of IP samples were loaded on each well. Data are representative of two independent experiments.

However, ZNF-385A did not produce specific bands in Drosha precipitates, showing similar bands in the IgG isotype control (Figure 3.16).

3.4.3 Investigating tenascin-C-mediated regulation of ZNF-346

Expression of ZNF-346 was analysed in *tnc+/+* and *tnc-/-* BMDMs during the response to LPS. Analysis of ZNF-346 transcript by qPCR showed that levels of ZNF-346 mRNA remained constant over 24 hours LPS-induction and that there was no difference between macrophages expressing or lacking tenascin-C (Figure 3.17).

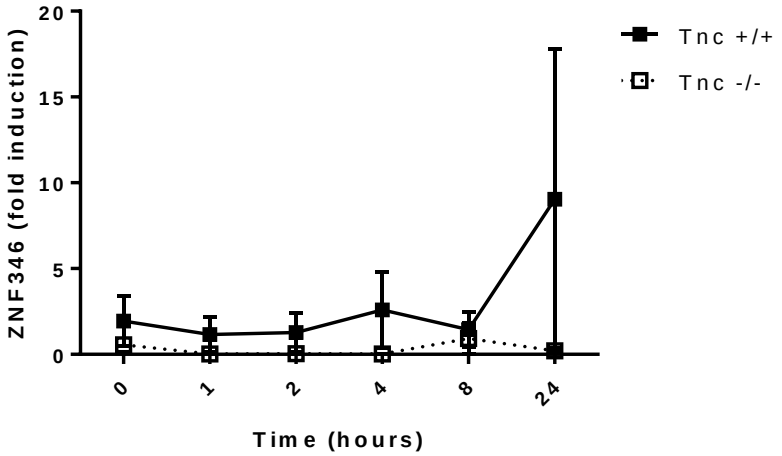


Figure 3.17 ZNF-346 mRNA expression in *tnc+/+* and *tnc-/-* BMDMs.
Total RNA was extracted from *tnc*+/+ and *tnc*-/- BMDMs untreated or stimulated with 100ng/ml LPS for the indicated duration. Expression levels of ZNF-346 transcript were measured by qPCR. HPRT1 was used as housekeeping gene and untreated samples were used as calibrator ($\Delta\Delta$Ct method). Data are represented as mean fold induction relative to untreated *tnc*+/+ and *tnc*-/- BMDMs ± n=3 mice per genotype, measured in triplicate.

Protein expression analysis performed by western blot showed similar results. Total cell lysates from *tnc+/+* and *tnc-/-* BMDMs showed similar ZNF-346 protein levels, which seemed to be only partially induced 4 hours after LPS treatment (Figure 3.18).

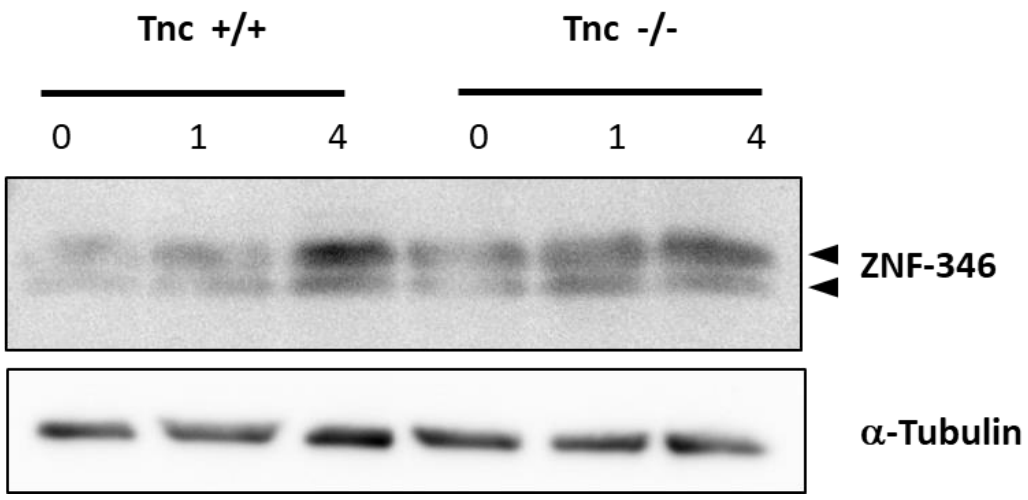


Figure 3.18 ZNF-346 protein expression in *tnc+/+* and *tnc-/-* BMDMs.
Total proteins were extracted from *tnc+/+* and *tnc-/-* BMDMs at the indicated time points after stimulation with LPS and 10 µg of each sample was loaded on each well. α-Tubulin was used as loading control. Representative of 3 biological replicates.

The localisation of ZNF-346 did not seem to change with LPS treatment and was found to be similar in *tnc+/+* and *tnc-/-* cells (Figure 3.19). However, nuclear and cytoplasmic distribution of ZNF-346 isoforms remained challenging to interpret due to the lack of a better antibody for ZNF-346 detection.

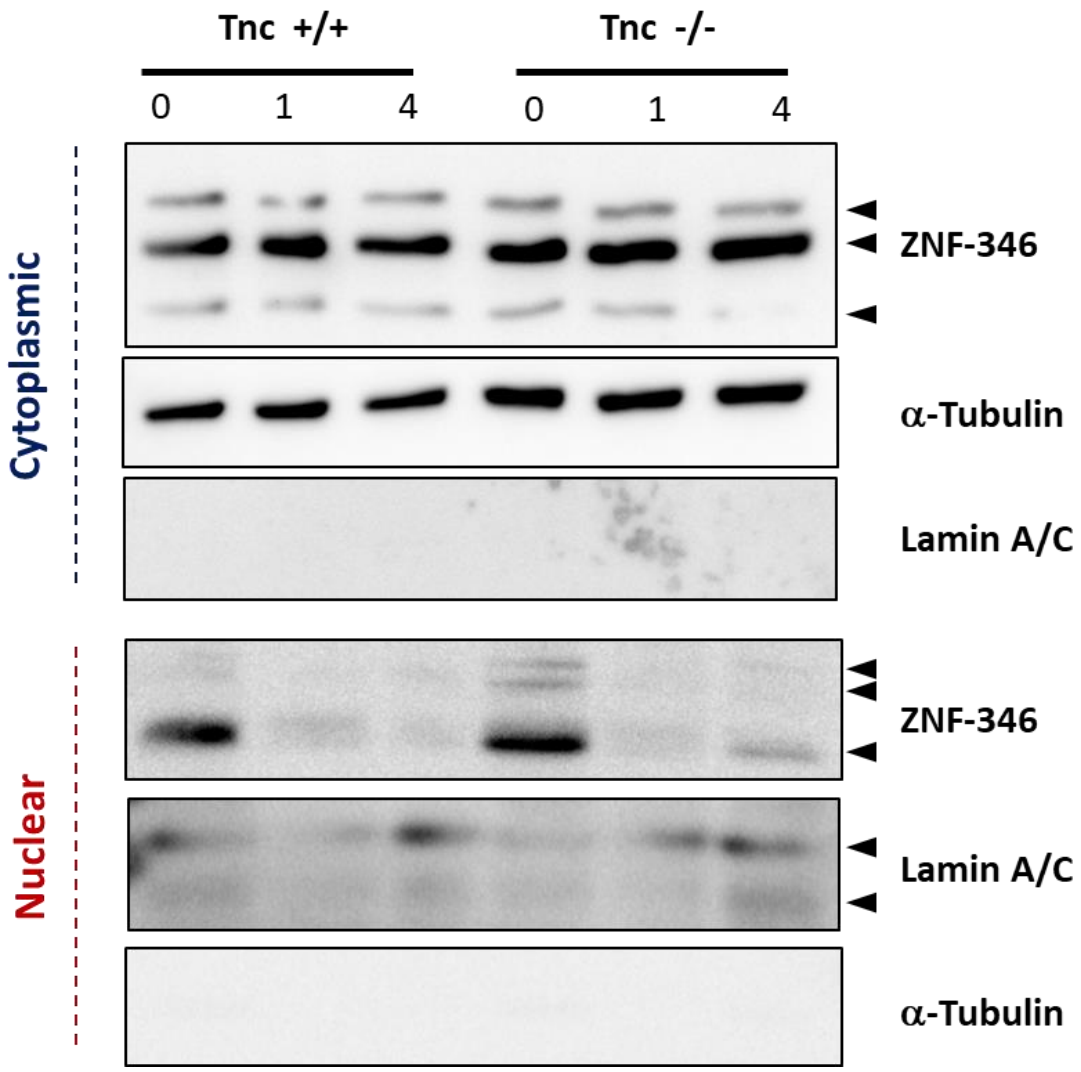


Figure 3.19 ZNF-346 nuclear-cytoplasmic distribution in *tnc+/+* and *tnc-/-* BMDMs.

Protein extracted from cytoplasmic and nuclear fractions of *tnc+/+* and *tnc-/-* BMDMs at the indicated time points after stimulation with LPS and 10 µg of each sample was loaded on each well. α-Tubulin or Lamin A/C were used as loading controls for cytoplasmic and nuclear fractions, respectively. Representative of 2 independent experiments.

3.4.4 Investigating tenascin-C-mediated regulation of TTP

The study of miRNA biogenesis and co-factors involved in regulating miRNA processing is still in its infancy. TTP role in miRNA biogenesis has not been characterised yet. However, its possible role in miR-155 expression, importance in innate immunity and cytokine production, could not exclude it as a candidate for tenascin-C-mediated regulation of the innate immune response [329].

Expression of TTP was measured by qPCR in *tnc+/+* and *tnc-/-* BMDMs to verify if genetic ablation of tenascin-C could affect it. LPS induced TTP transcription in macrophages, peaking at 1 hour after stimulation and gradually decreasing to levels close to unstimulated samples by 24 hours (Figure 3.20). Macrophages lacking tenascin-C showed significantly reduced TTP mRNA levels 1 hour after LPS induction, compared to their wild-type counterparts, and did not recover after 2 and 4 hours. At 8 hours after LPS stimulation, TTP mRNA levels in *tnc+/+* BMDMs decreased to levels similar to *tnc-/-* and stayed low until 24 hours.

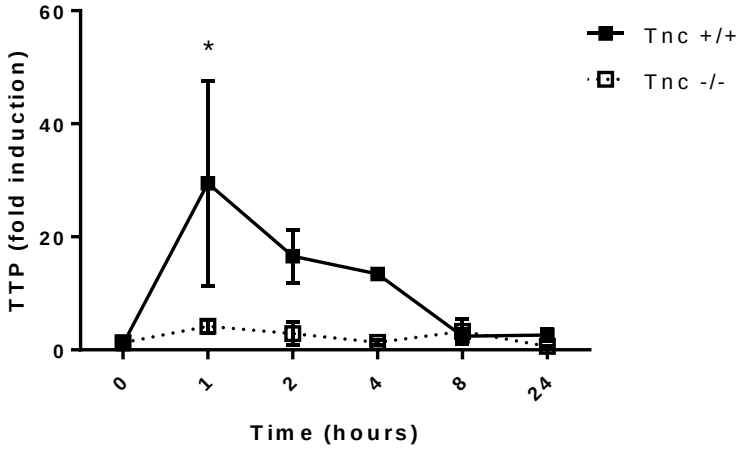


Figure 3.20 TTP mRNA expression in *tnc+/+* and *tnc-/-* BMDMs.
Total RNA was extracted from *tnc*+/+ and *tnc*-/- BMDMs untreated or stimulated with 100ng/ml LPS for the indicated duration. Expression levels of TTP transcript were measured by qPCR. HPRT1 was used as housekeeping gene, and untreated samples were used as calibrator (ΔΔCt method). Data are represented as mean fold induction relative to untreated *tnc*+/+ and *tnc*-/- BMDMs ± SEM; n=3 mice per genotype, measured in triplicate. *=p<0.05; two-way Anova with Sidak's post-hoc test.

To understand if tenascin-C could be involved in the expression of TTP during the early innate immune response, and if this could affect miR-155 expression, TTP protein levels were analysed by western blot.

Total protein extracts from *tnc+/+* and *tnc-/-* BMDMs were resolved on SDS-page gels, after macrophage activation with LPS for 1 and 4 hours (Figure 3.21).

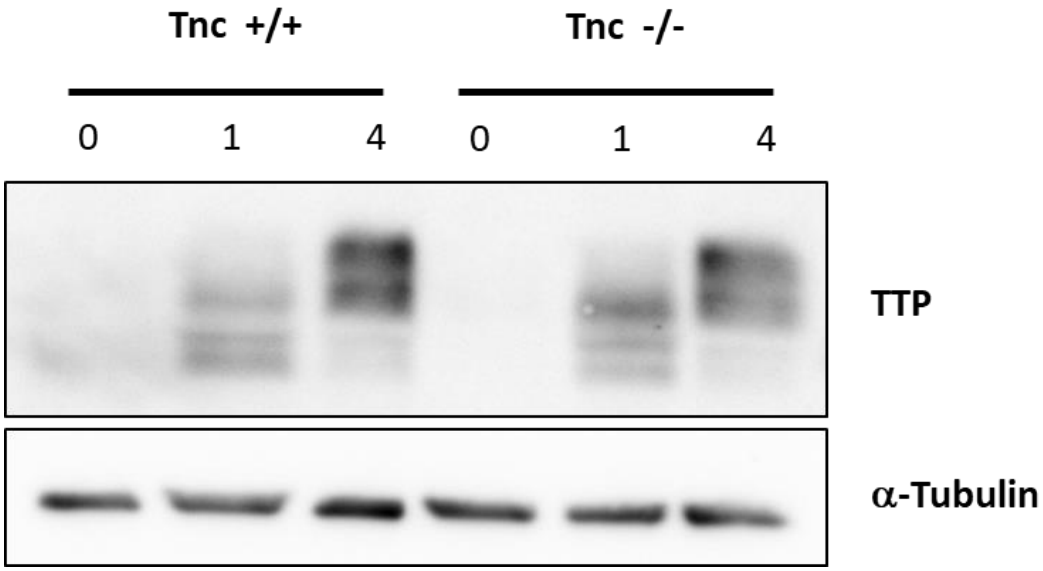


Figure 3.21 TTP protein expression in *tnc+/+* and *tnc-/-* BMDMs.
Total protein was extracted from *tnc+/+* and *tnc-/-* BMDMs at the indicated time points after stimulation with LPS and 10 µg of each sample was loaded on each well. α-Tubulin was used as loading control. Representative of 3 biological replicates.

TTP was not detected at steady-state but was rapidly induced upon LPS treatment from 1 to 4 hours, similarly in *tnc+/+* and *tnc-/-* BMDMs. Quantification by densitometric analysis could not be performed due to partial resolution of multiple protein bands, corresponding to different phosphorylated isoforms.

Cellular localisation of TTP was analysed to understand if tenascin-C could be associated with changes in its translocation. TTP was found to be mainly present in cytoplasmic fractions of BMDMs from *tnc+/+* and *tnc-/-* mice stimulated with LPS. The two genotypes expressed comparable levels of TTP in both cytoplasmic and nuclear fractions (Figure 3.22).

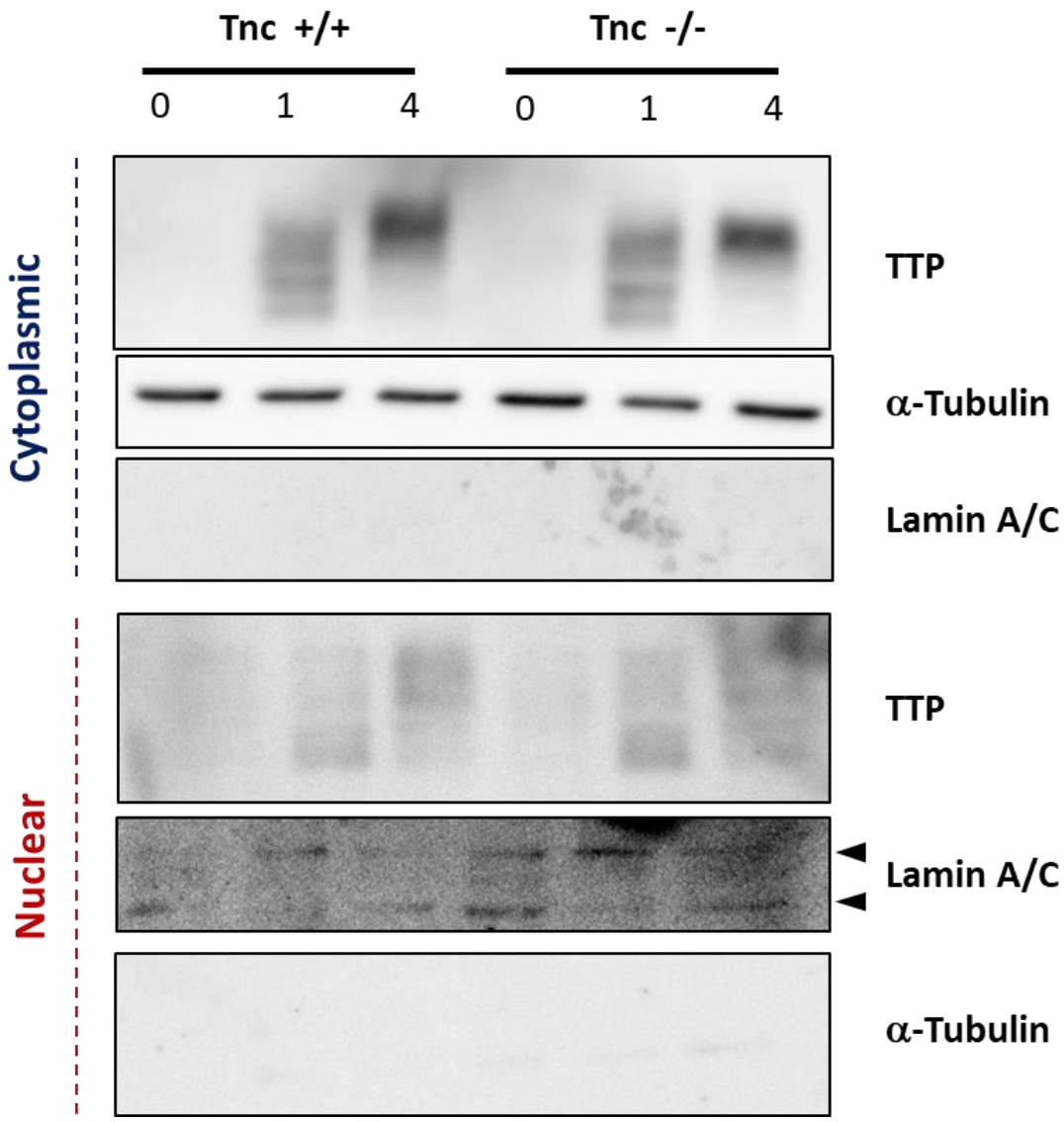


Figure 3.22 TTP nuclear-cytoplasmic distribution in *tnc+/+* and *tnc-/-* BMDMs.
Protein extracted from cytoplasmic and nuclear fractions of *tnc+/+* and *tnc-/-* BMDMs at the indicated time points after stimulation with LPS and 10 μg of each sample was loaded on each well. α-Tubulin or Lamin A/C were used as loading controls for cytoplasm and nuclei, respectively. Representative of 2 independent experiments.

Even if at lower levels, TTP could be detected in BMDMs nuclear fractions, after stimulation with LPS.

Preliminary co-immunoprecipitation experiments were performed on RAW 264.7 macrophages stimulated with LPS for 1 hour to investigate if TTP could associate with the Microprocessor, and be linked to miRNA biogenesis.

Total cell lysates were immunoprecipitated with anti-Drosha, DGCR8, TTP antibodies or IgG isotype control, and interaction between Microprocessor complex components and TTP was analysed by western blot.

Interaction of Drosha and DGCR8 was confirmed in pull-downs of both proteins (Figure 3.23 a). However, the analysis of Drosha and DGCR8 interaction with TTP produced unclear bands, only possibly corresponding to TTP. Immunoprecipitation experiments for both Drosha and TTP were repeated. Drosha IP showed potential bands at the molecular weight corresponding to TTP again. However, immunoprecipitation of TTP did not seem to show interaction with Drosha (Figure 3.23 b).

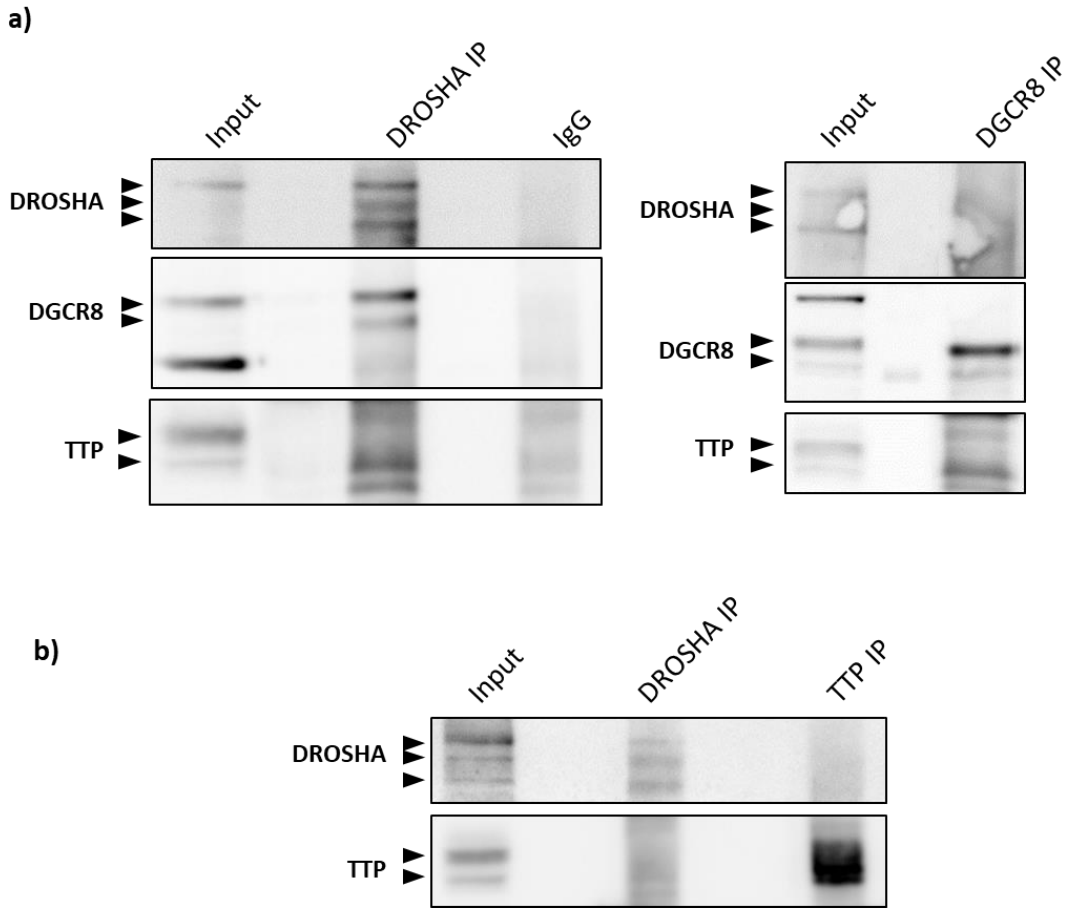


Figure 3.23 Microprocessor interaction with TTP.

Total cell extracts from RAW 264.7 cells stimulated with 100ng/ml LPS for 1 hour were immunoprecipitated with anti-Drosha, anti-DGCR8, anti-TTP antibody or IgG isotype control. Expression analysis of Drosha, DGCR8 and TTP were analysed by Western blot. **a)** Drosha and IgG control (left) and DGCR8 IP samples (right) were tested for Drosha, DGCR8 and TTP expression. **b)** Drosha and TTP IP samples were tested for Drosha and TTP expression. 100 µg input samples and 30µl of IP samples were loaded on each well. Data represent single independent experiments.

3.5. Discussion

During infection, the innate immune response is strictly modulated by a complex network of signalling pathways. Post-transcriptional regulators such as miR-155 play fundamental roles in these pathways by fine-tuning the expression of cytokines and inflammatory molecules, such as TNF-α, SHIP-1 and SOCS-1 [258-261]. The ECM protein tenascin-C, whose expression is rapidly induced by LPS in human and mice [296, 365], was required for optimal TNF-α expression through regulation of miR-155 levels in BMDMs in response to LPS [296].

The expression of tenascin-C was confirmed to be required for miR-155 expression, corroborating work from Piccinini *et al*. [296]. By expanding from the available published literature, miR-155 was analysed with different techniques, cell models and stimuli. For instance, preliminary data confirmed that knock-down of tenascin-C in macrophage cell lines stimulated with LPS leads to a reduction of miR-155 expression, matching what observed in BMDMs from wild type and *tnc-/-* mice. Interestingly, tenascin-C appeared to operate its regulatory function on miR-155 expression only upon an LPS- and TNF-α-mediated activation of macrophages, not upon Poly(I:C) stimulation. Importantly, it was provided evidence that tenascin-C regulates miR-155 biogenesis, potentially during Drosha-mediated processing. Finally, candidate RBPs were characterised and analysed for their expression and potential physical interaction with the Microprocessor.

Several distinct ligands and signalling pathways have been shown to induce miR-155 expression. For the first time, it was shown how ligation of specific receptors located on the plasma membrane, activated during both pathogenic and sterile

inflammation, is linked to tenascin-C-mediated modulation of miR-155 expression. Specifically, activation of TLR4 and TNFR, both present on the plasma membrane, showed significantly reduced induction of miR-155 expression in the absence of tenascin-C. Conversely, activation of the intracellular receptor TLR3 by Poly(I:C) did not show differences in miR-155 expression in BMDMs with or without tenascin-C. Poly(I:C) is a synthetic dsRNA widely used as a model of viral infection. While this at first suggests that tenascin-C may regulate miR-155 expression exclusively during bacterial infection and sterile inflammation, models of infection using intact microbes, rather than purified pathogenic components, should be carried out.

At this stage, how tenascin-C modulates miR-155 expression remained elusive. For the first time, we showed here that transcription of miR-155 is not perturbed by tenascin-C depletion. Distinct primer sets were designed to detect both total and unspliced pri-miR-155 transcripts (*Bic*). In this way, possible changes in splicing events caused by the absence of tenascin-C could be considered.

Nevertheless, *Bic* mRNA levels in *tnc+/+* and *tnc-/-* BMDMs were comparable and confirmed similar in nuclear RNA fractions. These results were in line with the original finding by Piccinini *et al*. (2012), using pre-designed, commercially available TaqMan™ pri-miRNA Assay primers for pri-miR-155 [296]. Importantly, it was not disclosed the exact binding position of TaqMan™ probes on pri-miR-155. By using custom-designed primers, it was possible to determine with greater confidence that tenascin-C post-transcriptionally regulates miR-155.

Levels of pre-miR-155 detected by northern blot were found to be lower in *tnc-/-* BMDMs than *tnc+/+* upon induction with LPS. This result was later confirmed by qPCR

analysis of cytoplasmic RNA fractions from BMDMs, which showed reduced induction of pre-miR-155 in *tnc-/-* macrophages at 4 hours after LPS induction. However, it was not possible to conclude if the tenascin-C-mediated regulation of miR-155 occurs in the nucleus or the cytoplasm due to the simultaneous presence of primary transcript and precursor in the nucleus that cannot be differentiated by qPCR using any primers for pre-miR-155. Based on these results, it was hypothesised that tenascin-C might impact the efficiency of Drosha-mediated cleavage of pri-miR-155 in the nucleus or affect pre-miR-155 export into the cytoplasm.

Therefore, RNA immunoprecipitation (RIP) analysis was performed to analyse and compare levels of pri-miR-155 in complex with Drosha during the LPS response in macrophages, aiming to overcome the limitations of pre-miR-155 quantification by qPCR and test our hypothesis. The technique was initially optimised in LPS-activated RAW 264.7 macrophages, and different sets of primers were tested for the experiment. Tenascin-C was knocked-down in RAW 264.7 cells by siRNAs, and levels of pri-miR-155 in complex with Drosha were measured and compared to those of cells normally expressing tenascin-C.

Lack of tenascin-C was associated with a marked reduction in binding of pri-miR-155 to Drosha in LPS-activated macrophages, potentially explaining why *tnc-/-* BMDMs presented lower levels of pre-miR-155 in the cytoplasm. Although evident, differences in pri-miR-155-Drosha association with and without tenascin-C did not reach significant levels. However, more repeats are necessary to reduce variability caused by the complexity of the experiment and the challenge of maintaining native conditions.

Impaired Microprocessor cleavage of pri-miR-155 in *tnc-/-* BMDMs could be responsible for the differences in miR-155 levels detected in LPS-activated cells. Nevertheless, levels of other mature, LPS-responsive miRNAs such as miR-146a and miR-21 were not affected by tenascin-C in the same way as miR-155 [296]. Primary transcripts of miRNAs identified as affected by tenascin-C by microarray should be analysed in association with Drosha, to investigate if tenascin-C could regulate miRNAs sharing specific characteristics and RBPs binding.

RBPs can promote the biogenesis of specific miRNAs classes, playing accessory roles to the miRNA biogenesis machinery. Therefore, four RBPs, KH-SRP, ZNF385A, ZNF-346 and TTP, were selected from careful literature research for their ability to regulate the expression of miR-155 specifically. The role of tenascin-C in regulating transcription, protein expression, and cellular translocation of the selected RBPs was tested by comparing BMDMs from tenascin-C knock-out and wild-type mice. Additionally, interaction with Drosha and DGCR8 was tested for those proteins localising in the nucleus and for which the antibodies available could produce reliable results.

Surprisingly, TTP mRNA expression was significantly lower in tnc-/- BMDM than *tnc+/+* macrophages during the early LPS response, but KH-SRP, ZNF385A and ZNF-346 did not show any difference in expression between the two genotypes.

LPS induces TTP transcription through an NF-kB dependent mechanism, also activated by TNF-α [492]. Interestingly a similar mechanism of activation is shared by miR-155 [121]. However, what was more striking was that since TTP is considered an anti-inflammatory protein, best known for downregulating TNF-α [484, 485] and IL-6

mRNAs [486], levels of TTP mRNA were expected to be higher in *tnc-/-*, compared to *tnc+/+* BMDMs.

Nevertheless, protein expression and cellular distribution of all four RBPs was found not to change with or without tenascin-C, which was surprisingly also confirmed for TTP. However, TTP has an auto-regulatory negative feedback-loop mechanism, in which TTP promotes its degradation within 45 minutes from LPS activation by binding to AREs on its transcript [493, 494]. Expression of TTP was also shown to be regulated post-transcriptionally by miR-29a in human breast cancer models [495, 496], HEK-293 T cells, and possibly in monocyte-derived macrophages [490]. TTP was also found regulated by miR-29c in podocytes from kidney tissue in hyperglycaemic conditions [489]. Studies on TTP function in miRNA regulation are still at very early stages, and the mechanism of action of TTP is now believed to go further than mRNA decay. Recent studies described TTP as a switch balancing between mRNA decay and translation regulation [497, 498], with TTP found localised in cytoplasmic polysomes [499, 500].

Additionally, cytoplasmic TTP was found associated with Dicer [333] and with KH-SRP to indirectly promote iNOS (inducible nitric oxide) mRNA decay [501, 502]. These examples represent the frequent association of TTP with components of the miRNA processing machinery.

These results indicated that tenascin-C might be not involved in the expression and localisation of KH-SRP, ZNF-385A, ZNF-346 and TTP in BMDMs. However, protein and signalling activation is frequently driven by post-translational modifications such as phosphorylation, which is involved in protein activation and complexing. For

example, the tenascin-C FBG domain can phosphorylate ZNF-385A in human peripheral blood monocyte-derived macrophages [356]. Therefore, it was decided to investigate if KH-SRP, ZNF-385A and TTP could associate with the Microprocessor during miRNA biogenesis. However, ZNF-346 was not included in the analysis due to a lack of high-quality reagents for IP and limited data.

Preliminary co-immunoprecipitation experiments using LPS-stimulated RAW 264.7 macrophages confirmed the interaction between Drosha and DGCR8. However, it was not possible to confirm any interaction between the Microprocessor components and the selected RBPs, often resulting in difficult to interpret or inconclusive results.

Possibly, a weaker interaction between these RBPs and the Microprocessor, compared to DGCR8 and Drosha, will require optimisation of co-immunoprecipitation conditions, such as changes in the lysis buffer composition. Indeed, KH-SRP was previously found to interact with Drosha in HeLa cells [229] and osteosarcoma cell lines [327]. However, other studies did not show a direct interaction between KH-SRP and Microprocessor or Dicer but attributed an effect of KH-SRP on miRNA regulation regardless [328]. Notably, Treiber *et al*. (2017) failed to detect KH-SRP in a miRNA processing context in 13 human cell lines, suggesting possible different experimental conditions compared to previous literature [233].

Nevertheless, TTP involvement with the nuclear Microprocessor and pri-miRNA processing is challenging to justify from the results obtained thus far. Low levels of nuclear TTP were previously detected in endogenous conditions [503], but its role in the nucleus remains elusive. It was suggested that nuclear TTP could be involved in

nuclear deadenylation of ARE-containing mRNAs [504] or act as a transcriptional co-repressor of NF-kB in B cells [505-507]. However, there was no previous indication of binding to Drosha, as the co-IP experiments seem to indicate. Tiedje *et al*. (2016) performed TTP iCLIP experiments, and RNA sequencing in LPS stimulated mouse macrophages and did not identify miR-155 host-gene *Bic* or pre-miR-155 among the TTP mRNA targets [508]. However, it could have been excluded from the selection as not a coding transcript. RIP on TTP and testing pri-miR-155 expression could investigate if an interaction between the RBP and the miRNA exists.

A more direct approach to tackle if the selected RBPs are involved in the regulation of miR-155 could use RNAi-mediated knockdown of the candidate proteins. However, first, it will be fundamental to identify the tenascin-C-regulated RBP(s) through an unbiased experimental approach. For example, Co-IP of Drosha and DGCR8 followed by proteomics analysis in macrophages could identify if tenascin-C-mediated regulation of miRNAs involves novel protein candidates or confirm if any of the RBPs analysed here is affected.

Moreover, by identifying differentially expressed miRNAs in tnc+/+ and tnc-/- BMDMs by small RNA-Seq and analysing common sequences and motifs between them, it could confirm if these share RBPs partners, regulated by tenascin-C.

3.6. Summary

In conclusion, it was shown here for the first time how tenascin-C is linked to the expression of miR-155 in response to specific inflammatory stimuli in macrophages activated at the plasma membrane. Furthermore, it was demonstrated that tenascin-C modulates miR-155 expression post-transcriptionally, likely at the Drosha-mediated pri-miR-155 cleavage step. However, it was not possible to determine which RBP is involved in this regulation; this could be one or more protein(s) involved in the biogenesis of tenascin-C-regulated miRNA subsets.

The next chapter investigates the form (soluble versus ECM-assembled) required for tenascin-C to signal miR-155 induction in activated macrophages. In particular, the rescue of impaired miR-155 expression in *tnc-/-* BMDMs will be attempted by culturing cells in the context of a tenascin-C-containing ECM.

Chapter 4

FORM VERSUS FUNCTION: REQUIREMENTS FOR TENASCIN-C IMMUNE-MODULATORY FUNCTION

Chapter 4. Form versus function: requirements for tenascin-C immune-modulatory function

A novel role for tenascin-C in miR-155 biogenesis was described for the first time in the previous chapter, where the ECM glycoprotein was found to be linked to enhanced cleavage of pri-miR-155 in macrophages responding to LPS.

Tenascin-C is an ECM secreted protein that can bind to other ECM molecules such as fibronectin [444], collagen [374] and proteoglycans [454], forming part of an insoluble three-dimensional network. However, tenascin-C is also found in a soluble form, in biological fluids (e.g. in sera from patients with rheumatoid arthritis or sepsis) during disease [509, 510]. Through its several domains, it can activate distinct receptors on the cell surface, including TLR4 [64], integrins [439], EGFR [511] and heparan sulfate proteoglycans, inducing intracellular signalling pathways [452, 512].

In this chapter, tenascin-C expression in its different forms will be analysed in LPS-activated macrophages. Moreover, it will be investigated in which form tenascin-C can regulate miR-155 expression.

Different cell-derived matrices (CDMs) will be generated using mouse embryonic fibroblasts (MEFs) and primary adult skin fibroblasts from *tnc+/+* and *tnc-/-* mice. These will be used to analyse tenascin-C function when in complex with the ECM. Through protein expression techniques, the deposition of ECM proteins in the generated CDMs will be characterised before and after removal of cells.

Finally, the role of ECM-assembled tenascin-C in regulating miR-155 expression will be tested in miR-155 rescue experiments in *tnc-/-* macrophages.

In this chapter, the immune-modulatory, tenascin-C form versus function will be explored.

4.1. Induction of tenascin-C expression in LPS-stimulated macrophages

4.1.1 LPS induces tenascin-C expression in RAW 264.7 cells

Expression of tenascin-C was investigated in RAW 264.7 macrophages at steady state or after stimulation with LPS for 24 hours. Tenascin-C mRNA could be detected at low levels in untreated cells, with Ct values ranging from 29 to 32. Upon LPS activation for 24 hours, tenascin-C expression increased to 1000-folds over untreated samples (Figure 4.1). High levels of tenascin-C expression in RAW 264.7 cells at 24-hours LPS stimulation seem to differ from BMDMs and human myeloid cells, where tenascin-C mRNA peaks between 4 and 8 hours after LPS stimulation and decreases nearly to basal levels at 24 hours [296, 365].

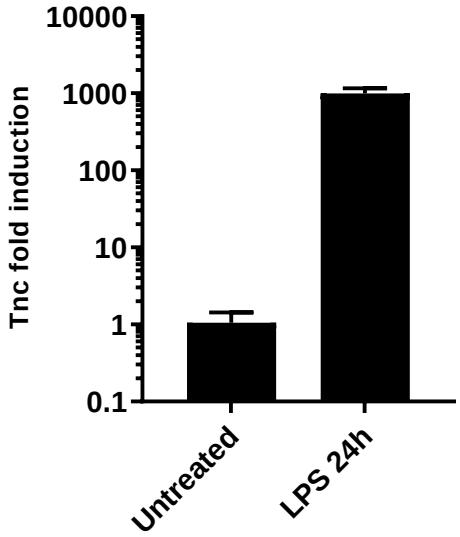


Figure 4.1 LPS induces tenascin-C mRNA expression in RAW 264.7 cells.
Total RNA extracted from RAW 264.7 stimulated with LPS for 24 hours was tested for expression of tenascin-C (Tnc), measured by qPCR. HPRT1 was used as endogenous housekeeping gene, and untreated samples were used as calibrator ($\Delta\Delta$Ct method). Data is represented in log10 scale mean fold induction relative to untreated ± SEM of 3 independent experiments measured in triplicate.

4.1.2 Extracellular localisation of tenascin-C in RAW 264.7 cells

Since LPS strongly induced tenascin-C transcription, protein expression was also expected to be enhanced. Piccinini *et al.* (2012) found that LPS-induced tenascin-C protein was both associated with cells and secreted in the conditioned medium of BMDMs [296]. By interacting with cell membrane receptors, tenascin-C can stimulate intracellular signalling cascades in response to changes of the microenvironment. Extracellular localisation of tenascin-C in LPS-stimulated RAW 264.7 cells was analysed by immunocytochemistry. Untreated or LPS-stimulated macrophages were left unpermeabilised to detect proteins expressed on the outer cellular membrane.

Notably, tenascin-C was expressed at comparable levels and with similar localisation in both unstimulated and LPS-stimulated RAW 264.7 cells (Figure 4.2). Tenascin-C appeared to localise pericellularly, possibly interacting with heparan sulfate chains of extracellular proteoglycans on the cell surface or with other ECM proteins. The proximity of some cells to each other could have affected the signal, showing higher fluorescence caused by cell clusters. However, an intense signal was also detected around cells which were not in such proximity.

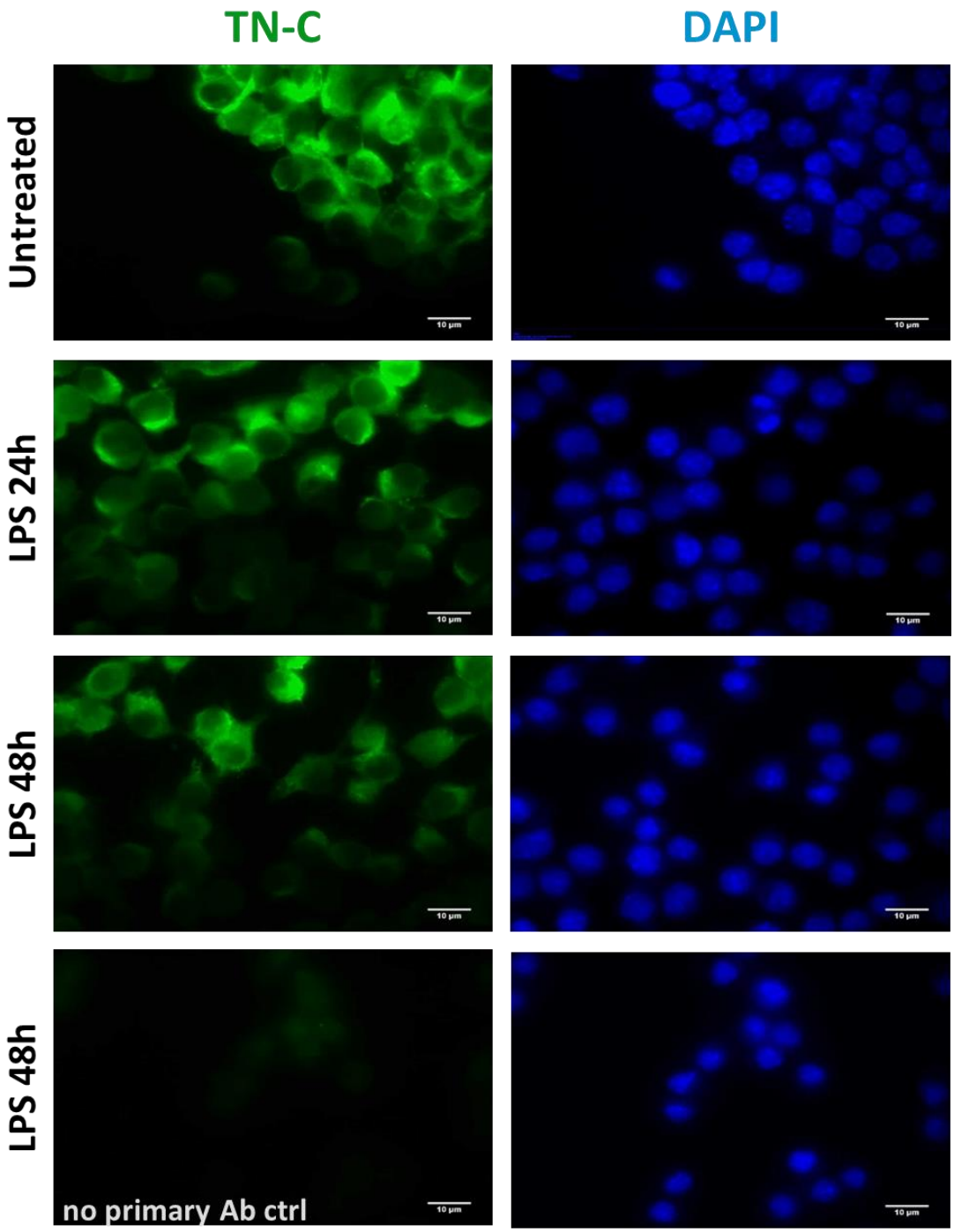


Figure 4.2 Tenascin-C localisation on the outer cell membrane of RAW 264.7 cells.
Immunofluorescence staining of tenascin-C (TN-C) in RAW 264.7 macrophages. Cells were stimulated with LPS at the indicated time points, fixed and left unpermeabilised before staining. TN-C in green and DAPI in blue. Images were visualised by the Leica DM2000 microscope with a 100x objective. Scale bar is 10µm.

As staining for additional cellular compartment markers such as the macrophage membrane marker CD11b (integrin alpha M) or the ECM marker fibronectin was not conducted in this study, it was challenging to define the exact localisation of tenascin-C with respect to the cell and the extracellular microenvironment. To overcome this limitation, LPS stimulated and unstimulated RAW 264.7 cells stained for tenascin-C were analysed by Z-stack confocal microscopy imaging. Z-stacking combines multiple images from different focal points, allowing the creation of a 3D composite image with a greater in-depth resolution than individual images. Tenascin-C seemed to localise on the outer layer of macrophage cell-membranes in unstimulated, 8 and 24 hours LPS-stimulated RAW 264.7 cells, as reported in Figure 4.3. As in Figure 4.2, it was not possible to see a clear induction of tenascin-C after LPS-activation of cells. However, in LPS-induced cells, tenascin-C expression seemed to relocate to the extremities of elongated cells.

The specificity of tenascin-C antibody binding was confirmed by testing signal detection in CDMs from *tnc-/-* skin fibroblasts, later shown in Figure 4.11, while any secondary antibody signal noise was adjusted to no primary antibody controls.

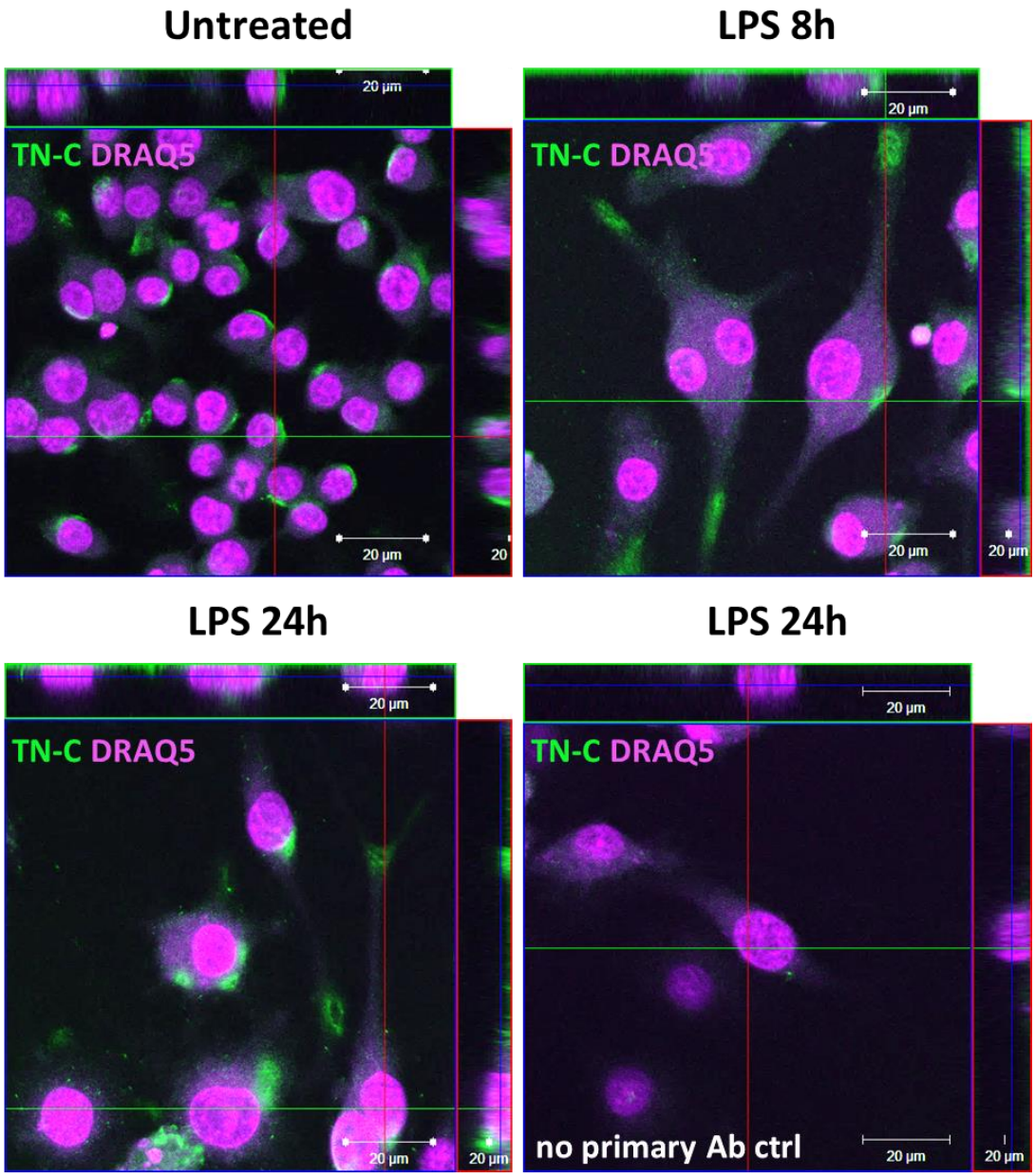


Figure 4.3 Tenascin-C distribution on the outer side of RAW 264.7 cell membrane.

Immunofluorescence staining of tenascin-C (TN-C) in RAW 264.7 macrophages. Cells were stimulated with LPS at the indicated time points, fixed and left unpermeabilised before staining. TN-C in green and DRAQ5 in purple. Images were visualised with the Zeiss LSM-510 Confocal System, with an EC-Plan-Nuofluar 40X/1.30 Oil DIC objective. Z-stacked cross-sections were compiled from n=14 1mm step size scans. Scale bar, 20µm.

4.1.3 LPS induces secretion of soluble tenascin-C by RAW 264.7 cells

To investigate if LPS could induce soluble tenascin-C secretion, cell supernatants of RAW 264.7 macrophages were analysed by western blotting. Cell media were collected 16, 24, or 48 hours after LPS stimulation (Figure 4.4). Abundant tenascin-C levels were secreted by RAW 264.7 cells at 16 hours after LPS treatment. At later time-points, tenascin-C levels started to decrease but were still easily detectable in macrophage supernatants. Tenascin-C could not be detected in untreated samples.

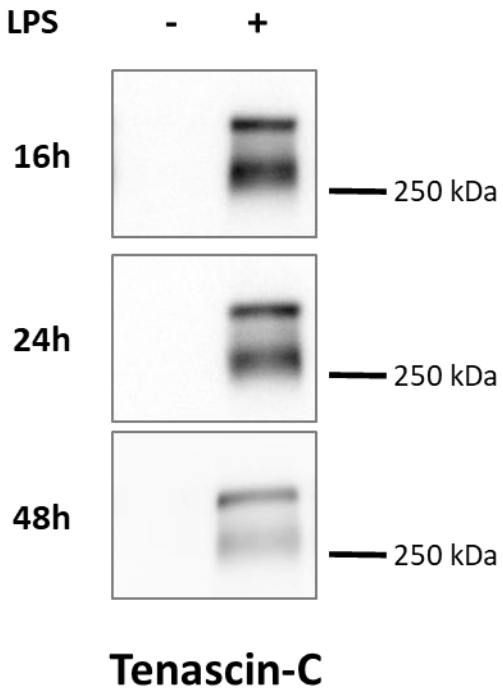


Figure 4.4 Tenascin-C is secreted as a soluble protein in LPS-induced RAW 264.7 cells.
Supernatants from RAW 264.7 stimulated with LPS for the indicated times. 50µl of supernatants were tested for TN-C expression by Western blot analysis.

These and previous experiments showed that macrophages at steady-state express tenascin-C protein, which localises on the outer side of the cell membrane and is not

secreted as a soluble protein in the cell supernatant. LPS stimulation of macrophages leads to a rearrangement of cell-associated tenascin-C localization on the cell and secretion of soluble protein in the cell supernatant. However, which of these forms regulates cytokine production and miR-155 expression remains to be established.

4.1.4 Not soluble, but cell-associated tenascin-C is involved in the regulation of miR-155

The existence of both soluble and insoluble (cell-associated) tenascin-C, and the complex network of interactions that tenascin-C can trigger with its different isoforms and domains, raises the question as to which form of tenascin-C is responsible for its function in miR-155 regulation.

Figure 4.5 shows preliminary published (a) and unpublished (b) experiments from Dr Piccinini, investigating which form of tenascin-C influences the synthesis of TNF-α and miR-155 in *tnc-/-* BMDMs. Cells were supplemented with increasing doses of soluble recombinant purified tenascin-C before stimulation with LPS (Figure 4.5a). However, soluble tenascin-C addition did not rescue but further impaired cytokine synthesis in *tnc-/-* BMDMs.

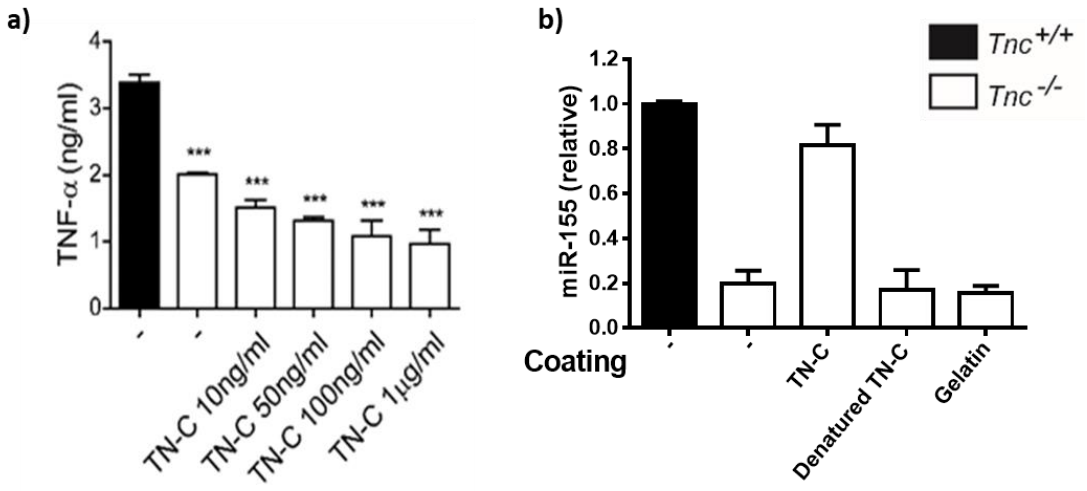


Figure 4.5 Insoluble, ECM-assembled tenascin-C is required for its immunomodulatory function.
a) TNF-α levels from 8-hours LPS stimulated *tnc+/+* and *tnc-/-* BMDMs were analysed by ELISA. *Tnc-/-* BMDMs were treated with increasing doses of recombinant purified tenascin-C (TN-C). Data are represented as mean ± SEM. *** = $p < 0.001$ compared to *tnc+/+* BMDMs stimulated with LPS (Data from three independent experiments from cells from 3 mice per genotype), Piccinini and Midwood 2012). **b)** Expression of mature miR-155 was measured by qPCR in LPS-stimulated *tnc+/+* and *tnc-/-* BMDMs cultured on TN-C-coated plates or heat-inactivated TN-C and gelatin-coated controls. snU6 was used as endogenous housekeeping gene, and untreated samples were used as calibrator (ΔΔCT method). Data are represented as mean ± SD, from one experiment measured in triplicate.

Soluble tenascin-C was not the form that was involved in cytokine production. Dr Piccinini next analysed if tenascin-C needed to be in its insoluble form (e.g. bound to the cell or ECM proteoglycans) to promote miR-155 expression. *Tnc-/-* BMDMs were cultured on tenascin-C-coated plates, which increased the expression of miR-155 to levels similar to *tnc+/+ cells* (Figure 4.5 b). The specificity of the effect of tenascin-C was addressed by plating *tnc-/-* cells on gelatin or heat-denatured tenascin-C, both of which did not rescue miR-155 production. Therefore, it was hypothesized that tenascin-C required assembly into an insoluble, multimolecular complex, most likely involving molecules such as proteoglycans present on the cell membrane or in a pericellular matrix, in order to be able to regulate miR-155 expression and, in turn,

inflammation. However, the effect of soluble tenascin-C on miR-155 expression was not tested.

By developing and characterising a physiological, cell-derived 3D-ECM model, we, therefore, aimed to test what tenascin-C assembly requirements are needed for the regulation of miR-155.

4.2. Development and characterisation of native ECM 3D culture models to study tenascin-C assembly into ECM from different cell-sources

Mouse embryonic fibroblasts (MEFs) were chosen to initially optimise and develop a model to study tenascin-C in its insoluble, ECM-assembled form. Since tenascin-C is strongly expressed during embryonic development [513], MEFs were used to generate a tenascin-C rich cell-derived matrix (CDM). Additionally, CDMs from adult skin fibroblasts (FBs) from *tnc-/-* and *tnc+/+* mice were generated, characterised for their ability to deposit ECMs, tested for their suitability as substrates for BMDM culture and applied to determine if tenascin-C requires assembly into a form of ECM to regulate miR-155 maturation.

4.2.1 Characterisation of Mouse Embryonic Fibroblast CDMs

ECMs are composed of an interlocking mesh of insoluble fibrous proteins. These include collagens, which form complexes with other molecules such as glycosaminoglycans and glycoproteins, and fibronectin. Additionally, they include ECM-associated molecules such as proteases and growth factors, which make up the soluble fraction of the ECM [358]. Soluble and insoluble components of de-cellularised MEF-derived matrices were extracted and analysed to verify matrix assembly and presence of tenascin-C.

Total protein extracts were quantified via Bradford assay and resolved by SDS-PAGE. Brilliant blue staining of resolved proteins showed high molecular weight proteins,

visible only in the insoluble fraction, with bands corresponding to putative sizes of fibronectin and collagen (Figure 4.6a).

Protein quantification found that protein concentration in the soluble fraction was two times higher than the insoluble fraction (Figure 4.6 b), reflecting the high abundance of soluble factors such as growth factors associated with the developmental status of the cells. Soluble factors have a lower molecular weight and did not appear in the SDS-gel in which higher molecular weight proteins (>55 kDa) were resolved.

Expression of tenascin-C mRNA was measured in MEFs by qPCR. Comparison between steady-state MEFs and RAW 264.7 cells showed that tenascin-C levels were much higher in MEFs (Ct 14.9 ±0.03) than RAW 264.7 cells (Ct 29.8 ±0.03) (Figure 4.6 c), confirming reports from the literature [513].

Tenascin-C expression was subsequently detected by Western blot in insoluble and soluble fractions of MEF-derived CDMs (Figure 4.6 d). While most tenascin-C was present as a large isoform of ~230 kDa in the insoluble, ECM-assembled form, lower tenascin-C levels were found in the soluble matrix fraction as a large and short isoform of ~230KDa and ~100kDa, respectively.

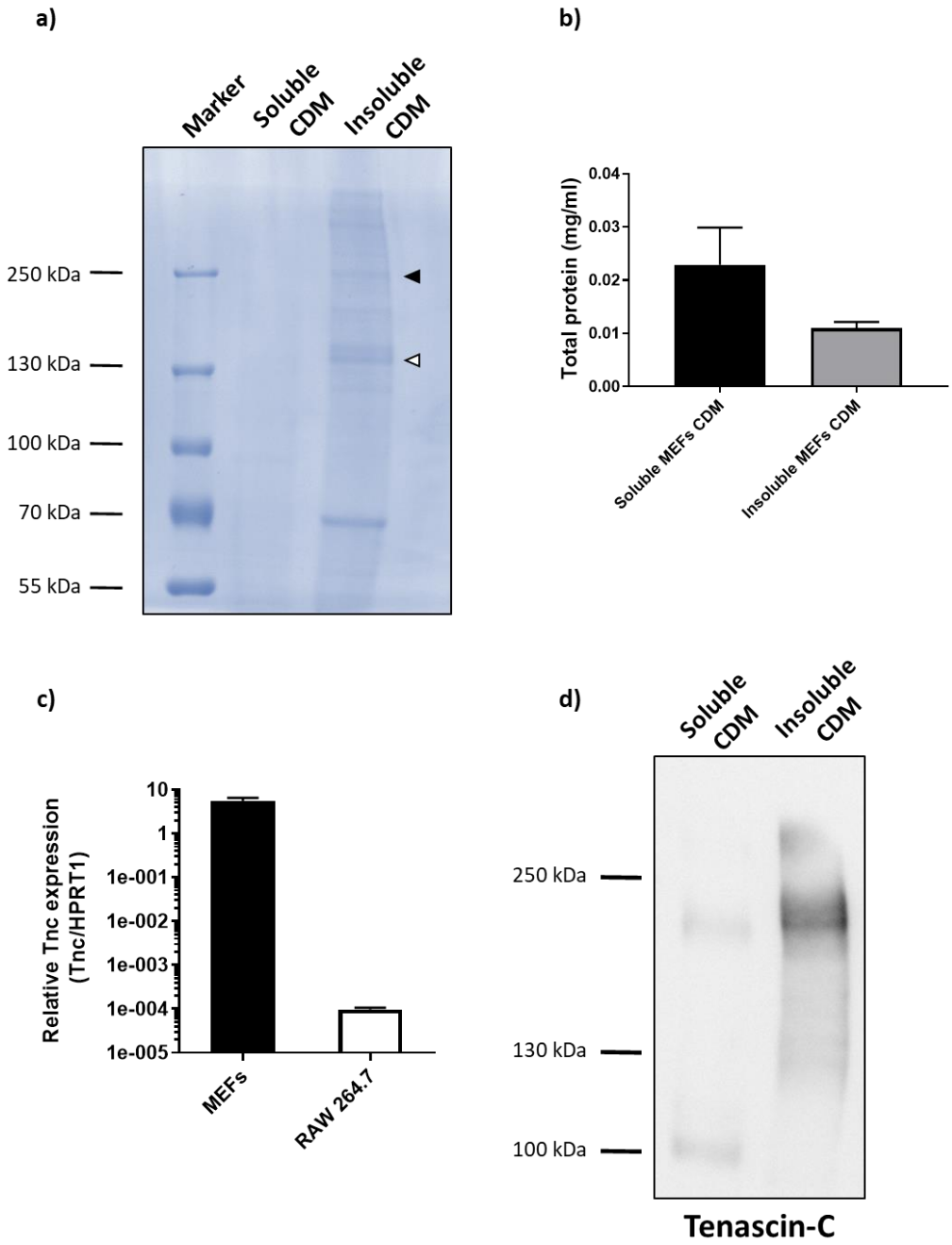


Figure 4.6 Characterisation of ECM deposited by MEFs.

Cell-derived matrices (CDMs) deposited by MEFs cultured on 10 cm dishes were de-cellularised, and soluble and insoluble matrix complexes were extracted, quantified and resolved by SDS-PAGE. **a)** 120µl of soluble and insoluble extracts from MEF-derived matrixes run on an 8% SDS-PAGE gel stained with brilliant blue G-colloidal. Arrows indicate sizes corresponding to putative positions for fibronectin (black arrow) and collagen (white arrow). **b)** Total protein quantification in soluble and insoluble MEF-derived matrix fractions measured by Bradford assay. Data are represented as mean ± SD, from one experiment measured in triplicate. **c)** cDNA reverse transcribed from WT MEFs and RAW 264.7 cells was tested for expression of tenascin-C (Tnc) by qPCR. HPRT1 was used as endogenous housekeeping gene. Data are represented as relative expression of Tnc against HPRT1 for one biological sample in three technical replicates ± SD. **d)** 120µl of soluble and insoluble CDM fractions of MEFs were tested for tenascin-C expression by Western blot. Tenascin-C (~230KDa) expression in insoluble fraction of

CDMs. Lower levels of different isoforms of tenascin-C in soluble CDM fractions (~230 KDa and ~100 KDa).

Results obtained with MEFs suggested that it was possible to use CDMs as a model to study the role of ECM-assembled tenascin-C in modulating miR-155 expression. Moreover, two extra models of CDM were introduced and optimised. In the following sections, the composition and characterisation of ECM proteins from MEFs, *tnc+/+* and *tnc-/-* adult skin fibroblasts (FBs) will be investigated.

4.2.2 Comparison of CDMs from adult and embryonic fibroblasts

The ECM is very dynamic, and its composition is strongly influenced by health status, localisation within the body, developmental stage and external stimuli [357].

Specific biochemical properties and protein abundance may vary between ECM of different origin, affecting how cells interact with each other and their microenvironment [358].

In this section, the expression of fundamental components of the ECM will be analysed in CDMs from MEFs, *tnc+/+* and *tnc-/-* adult skin fibroblasts (FBs), before and after removal of cells. These analyses will confirm if CDMs are suitable as a substrate for *tnc-/-* BMDMs, and the rescue of tenascin-C function.

ECM proteins considered for this analysis were collagen-I (Col-1), fibronectin (FN) and tenascin-C (TN-C), which were all expected to be abundant in these CDMs.

Collagen-I

Collagen-I, together with collagen-II and –III, are the main components of the ECM, constituting a fibrous insoluble scaffold surrounding cells [514].

Collagen-I was analysed by immunocytochemistry in CDMs before and after cell-denudation to confirm that the ECM structure was not affected by de-cellularisation.

Collagen-I was found to be distributed and expressed similarly across CDMs from *tnc+/+*, *tnc-/-* skin FBs and MEFs (Figure 4.7). Effective de-cellularisation was confirmed by DAPI staining showing complete removal of genomic DNA. Additionally, collagen-I composition was not visibly affected by cell removal, maintaining a high degree of complexity and structure.

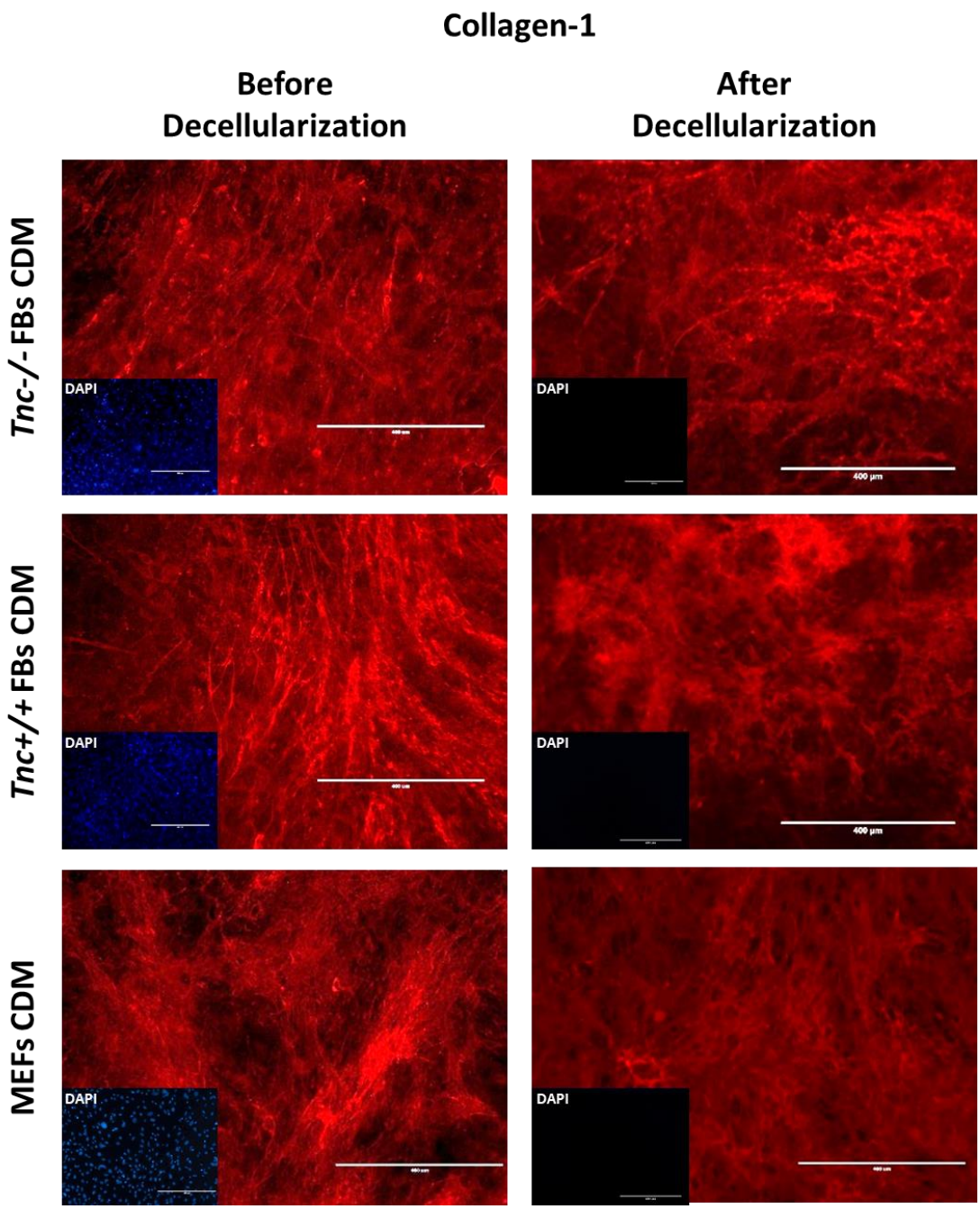


Figure 4.7 Collagen-I deposition in CDMs before and after de-cellularisation.

Skin FBs from *wild type* (WT) and *tnc-/-* mice and MEFs were cultured for 10 days in complete media supplemented with 50 µg/ml L-Ascorbic acid before de-cellularisation and DNase I treatment. Immunofluorescence analysis of collagen-I (Col-1) is shown in red. DAPI staining of genomic DNA (blue) was used to mark the nuclei (left panels) and to show complete cell removal (right panels). Images were visualised using an Evos FL Cell Imaging System with a 10x objective. Scale bar, 400µm.

Expression of collagen-I was further examined by resolution of decellularised CDM protein extracts on SDS-pages and western blotting.

Tnc-/-, tnc+/+ skin FB and MEF CDMs similarly expressed the main form of collagen-I (140kDa), with some differences between adult and embryonic FBs. For example, in the high molecular weight region for MEF CDMs, the crosslinked trimeric (~400kDa) and dimeric (~270kDa) forms of collagen-I were more abundant than in adult tissues. However, differences in the abundance of collagen-I levels between *tnc+/+* and *tnc-/-* skin FB CDMs were not considered significant since total protein staining showed minor protein loading differences between *tnc-/-* and *tnc+/+* skin FB CDMs (Appendix Figure 7.5a). For reproducibility, experimental conditions were maintained the same during all procedures. However, due to the lack of classical protein normalisers, relative quantification could not be performed with CDMs.

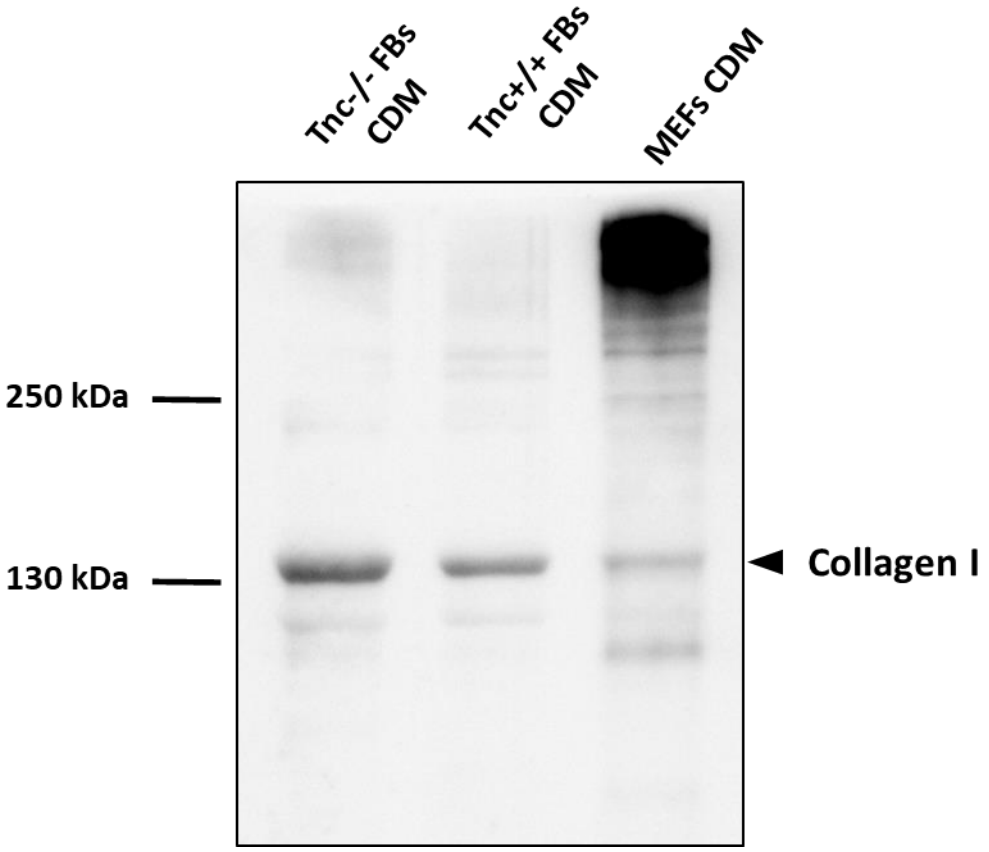


Figure 4.8 Deposition of ECM protein collagen-1 in CDMs from *tnc+/+* and *tnc-/-* FBs and MEFs.
Decellularized CDMs from wild type and *tnc-/-* skin FBs and MEFs were analysed by western blot for expression of the ECM protein COL1. 30 µl of sample was loaded on each well. Representative of 3 biological replicates.

Fibronectin

Fibronectin is a fundamental and abundant component of the ECM and plays both structural and modulatory roles [515, 516]. Additionally, fibronectin expression is often linked to tenascin-C [370, 392, 470, 517, 518].

Immunofluorescence analysis of fibronectin deposited by adult *tnc-/-* and *tnc+/+* skin FB CDMs appeared to be different from MEF CDMs (Figure 4.9). Moreover, the absence of tenascin-C in adult skin FB CDMs seemed to affect the overall abundance of fibronectin in *tnc-/-* skin FB CDMs. Cell removal revealed a more compact distribution of fibronectin, compared to images with cells. The difference could be partly due to cells covering the fluorescent signal of lower layers, uncovered by decellularisation, or higher permeability of antibody to CDMs without cells.

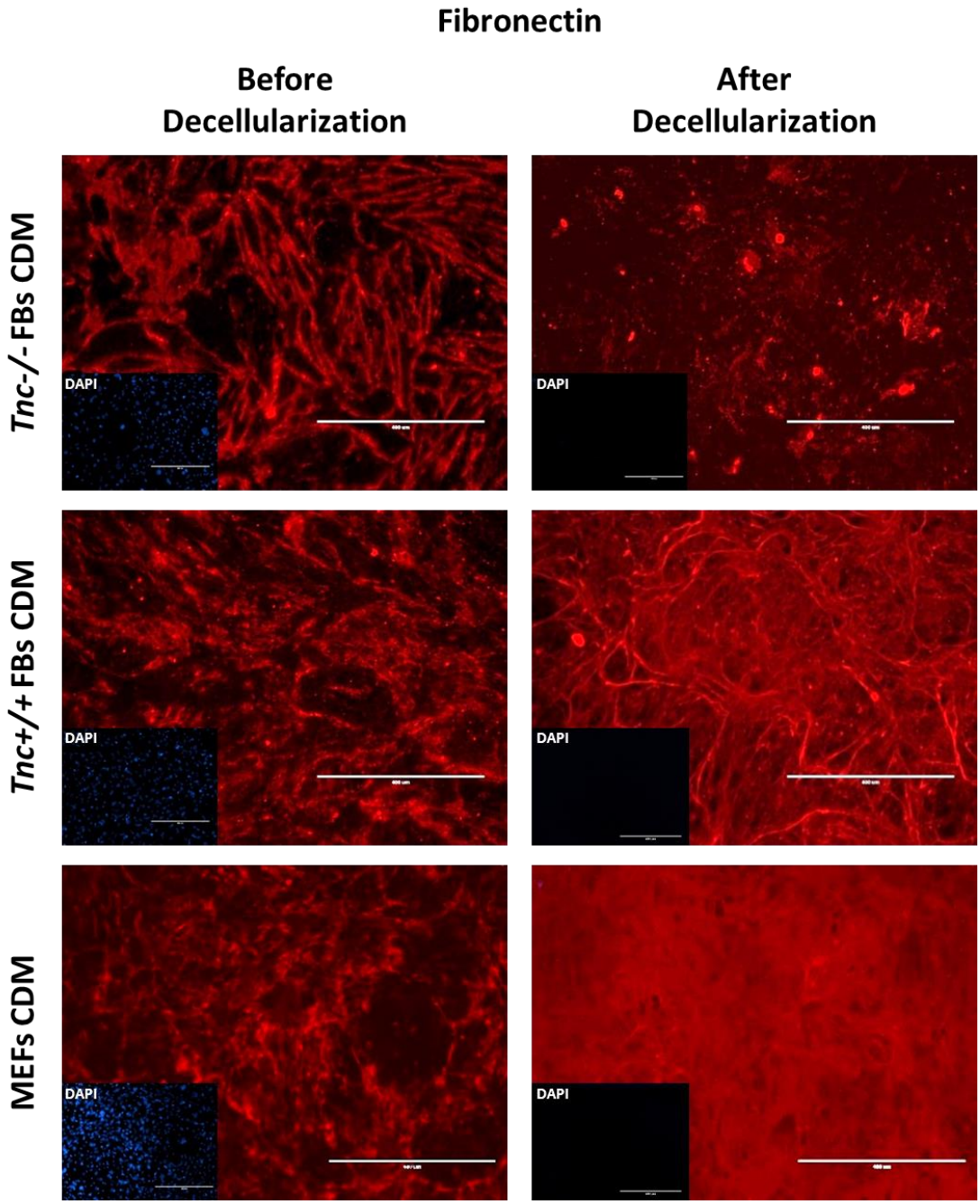


Figure 4.9 Fibronectin deposition in CDMs before and after de-cellularisation.

Skin FBs from *wild type* (WT) and *tnc-/-* mice and MEFs were cultured for 10 days in complete media supplemented with 50 µg/ml L-Ascorbic acid, before de-cellularisation and DNase I treatment. Immunofluorescence analysis of fibronectin (FN) is shown in red. DAPI staining of genomic DNA (blue) was used to mark the nuclei (left panels) and to show complete cell removal (right panels). Images were visualised using an Evos FL Cell Imaging System with a 10x objective. Scale bar, 400µm.

Decellularized CDMs were further analysed by western blotting. All three CDMs presented a band at the expected molecular weight size for fibronectin (220kDa) (Figure 4.10). Nevertheless, differences for higher molecular weight bands, presumably corresponding to different isoforms and post-translational modifications (e.g. glycosylation), were detected between the CDMs.

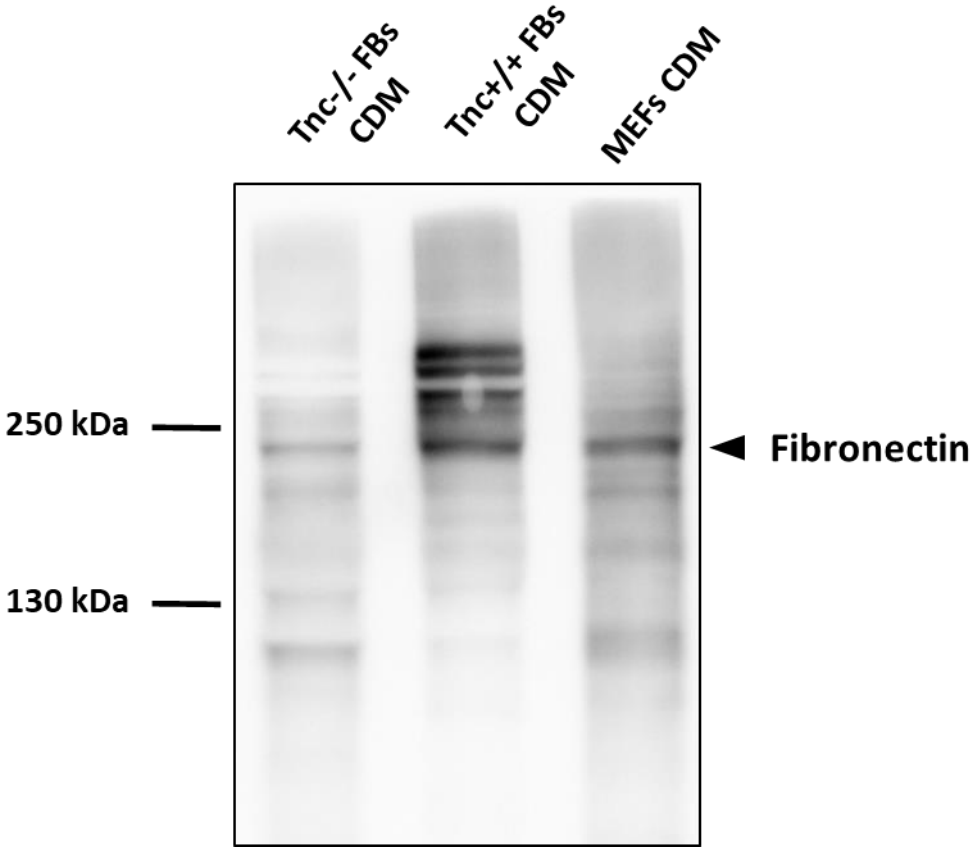


Figure 4.10 Deposition of ECM protein fibronectin in CDMs from *tnc +/+* and *tnc-/-* FBs and MEFs.
Decellularized CDMs from wild type and tnc-/- skin FBs and MEFs were analysed by western blot for expression of the ECM protein FN. 30 µl of sample was loaded on each well. Representative of 3 biological replicates.

Noticeably, *tnc+/+* skin FB CDM seemed to express higher fibronectin levels and more abundant high molecular weight bands, compared to *tnc-/-* skin FB or MEF CDMs.

Despite trying to maintain consistent conditions for all the samples, Ponceau S staining showed a higher protein loading in *tnc-/-* skin FB CDM samples, than *tnc+/+* skin FB CDM (Appendix Figure 7.5b). However, a more abundant protein loading in *tnc-/-* than in *tnc+/+* skin FB CDM, further confirmed that the decreased fibronectin expression seen in *tnc-/-* skin FB CDM was genuine.

Tenascin-C

Tenascin-C expression is characterised by strict spatio-temporal control, dramatically changing from embryonic to adult tissues [374, 392, 428]. During morphological events, tenascin-C is maintained at high levels, allowing rapid tissue remodelling and cellular turnover. In healthy adults, tenascin-C expression drops to very low levels, with transient induction in response to inflammation and tissue injury [376, 389]. Nevertheless, adult tissues characterised by constant remodelling and subject to tensile forces such as the epithelium consistently express basal levels of tenascin-C [425, 427].

Deposition of tenascin-C in ECMs from embryonic and adult skin fibroblasts was analysed by immunofluorescence, before and after cell-removal (Figure 4.11). No primary antibody controls for CDMs are reported in appendix inFigure 7.6.

As expected, tenascin-C was not detectable in CDMs from *tnc-/-* skin FBs, both with and without cells. *Tnc+/+* skin FB and MEF CDMs both showed abundant expression of tenascin-C in the ECM, which was confirmed after removal of cells. As seen with fibronectin, denuded CDMs showed a more compact structure, revealing the intricated meshwork which was previously surrounding cells.

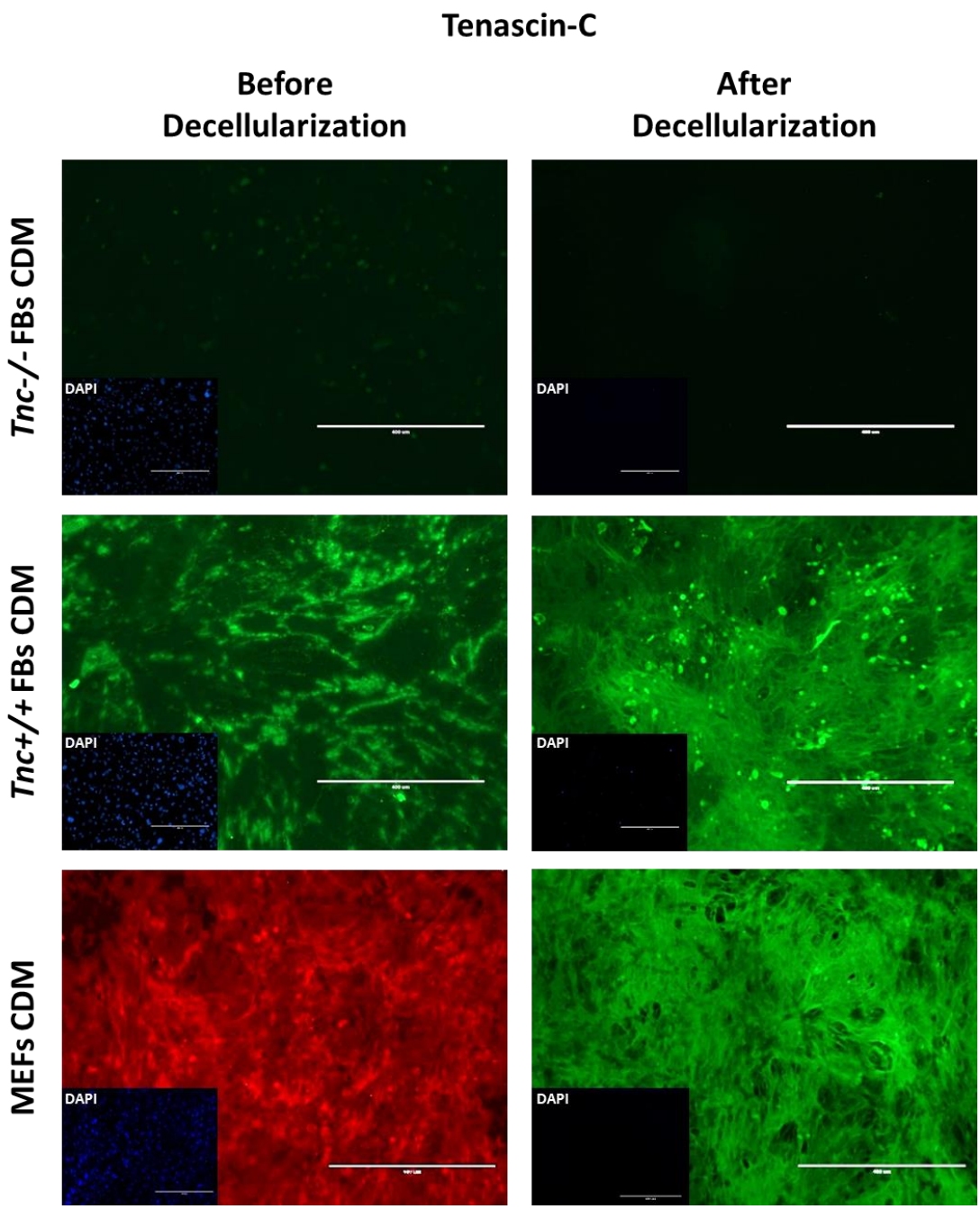


Figure 4.11 Tenascin-C deposition in CDMs before and after decellularisation.

Skin FBs from *wild type* (WT) and *tnc-/-* mice and MEFs were cultured for 10 days in complete media supplemented with 50 µg/ml L-Ascorbic acid, before decellularisation and DNase I treatment. Immunofluorescence analysis of tenascin-C (TN-C) is shown in green or in red (bottom left panel). DAPI staining of genomic DNA (blue) was used to mark the nuclei (left panels) and to show complete cell removal (right panels). Images were visualised using an Evos FL Cell Imaging System with a 10x objective. Scale bar, 400µm.

Western blot analysis of decellularised CDMs confirmed the absence of tenascin-C in *tnc-/-* skin FB CDMs (Figure 4.12). Additionally, tenascin-C expression was

investigated by comparing *tnc+/+* skin FB and MEF CDMs. The molecular weight of tenascin-C ranges between species from 190 to 320 kDa. It was possible to identify the main tenascin-C isoforms in mouse in both cell types, corresponding to 260 and 210 kDa. A higher band, likely corresponding to the 320 kDa isoform, was also present in adult skin and embryonic FB CDMs. However, differences in expression were identified around 280 and 190 kDa molecular weight sizes, showing potential differences in isoform expression or post-translational modification between the two cell types.

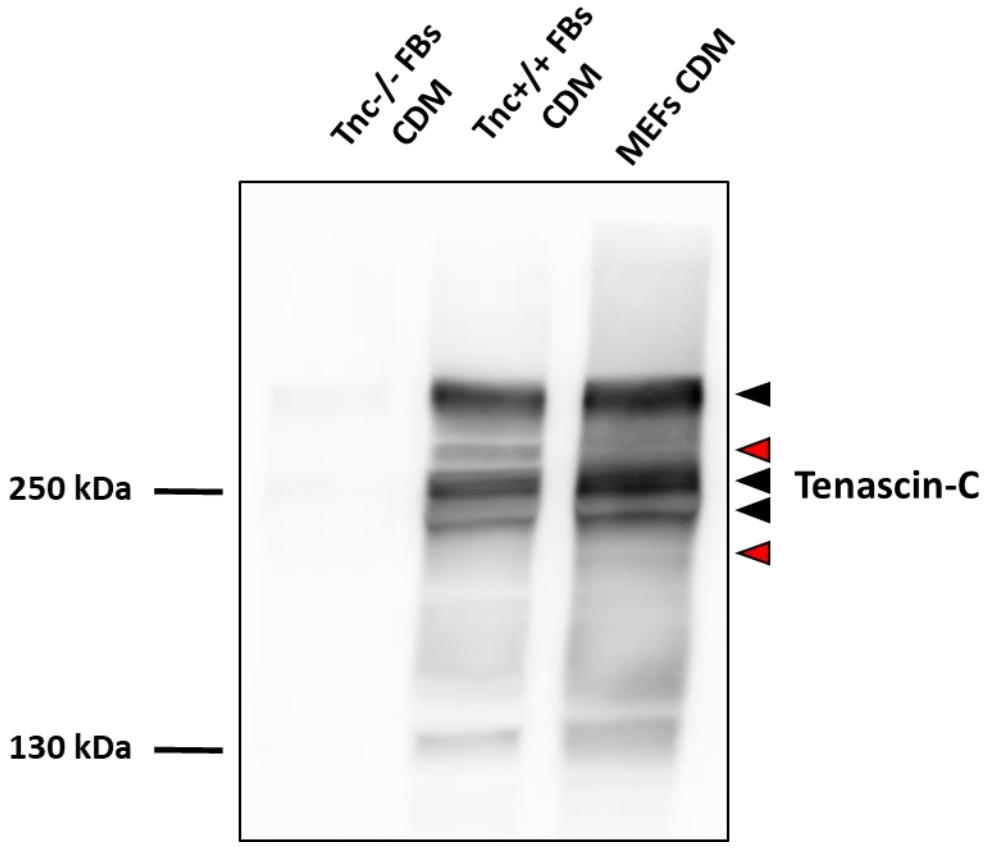


Figure 4.12 Deposition of extracellular proteins in CDMs from *tnc +/+* and *tnc-/-* FBs and MEFs.
Decellularized CDMs from wild type and *tnc-/-* skin FBs and MEFs were analysed for expression of the ECM protein TN-C. 30 µl of sample was loaded on each well. Representative of 3 biological replicates. Black arrows indicate main isoforms; red arrows point at different putative isoforms in MEFs and adult skin FBs.

In summary, CDMs from *tnc+/+* adult skin FBs and MEFs exhibited abundant tenascin-C expression, but also distinctive characteristics in protein expression and matrix deposition. Decellularisation did not affect ECM structures and protein composition, supporting the use of CDMs as a substrate to culture *tnc-/-* BMDMs and study tenascin-C form versus function.

4.3. Analysis of ECM-associated tenascin-C effect on miR-155 modulation

CDMs from *tnc-/-* and *tnc+/+* skin FBs and MEFs were confirmed to be valid models of physiological ECMs. However, whether insoluble, ECM-associated tenascin-C could fine-tune miR-155 expression was yet unclear.

BMDMs differentiated from *tnc-/-* mice were seeded either on classic tissue culture 6-well plates or on decellularised matrices deposited by the cell-types indicated above.

BMDMs seeded in equal numbers on plastic or CDMs showed a drastic difference in distribution, shape and cell-to-cell contact (Figure 4.13). Compared to the two-dimensional, stiff surface of plastic plates, unstimulated and LPS-activated macrophages appeared more spread and less flattened on CDMs where cells could distribute over a three-dimensional space. Additionally, LPS-stimulated cells seeded on CDMs appeared to be more rounded and motile than BMDMs on tissue-culture plates.

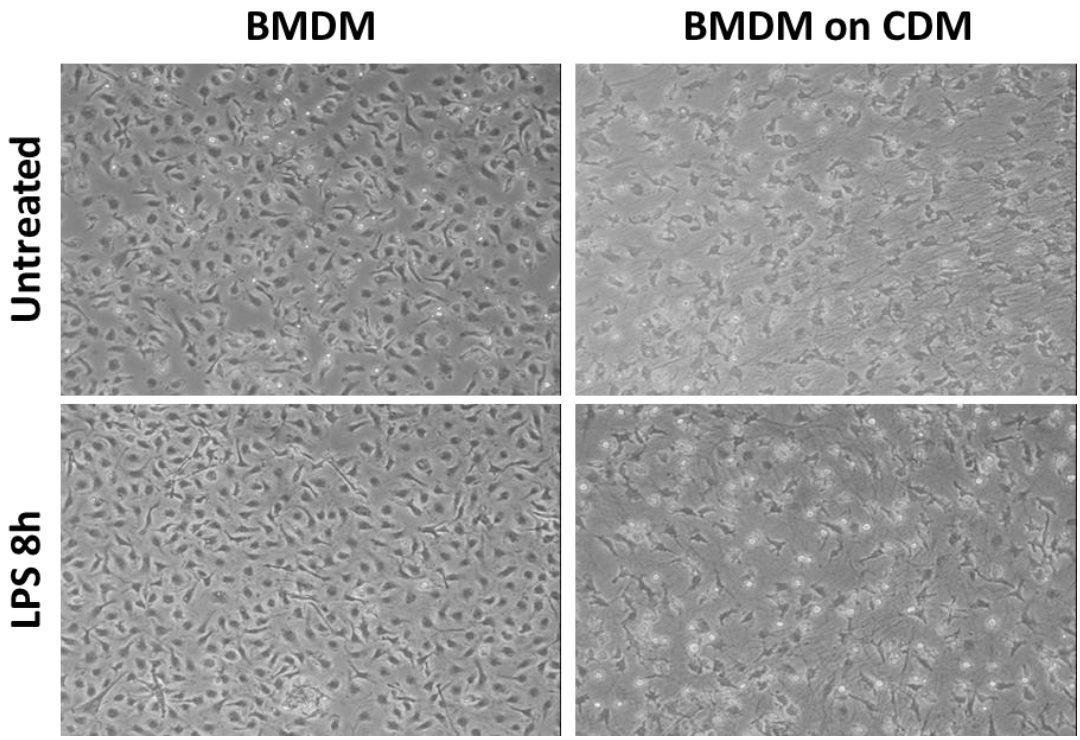


Figure 4.13 Seeding of BMDMs on CDMs.

BMDMs were cultured for 7 days in medium containing M-CSF. Differentiated *tnc-/-* BMDMs were seeded on tissue culture 6-well plates (left) or CDMs (right), originated by *tnc+/+* FBs. After resting overnight, cells were stimulated with LPS (bottom) or left untreated (top). Images were taken using phase-contrast microscopy, magnification 10X.

Tnc-/- BMDMs were seeded on tissue culture 6-well plates and CDMs from *tnc-/-* and *tnc+/+* skin FBs and MEFs. Induction of miR-155 expression was analysed after LPS treatment for 8 and 24 hours, and it was compared to levels of miR-155 in *tnc+/+* BMDMs seeded on plastic plates (Figure 4.14).

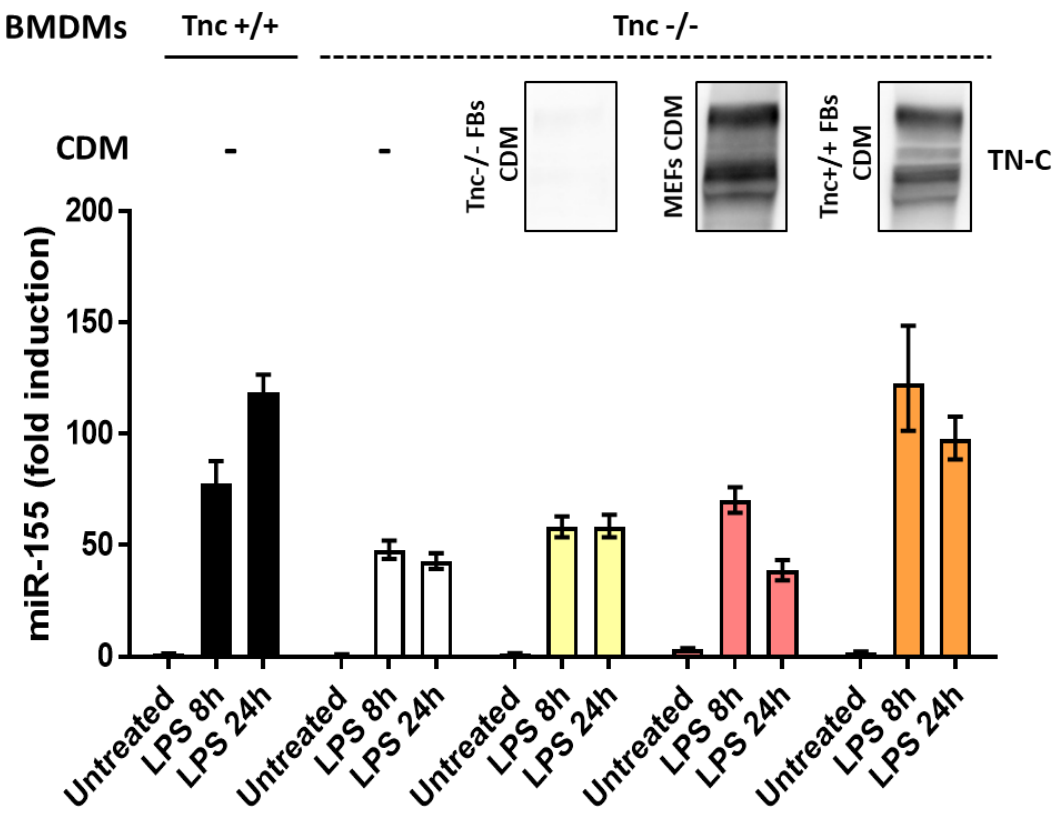


Figure 4.14 Rescuing miR-155 in *tnc-/-* BMDMs.
M-CSF-differentiated BMDMs were seeded on tissue culture 6-well plates and CDMs originated from *tnc+/+* and *tnc-/-* skin FBs, and MEFs. Total RNA was extracted from *tnc+/+* and *tnc-/-* BMDMs after stimulation with LPS for the indicated duration. Expression of mature miR-155 was measured by qPCR. snU6 was used as endogenous housekeeping gene and *tnc-/-* untreated samples as calibrator ($\Delta\Delta$Ct method). Data from one experiment is represented as mean fold induction ± SD, measurements taken in triplicates.

As reported in Chapter 3, miR-155 levels were lower in LPS-stimulated *tnc-/-* cells seeded on plastic compared to *tnc+/+* BMDMs. In line with this, miR-155 expression did not increase in *tnc-/-* BMDMs seeded on CDMs lacking tenascin-C, with levels similar to *tnc-/-* BMDMs on plastic. Notably, *tnc-/-* BMDMs plated on tenascin-C-expressing MEF CDM did not replenish miR-155 expression, remaining lower than that of *tnc+/+* BMDMs. On the other hand, CDMs obtained from *tnc+/+* adult skin FBs were able to rescue miR-155 expression to levels comparable to *wild-type*

macrophages. Additional biological replicates will be required to confirm these results.

4.4. Discussion

The concept of DAMPs being active components in response to infection is relatively new. Tenascin-C was found to be induced early upon LPS-activation, both in human myeloid cells [365] and *in vivo* in mice [296]. Its expression was required for an effective pro-inflammatory response to experimental sepsis, induced by LPS [296].

However, tenascin-C comes in different forms, influencing what function and interactions will prevail [392].

This chapter addressed the question as to what form of tenascin-C regulates miR-155 expression: soluble or ECM-assembled?

Tenascin-C expression was analysed in RAW 264.7 cells in response to LPS. Transient transcription of tenascin-C was previously found to be significantly induced in BMDMs from 4 to 8 hours after LPS treatment and decreasing to almost basal levels after 24 hours [296]. Similar results were obtained in human primary monocytes, monocyte-derived dendritic cells (MDDCs) and monocyte-derived macrophages (MDMs) [365]. Here, we showed that tenascin-C mRNA levels were still strongly induced 24 hours after LPS treatment of RAW 264.7 macrophages. Lack of other time-points did not allow us to understand if transcription was at this point still increasing, plateauing or decreasing. However, it is essential to consider that cell lines often show exacerbated situations, compared to primary cells, and that RAW 264.7 cells are macrophages derived from tumorigenic tissues, where tenascin-C is usually found upregulated [389]. Overall, we confirmed that LPS-stimulated RAW 264.7 cells strongly induced transcription of tenascin-C. Additionally, it was noticed that low

basal levels of tenascin-C mRNA could be detected in untreated macrophages, but the semi-quantitative analysis does not allow absolute quantification of the transcript levels. Still, Giblin et al. (2020) recently reported detecting basal mRNA levels of tenascin-C in different untreated immune cells, including human M-CSF-macrophages and MDDCs, but not in neutrophils [519].

Immunocytochemistry analysis found that tenascin-C localised extracellularly around the cell membrane of RAW 264.7 cells and was more concentrated in regions of contact between cells. On the outer side of the cell membrane, tenascin-C could bind to heparan sulfate proteoglycans such as syndecan-4 [419, 452], integrins, including $\alpha 9\beta 1$ [371] and $\alpha v\beta 3$ [456], or other ECM proteins such as collagen [374] and fibronectin [370, 518]. Nevertheless, to address more precisely where tenascin-C is localised outside of cells, tenascin-C will have to be detected in combination with additional protein markers such as CD11b for the cellular membrane, and fibronectin for the ECM.

The overall amount of tenascin-C present on the cell surface was not affected by LPS stimulation. De novo synthesized tenascin-C could be secreted as a soluble protein in the cell supernatant, similarly to what occurs *in vivo* during inflammation where soluble tenascin-C is detected in body fluids. It is also possible that newly-produced, cell-associated tenascin-C does not bind strongly to the cells or that the macrophage cell surface is already saturated with tenascin-C, and that any soluble excess is washed away during preparation for the experiment. Tenascin-C was previously detected at various levels in association with cells in BMDMs and MDDCs by ELISA [296, 519].

Macrophages are now known to synthesise a variety of ECM molecules, albeit in smaller quantities than stromal and epithelial cells [[520-522]]. They can also release molecules and signals for other cells to modify the environment in which they reside [356, 523]. It is yet unclear if tenascin-C secreted by immune cells during inflammation gets integrated into their pericellular ECM or if secreted tenascin-C is meant to be delivered to more distant sites through the circulation where it could act as DAMP, alerting other cells of the presence of infection or tissue damage.

It was shown here that the addition of soluble tenascin-C was not able to recover cytokine expression in *tnc-/-* BMDMs. On the contrary, coating plates with tenascin-C could rescue miR-155 expression in the same cells. These results were in line with the idea that assembly of tenascin-C into the ECM surrounding cells could modify how its domains are presented to cellular receptors and interacting molecules, activating distinct intracellular pathways. For example, soluble tenascin-C can easily interact with fibronectin in glycerol gradients assays [444], but if tenascin-C is immobilised to ELISA plates, interaction with fibronectin is reduced [444, 451, 524]. On the other side, oligomerisation of tenascin-C and its assembly into an insoluble matrix-associated hexabrachion might be required for binding of multiple partners simultaneously, leading to activation of the cell surface receptor responsible for miR-155 regulation.

To analyse the role of matrix-assembled tenascin-C in regulating miR-155 expression and LPS-induced immune response, CDMs were generated and characterised from adult and embryonic fibroblasts. Matrix protein expression and deposition were confirmed by analysing soluble and insoluble matrix fractions, and was initially

described in MEFs. MEF-derived matrices deposited an abundant ECM, presenting high molecular weight ECM proteins in their insoluble fraction. Total protein concentration in the insoluble fraction was lower than that of the soluble, possibly due to high levels of growth factors and tissue degrading enzymes in embryonic tissues [525]. In MEF CDMs, tenascin-C was found mostly in complex with ECM molecules in the insoluble fraction. These data are in line with previous studies, showing that tenascin-C is a significant component of MEF ECM [526].

Deposition of ECM proteins collagen-I, fibronectin and tenascin-C was analysed in CDMs from *tnc-/-* and *tnc+/+* adult skin FBs and MEFs. Quality and efficiency of decellularisation were assessed by fluorescent microscopy and confirmed the complete removal of cells as well as maintenance of intact ECM structures. Differences in protein abundance and matrix-complexation were identified between embryonic and adult skin FBs, and between *wild-type* and tenascin-C knockout cells. In particular, fibronectin was found to be expressed at lower levels in CDMs from *tnc-/-* skin FBs, compared to *tnc+/+* CDMs, both by immunofluorescence and western blot analysis.

The relationship between tenascin-C and fibronectin has solid foundations. They are found co-localised in cell culture and embryos [444], and they are co-dependent on each other. It was shown that inhibition of fibronectin matrix formation by mutating heparan sulfate proteoglycans (HSPGs) blocked tenascin-C integration into the ECM [527]. In agreement with that, a fibronectin template was found to be required for tenascin-C assembly in the ECM of squamous cell carcinoma [528].

On the other hand, fibronectin expression depends on tenascin-C. Tenascin-C knockout mice expressed reduced levels of fibronectin in skin and corneal wound healing, compared to *wild-type* mice [430, 470]. More recent studies found that tenascin-C is involved in production and matrix incorporation of fibronectin in skin lesions, contributing to fibrosis [370]. Additionally, tenascin-C was found to induce fibronectin expression in human endothelial cells [518].

Why fibronectin and tenascin-C seem to interact and oppose each other's action is still not well understood. However, a balanced and temporally controlled expression of both proteins seems to be essential in tissue repair and inflammatory response.

In addition to fibronectin, analysis of tenascin-C in the different CDMs revealed differences between adult skin and embryonic fibroblasts. As expected, tenascin-C was found to be absent in *tnc-/-* skin FBs CDM. Interestingly, *tnc+/+* skin FB and MEF CDMs expressed different matrix-assembled tenascin-C isoforms with potentially different protein post-translational modifications. For instance, tenascin-C contains several sites for *N*- and *O*-glycosylation [392, 412, 413] and citrullination [414]. The idea that different tenascin-C isoforms are dictating specific events during embryogenesis and tumorigenesis was previously reviewed by Giblin et al. (2015) [392]. More recently, the same authors demonstrated how alternative splicing of tenascin-C is affected in myeloid cells responding to LPS [519]. LPS-activated myeloid cells specifically induced upregulation of alternatively spliced FnIII isoforms of tenascin-C which were lacking AD2 and AD1 domains. AD2AD1 domain appeared to have an inhibitory role in MDDCs chemotaxis and TLR4-dependent cytokine release.

Notably, the CDM generated from *tnc+/+* adult skin FBs, which expressed different tenascin-C isoforms compared to MEF CDM, was the only form of CDM tested that was able to rescue miR-155 expression in *tnc-/-* BMDMs. In contrast, embryonic cell-derived tenascin-C in MEF CDM was unable to rescue miR-155 expression in *tnc-/-* BMDMs, as was the lack of tenascin-C in the control skin FB CDMs. Importantly, due to experimental difficulties and lack of time, this experiment was only performed once, and further repeats are necessary. Nevertheless, unpublished results from a colleague demonstrated that LPS-induced miR-155 expression in primary human macrophages is enhanced by seeding cells on tenascin-C expressing adult, skin FB CDMs, but not on TNC knockout skin FB CDMs.

The idea that the form and function of tenascin-C are deeply interconnected is not new, but there is yet a limited number of studies describing this relationship in detail [474, 519, 529, 530]. Emerging studies are demonstrating unique roles for specific tenascin-C splice variants in innate immunity. For example, internalisation of the T-cell receptor complex was found inhibited by alternatively spliced tenascin-C containing FnIII A1A2 domains, leading to blockade of T-lymphocytes polarisation [474]. Different isoforms may uncover cryptic binding sites for interacting molecules and have different affinity for ECM molecules and cell-membrane receptors. For example, alternatively spliced FnIII D domain of tenascin-C contains an active integrin $\alpha 7\beta 1$ binding site that can promote rat hippocampal neurite outgrowth [531].

Confirming what form of tenascin-C is regulating miR-155 expression, for example by analysing miR-155 levels in *tnc-/-* BMDMs plated on different recombinant isoforms

of tenascin-C, could also help in identifying the cellular receptor that is involved in this regulation.

4.5. Summary

In this chapter, form versus function of tenascin-C was investigated in the context of LPS-induced innate immune response. Expression of tenascin-C in LPS-activated macrophages was analysed through different techniques. LPS stimulation enhanced tenascin-C transcription but did not result in increased amounts of tenascin-C protein associated to the cell surface. Instead, *de novo* synthesized tenascin-C was mainly released as a soluble protein in the cell supernatant. Notably, insoluble, ECM-associated tenascin-C, and not soluble tenascin-C, seemed to be the form involved in mediating miR-155 expression. Given that in inflammation miR-155 and TNF-α are very early response genes, it is not surprising that insoluble, cell-associated tenascin-C, which is available to the macrophage when it is activated, and not soluble tenascin-C, which requires *de novo* synthesis, operates regulation of miR-155 expression. Furthermore, this regulation appears to be linked to specific isoform(s) of ECM-assembled tenascin-C that are not present in embryonic FB CDMs, but in adult skin FB CDMs.

The tenascin-C isoform(s) involved in the regulation of miR-155 could reveal cryptic binding sites for specific cell membrane receptors, among the ones already known or yet unidentified. The next chapter will investigate candidate tenascin-C receptors responsible for miR-155 induction in LPS-activated macrophages.

Chapter 5

INVESTIGATING THE CELL-SURFACE RECEPTOR INVOLVED IN TENASCIN-C-MEDIATED REGULATION OF miR-155

Chapter 5. Investigating the cell-surface receptor involved in tenascin-C-mediated regulation of miR-155

In the previous chapter, it was found that tenascin-C is already present on the cell surface of macrophages in their steady-state and that it must be in an ECM-assembled form to regulate miR-155 levels in macrophages. This original finding attributes the gene regulation ability of tenascin-C to its insoluble form and not its soluble form, *de novo* synthesized upon inflammation and may act at a later stage of the inflammatory response triggering different signalling pathways. Therefore, when tenascin-C is bound to cell surface proteoglycans or other ECM components, its conformation may reveal specific ligand binding sites, allowing interaction with the receptor(s) and potentially co-receptor(s) expressed on the macrophage cell membrane, whose activation induces intracellular signalling cascades.

In this chapter, candidate tenascin-C receptors, expressed in macrophages, were investigated for their ability to activate signalling pathways leading to the regulation of miR-155 expression.

Candidate receptors included the experimentally validated tenascin-C receptors TLR4, integrins $\alpha 9\beta 1$, $\alpha v\beta 3$ and $\alpha 5\beta 1$, and EGFR, selected for their roles in regulating inflammation in collaboration with tenascin-C, as described in Chapter 1 (Section 1.6.3). A summary of their biological effects upon tenascin-C binding is presented in Table 21. In addition, their involvement in miR-155 expression was analysed in LPS-induced macrophages after inhibition of receptors with commercially available

function-blocking antibodies, cell signalling small molecule inhibitors or receptor binding peptides.

Receptor	TN-C binding domain	Biological effect	References
TLR4	FBG	NF-kB signalling activation; cytokine production.	[64, 356, 366-370, 441]
Integrin alpha-9 beta-1 (α9β1)	FNIII3	Cell adhesion and migration; cytokine & chemokine expression.	[371-373]
Integrin alpha-V beta-3 (αvβ3)	FBG + FNIII3	Cell adhesion and migration; NF-kB signalling activation; cytokine production; promotion of pro-inflammatory macrophage phenotypes.	[456, 457, 532]
Integrin alpha-5 beta-1 (α5β1)	FNIII	Cell adhesion and migration; intracellular signalling activation.	[452, 455, 475]
EGFR	EGF-L	EGFR phosphorylation; mitogenesis; MAPK and ERK activation.	[437, 438, 511]

Table 21 Experimentally validated, candidate tenascin-C receptors investigated in this study
TLR4: Toll-like Receptor 4; FBG: fibrinogen-like globe; FNIII: fibronectin type III-like repeats; EGFR: Epidermal Growth Factor Receptor; EGF-L: EGF-like repeats.

Additionally, two novel candidates were investigated here for their potential ability to bind to tenascin-C and regulate miR-155 expression (Table 22). The first candidate, macrophage-1 antigen (Mac-1), binds to ligands with a high degree of homology with specific tenascin-C domains. This similarity prompted us to examine whether tenascin-C could interact with Mac-1 and if this cell surface receptor could be

involved in regulating miR-155 expression. The second candidate, neuropilin-1 (NRP1), is a non-tyrosine kinase transmembrane co-receptor only recently found to be involved in innate immunity [533-537] that shares several binding partners and functions with tenascin-C, as summarised below. Herein we analysed NRP1 expression upon LPS-activation of macrophages and its role in regulating miR-155.

Receptor	Potential TN-C binding domain	Involved in	References
CD11b/CD18 (Mac-1, integrin αMβ2)	FBG	Phagocytosis; cell adhesion, migration & spreading; TLR-signalling pathways.	[538-543]
Neuropilin-1	Unknown	Co-receptor for VEGF family members & TGFβ1; surface marker of T_{Reg} cells; regulation of adhesion and clustering between DCs and resting T-cells; macrophage polarisation;macrophage function in sepsis.	[534, 535, 544-549]

Table 22 Novel candidate tenascin-C receptors and co-receptors investigated in this study.
Mac-1: macrophage-1 antigen; FBG: fibrinogen-like globe; VEGF: Vascular Endothelial Growth Factor; TGFβ1: Transforming Growth Factor Beta-1; DCs: Dendritic Cells

Mac-1, also known as integrin αMβ2 or complement receptor 3 (CR3), is composed of a heterodimer of αM (CD11b) and β2 (CD18) chains, primarily expressed on myeloid cells such as macrophages, dendritic cells and neutrophils [540, 550-554]. Mac-1 drives key events of the inflammatory response such as cell adhesion, migration, activation, chemotaxis and phagocytosis upon binding-mediated activation [538, 539]. Reflecting the diversity of its functions, Mac-1 can bind to an

extensive range of molecules, such as intercellular adhesion molecule 1 (ICAM-1), and platelet glycoprotein Iβα (GPIβα), and ECM glycoproteins, including fibrinogen and fibronectin [555]. Additionally, Mac-1 can act as PRR to recognise PAMPs and DAMPs such as LPS [540-543], dsRNA [543], HMGB1 [542, 556] and β–amyloid aggregates [557], mediating outside-in signalling translation. However, the role of Mac-1 in TLR-signalling remains controversial, seemingly both protective against endotoxin shock and sepsis [541, 542, 555, 558] and positively regulating pro-inflammatory molecule expression [540, 543, 558].

One of the best-characterised ligands of Mac-1 is fibrinogen-gamma (FBG-γ) [559]. FBG-γ and the C-terminal FBG domain of tenascin-C share 30% sequence homology (Table 23). Therefore, the interaction between Mac-1 and tenascin-C was investigated by *in silico* alignment of the FBG-γ protein sequence with the C-terminal FBG domain of tenascin-C. Moreover, known residues involved in FBG-γ interaction with the αM subunit (CD11b) of Mac-1 [560, 561] were used to identify corresponding motifs and potential binding sites on tenascin-C.

Additionally, the expression of miR-155 was analysed in LPS-activated macrophages after antibody-mediated blockade of Mac-1. This experiment allowed us to investigate if Mac-1 could have a role in miR-155 regulation.

Previous studies have found that tenascin-C can exert intracellular signalling by recruiting receptors and co-receptors. For example, tenascin-C can prevent syndecan-4 binding to fibronectin, reducing α5β1 integrin signalling amplification [452]. A novel tenascin-C co-receptor was potentially identified in neuropilin-1 (NRP1).

NRP1 has been characterised in several immune cells, including macrophages, DCs, subpopulations of T-cells and mast cells [562], where it plays a critical role in inflammation and immune responses [533, 535, 549]. It remains unclear what role NRP1 plays in immunity, but it appears to negatively regulate inflammation. For example, NRP1 deficiency in myeloid cells exacerbated cytokine production and enhanced LPS-induced sepsis mortality in mice [535]. Moreover, in the presence of VEGF, NRP1 could bind to TLR4, abrogating secretion of cytokines such as IL-6, IL-12 and TNF-α in BMDC (bone marrow-derived dendritic cells) [549]. In agreement with its anti-inflammatory roles, recent studies found that NRP1 mediates the entry of SARS-CoV-2 (Severe acute respiratory syndrome coronavirus 2) into epithelial and endothelial cells, enhancing viral infectivity [536, 537]. Protease-cleaved Spike protein of SARS-CoV-2 binds to the VEGF-A binding domain on NRP1, blocking VEGF-A/NRP1 signalling and reducing pain de-sensitising nociceptor activity [563].

In addition to TLR4 [64, 549], tenascin-C and NRP1 share other binding partners. For instance, NRP1 was found to modulate ECM signalling in endothelial cells by binding to fibronectin and integrins [564, 565], including integrin $\alpha5\beta1$ [564] and $\alpha v\beta3$ [566, 567], all well-known tenascin-C binding partners [452, 455-457, 475, 532]. Additionally, NRP1 is known to act as co-receptor for growth factors such as the previously mentioned VEGF [564] and TGF-β [545] and can cross-talk with several other growth factors signalling pathways, similarly to tenascin-C [450, 533].

In regards to their functions, tenascin-C and NRP1 are both involved in cytoskeletal rearrangement and cell motility mediated through FAK phosphorylation and activation of Rho-GTPase [568-570], axon guidance and angiogenesis (reviewed in

[374] and [571]), amongst others. Moreover, they are both recognised hallmarks of tumorigenic conditions, where both are found upregulated and promoting malignant cell-survival (reviewed in [389] and [572]).

The overlapping cellular functions and binding partners between tenascin-C and NRP1 could indicate interaction or competition between the two proteins. Therefore, NRP1 was analysed, together with the other receptors, for its potential role in regulating miR-155 expression in macrophages.

5.1. Experimentally validated, candidate tenascin-C receptors

5.1.1 Toll-like receptor 4 (TLR4)

Analysis of tenascin-C validated receptors began with TLR4, which is activated by both LPS and tenascin-C. The levels of miR-155 were quantified in *tnc+/+* BMDMs or RAW 264.7 macrophages pre-incubated with the specific TLR4 signalling inhibitor CLI-095 (also known as TAK-242) before treatment with poly(I:C) or TNF-α to determine whether tenascin-C regulates miR-155 expression downstream of TLR4 pathways. Both poly(I:C) and TNF-α are established inducers of miR-155 expression in macrophages [123, 208]. These molecules activate NF-kB through TLR3 and TNFR, respectively, but not TLR4, allowing blockade of TLR4 function without compromising NF-kB-mediated induction of miR-155.

After poly(I:C) stimulation for 24 hours, *tnc+/+* BMDMs were expressed at similar levels of miR-155 to non-inhibited cells, whether TLR4 signalling was inhibited (Cli-095) or treated with the DMSO control solution (Figure 5.1 a)

TLR4 involvement was further analysed using a macrophage activator, previously found to depend on tenascin-C for an appropriate expression of miR-155, dissimilarly to poly (I:C) (Chapter 3, section 3.1.1). Levels of miR-155 were measured in TNF-α–stimulated RAW 264.7 macrophages after inhibition of TLR4 signalling. However, preliminary results from a single experiment showed little activation of miR-155 upon stimulation with TNF-α, accompanied by no detectable difference in miR-155 levels between TLR4-inhibited cells and controls (Figure 5.1 b, experiment performed by Alessandro Nunziata under my supervision).

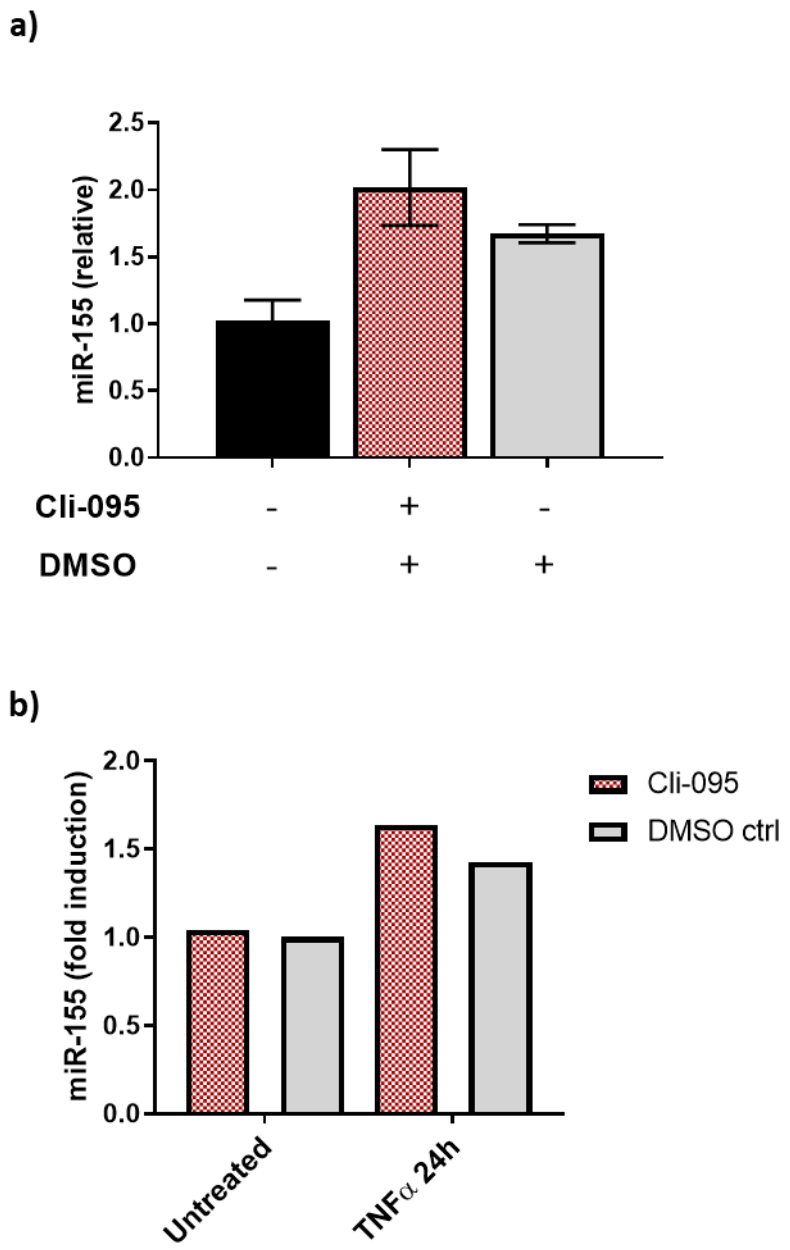


Figure 5.1 TLR4 signalling in tenascin-C-mediated regulation of miR-155 expression.
a) Total RNA was extracted from *tnc+/+* BMDMs, stimulated with 20mg/ml poly(I:C) for 24 hours, in the presence or absence of 3μM TLR4 inhibitor (CLI-095) or dimethyl sulfoxide (DMSO). Expression levels of mature miR-155 were measured by qPCR. snU6 was used as endogenous housekeeping gene and non-inhibited samples used as calibrators (ΔΔCt method). Data are represented as mean relative induction ± SEM (3 mice per genotype measured in triplicates). **b)** Total RNA extracted from Raw 264.7 cells, stimulated with 10ng/ml recombinant TNFα for 24 hours, in the presence or absence of 3μM TLR4 inhibitor (CLI-095) or dimethyl sulfoxide (DMSO). Expression levels of mature miR-155 were measured by qPCR. snU6 was used as endogenous housekeeping gene, and unstimulated DMSO control was used as calibrator (ΔΔCt method). Data represent a single experiment.

5.1.2 Integrins α5β1, αvβ3 and α9β1

Tenascin-C can initiate intracellular signalling by binding to integrins such as α5β1, αvβ3 and α9β1, located on the macrophage cell membrane.

To test if these integrins are involved in the regulation of miR-155, integrin receptors were inhibited with function-blocking antibodies targeting integrin α5β1 (BMC5) and integrin β1 (CD-29), and an RGD-peptide, targeting integrin αvβ3. Integrin receptors were inhibited for 30 minutes before 24-hours LPS stimulation and RNA extraction. Expression of miR-155 in *tnc+/+* BMDMs was then quantified by qPCR.

Blockade of integrin receptors was expected to result in reduced miR-155 expression in the case tenascin-C-mediated regulation was dependent on integrin receptors or remain unchanged if miR-155 levels were not dependent on integrin signalling. However, the blocking of integrin receptors induced an unexpected but not statistically significant up-regulation of miR-155 expression in BMDMs (Figure 5.2). Furthermore, a stronger difference in miR-155 was detected in cells in which α5β1 and αvβ3 were inhibited (Figure 5.2 a and b), while inhibition of integrin β1 alone showed a more modest variation (Figure 5.2 c).

Endotoxin contamination of reagents is often a cause of unwanted, non-specific activation of immune responses in cells that very likely occurred here.

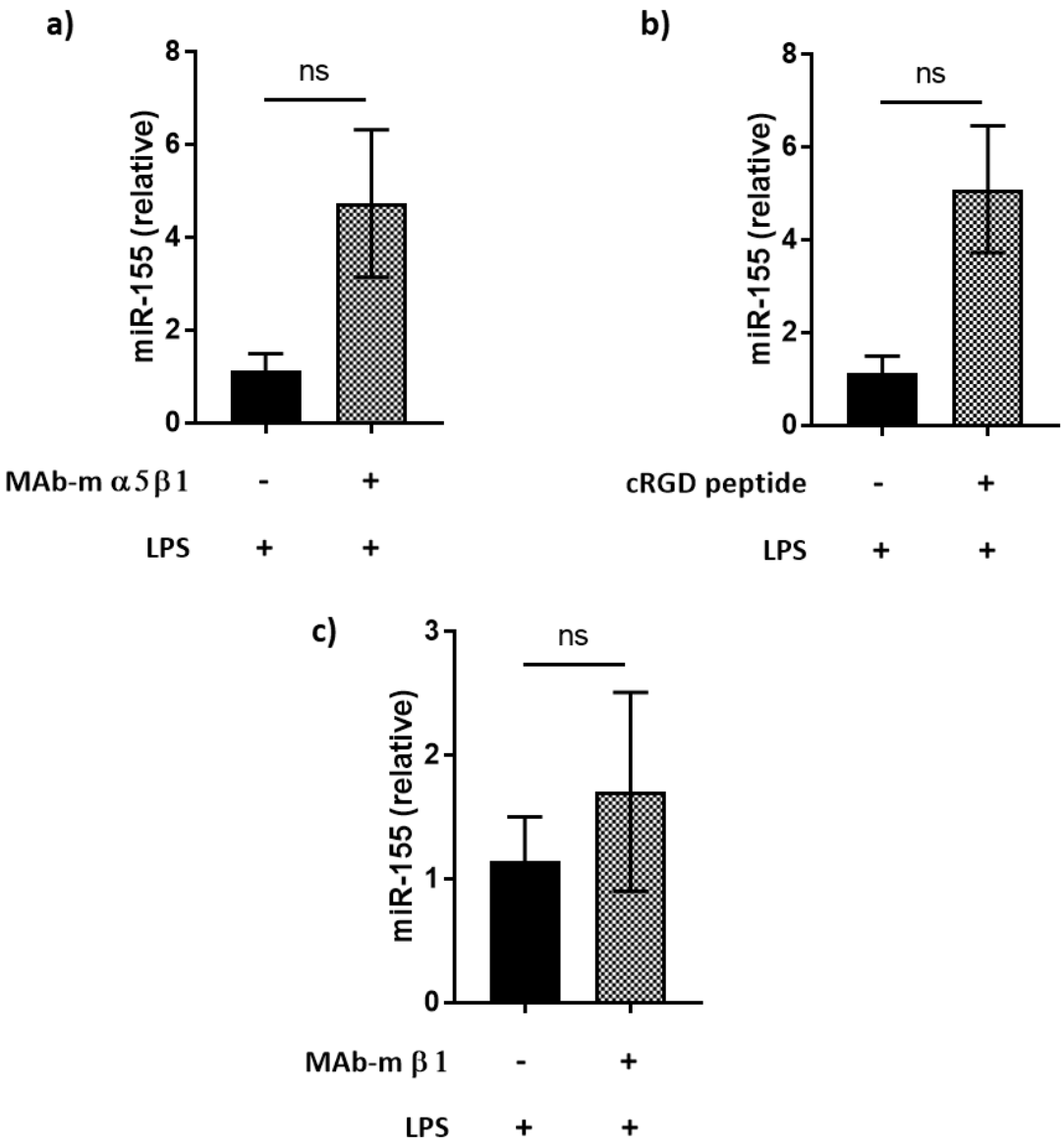


Figure 5.2 Investigating integrin signalling regulation of miR-155 expression in BMDMs.
Total RNA was extracted from *tnc+/+* BMDMs, stimulated with 100ng/ml LPS for 24 hours, in the presence or absence of 25μg/ml of anti-integrin alpha5-beta1 (Mab-m α5β1; **a**) or anti-integrin beta1 (Mab-m β 1; **c**), or 100mg/ml of alphaV-beta3 integrin binding cyclic RGD peptide (cRGD peptide, αvβ3; **b**) Expression levels of mature miR-155 were measured by qPCR. snU6 was used as endogenous housekeeping gene and non-inhibited samples used as calibrators (ΔΔCt method). Data are represented as mean relative induction ± SEM (3 mice, measured in triplicates).

In order to further characterise the potential role of integrins in tenascin-C-mediated miR-155 regulation, it was decided to re-test only the anti-integrin β1 antibody,

whose levels of endotoxins were measured by the LAL (Limulus Amebocyte Lysate) assay and indicated by the manufacturer as <0.001ng/μg.

RAW 264.7 macrophages were treated overnight with integrin β1 blocking antibody before stimulation with LPS for the indicated times (Figure 5.3; experiment performed by Alessandro Nunziata under my supervision).

Similarly to BMDMs, LPS-induced expression of miR-155 in RAW 264.7 cells remained comparable at all time-points in controls and integrin β1-inhibited macrophages.

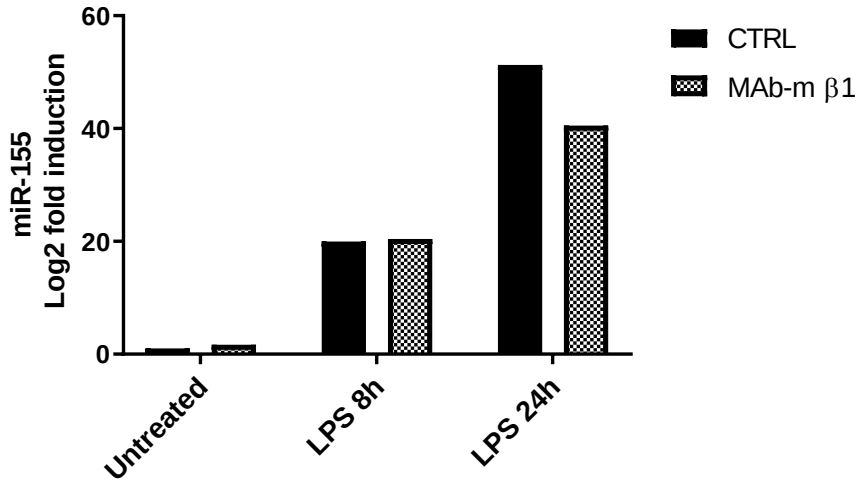


Figure 5.3 Investigating integrin signalling regulation of miR-155 in RAW 264.7 cells.
Total RNA extracted from RAW 264.7 cells, stimulated with 100ng/ml LPS for 24 hours, in the presence or absence of 10μg/ml anti-integrin beta1 antibody (MAb-m β1). Expression levels of mature miR-155 were measured by qPCR. snU6 was used as endogenous housekeeping gene, and non-inhibited untreated control was used as calibrator (ΔΔCt method). Data represent a single experiment.

5.1.3 Epithelial Growth Factor Receptor (EGFR)

In addition to integrins, tenascin-C can bind to EGFR, inducing its phosphorylation and activation of downstream MAP kinase signalling pathways [437, 438, 460].

In this section, it was tested if EGFR could be involved in miR-155 regulation in macrophages. BMDMs were treated for 30 minutes with an anti-EGFR blocking antibody before a 24-hour LPS stimulation, RNA extraction and qPCR for miR-155 quantification.

Compared to controls, relative miR-155 levels showed a variable and statistically not significant up-regulation when EGFR was inhibited (Figure 5.4)

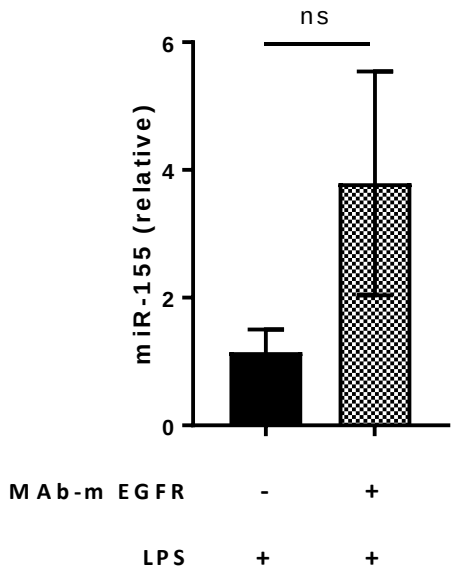


Figure 5.4 Investigating EGFR signalling regulation of miR-155 expression in BMDMs.
Total RNA was extracted from *tnc+/+* BMDMs, stimulated with 100ng/ml LPS for 24 hours, in the presence or absence of 25μg/ml anti-EGFR antibody (MAb-m EGFR). Expression levels of mature miR-155 were measured by qPCR. snU6 was used as endogenous housekeeping gene, and non-inhibited samples used as calibrators (ΔΔCt method). Data are represented as mean relative induction ± SEM (3 mice, measured in triplicates).

5.2. Novel candidate tenascin-C-receptors

5.2.1 Macrophage Receptor 1 (MAC-1)

Sequence homology analysis of tenascin-C and a validated Mac-1 ligand

In this section, potential interactions between Mac-1 and tenascin-C were investigated using *in silico* analysis.

The C-terminal domain of fibrinogen gamma (FBG-γ) is known to bind to the αM subunit of Mac-1 (αMI-domain) [573] . The FBG-γ sequence was analysed and compared to that of the tenascin-C FBG domain by pairwise alignment. Human and mouse FBG domains of tenascin-C are approximately 30% identical to human and mouse FBG-γ, respectively (Table 23).

	Human FBG γ	**Mouse FBG γ**
Human FBG-γ	-	79.5%
Mouse FBG-γ	79.5%	-
Human TN-C FBG	30.6%	-
Mouse TN-C FBG	-	30.6%

Table 23 Identity between FBG-γ and tenascin-C FBG domains in human and mouse.
Percentage of identity of human and mouse C-terminus fibrinogen-γ (FBG-γ) chain against human and mouse tenascin-C FBG determined by pairwise alignment with Clustal Omega.

However, Mac-1 is known to be able to bind to a diversified range of host-specific ligands, fitting a mosaic model of binding [574]. Distinct amino acid sequences can interact with the αMI-domain, providing that they present common binding surfaces and specific residues organisation [575, 576].

Mac-1 was found to interact with human FBG-γ on its D-domain [559], where two unrelated sequences were identified as binding sites for Mac-1 receptor: P1 γ190–202 (GWTVFQKRLDGSV) and P2 γ377–395 (YSMKKTTMKIIPFNRLTIG) [560, 561]. The P1 and P2 sequences were later validated, together with several other sequences identified as positive binding sites for Mac-1 [575]. The γ368-395 sequence contained in P2 formed the most prominent αMI-domain binding cluster.

In the three-dimensional structure of the FBG-γ C-terminus, the P1 and P2 sequences reside in close proximity, forming two antiparallel β strands (Figure 5.5 a). Tenascin-C FBG domain forms a very similar three-dimensional structure (Figure 5.5 b). Moreover, the sequences matching the predicted Mac-1 binding sites on tenascin-C FBG closely resemble the structural organisation and location of FBG-γ.

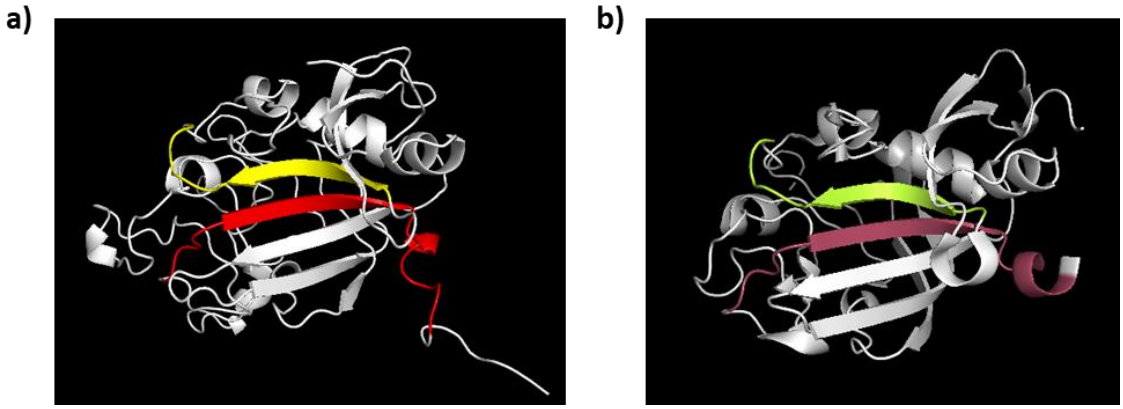


Figure 5.5 Three-dimensional structure of human FBG-γ and tenascin-C FBG domains.
a) Crystal structure of human C-terminal fragment of fibrinogen-gamma (FBG-γ, PDB: 1FID). Binding sequences for Mac-1 (αMβ2 integrin) are coloured in yellow (G190-V202) and red (Y377-E396). **b)** Crystal structure of human fibrinogen-like domain (FBG) of tenascin-C (PDB: 6QNV). Predicted binding sequences for Mac-1 (αMβ2 integrin) are coloured in lemon (G2022-E2034) and raspberry (H2177-N2193).
Protein residues were coloured using PyMOL Molecular Graphic System v2.4.0.

To further address if the similarities within the two proteins could indicate a potential interaction between Mac-1 and tenascin-C, sequences of C-terminal FBG-γ and FBG domain of tenascin-C were analysed using multiple sequence alignment tools. Sequences were aligned according to their identity, and groups of amino acids were coloured according to their properties, including hydrophobicity, positive or negative charge, and polarity.

The attention was mainly focused on the two sequences P1 and P2 on FBG-γ, indicated with red boxes in Figure 5.6, and the corresponding sequences on tenascin-C.

A minimal recognition motif in human FBG-γ is composed of a short sequence with a central basic residue, surrounded by hydrophobic residues [575]. The putative binding sites on tenascin-C FBG domain maintain similar characteristics, with alternate short hydrophobic and basic sequences (e.g. W2023-N2031 (WIVF**LRRK**N), or I2179-R2187 (IQFAE**MKLR**)). Together, these data supported the hypothesis of the potential interaction of tenascin-C with Mac-1. However, it remained to be clarified whether Mac-1 contributes to the regulation of miR-155 expression.

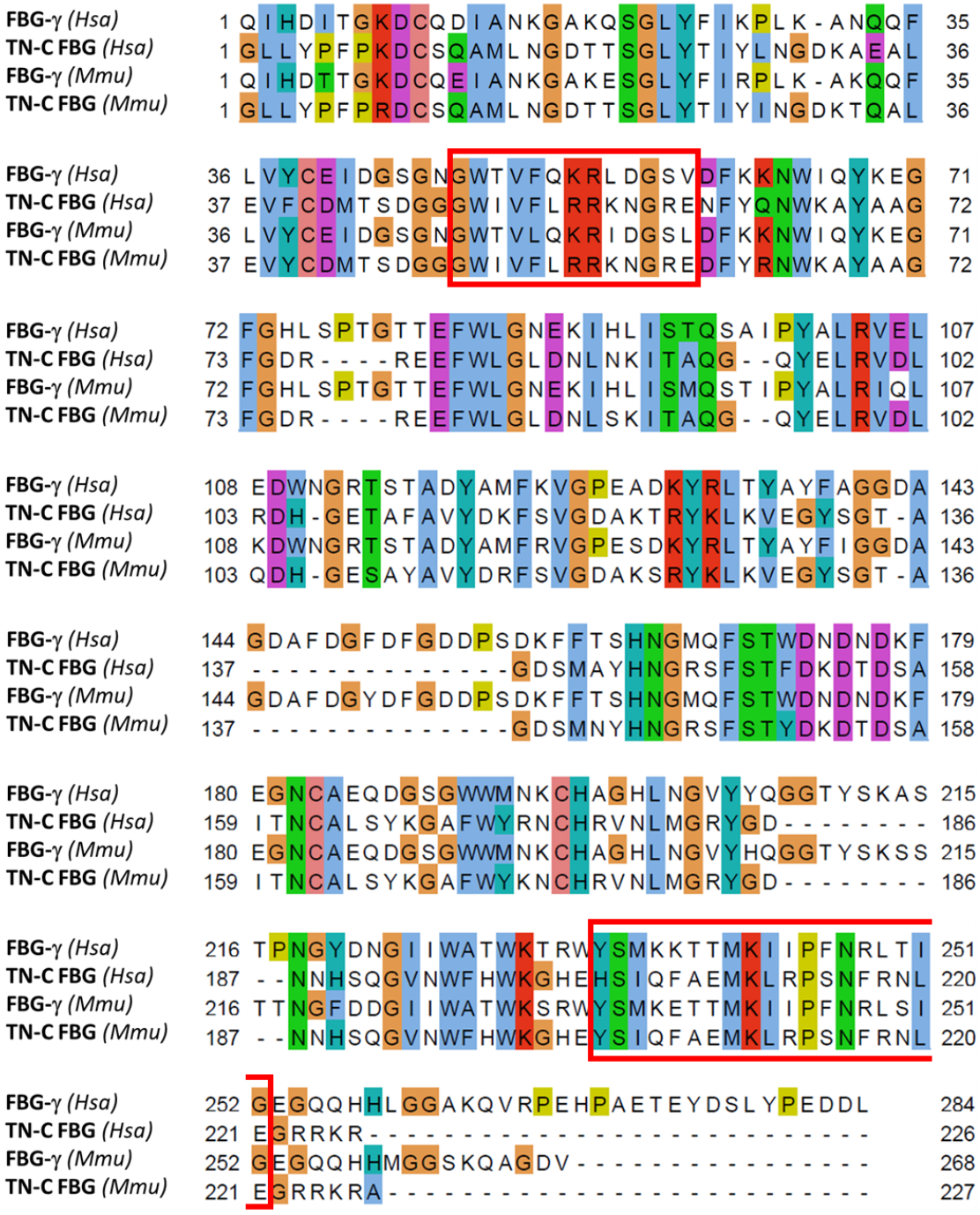


Figure 5.6 Homology between FBG-γ and tenascin-C FBG domains in human and mouse.

Conserved regions between human and mouse FBG-gamma (γ) and tenascin-C FBG domains detected using Clustal Omega software. Alignments were coloured with Jalview software according to the Clustal colour scheme. Light blue: hydrophobic. Red: positively charged. Magenta: negative charge. Green: polar. Pink: conserved cysteine. Orange: glycines. Yellow: prolines. Cyan: aromatics. Red boxed indicate two confirmed binding sites for αMβ2 integrin with human FBG-γ, and corresponding regions on aligned sequences.

Mac-1 role in miR-155 regulation

In this section, it was analysed the potential role of Mac-1 in regulating the expression of miR-155.

BMDMs and RAW 264.7 macrophages were treated with antibodies blocking CD11b, the ligand-binding subunit of Mac-1, before LPS stimulation and RNA extraction.

Inhibition of Mac-1 receptor in LPS-induced BMDMs did not affect the induction of miR-155, which remained comparable to controls (Figure 5.7 a). Similarly, levels of miR-155 did not vary in a statistically significant manner in CD11b-inhibited RAW 264.7 cells and controls both at 8 and 24 hours after LPS stimulation (Figure 5.7 b). Additionally, the introduction of an isotype antibody control showed that the evident but not significant reduction of miR-155 levels in cells treated with the CD11b blocking antibody was likely not linked to Mac-1 inhibition. Both CD11b and isotype control antibodies endotoxin contamination levels were certified by the manufacturer as <0.01 EU/μg.

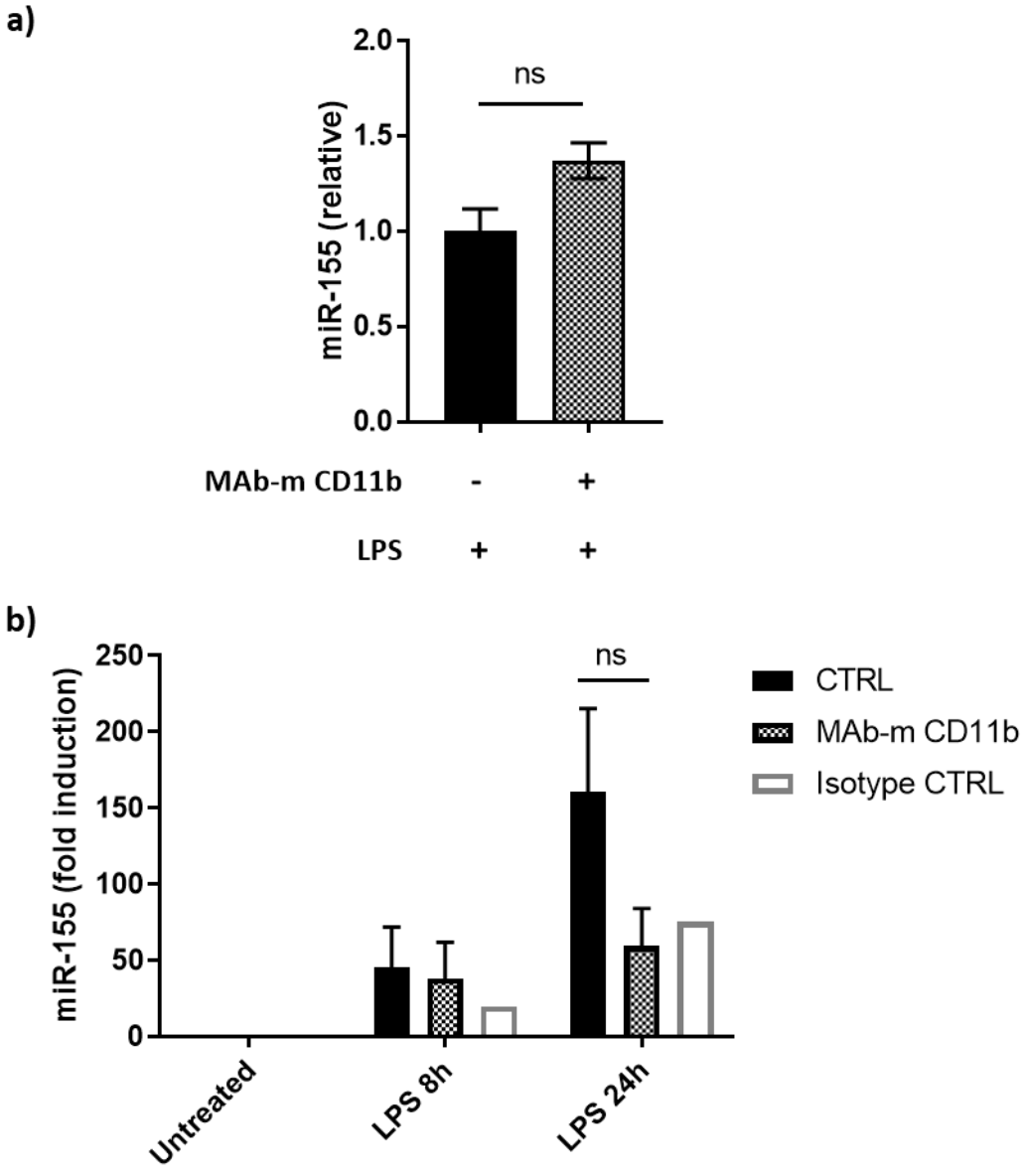


Figure 5.7 Role of Mac-1 in regulating miR-155 expression in BMDMs and RAW 264.7 cells.
a) Total RNA was extracted from *tnc+/+* and *tnc-/-* BMDMs, stimulated with 100ng/ml LPS for 24 hours, in the presence or absence of 25μg/ml LEAF™ anti-CD11b antibody (MAb-m CD11b). Expression levels of mature miR-155 were measured by qPCR. snU6 was used as endogenous housekeeping gene and non-inhibited *tnc+/+* samples used as calibrators (ΔΔCt method). Data from one experiment are represented as mean relative induction ± SD, from triplicate measurements. **b**) Total RNA extracted from RAW 264.7 cells, stimulated with 100ng/ml LPS for 24 hours, in the presence or absence of 10μg/ml monoclonal Ultra-LEAF™ anti-CD11b antibody or isotype control. Expression levels of mature miR-155 were measured by qPCR. snU6 was used as endogenous housekeeping gene and non-inhibited untreated control was used as calibrator (ΔΔCt method). Data from 3 independent experiments are represented as mean fold induction ± SEM (isotype control n=1).

5.2.2 Neuropilin-1 (NRP1)

Neuropilin 1 (NRP1) is the best-known member of the neuropilin family of transmembrane co-receptors, which also includes the NRP1 homologous isoform, neuropilin-2 (NRP2). The importance of neuropilins in immune responses and inflammation has only recently been discovered, and little is known about their roles in regulating immune reactions. Despite being highly similar, NRP1 and NRP2 play distinct and sometimes opposite roles in immunity [562].

Expression of NRP1 and NRP2 was measured by qPCR 24 hours after LPS-induction of RAW 264.7 cells (Figure 5.8). Neuropilins expression was differently affected by LPS, with detectable but not significant changes: NRP1 mRNA was partially downregulated by LPS, while NRP2 expression was induced upon LPS-activation.

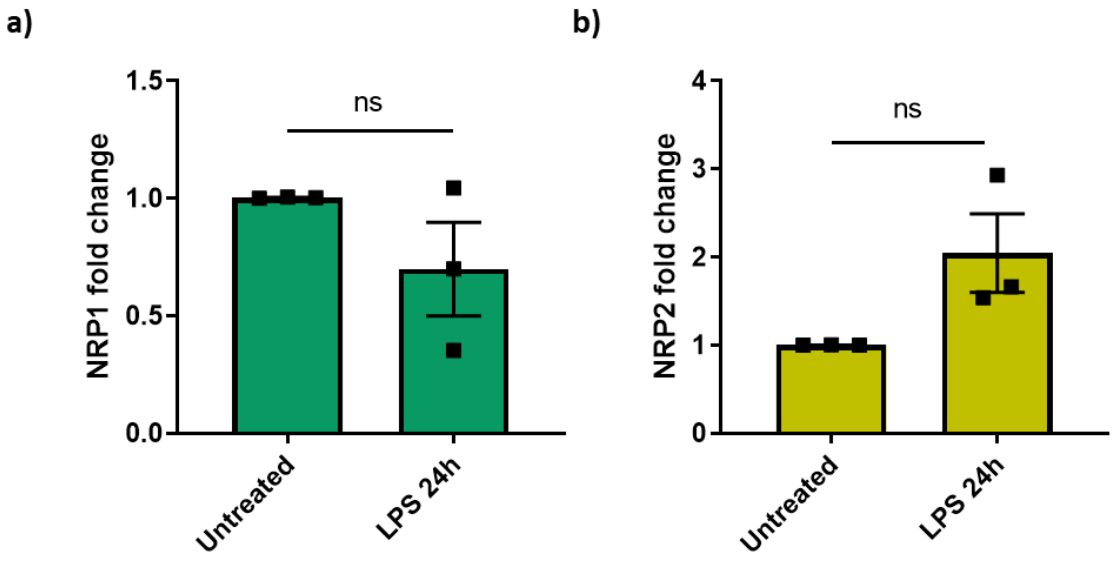


Figure 5.8 Expression of NRP1 and NRP2 in RAW 264.7 macrophages upon LPS stimulation.
RAW 264.7 cells were stimulated with LPS for 24 hours, before RNA extraction. Expression levels of NRP1 **a)** and NRP2 **b)** were measured by qPCR. HPRT1 was used as endogenous housekeeping gene, and untreated samples were used as calibrator ($\Delta\Delta$Ct method). Data from 3 independent experiments are represented as mean fold change ± SEM.

The expression of miR-155 was then analysed to investigate the potential role of NRP1 in RAW 264.7 cells. Before LPS activation for 24 hours and RNA extraction, cells were transfected with either siRNAs targeting NRP1 or NRP2 or non-targeting siRNA controls.

The efficiency of siRNA transfection was confirmed by measuring NRP1 and NRP2 mRNA levels in RAW 264.7 cells by qPCR. NRP1 levels were between 54 and 63% lower than controls, while NRP2 levels decreased by 44 to 53% (Figure 5.9 a and b).

NRP1 knock-down led to increased levels of miR-155 at steady-state, while NRP2 knock-down did not affect macrophage expression of miR-155, which remained similar to control cells. However, 24 hours after LPS activation, levels of miR-155 were overall similarly induced in all conditions (Figure 5.9 c).

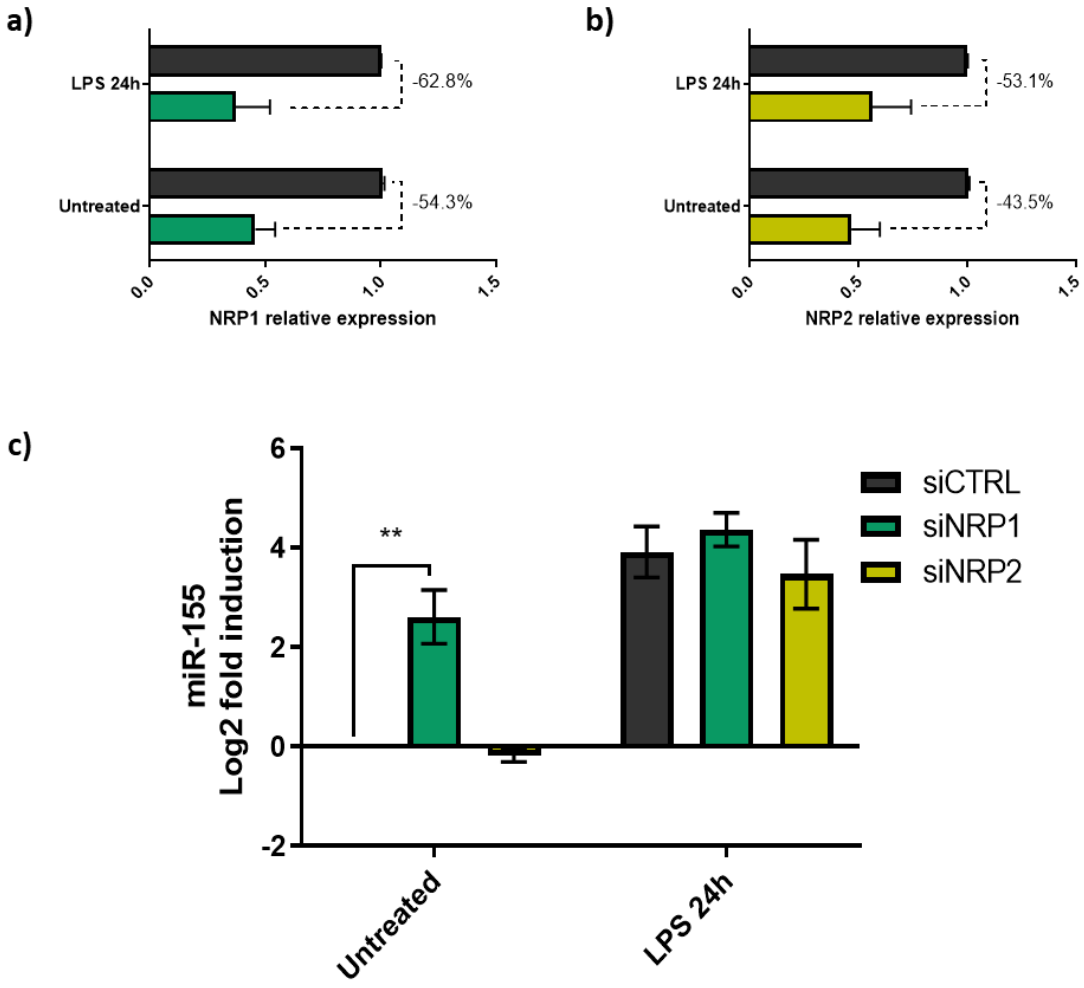


Figure 5.9 Expression of miR-155 in RAW 264.7 macrophages is affected by NRP1 knock-down but not by NRP2.

RAW 264.7 cells were transfected for 72 hours with non-targeting control, NRP1 or NRP2 siRNAs and stimulated with LPS for 24 hours before RNA extraction. **a)** Expression levels of mature miR-155 were measured by qPCR. snU6 was used as endogenous housekeeping gene, and untreated siCTRL samples were used as calibrator (ΔΔCt method). Data represented as mean log2 fold induction ± SEM. ** = $p<0.01$; two-way Anova with Sidak's post-hoc test. **b)** NRP1 transcripts were measured by qPCR using HPRT1 as endogenous housekeeping gene. Relative expression of NRP1 was calculated using siCTRL as calibrator (ΔΔCt method). **c)** Relative expression of NRP2 was measured and calculated as explained in b). Data represent 3 independent experiments.

5.3. Discussion

Tenascin-C triggers intracellular signalling pathways by interacting with different cell surface receptors in health and disease in a time- and space-dependent manner. Its multimeric domain structure allows tenascin-C to bind to a varied range of receptors, activating distinct molecular pathways, depending on the cell type involved.

In this chapter, experimentally validated and novel candidate tenascin-C receptors expressed by macrophages were tested for their ability to modulate miR-155 expression during LPS-induced inflammation.

The first receptor to be tested was TLR4, known to be activated by both LPS and tenascin-C [64, 356]. Poly(I:C) and TNF-α were used instead of LPS as macrophage activators and miR-155 inducers to investigate the specific effect of tenascin-C on TLR4. Expression of miR-155 was not affected by TLR4 blockade in any of the conditions tested. However, TNF-α stimulation of RAW 264.7 macrophages resulted in low induction of miR-155 expression and represented only a single experiment. Notably, miR-155 levels were previously found to be induced to approximately 15-fold in 24-hour TNF-α activated BMDMs (Chapter 3, Figure 3.1 d), similarly to Mann et al. (2018), who reported miR-155 induction as being up to 40-fold over the control in the same cells and conditions [208]. Moreover, as shown in Chapter 3, Figure 3.1b, previous experiments in RAW 264.7 found that levels of miR-155 were induced by at least 10-fold upon TNF-α treatment, indicating suboptimal miR-155 induction in this instance. Previous results (Chapter 3, section 3.1) showed that tenascin-C regulates miR-155 levels in LPS- and TNF-α–induced, but not poly(I:C)-induced macrophages. One main difference between these inducers is the localisation of their binding

receptors, namely TLR4 and TNFR on plasma membranes and TLR3 on endosomal membranes. Also, contrary to TLR4 and TNFR [365, 577], activation of TLR3 does not induce tenascin-C expression [365], suggesting that the TLR3 signalling pathway could be tenascin-C-independent.

Poor results with TNF-α stimulation of RAW 264.7 and previous indications of a tenascin-C-mediated regulation in TNFR induction of miR-155 prompts to repeat the experiment with the TLR4 inhibitor, which could be further improved with additional LPS-treatment positive controls to test that TLR4 inhibition could reduce miR-155 expression.

In addition to TLR4, tenascin-C is known to bind to several macrophage-expressed integrins to induce the production of cytokines, chemokines, and activation of pro-inflammatory pathways, as summarised in Table 21. Integrins are fundamental mediators in the communication of extracellular signals to cells. Blocking of integrin β1, α5β1 and αvβ3 in *tnc+/+* BMDMs did not show significant variations in levels of miR-155 in LPS-activated macrophages. In this instance, the same experiment was not carried out in *tnc-/-* BMDMs to analyse if the selected receptors could regulate miR-155 expression in the first place.

Nevertheless, a 4-fold upregulation of miR-155 was observed in cells in which α5β1 and αvβ3 were inhibited. A similar non-significant induction of miR-155 was also noticed when blocking the EGF receptor. However, LPS contamination of function-blocking antibodies against integrin α5β1 and EGFR and cRGD peptide targeting integrin αvβ3 is the most likely cause of the unexpected up-regulation of miR-155.

Therefore, to analyse any aspecific miR-155 induction in untreated cells caused by endotoxin contamination, the experiment should be repeated with antibodies, peptide-only control, or, more importantly, include an LPS inhibitor Polymyxin B control. Ideally, endotoxin content of antibodies and peptide should be quantified by LAL assay and, when using function-blocking antibodies, isotype controls should be included to exclude any non-specific effects.

Alternatively, receptors could be temporarily knocked down by siRNAs. This solution would reduce unwonted activation of macrophages, avoid potential tenascin-C binding to non-blocked epitopes on the receptor and allow the study of specific tenascin-C ligands, including integrin subunit α9. Indeed, blocking of α9 integrin in human synovial macrophages activated by tenascin-C resulted in reduced TNF-α and IL-1β production [373], as well as reducing expression of IL-6 in murine synovial macrophages [371].

The possibility that tenascin-C could be regulating gene expression through a yet unknown binding partner was also considered. Mac-1 and NRP1 were identified as two potential candidates based on the scientific literature and *in silico* prediction of binding.

In silico analysis of Mac-1 ligand, FBG-γ, and the FBG domain of tenascin-C corroborated the hypothesis that tenascin-C could interact with Mac-1 when expressed as an insoluble protein assembled into the ECM. The primary binding peptide for Mac-1 on FBG-γ, P2-C, is buried in a cryptic site in the soluble form of the protein. However, it becomes exposed when deposited in the extracellular matrix [578]. Similarly, tenascin-C peptide I2179-R2187 (IQFAEMKLR), which is located in the

same 3D-structural position as FBG-γ and has similar biochemical properties, could present itself to Mac-1 only once integrated into the ECM. Therefore, the structural protein requirements for binding will have to be considered when confirming the interaction between tenascin-C and Mac-1, for example, through protein binding assays, co-immunoprecipitation or co-localisation analysis.

Despite the predicted tenascin-C and Mac-1 interaction, experimentally, miR-155 did not appear to be affected by the Mac-1 signalling network in macrophages. Indeed, miR-155 levels remained stable upon inhibition of Mac-1 in both BMDMs and RAW 264.7 cells. However, Mac-1 could be regulating TLR signalling pathways in a cell-specific and ligand-specific manner. For example, TLR4-induced cytokine production was found to be affected by Mac-1 subunit CD11b in dendritic cells, but not in steady-state macrophages [540], while Mac-1 could induce pro-inflammatory cytokine production in macrophages upon binding with poly (I:C) [543]. In both studies, Mac-1 was involved in the internalisation of the PAMPs, indicating a possible role for Mac-1 in the endocytosis, while tenascin-C effect seems to activate intracellular signalling through outer membrane receptors.

However, the function-blocking antibody for CD11b used in the experiments was based on clone M1/70, which is known to involve integrin outside-in signalling. Anti-Mac-1 (M1/70) treatment induced aberrant IL-6, TNF-α and CCL2 production in mice circulating serum and cultured peritoneal macrophages [555]. Blockade of the Mac-1 receptor could be verified by measuring macrophage released factors by ELISA. Additionally, to avoid unwonted ligand binding to still available CD11b binding sites

[579], the receptor could be temporarily knock-down in macrophages by siRNA, or BMDMs from Mac-1 knockout mice could be used [540].

However, tenascin-C and Mac-1 depletion seem to have opposite effects on cytokine production [296], with Mac-1 blockade promoting IL-6 and TNF-α expression in thyoglycolate-elicited peritoneal macrophages [540, 555]. Thus, Mac-1 might not be involved in regulating miR-155 expression in light of presented experimental results and literature review. Nevertheless, this does not exclude that tenascin-C and Mac-1 could interact to regulate other cellular events.

Notably, tenascin-C regulation of miR-155 could involve a very early protein-protein interaction on the macrophage cell surface. As seen in Chapter 4 (Figure 4.2), tenascin-C could be detected on the surface of untreated macrophages. Interestingly, miR-155 expression was found to be upregulated in untreated macrophages in which the expression of the transmembrane co-receptor NRP1 was silenced. This effect appeared to be specific as NRP2 knock-down did not affect miR-155 expression.

NRP1 and NRP2 roles in the immune response remain elusive. Analysis of NRP1 and NRP2 mRNA expression in macrophages showed partially opposite effects upon LPS stimulation, with decreasing levels for NRP1 and increasing NRP2. This result was in line with the literature, which shows that NRP1 was downregulated in a TLR4-NF-kB-mediated manner in peritoneal macrophages, BMDMs and RAW 264.7 cells [535], while upregulation of NRP2 by LPS was identified in differentiating human dendritic cells [580].

NRP1 depletion was reported to enhance the susceptibility of mice to LPS-induced sepsis, leading to an enhanced pro-inflammatory cytokine production [535]. In

agreement with this, Oussa et al. (2016) showed that upon specific binding to VEGF, NRP1 could bind to TLR4, inhibiting LPS-dependent BMDC maturation and secretion of cytokines such as IL-6, IL-12 and TNF-α. Interestingly, TLR3 and TLR9 signalling were not affected by VEGF and NRP1 [549].

The indication that NRP1 could negatively regulate inflammation suggests that tenascin-C and NRP1 could have opposite effects on cytokine expression during LPS challenge *in vivo* [296]. This raises the possibility that tenascin-C and NRP-1 may compete for the same receptor. Upon LPS-activation of TLR4, ECM-associated tenascin-C, which is available before inflammation develops, could bind to one or more of its binding partners, displacing NRP1 and inhibiting its anti-inflammatory function. This event would allow early pro-inflammatory responses involving miR-155 and TNF-α, to occur. At later stages, macrophage released molecules, including soluble tenascin-C, would lead to a switch to reparative phenotypes, enhancing the expression of tissue repair molecules, such as VEGF [356, 518], and activating NRP1.

In agreement with this, NRP1 can interact with several tenascin-C binding partners such as TLR4 [549], integrin $\alpha5\beta1$ in endothelial cells [564] and integrin $\beta1$ in pancreatic ductal adenocarcinoma (PDAC) cells [581]. Therefore, further analysis should focus on the possible interaction between NRP1, tenascin-C and respective ligands. For example, it could be determined if the two proteins co-localise on the cell membrane and can be immunoprecipitated together.

Finally, proteomics analysis of cell membrane proteins that immunoprecipitate together with tenascin-C should be carried out to test our hypothesis. These

experiments would allow us to confirm or rule out candidate tenascin-C-receptor(s) or identify novel binding partner(s).

5.4. Summary

In this chapter, experimentally validated and novel candidate tenascin-C receptors were analysed for their ability to regulate miR-155 expression. Preliminary experiments suggested that, among the validated tenascin-C receptors, TLR4, β1 and αvβ3 integrins and EGFR might not be involved in regulating miR-155. However, further experiments are necessary to confirm or rule out the potential role of integrin α9β1 and TLR4.

Amongst the novel candidate receptors, Mac-1 emerged as a potential binding partner for tenascin-C in *silico* analysis. However, Mac-1 was not linked to the expression of miR-155 when blocked with the anti-CD11b (clone M1/70) antibody. Thus, Mac-1 gene depletion or complete blockade of Mac-1 function should be performed to be able to exclude Mac-1 as a miR-155 regulator. On the other hand, miR-155 expression increased in the absence of NRP1, but not NRP2. Therefore, further studies should focus on understanding if tenascin-C and NRP1 are competing for and binding to the same receptor to regulate miR-155 expression. Finally, through tenascin-C pull-down and proteomics analyses, it will be possible to identify if other receptor(s) or co-receptor(s) interact with tenascin-C to regulate miR-155 expression.

Chapter 6. Final Discussion

A prompt and effective yet self-limited immune response requires fine-tuning of pro-inflammatory gene expression. In this context, the expression of miRNAs such as miR-155 requires tight control, with pathological effects when the balance is lost.

In this context, tenascin-C, an ECM glycoprotein specifically induced during inflammation and the immune response [64, 296, 365], was found to regulate the expression of miR-155 in LPS induced macrophages [296], revealing a novel mechanism of regulation of miRNA biogenesis. Thus, this work aimed to shed light on the role of tenascin-C in the regulation of miR-155.

For the first time, it was demonstrated that tenascin-C-mediated regulation of miR-155 is linked explicitly to activation of receptors that localise on the cell surface, such as TLR4 and TNFR, while it does not affect endosomal receptors, such as TLR3. The internalisation of receptors is involved in activating specific intracellular pathways and involves different adaptor proteins and factors (reviewed in [582, 583]). Similarly to miR-155 [208, 264], tenascin-C expression is also induced by TNF-α and LPS through an NF-kB-dependent mechanism [365, 584], while Poly(I:C) does not promote tenascin-C expression in human MDDC cells [365]. It seems, therefore, reasonable to ask whether the absence of tenascin-C could affect NF-kB-mediated transcription of miR-155. Nevertheless, the lack of tenascin-C was not found to affect miR-155 transcription or splicing. Together, this suggested that tenascin-C regulated miR-155 processing, following its NF-kB-mediated transcription induced by LPS.

Tenascin-C was found involved in a post-transcriptional event of miR-155 biogenesis, leading to defective processing of pri-miR-155 into pre-miR-155. This defect was likely due to the reduced efficiency of Drosha-mediated cleavage for pri-miR-155 in cells without tenascin-C. However, further work will need to confirm this finding.

The regulation exerted by tenascin-C is not limited to miR-155 but includes selected LPS-induced miRNAs [296], likely regulated by miRNA-specific RBPs.

Nevertheless, the analysis of miR-155-associated candidate RBPs, KH-SRP, ZNF-385A, ZNF-346 and TTP, could not clarify if these are involved in the tenascin-C mediated regulation. It was surprising to find that lack of tenascin-C negatively influenced TTP mRNA levels. However, we could not detect any difference in protein expression and cellular localisation for TTP, nor for KH-SRP, ZNF-385A and ZNF-346. This result was not unexpected since the effect on pri-miR155 regulation that we detected appeared to occur very early, between 2 and 4 hours after LPS stimulation. The protein(s) involved in miR-155 biogenesis would either need to be produced exceptionally rapidly or be already expressed and activated through post-translational regulators. Notably, it is known that different phosphorylation events can activate KH-SRP [327] and ZNF-385A [356]. Alternatively, phosphorylation of TTP by the MAPK p38/MK2 pathway stabilises the protein, but it decreases its RNA-binding capacity, inactivating it [499].

The idea that tenascin-C would regulate the expression of inflammatory molecules such as miR-155, TNF-α and IL-6 through activation of the MAPK p38 signalling is very enticing but not surprising. Indeed, the FBG domain of tenascin-C is known to induce phosphorylation of p38α and p38β in human M-CSF-MDMs (Monocyte Derived

Macrophages) [356]. Without tenascin-C, the MAPK p38 activation might be impaired, resulting in increased activation of TTP and degradation of TNF-α mRNA [499, 508]. Similarly to what was found for tenascin-C [296], LPS-induced MK2-deficient macrophages showed reduced TNF-α protein expression but no differences in mRNA levels [585, 586]. Moreover, de-regulated MK2-activation could also explain differences in expression of miR-155 and other RBPs-associated miRNAs found in tenascin-C knock-out cells compared to wild type cells. MK2-mediated phosphorylation of p68 was required for its nuclear translocation and promotion of processing of selected pri-miRNAs in MEFs [587]. RNA helicases p68 and p72 can interact with Drosha, influencing Microprocessor cleavage, and influence miRNA biogenesis of miRNAs possibly regulated by tenascin-C, like miR-15a, miR-15b, miR-145 and miR-9 [220, 221, 588].

Interestingly, the specific tenascin-C-mediated regulation of miR-155 biogenesis is linked to the activation of receptors on the outer cell membrane. Indeed, tenascin-C can be found in different forms, including soluble (in biological fluids) and insoluble (ECM-associated), and isoforms, resulting from alternative splicing, which can exert different function, depending on the inflammatory cellular microenvironment context [392]. However, it remained to be clarified in which form tenascin-C can regulate miR-155 expression.

LPS activation of macrophages induced tenascin-C transcription and abundant soluble tenascin-C protein in the cell supernatants. However, insoluble tenascin-C protein was found to detected extracellularly around the macrophage cell membrane also at steady-state, at levels similar to LPS-induced cells.

In vivo, high levels of tenascin-C are found in synovial joints [365, 509, 510] and serum of rheumatoid arthritis patients [589]. Interestingly, the ECM-associated and soluble tenascin-C seem to have different effects on intracellular signalling cascades. For example, tenascin-C promotes Wnt signalling by interacting with Wnt3a and stabilising β-catenin when human adenocarcinoma cells are seeded on tenascin-C coated plates. However, treatment of the same cells with soluble tenascin-C reduces Wnt signalling, possibly by sequestering available Wnt ligands, preventing them from interacting with cell membrane receptors for signalling activation [590]. Similarly, here we showed that soluble tenascin-C did not rescue but further inhibited cytokine synthesis in *tnc*-/- BMDMs, while surface-bound tenascin-C could re-establish miR-155 expression in *tnc*-/- BMDMs back to wild type levels. Thus, it could be that soluble, *de novo* synthesized tenascin-C, which is made later when the inflammatory response is already established, acts as a DAMP competing with LPS for TLR4, explaining inhibition of cytokine synthesis when recombinant tenascin-C is added to BMDMs in the presence of LPS. Whereas ECM-associated tenascin-C, which forms large hexamers and is readily available at steady state, could trigger the formation of a different receptor/co-receptor complex, enhancing miR-155 expression during the very early response to infection and injury.

Notably, other ECM molecules have been shown to contribute to miRNA regulation, in addition to tenascin-C. For example, excessive deposition of collagen by breast cancer cells promoted the expression of miR-18a, contributing to tumour progression by targeting PTEN [362]. Moreover, the antiangiogenic protein thrombospondin (TSP)2 downregulated miR-29, contributing to decreased fibrillar collagen crosslinking in mouse dermal fibroblasts [591]. Finally, the pericellular proteoglycan

decorin negatively regulated miR-21 expression by inhibiting TGF-β signalling in LPS –induced macrophages [56]. However, the involvement of the ECM and its components in miRNA regulation is underinvestigated, and further research is required to elucidate the molecular mechanisms underpinning it.

Therefore, we optimised a physiological CDM model to recapitulate the three-dimensional microenvironment inclusive of the ECM, macrophages and signalling molecules. This model was utilised to investigate the role of ECM-associated tenascin-C in miRNA regulation. Fibroblasts, the most abundant cellular source of ECM, were chosen as cell factories to deposit ECMs inclusive of tenascin-C. During the characterisation of this model, we uncovered how the absence of tenascin-C affected fibronectin deposition. Indeed, tenascin-C is involved in the production and incorporation of fibronectin in skin lesions [370], and the lack of tenascin-C in mice induced less fibronectin in response to skin and corneal wound healing [430, 470],

By applying the model we developed, we could demonstrate that adult CDM-expressed tenascin-C specifically regulates miR-155 during the LPS-response in macrophages. Conversely, tenascin-C assembled within embryonic tissues expressed similar levels of miR-155 to negative controls.

Differences in isoform and post-translational modifications are known to be pivotal for specific tenascin-C functions [392]. To that extent, we showed that MEF and adult skin FB CDMs expressed different putative isoforms of tenascin-C.

Selective exclusion of alternatively spliced isoforms has been reported for tenascin-C expressed in myeloid cells. Specifically, the alternatively spliced forms, including the AD2AD1 domain, were not upregulated in LPS-responding MDDCs, thus eluding

AD2AD1 domain inhibitory effect on chemotaxis and cytokine release [519]. Others found that alternatively spliced tenascin-C isoform containing FnIII A1A2 domains could block T-cell polarization by inhibiting T-cell receptor complex internalisation [474]. In addition, specific tenascin-C isoforms could contain cryptic binding sites for cell-membrane receptors and ECM molecules such as the integrin $\alpha7\beta1$ binding site included in the alternatively spliced FnIII D domain that is involved in neurite outgrowth in rats [531]. Indeed, to induce intracellular signalling, tenascin-C can directly interact with several receptors on the cell membrane. However, it remained to define what cell membrane receptor was linked to tenascin-C for the regulation of miR-155.

Analyses of experimentally validated tenascin-C receptors, TLR4, integrins $\alpha9\beta1$, $\alpha v\beta3$ and $\alpha5\beta1$, and EGFR, did not seem to link to miR-155 expression per se. However, certain aspects and issues with cell treatments should be considered when interpreting the results obtained, leaving still open questions on the involvement of receptors like TLR4 and integrins.

On the other side, through the analysis of novel tenascin-C candidate receptors, such as Mac-1, we could identify putative binding sites for Mac-1 on tenascin-C *in silico*. These sites would allow interaction between the two proteins when tenascin-C is integrated into the ECM, similarly to FBG-γ [578].

However, blocking CD11b revealed that the ligand-binding subunit of the Mac-1 receptor was not involved in regulating miR-155 expression. Cell-specific events could be regulating Mac-1 outside-in signalling. Indeed, cytokine and chemokine production was found upregulated in thioglycolate-elicited peritoneal macrophages

where CD11b was either blocked with a function-blocking antibody (clone M1/70) or measured from CD11b knock-out mice [540, 555]. In contrast, cytokine and chemokine expression was not affected in CD11b-/- BMDMs and resident peritoneal macrophages [540]. If true, the predicted interaction between tenascin-C and Mac-1 might involve other cellular events rather than miR-155 expression. Mac-1 plays an important role in immune cell recruitment, adhesion and mobility. In mice with depleted FBG-γ binding site for Mac-1, leukocytes cannot clear peritoneal bacteria [592]. Defective macrophage migration and adhesion were observed in Mac-1 knock-out mice, leading to a reduced macrophage migration to the lymphatic system [593]. Moreover, Mac-1 could regulate phagocytosis by inducing actin cytoskeletal reorganisation through FAK activation [594]. Tenascin-C could be binding to Mac-1 receptor to contribute to cellular mobility and adhesion [518, 519] and cytoskeletal reorganisation [570]. Additionally, tenascin-C and Mac-1 interaction could be regulating the release of late inflammatory molecules such as HMGB1, which was differentially regulated in septic *tnc-/-* mice [296, 542].

Ultimately, the cell membrane receptor involved in the tenascin-C-mediated regulation of miR-155 remained elusive at this stage. However, we found that the cell membrane co-receptor NRP1 was involved in maintaining miR-155 levels at steady state in LPS-unstimulated macrophages. As seen in Chapter 4, the basal expression of tenascin-C surrounding cells in unstimulated macrophages indicated that tenascin-C might be required before initiating an immune response in cells. There is substantial correspondence between several NRP1 and tenascin-C binding partners, which include TLR4 [64, 549], fibronectin and integrin $\alpha5\beta1$ [452, 455, 564, 565], integrin $\alpha\nu\beta3$ [456, 595], VEGF [450, 564] and TGF-β [533, 545]. Noticeably, VEGF-induced

activation of NRP1 promoted specific NRP1 binding to TLR4 in LPS-induced BMDCs, inhibiting the production of IL-6, IL-12 and TNF-α [549]. However, TLR3 was not activated by NRP1/VEGF, similarly to what seen for tenascin-C. Tenascin-C and NRP1 seemed to have opposite effects on inflammation, possibly competing for the same cell membrane receptors. At steady-state and early stages of inflammation, tenascin-C could bind to cell membrane receptors, such as integrin $\alpha5\beta1$ or $\alpha v\beta3$, preventing them from binding to NRP1. Alternatively, tenascin-C could sequester NRP-1, preventing it from binding to VEGF and cell membrane receptors. Thus, inactivated NRP1 would not exert its anti-inflammatory effects until activated by soluble factors released later during inflammation, like VEGF.

Finally, tenascin-C and NRP1 could be linked in their intracellular effect by activating FAK signalling and YAP regulation, ultimately controlling miRNA expression [221]. Indeed, in cancer cells, tenascin-C could inhibit YAP by activating integrins $\alpha9\beta1$ or $\alpha5\beta1$, leading to YAP phosphorylation and cytoplasmic localisation [596, 597], while NRP1 could promote YAP activity via integrin $\alpha6\beta4$ [598].

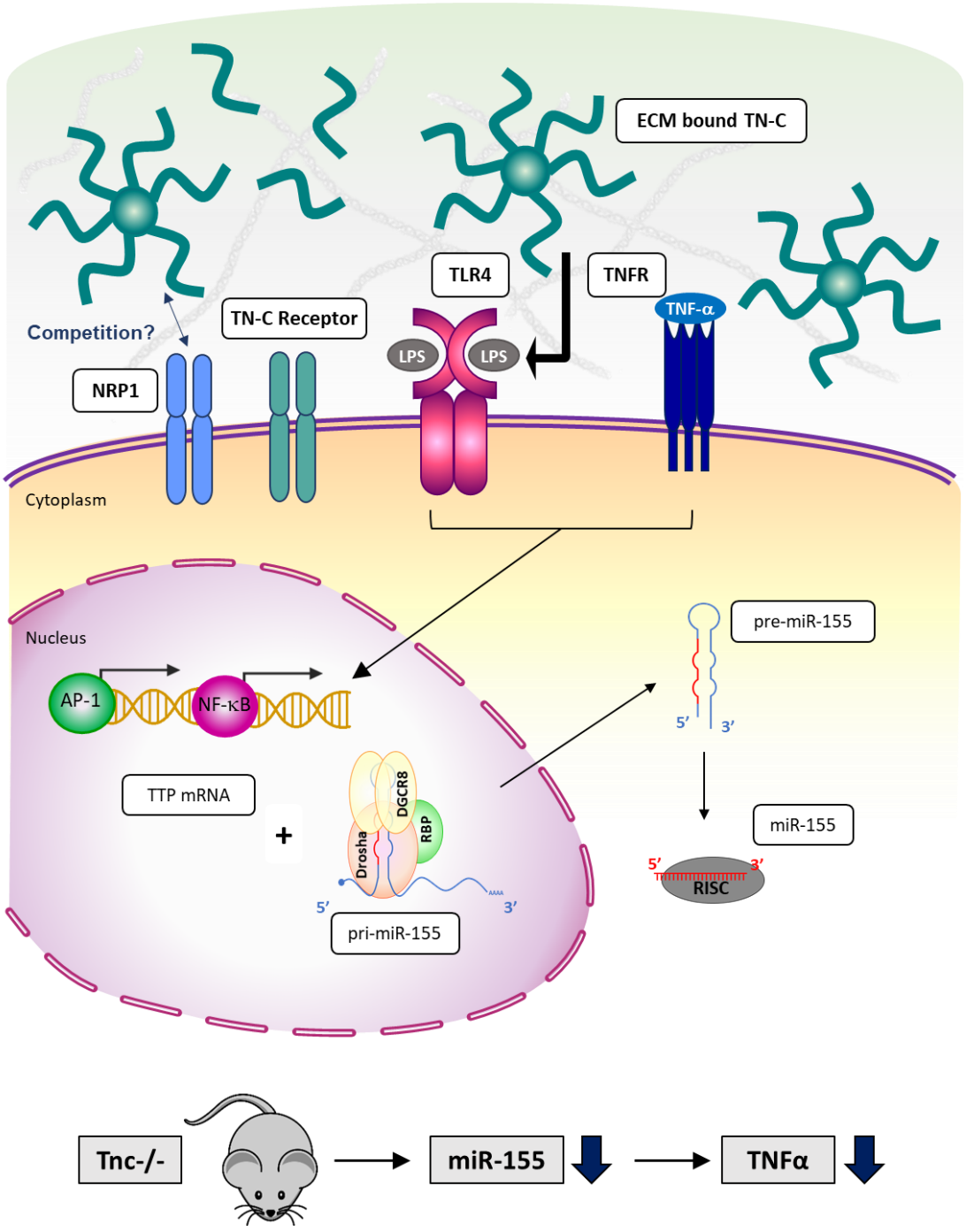


Figure 6.1 Summary of discoveries.

Expression of miR-155 was found to be regulated by tenascin-C (TN-C) during LPS- and TNF-α-induced immune responses in macrophages. Tenascin-C needs to be localised on the outer cellular membrane and assembled into the ECM to regulate miR-155 expression. We hypothesised that only the ECM-bound tenascin-C has the necessary conformation to interact with the cell membrane-bound receptor(s), transducing the outside-in signalling for miR-155 regulation. The TN-C receptor remains unknown at this stage, but neuropilin-1 (NRP1) was identified as a possible antagonist of tenascin-C regulating miR-155 at steady state. During early LPS-induction, the lack of tenascin-C induced lower TTP mRNA expression, and deficient Drosha-mediated cleavage of pri-miR-155, resulting in lower levels of pre-miR-155 in the cytoplasm. The reduced availability of pre-miR155 led to express lower levels of mature miR-155, previously linked to reduced TNF-α production and release.

6.1. Concluding Remarks and Future work

In conclusion, this work revealed a novel mechanism of control of the innate immune response in LPS-induced macrophages, possibly extending to other types of infection, cancer and autoimmunity. This mechanism included regulation of miR-155, a master regulator of immunity whose expression is dysregulated in patients with tuberculosis, pneumonia and sepsis [164, 599], where its upregulation correlates with tenascin-C levels and disease severity [296, 476]. Beyond infection, miR-155 and tenascin-C prognostic significance has been confirmed in cancer and autoimmune disorders such as rheumatoid arthritis [64, 308]. Thus, understanding the molecular mechanisms involved in innate immunity activation could identify novel targets to prevent excessive and chronic inflammation.

Future plans will include:

- To determine if tenascin-C regulates miR-155 expression in infection models different from Gram-negative bacteria, using intact microbes and *in vivo* models.
- To identify tenascin-C-regulated RBP(s) involved in Drosha-mediated cleavage of pri-miR-155 by pull-down of Drosha in *tnc+/+* and *tnc-/-* BMDMs, followed by mass spectrometry analysis of proteins.
- To identify other potential pri-miRNAs regulated by tenascin-C by RIP-seq following Drosha IP from *tnc+/+* and *tnc-/-* cell lysates.
- To investigate the role of tenascin-C in TTP expression and regulation. Analyses of RNA precipitates after pull-down of TTP protein to measure any

difference in RNA binding in known TTP targets, including TNF-α mRNA, and novel candidates, such as pri-miR-155.

- To analyse the activation of p38 MAPK pathways in *tnc+/+* and *tnc-/-* cells and link it to possible differential activation of p72 and p68 Microprocessor components, which would regulate miRNA biogenesis.
- To determine the exact localisation and pericellular expression of tenascin-C in BMDMs, by detecting tenascin-C in combination with cell-membrane and ECM components.
- To confirm the requirements for tenascin-C form in regulating miR-155 expression by completing miR-155 rescue experiments in *tnc-/-* BMDMs with CDMs from skin fibroblasts and, additionally, CDMs deposited by *tnc+/+* BMDMs.
- To identify the tenascin-C-binding receptor involved in miR-155 expression using an unbiased approach such as tenascin-C pull-down in macrophages followed by mass spectrometry analysis. In parallel, pursue candidate approach analysis, using siRNA knock-down in macrophages.

Chapter 7. Bibliography

1. Janeway, C.A., Jr., *Approaching the asymptote? Evolution and revolution in immunology.* Cold Spring Harb Symp Quant Biol, 1989. **54 Pt 1**: p. 1-13.
2. Kono, H. and K.L. Rock, *How dying cells alert the immune system to danger.* Nat Rev Immunol, 2008. **8**(4): p. 279-89.
3. Gong, T., et al., *DAMP-sensing receptors in sterile inflammation and inflammatory diseases.* Nat Rev Immunol, 2019.
4. Matzinger, P., *Tolerance, danger, and the extended family.* Annu Rev Immunol, 1994. **12**: p. 991-1045.
5. Beutler, B., *Neo-ligands for innate immune receptors and the etiology of sterile inflammatory disease.* Immunol Rev, 2007. **220**: p. 113-28.
6. Gordon, S., *Pattern recognition receptors: doubling up for the innate immune response.* Cell, 2002. **111**(7): p. 927-30.
7. Orkin, S.H. and L.I. Zon, *Hematopoiesis: an evolving paradigm for stem cell biology.* Cell, 2008. **132**(4): p. 631-44.
8. Epelman, S., K.J. Lavine, and G.J. Randolph, *Origin and functions of tissue macrophages.* Immunity, 2014. **41**(1): p. 21-35.
9. Swirski, F.K., et al., *Identification of splenic reservoir monocytes and their deployment to inflammatory sites.* Science, 2009. **325**(5940): p. 612-6.
10. Leuschner, F., et al., *Rapid monocyte kinetics in acute myocardial infarction are sustained by extramedullary monocytopoiesis.* J Exp Med, 2012. **209**(1): p. 123-37.
11. Takeuchi, O. and S. Akira, *Pattern recognition receptors and inflammation.* Cell, 2010. **140**(6): p. 805-20.
12. Lau, C.M., et al., *RNA-associated autoantigens activate B cells by combined B cell antigen receptor/Toll-like receptor 7 engagement.* J Exp Med, 2005. **202**(9): p. 1171-7.
13. Qin, C., et al., *Critical Role of P2Y12 Receptor in Regulation of Th17 Differentiation and Experimental Autoimmune Encephalomyelitis Pathogenesis.* J Immunol, 2017. **199**(1): p. 72-81.
14. Akira, S., S. Uematsu, and O. Takeuchi, *Pathogen recognition and innate immunity.* Cell, 2006. **124**(4): p. 783-801.
15. Janeway, C.A., Jr. and R. Medzhitov, *Innate immune recognition.* Annu Rev Immunol, 2002. **20**: p. 197-216.
16. Cao, X., *Self-regulation and cross-regulation of pattern-recognition receptor signalling in health and disease.* Nat Rev Immunol, 2016. **16**(1): p. 35-50.
17. Mogensen, T.H., *Pathogen recognition and inflammatory signaling in innate immune defenses.* Clin Microbiol Rev, 2009. **22**(2): p. 240-73, Table of Contents.
18. Zelensky, A.N. and J.E. Gready, *The C-type lectin-like domain superfamily.* FEBS J, 2005. **272**(24): p. 6179-217.
19. Yamasaki, S., et al., *C-type lectin Mincle is an activating receptor for pathogenic fungus, Malassezia.* Proc Natl Acad Sci U S A, 2009. **106**(6): p. 1897-902.
20. Mayer, S., et al., *C-Type Lectin Receptor (CLR)-Fc Fusion Proteins As Tools to Screen for Novel CLR/Bacteria Interactions: An Exemplary Study on Preselected Campylobacter jejuni Isolates.* Front Immunol, 2018. **9**: p. 213.

21. Bermejo-Jambrina, M., et al., *C-Type Lectin Receptors in Antiviral Immunity and Viral Escape.* Front Immunol, 2018. **9**: p. 590.

22. Suzuki, Y., et al., *Involvement of Mincle and Syk in the changes to innate immunity after ischemic stroke.* Sci Rep, 2013. **3**: p. 3177.

23. Yoneyama, M., et al., *Shared and unique functions of the DExD/H-box helicases RIG-I, MDA5, and LGP2 in antiviral innate immunity.* J Immunol, 2005. **175**(5): p. 2851-8.

24. Yoneyama, M., et al., *The RNA helicase RIG-I has an essential function in double-stranded RNA-induced innate antiviral responses.* Nat Immunol, 2004. **5**(7): p. 730-7.

25. Roers, A., B. Hiller, and V. Hornung, *Recognition of Endogenous Nucleic Acids by the Innate Immune System.* Immunity, 2016. **44**(4): p. 739-54.

26. Takahasi, K., et al., *Solution structures of cytosolic RNA sensor MDA5 and LGP2 C-terminal domains: identification of the RNA recognition loop in RIG-I-like receptors.* J Biol Chem, 2009. **284**(26): p. 17465-74.

27. Nallagatla, S.R., et al., *5'-triphosphate-dependent activation of PKR by RNAs with short stem-loops.* Science, 2007. **318**(5855): p. 1455-8.

28. Li, X.D., et al., *Pivotal roles of cGAS-cGAMP signaling in antiviral defense and immune adjuvant effects.* Science, 2013. **341**(6152): p. 1390-4.

29. Rathinam, V.A., et al., *The AIM2 inflammasome is essential for host defense against cytosolic bacteria and DNA viruses.* Nat Immunol, 2010. **11**(5): p. 395-402.

30. Li, T. and Z.J. Chen, *The cGAS-cGAMP-STING pathway connects DNA damage to inflammation, senescence, and cancer.* J Exp Med, 2018. **215**(5): p. 1287-1299.

31. Komada, T., et al., *Macrophage Uptake of Necrotic Cell DNA Activates the AIM2 Inflammasome to Regulate a Proinflammatory Phenotype in CKD.* J Am Soc Nephrol, 2018. **29**(4): p. 1165-1181.

32. Takaoka, A., et al., *DAI (DLM-1/ZBP1) is a cytosolic DNA sensor and an activator of innate immune response.* Nature, 2007. **448**(7152): p. 501-5.

33. Gong, T., W. Jiang, and R. Zhou, *Control of Inflammasome Activation by Phosphorylation.* Trends Biochem Sci, 2018. **43**(9): p. 685-699.

34. Halle, A., et al., *The NALP3 inflammasome is involved in the innate immune response to amyloid-beta.* Nat Immunol, 2008. **9**(8): p. 857-65.

35. Bell, J.K., et al., *Leucine-rich repeats and pathogen recognition in Toll-like receptors.* Trends Immunol, 2003. **24**(10): p. 528-33.

36. Bryant, C.E., et al., *Advances in Toll-like receptor biology: Modes of activation by diverse stimuli.* Crit Rev Biochem Mol Biol, 2015. **50**(5): p. 359-79.

37. Takeuchi, O., et al., *Cutting edge: role of Toll-like receptor 1 in mediating immune response to microbial lipoproteins.* J Immunol, 2002. **169**(1): p. 10-4.

38. Wyllie, D.H., et al., *Evidence for an accessory protein function for Toll-like receptor 1 in anti-bacterial responses.* J Immunol, 2000. **165**(12): p. 7125-32.

39. Funderburg, N., et al., *Human -defensin-3 activates professional antigen-presenting cells via Toll-like receptors 1 and 2.* Proc Natl Acad Sci U S A, 2007. **104**(47): p. 18631-5.

40. Aliprantis, A.O., et al., *Cell activation and apoptosis by bacterial lipoproteins through toll-like receptor-2.* Science, 1999. **285**(5428): p. 736-9.

41. Takeuchi, O., et al., *Differential roles of TLR2 and TLR4 in recognition of gram-negative and gram-positive bacterial cell wall components.* Immunity, 1999. **11**(4): p. 443-51.

42. Schwandner, R., et al., *Peptidoglycan- and lipoteichoic acid-induced cell activation is mediated by toll-like receptor 2.* J Biol Chem, 1999. **274**(25): p. 17406-9.

43. Boehme, K.W., M. Guerrero, and T. Compton, *Human cytomegalovirus envelope glycoproteins B and H are necessary for TLR2 activation in permissive cells.* J Immunol, 2006. **177**(10): p. 7094-102.

44. Underhill, D.M., et al., *The Toll-like receptor 2 is recruited to macrophage phagosomes and discriminates between pathogens.* Nature, 1999. **401**(6755): p. 811-5.

45. Mariano, V.S., et al., *Recognition of TLR2 N-glycans: critical role in ArtinM immunomodulatory activity.* PLoS One, 2014. **9**(6): p. e98512.

46. Yu, L., L. Wang, and S. Chen, *Endogenous toll-like receptor ligands and their biological significance.* J Cell Mol Med, 2010. **14**(11): p. 2592-603.

47. Lin, Q., et al., *The essential roles of Toll-like receptor signaling pathways in sterile inflammatory diseases.* Int Immunopharmacol, 2011. **11**(10): p. 1422-32.

48. Asea, A., et al., *Novel signal transduction pathway utilized by extracellular HSP70: role of toll-like receptor (TLR) 2 and TLR4.* J Biol Chem, 2002. **277**(17): p. 15028-34.

49. Park, J.S., et al., *Involvement of toll-like receptors 2 and 4 in cellular activation by high mobility group box 1 protein.* J Biol Chem, 2004. **279**(9): p. 7370-7.

50. Klune, J.R., et al., *HMGB1: endogenous danger signaling.* Mol Med, 2008. **14**(7-8): p. 476-84.

51. Park, J.S., et al., *High mobility group box 1 protein interacts with multiple Toll-like receptors.* Am J Physiol Cell Physiol, 2006. **290**(3): p. C917-24.

52. Murakami, S., et al., *Surfactant protein A inhibits peptidoglycan-induced tumor necrosis factor-alpha secretion in U937 cells and alveolar macrophages by direct interaction with toll-like receptor 2.* J Biol Chem, 2002. **277**(9): p. 6830-7.

53. Ohya, M., et al., *Human pulmonary surfactant protein D binds the extracellular domains of Toll-like receptors 2 and 4 through the carbohydrate recognition domain by a mechanism different from its binding to phosphatidylinositol and lipopolysaccharide.* Biochemistry, 2006. **45**(28): p. 8657-64.

54. Yang, D., et al., *Eosinophil-derived neurotoxin acts as an alarmin to activate the TLR2-MyD88 signal pathway in dendritic cells and enhances Th2 immune responses.* J Exp Med, 2008. **205**(1): p. 79-90.

55. Liu, S., et al., *TLR2 is a primary receptor for Alzheimer's amyloid beta peptide to trigger neuroinflammatory activation.* J Immunol, 2012. **188**(3): p. 1098-107.

56. Merline, R., et al., *Signaling by the matrix proteoglycan decorin controls inflammation and cancer through PDCD4 and MicroRNA-21.* Sci Signal, 2011. **4**(199): p. ra75.

57. Alexopoulou, L., et al., *Recognition of double-stranded RNA and activation of NF-kappaB by Toll-like receptor 3.* Nature, 2001. **413**(6857): p. 732-8.

58. Cavassani, K.A., et al., *TLR3 is an endogenous sensor of tissue necrosis during acute inflammatory events.* J Exp Med, 2008. **205**(11): p. 2609-21.

59. Kariko, K., et al., *mRNA is an endogenous ligand for Toll-like receptor 3.* J Biol Chem, 2004. **279**(13): p. 12542-50.

60. Poltorak, A., et al., *Defective LPS signaling in C3H/HeJ and C57BL/10ScCr mice: mutations in Tlr4 gene.* Science, 1998. **282**(5396): p. 2085-8.

61. Rassa, J.C., et al., *Murine retroviruses activate B cells via interaction with toll-like receptor 4.* Proc Natl Acad Sci U S A, 2002. **99**(4): p. 2281-6.

62. Oliveira, A.C., et al., *Expression of functional TLR4 confers proinflammatory responsiveness to Trypanosoma cruzi glycoinositolphospholipids and higher resistance to infection with T. cruzi.* J Immunol, 2004. **173**(9): p. 5688-96.

63. Tada, H., et al., *Saccharomyces cerevisiae- and Candida albicans-derived mannan induced production of tumor necrosis factor alpha by human monocytes in a CD14- and Toll-like receptor 4-dependent manner.* Microbiol Immunol, 2002. **46**(7): p. 503-12.

64. Midwood, K., et al., *Tenascin-C is an endogenous activator of Toll-like receptor 4 that is essential for maintaining inflammation in arthritic joint disease.* Nat Med, 2009. **15**(7): p. 774-80.

65. Ohashi, K., et al., *Cutting edge: heat shock protein 60 is a putative endogenous ligand of the toll-like receptor-4 complex.* J Immunol, 2000. **164**(2): p. 558-61.

66. Babelova, A., et al., *Biglycan, a danger signal that activates the NLRP3 inflammasome via toll-like and P2X receptors.* J Biol Chem, 2009. **284**(36): p. 24035-48.

67. Smiley, S.T., J.A. King, and W.W. Hancock, *Fibrinogen stimulates macrophage chemokine secretion through toll-like receptor 4.* J Immunol, 2001. **167**(5): p. 2887-94.

68. Okamura, Y., et al., *The extra domain A of fibronectin activates Toll-like receptor 4.* J Biol Chem, 2001. **276**(13): p. 10229-33.

69. Biragyn, A., et al., *Toll-like receptor 4-dependent activation of dendritic cells by beta-defensin 2.* Science, 2002. **298**(5595): p. 1025-9.

70. Guillot, L., et al., *Cutting edge: the immunostimulatory activity of the lung surfactant protein-A involves Toll-like receptor 4.* J Immunol, 2002. **168**(12): p. 5989-92.

71. Hayashi, F., et al., *The innate immune response to bacterial flagellin is mediated by Toll-like receptor 5.* Nature, 2001. **410**(6832): p. 1099-103.

72. Takeuchi, O., et al., *Discrimination of bacterial lipoproteins by Toll-like receptor 6.* Int Immunol, 2001. **13**(7): p. 933-40.

73. Ozinsky, A., et al., *The repertoire for pattern recognition of pathogens by the innate immune system is defined by cooperation between toll-like receptors.* Proc Natl Acad Sci U S A, 2000. **97**(25): p. 13766-71.

74. Hemmi, H., et al., *Small anti-viral compounds activate immune cells via the TLR7 MyD88-dependent signaling pathway.* Nat Immunol, 2002. **3**(2): p. 196-200.

75. Heil, F., et al., *The Toll-like receptor 7 (TLR7)-specific stimulus loxoribine uncovers a strong relationship within the TLR7, 8 and 9 subfamily.* Eur J Immunol, 2003. **33**(11): p. 2987-97.

76. Heil, F., et al., *Species-specific recognition of single-stranded RNA via toll-like receptor 7 and 8.* Science, 2004. **303**(5663): p. 1526-9.

77. Diebold, S.S., et al., *Innate antiviral responses by means of TLR7-mediated recognition of single-stranded RNA.* Science, 2004. **303**(5663): p. 1529-31.

78. Vollmer, J., et al., *Immune stimulation mediated by autoantigen binding sites within small nuclear RNAs involves Toll-like receptors 7 and 8.* J Exp Med, 2005. **202**(11): p. 1575-85.

79. Christensen, S.R., et al., *Toll-like receptor 7 and TLR9 dictate autoantibody specificity and have opposing inflammatory and regulatory roles in a murine model of lupus.* Immunity, 2006. **25**(3): p. 417-28.

80. Hemmi, H., et al., *A Toll-like receptor recognizes bacterial DNA.* Nature, 2000. **408**(6813): p. 740-5.

81. Bao, W., et al., *Toll-like Receptor 9 Can be Activated by Endogenous Mitochondrial DNA to Induce Podocyte Apoptosis.* Sci Rep, 2016. **6**: p. 22579.

82. Akira, S. and K. Takeda, *Toll-like receptor signalling.* Nat Rev Immunol, 2004. **4**(7): p. 499-511.

83. Piccinini, A.M. and K.S. Midwood, *DAMPening inflammation by modulating TLR signalling.* Mediators Inflamm, 2010. **2010**.

84. Wright, S.D., et al., *CD14, a receptor for complexes of lipopolysaccharide (LPS) and LPS binding protein.* Science, 1990. **249**(4975): p. 1431-3.

85. Gioannini, T.L., et al., *Isolation of an endotoxin-MD-2 complex that produces Toll-like receptor 4-dependent cell activation at picomolar concentrations.* Proc Natl Acad Sci U S A, 2004. **101**(12): p. 4186-91.

86. Park, B.S. and J.O. Lee, *Recognition of lipopolysaccharide pattern by TLR4 complexes.* Exp Mol Med, 2013. **45**: p. e66.

87. Adachi, O., et al., *Targeted disruption of the MyD88 gene results in loss of IL-1- and IL-18-mediated function.* Immunity, 1998. **9**(1): p. 143-50.

88. Horng, T., et al., *The adaptor molecule TIRAP provides signalling specificity for Toll-like receptors.* Nature, 2002. **420**(6913): p. 329-33.

89. Chang, L. and M. Karin, *Mammalian MAP kinase signalling cascades.* Nature, 2001. **410**(6824): p. 37-40.

90. Kawai, T. and S. Akira, *The role of pattern-recognition receptors in innate immunity: update on Toll-like receptors.* Nat Immunol, 2010. **11**(5): p. 373-84.

91. Kawai, T., et al., *Unresponsiveness of MyD88-deficient mice to endotoxin.* Immunity, 1999. **11**(1): p. 115-22.

92. Kawai, T., et al., *Lipopolysaccharide stimulates the MyD88-independent pathway and results in activation of IFN-regulatory factor 3 and the expression of a subset of lipopolysaccharide-inducible genes.* J Immunol, 2001. **167**(10): p. 5887-94.

93. Kagan, J.C., et al., *TRAM couples endocytosis of Toll-like receptor 4 to the induction of interferon-beta.* Nat Immunol, 2008. **9**(4): p. 361-8.

94. Drexler, S.K. and B.M. Foxwell, *The role of toll-like receptors in chronic inflammation.* Int J Biochem Cell Biol, 2010. **42**(4): p. 506-18.

95. Marshak-Rothstein, A., *Toll-like receptors in systemic autoimmune disease.* Nat Rev Immunol, 2006. **6**(11): p. 823-35.

96. Tsujimoto, H., et al., *Role of Toll-like receptors in the development of sepsis.* Shock, 2008. **29**(3): p. 315-21.

97. Joosten, L.A., et al., *Toll-like receptors and chronic inflammation in rheumatic diseases: new developments.* Nat Rev Rheumatol, 2016. **12**(6): p. 344-57.

98. Roger, T., et al., *Protection from lethal gram-negative bacterial sepsis by targeting Toll-like receptor 4.* Proc Natl Acad Sci U S A, 2009. **106**(7): p. 2348-52.

99. Bergt, S., et al., *Hydrocortisone reduces the beneficial effects of toll-like receptor 2 deficiency on survival in a mouse model of polymicrobial sepsis.* Shock, 2013. **40**(5): p. 414-9.

100. Ospelt, C., et al., *Overexpression of toll-like receptors 3 and 4 in synovial tissue from patients with early rheumatoid arthritis: toll-like receptor expression in early and longstanding arthritis.* Arthritis Rheum, 2008. **58**(12): p. 3684-92.

101. Kowalski, M.L., et al., *Increased responsiveness to toll-like receptor 4 stimulation in peripheral blood mononuclear cells from patients with recent onset rheumatoid arthritis.* Mediators Inflamm, 2008. **2008**: p. 132732.

102. Yang, Y., et al., *Heat shock protein gp96 is a master chaperone for toll-like receptors and is important in the innate function of macrophages.* Immunity, 2007. **26**(2): p. 215-26.

103. Ewald, S.E., et al., *The ectodomain of Toll-like receptor 9 is cleaved to generate a functional receptor.* Nature, 2008. **456**(7222): p. 658-62.

104. Park, B., et al., *Proteolytic cleavage in an endolysosomal compartment is required for activation of Toll-like receptor 9.* Nat Immunol, 2008. **9**(12): p. 1407-14.

105. Garcia-Cattaneo, A., et al., *Cleavage of Toll-like receptor 3 by cathepsins B and H is essential for signaling.* Proc Natl Acad Sci U S A, 2012. **109**(23): p. 9053-8.

106. Langjahr, P., et al., *Metalloproteinase-dependent TLR2 ectodomain shedding is involved in soluble toll-like receptor 2 (sTLR2) production.* PLoS One, 2014. **9**(12): p. e104624.

107. Iwami, K.I., et al., *Cutting edge: naturally occurring soluble form of mouse Toll-like receptor 4 inhibits lipopolysaccharide signaling.* J Immunol, 2000. **165**(12): p. 6682-6.

108. Mitsuzawa, H., et al., *Recombinant soluble forms of extracellular TLR4 domain and MD-2 inhibit lipopolysaccharide binding on cell surface and dampen lipopolysaccharide-induced pulmonary inflammation in mice.* J Immunol, 2006. **177**(11): p. 8133-9.

109. Jiang, Z., et al., *CD14 is required for MyD88-independent LPS signaling.* Nat Immunol, 2005. **6**(6): p. 565-70.

110. Lee, H.K., et al., *Double-stranded RNA-mediated TLR3 activation is enhanced by CD14.* Immunity, 2006. **24**(2): p. 153-63.

111. Lee, K.G., et al., *Bruton's tyrosine kinase phosphorylates Toll-like receptor 3 to initiate antiviral response.* Proc Natl Acad Sci U S A, 2012. **109**(15): p. 5791-6.

112. Yamashita, M., et al., *Epidermal growth factor receptor is essential for Toll-like receptor 3 signaling.* Sci Signal, 2012. **5**(233): p. ra50.

113. Medvedev, A.E., et al., *Role of TLR4 tyrosine phosphorylation in signal transduction and endotoxin tolerance.* J Biol Chem, 2007. **282**(22): p. 16042-53.

114. Jefferies, C.A., et al., *Bruton's tyrosine kinase is a Toll/interleukin-1 receptor domain-binding protein that participates in nuclear factor kappaB activation by Toll-like receptor 4.* J Biol Chem, 2003. **278**(28): p. 26258-64.

115. Gray, P., et al., *MyD88 adapter-like (Mal) is phosphorylated by Bruton's tyrosine kinase during TLR2 and TLR4 signal transduction.* J Biol Chem, 2006. **281**(15): p. 10489-95.

116. Piao, W., et al., *Tyrosine phosphorylation of MyD88 adapter-like (Mal) is critical for signal transduction and blocked in endotoxin tolerance.* J Biol Chem, 2008. **283**(6): p. 3109-19.

117. Xiong, Y., et al., *Endotoxin Tolerance Inhibits Lyn and c-Src Phosphorylation and Association with Toll-Like Receptor 4 but Increases Expression and Activity of Protein Phosphatases.* J Innate Immun, 2016. **8**(2): p. 171-84.

118. Burns, K., et al., *Inhibition of interleukin 1 receptor/Toll-like receptor signaling through the alternatively spliced, short form of MyD88 is due to its failure to recruit IRAK-4.* J Exp Med, 2003. **197**(2): p. 263-8.

119. Palsson-McDermott, E.M., et al., *TAG, a splice variant of the adaptor TRAM, negatively regulates the adaptor MyD88-independent TLR4 pathway.* Nat Immunol, 2009. **10**(6): p. 579-86.

120. Kobayashi, K., et al., *IRAK-M is a negative regulator of Toll-like receptor signaling.* Cell, 2002. **110**(2): p. 191-202.

121. He, X., Z. Jing, and G. Cheng, *MicroRNAs: new regulators of Toll-like receptor signalling pathways.* Biomed Res Int, 2014. **2014**: p. 945169.

122. O'Connell, R.M., et al., *Physiological and pathological roles for microRNAs in the immune system.* Nat Rev Immunol, 2010. **10**(2): p. 111-22.

123. O'Connell, R.M., et al., *MicroRNA-155 is induced during the macrophage inflammatory response.* Proc Natl Acad Sci U S A, 2007. **104**(5): p. 1604-9.

124. Ambros, V., *A hierarchy of regulatory genes controls a larva-to-adult developmental switch in C. elegans.* Cell, 1989. **57**(1): p. 49-57.

125. Wightman, B., I. Ha, and G. Ruvkun, *Posttranscriptional regulation of the heterochronic gene lin-14 by lin-4 mediates temporal pattern formation in C. elegans.* Cell, 1993. **75**(5): p. 855-62.

126. Lee, R.C., R.L. Feinbaum, and V. Ambros, *The C. elegans heterochronic gene lin-4 encodes small RNAs with antisense complementarity to lin-14.* Cell, 1993. **75**(5): p. 843-54.

127. Pasquinelli, A.E., et al., *Conservation of the sequence and temporal expression of let-7 heterochronic regulatory RNA.* Nature, 2000. **408**(6808): p. 86-9.

128. Alles, J., et al., *An estimate of the total number of true human miRNAs.* Nucleic Acids Res, 2019. **47**(7): p. 3353-3364.

129. Berezikov, E., *Evolution of microRNA diversity and regulation in animals.* Nat Rev Genet, 2011. **12**(12): p. 846-60.

130. Obernosterer, G., et al., *Post-transcriptional regulation of microRNA expression.* RNA, 2006. **12**(7): p. 1161-7.

131. Siegel, G., et al., *A functional screen implicates microRNA-138-dependent regulation of the depalmitoylation enzyme APT1 in dendritic spine morphogenesis.* Nat Cell Biol, 2009. **11**(6): p. 705-16.

132. Jopling, C., *Liver-specific microRNA-122: Biogenesis and function.* RNA Biol, 2012. **9**(2): p. 137-42.

133. Landgraf, P., et al., *A mammalian microRNA expression atlas based on small RNA library sequencing.* Cell, 2007. **129**(7): p. 1401-14.

134. Garzon, R. and C.M. Croce, *MicroRNAs in normal and malignant hematopoiesis.* Curr Opin Hematol, 2008. **15**(4): p. 352-8.

135. Lee, Y., et al., *MicroRNA maturation: stepwise processing and subcellular localization.* EMBO J, 2002. **21**(17): p. 4663-70.

136. Liu, H., et al., *Nuclear functions of mammalian MicroRNAs in gene regulation, immunity and cancer.* Mol Cancer, 2018. **17**(1): p. 64.

137. Meister, G., et al., *Human Argonaute2 mediates RNA cleavage targeted by miRNAs and siRNAs.* Mol Cell, 2004. **15**(2): p. 185-97.

138. Hwang, H.W., E.A. Wentzel, and J.T. Mendell, *A hexanucleotide element directs microRNA nuclear import.* Science, 2007. **315**(5808): p. 97-100.

139. Taft, R.J., et al., *Nuclear-localized tiny RNAs are associated with transcription initiation and splice sites in metazoans.* Nat Struct Mol Biol, 2010. **17**(8): p. 1030-4.

140. Leung, A.K.L., *The Whereabouts of microRNA Actions: Cytoplasm and Beyond.* Trends Cell Biol, 2015. **25**(10): p. 601-610.

141. Selbach, M., et al., *Widespread changes in protein synthesis induced by microRNAs.* Nature, 2008. **455**(7209): p. 58-63.

142. Uhlmann, S., et al., *Global microRNA level regulation of EGFR-driven cell-cycle protein network in breast cancer.* Mol Syst Biol, 2012. **8**: p. 570.

143. Lujambio, A. and S.W. Lowe, *The microcosmos of cancer.* Nature, 2012. **482**(7385): p. 347-55.

144. Im, H.I. and P.J. Kenny, *MicroRNAs in neuronal function and dysfunction.* Trends Neurosci, 2012. **35**(5): p. 325-34.

145. Liu, J., et al., *Argonaute2 is the catalytic engine of mammalian RNAi.* Science, 2004. **305**(5689): p. 1437-41.

146. Agarwal, V., et al., *Predicting effective microRNA target sites in mammalian mRNAs.* Elife, 2015. **4**.

147. Eulalio, A., E. Huntzinger, and E. Izaurralde, *Getting to the root of miRNA-mediated gene silencing.* Cell, 2008. **132**(1): p. 9-14.

148. Guo, H., et al., *Mammalian microRNAs predominantly act to decrease target mRNA levels.* Nature, 2010. **466**(7308): p. 835-40.

149. Jonas, S. and E. Izaurralde, *Towards a molecular understanding of microRNA-mediated gene silencing.* Nat Rev Genet, 2015. **16**(7): p. 421-33.

150. Huntzinger, E. and E. Izaurralde, *Gene silencing by microRNAs: contributions of translational repression and mRNA decay.* Nat Rev Genet, 2011. **12**(2): p. 99-110.

151. O'Brien, J., et al., *Overview of MicroRNA Biogenesis, Mechanisms of Actions, and Circulation.* Front Endocrinol (Lausanne), 2018. **9**: p. 402.

152. Rehwinkel, J., et al., *A crucial role for GW182 and the DCP1:DCP2 decapping complex in miRNA-mediated gene silencing.* RNA, 2005. **11**(11): p. 1640-7.

153. Bartel, D.P., *Metazoan MicroRNAs.* Cell, 2018. **173**(1): p. 20-51.

154. Wu, L., J. Fan, and J.G. Belasco, *MicroRNAs direct rapid deadenylation of mRNA.* Proc Natl Acad Sci U S A, 2006. **103**(11): p. 4034-9.

155. Eisen, T.J., et al., *MicroRNAs Cause Accelerated Decay of Short-Tailed Target mRNAs.* Mol Cell, 2020. **77**(4): p. 775-785 e8.

156. Ling, H., M. Fabbri, and G.A. Calin, *MicroRNAs and other non-coding RNAs as targets for anticancer drug development.* Nat Rev Drug Discov, 2013. **12**(11): p. 847-65.

157. Kiriakidou, M., et al., *An mRNA m7G cap binding-like motif within human Ago2 represses translation.* Cell, 2007. **129**(6): p. 1141-51.

158. Chendrimada, T.P., et al., *MicroRNA silencing through RISC recruitment of eIF6.* Nature, 2007. **447**(7146): p. 823-8.

159. Filipowicz, W., S.N. Bhattacharyya, and N. Sonenberg, *Mechanisms of post-transcriptional regulation by microRNAs: are the answers in sight?* Nat Rev Genet, 2008. **9**(2): p. 102-14.

160. Jing, Q., et al., *Involvement of microRNA in AU-rich element-mediated mRNA instability.* Cell, 2005. **120**(5): p. 623-34.

161. Vasudevan, S., Y. Tong, and J.A. Steitz, *Switching from repression to activation: microRNAs can up-regulate translation.* Science, 2007. **318**(5858): p. 1931-4.

162. Orom, U.A., F.C. Nielsen, and A.H. Lund, *MicroRNA-10a binds the 5'UTR of ribosomal protein mRNAs and enhances their translation.* Mol Cell, 2008. **30**(4): p. 460-71.

163. Dharap, A., et al., *MicroRNA miR-324-3p induces promoter-mediated expression of RelA gene.* PLoS One, 2013. **8**(11): p. e79467.

164. Tili, E., et al., *Modulation of miR-155 and miR-125b levels following lipopolysaccharide/TNF-alpha stimulation and their possible roles in regulating the response to endotoxin shock.* J Immunol, 2007. **179**(8): p. 5082-9.

165. Roush, S. and F.J. Slack, *The let-7 family of microRNAs.* Trends Cell Biol, 2008. **18**(10): p. 505-16.

166. He, L., et al., *microRNAs join the p53 network--another piece in the tumour-suppression puzzle.* Nat Rev Cancer, 2007. **7**(11): p. 819-22.

167. Kim, J., et al., *A MicroRNA feedback circuit in midbrain dopamine neurons.* Science, 2007. **317**(5842): p. 1220-4.

168. Cai, X., C.H. Hagedorn, and B.R. Cullen, *Human microRNAs are processed from capped, polyadenylated transcripts that can also function as mRNAs.* RNA, 2004. **10**(12): p. 1957-66.

169. Ozsolak, F., et al., *Chromatin structure analyses identify miRNA promoters.* Genes Dev, 2008. **22**(22): p. 3172-83.

170. de Rie, D., et al., *An integrated expression atlas of miRNAs and their promoters in human and mouse.* Nat Biotechnol, 2017. **35**(9): p. 872-878.

171. Ha, M. and V.N. Kim, *Regulation of microRNA biogenesis.* Nat Rev Mol Cell Biol, 2014. **15**(8): p. 509-24.

172. Chang, S., et al., *Tumor suppressor BRCA1 epigenetically controls oncogenic microRNA-155.* Nat Med, 2011. **17**(10): p. 1275-82.

173. Lee, Y., et al., *MicroRNA genes are transcribed by RNA polymerase II.* EMBO J, 2004. **23**(20): p. 4051-60.

174. Morlando, M., et al., *Primary microRNA transcripts are processed co-transcriptionally.* Nat Struct Mol Biol, 2008. **15**(9): p. 902-9.

175. Kwon, S.C., et al., *Structure of Human DROSHA.* Cell, 2016. **164**(1-2): p. 81-90.

176. Kwon, S.C., et al., *Molecular Basis for the Single-Nucleotide Precision of Primary microRNA Processing.* Mol Cell, 2019. **73**(3): p. 505-518 e5.

177. Partin, A.C., et al., *Cryo-EM Structures of Human Drosha and DGCR8 in Complex with Primary MicroRNA.* Mol Cell, 2020.

178. Jin, W., et al., *Structural Basis for pri-miRNA Recognition by Drosha.* Mol Cell, 2020.

179. Nguyen, T.A., et al., *Functional Anatomy of the Human Microprocessor.* Cell, 2015. **161**(6): p. 1374-87.

180. Quick-Cleveland, J., et al., *The DGCR8 RNA-binding heme domain recognizes primary microRNAs by clamping the hairpin.* Cell Rep, 2014. **7**(6): p. 1994-2005.

181. Nguyen, T.A., et al., *Microprocessor depends on hemin to recognize the apical loop of primary microRNA.* Nucleic Acids Res, 2018. **46**(11): p. 5726-5736.

182. Bohnsack, M.T., K. Czaplinski, and D. Gorlich, *Exportin 5 is a RanGTP-dependent dsRNA-binding protein that mediates nuclear export of pre-miRNAs.* RNA, 2004. **10**(2): p. 185-91.

183. Lund, E., et al., *Nuclear export of microRNA precursors.* Science, 2004. **303**(5654): p. 95-8.

184. Yi, R., et al., *Exportin-5 mediates the nuclear export of pre-microRNAs and short hairpin RNAs.* Genes Dev, 2003. **17**(24): p. 3011-6.

185. Gwizdek, C., et al., *Exportin-5 mediates nuclear export of minihelix-containing RNAs.* J Biol Chem, 2003. **278**(8): p. 5505-8.

186. Zeng, Y. and B.R. Cullen, *Structural requirements for pre-microRNA binding and nuclear export by Exportin 5.* Nucleic Acids Res, 2004. **32**(16): p. 4776-85.

187. Bernstein, E., et al., *Role for a bidentate ribonuclease in the initiation step of RNA interference.* Nature, 2001. **409**(6818): p. 363-6.

188. Hutvagner, G., et al., *A cellular function for the RNA-interference enzyme Dicer in the maturation of the let-7 small temporal RNA.* Science, 2001. **293**(5531): p. 834-8.

189. Ketting, R.F., et al., *Dicer functions in RNA interference and in synthesis of small RNA involved in developmental timing in C. elegans.* Genes Dev, 2001. **15**(20): p. 2654-9.

190. Lau, P.W., et al., *The molecular architecture of human Dicer.* Nat Struct Mol Biol, 2012. **19**(4): p. 436-40.

191. Macrae, I.J., et al., *Structural basis for double-stranded RNA processing by Dicer.* Science, 2006. **311**(5758): p. 195-8.

192. Park, J.E., et al., *Dicer recognizes the 5' end of RNA for efficient and accurate processing.* Nature, 2011. **475**(7355): p. 201-5.

193. Tian, Y., et al., *A phosphate-binding pocket within the platform-PAZ-connector helix cassette of human Dicer.* Mol Cell, 2014. **53**(4): p. 606-16.

194. Lee, H.Y., et al., *Differential roles of human Dicer-binding proteins TRBP and PACT in small RNA processing.* Nucleic Acids Res, 2013. **41**(13): p. 6568-76.

195. Chendrimada, T.P., et al., *TRBP recruits the Dicer complex to Ago2 for microRNA processing and gene silencing.* Nature, 2005. **436**(7051): p. 740-4.

196. Gregory, R.I., et al., *Human RISC couples microRNA biogenesis and posttranscriptional gene silencing.* Cell, 2005. **123**(4): p. 631-40.

197. MacRae, I.J., et al., *In vitro reconstitution of the human RISC-loading complex.* Proc Natl Acad Sci U S A, 2008. **105**(2): p. 512-7.

198. Khvorova, A., A. Reynolds, and S.D. Jayasena, *Functional siRNAs and miRNAs exhibit strand bias.* Cell, 2003. **115**(2): p. 209-16.

199. Nykanen, A., B. Haley, and P.D. Zamore, *ATP requirements and small interfering RNA structure in the RNA interference pathway.* Cell, 2001. **107**(3): p. 309-21.

200. Yoda, M., et al., *ATP-dependent human RISC assembly pathways.* Nat Struct Mol Biol, 2010. **17**(1): p. 17-23.

201. Schwarz, D.S., et al., *Asymmetry in the assembly of the RNAi enzyme complex.* Cell, 2003. **115**(2): p. 199-208.

202. Kim, H., et al., *A Mechanism for microRNA Arm Switching Regulated by Uridylation.* Mol Cell, 2020. **78**(6): p. 1224-1236 e5.

203. Berezikov, E., et al., *Mammalian mirtron genes.* Mol Cell, 2007. **28**(2): p. 328-36.

204. Ruby, J.G., C.H. Jan, and D.P. Bartel, *Intronic microRNA precursors that bypass Drosha processing.* Nature, 2007. **448**(7149): p. 83-6.

205. Cheloufi, S., et al., *A dicer-independent miRNA biogenesis pathway that requires Ago catalysis.* Nature, 2010. **465**(7298): p. 584-9.

206. Heo, I., et al., *Mono-uridylation of pre-microRNA as a key step in the biogenesis of group II let-7 microRNAs.* Cell, 2012. **151**(3): p. 521-32.

207. Gantier, M.P., et al., *Analysis of microRNA turnover in mammalian cells following Dicer1 ablation.* Nucleic Acids Res, 2011. **39**(13): p. 5692-703.

208. Mann, M., et al., *An NF-kappaB-microRNA regulatory network tunes macrophage inflammatory responses.* Nat Commun, 2017. **8**(1): p. 851.

209. Krol, J., et al., *Characterizing light-regulated retinal microRNAs reveals rapid turnover as a common property of neuronal microRNAs.* Cell, 2010. **141**(4): p. 618-31.

210. Rissland, O.S., S.J. Hong, and D.P. Bartel, *MicroRNA destabilization enables dynamic regulation of the miR-16 family in response to cell-cycle changes.* Mol Cell, 2011. **43**(6): p. 993-1004.

211. O'Donnell, K.A., et al., *c-Myc-regulated microRNAs modulate E2F1 expression.* Nature, 2005. **435**(7043): p. 839-43.

212. Ma, L., et al., *miR-9, a MYC/MYCN-activated microRNA, regulates E-cadherin and cancer metastasis.* Nat Cell Biol, 2010. **12**(3): p. 247-56.

213. Chang, T.C., et al., *Widespread microRNA repression by Myc contributes to tumorigenesis.* Nat Genet, 2008. **40**(1): p. 43-50.

214. Del Mar Diaz-Gonzalez, S., et al., *Transregulation of microRNA miR-21 promoter by AP-1 transcription factor in cervical cancer cells.* Cancer Cell Int, 2019. **19**: p. 214.

215. Yin, Q., et al., *B-cell receptor activation induces BIC/miR-155 expression through a conserved AP-1 element.* J Biol Chem, 2008. **283**(5): p. 2654-62.

216. Fukao, T., et al., *An evolutionarily conserved mechanism for microRNA-223 expression revealed by microRNA gene profiling.* Cell, 2007. **129**(3): p. 617-31.

217. Sun, Y., et al., *PU.1-dependent transcriptional regulation of miR-142 contributes to its hematopoietic cell-specific expression and modulation of IL-6.* J Immunol, 2013. **190**(8): p. 4005-13.

218. Zardo, G., et al., *Polycombs and microRNA-223 regulate human granulopoiesis by transcriptional control of target gene expression.* Blood, 2012. **119**(17): p. 4034-46.

219. Han, J., et al., *Posttranscriptional crossregulation between Drosha and DGCR8.* Cell, 2009. **136**(1): p. 75-84.

220. Auyeung, V.C., et al., *Beyond secondary structure: primary-sequence determinants license pri-miRNA hairpins for processing.* Cell, 2013. **152**(4): p. 844-58.

221. Mori, M., et al., *Hippo signaling regulates microprocessor and links cell-density-dependent miRNA biogenesis to cancer.* Cell, 2014. **156**(5): p. 893-906.

222. Gregory, R.I., et al., *The Microprocessor complex mediates the genesis of microRNAs.* Nature, 2004. **432**(7014): p. 235-40.

223. Dardenne, E., et al., *RNA helicases DDX5 and DDX17 dynamically orchestrate transcription, miRNA, and splicing programs in cell differentiation.* Cell Rep, 2014. **7**(6): p. 1900-13.

224. Suzuki, H.I., et al., *Modulation of microRNA processing by p53.* Nature, 2009. **460**(7254): p. 529-33.

225. Remenyi, J., et al., *The loop structure and the RNA helicase p72/DDX17 influence the processing efficiency of the mice miR-132.* Sci Rep, 2016. **6**: p. 22848.

226. Connerty, P., et al., *The miRNA biogenesis factors, p72/DDX17 and KHSRP regulate the protein level of Ago2 in human cells.* Biochim Biophys Acta, 2016. **1859**(10): p. 1299-305.

227. Davis, B.N., et al., *SMAD proteins control DROSHA-mediated microRNA maturation.* Nature, 2008. **454**(7200): p. 56-61.

228. Guil, S. and J.F. Caceres, *The multifunctional RNA-binding protein hnRNP A1 is required for processing of miR-18a.* Nat Struct Mol Biol, 2007. **14**(7): p. 591-6.

229. Trabucchi, M., et al., *The RNA-binding protein KSRP promotes the biogenesis of a subset of microRNAs.* Nature, 2009. **459**(7249): p. 1010-4.

230. Piskounova, E., et al., *Determinants of microRNA processing inhibition by the developmentally regulated RNA-binding protein Lin28.* J Biol Chem, 2008. **283**(31): p. 21310-4.

231. Viswanathan, S.R., G.Q. Daley, and R.I. Gregory, *Selective blockade of microRNA processing by Lin28.* Science, 2008. **320**(5872): p. 97-100.

232. Heo, I., et al., *TUT4 in concert with Lin28 suppresses microRNA biogenesis through pre-microRNA uridylation.* Cell, 2009. **138**(4): p. 696-708.

233. Treiber, T., et al., *A Compendium of RNA-Binding Proteins that Regulate MicroRNA Biogenesis.* Mol Cell, 2017. **66**(2): p. 270-284.e13.

234. Iwasaki, Y.W., et al., *Global microRNA elevation by inducible Exportin 5 regulates cell cycle entry.* RNA, 2013. **19**(4): p. 490-7.

235. Wan, G., et al., *DNA-damage-induced nuclear export of precursor microRNAs is regulated by the ATM-AKT pathway.* Cell Rep, 2013. **3**(6): p. 2100-12.

236. Melo, S.A., et al., *A genetic defect in exportin-5 traps precursor microRNAs in the nucleus of cancer cells.* Cancer Cell, 2010. **18**(4): p. 303-15.

237. Lee, Y., et al., *The role of PACT in the RNA silencing pathway.* EMBO J, 2006. **25**(3): p. 522-32.

238. Paroo, Z., et al., *Phosphorylation of the human microRNA-generating complex mediates MAPK/Erk signaling.* Cell, 2009. **139**(1): p. 112-22.

239. Maniataki, E. and Z. Mourelatos, *A human, ATP-independent, RISC assembly machine fueled by pre-miRNA.* Genes Dev, 2005. **19**(24): p. 2979-90.

240. Zeng, Y., et al., *Phosphorylation of Argonaute 2 at serine-387 facilitates its localization to processing bodies.* Biochem J, 2008. **413**(3): p. 429-36.

241. Horman, S.R., et al., *Akt-mediated phosphorylation of argonaute 2 downregulates cleavage and upregulates translational repression of MicroRNA targets.* Mol Cell, 2013. **50**(3): p. 356-67.

242. Shen, J., et al., *EGFR modulates microRNA maturation in response to hypoxia through phosphorylation of AGO2.* Nature, 2013. **497**(7449): p. 383-7.

243. Ameres, S.L. and P.D. Zamore, *Diversifying microRNA sequence and function.* Nat Rev Mol Cell Biol, 2013. **14**(8): p. 475-88.

244. Xhemalce, B., S.C. Robson, and T. Kouzarides, *Human RNA methyltransferase BCDIN3D regulates microRNA processing.* Cell, 2012. **151**(2): p. 278-88.

245. Ruegger, S. and H. Grosshans, *MicroRNA turnover: when, how, and why.* Trends Biochem Sci, 2012. **37**(10): p. 436-46.

246. Guo, S., et al., *MicroRNA miR-125a controls hematopoietic stem cell number.* Proc Natl Acad Sci U S A, 2010. **107**(32): p. 14229-34.

247. O'Connell, R.M., et al., *MicroRNAs enriched in hematopoietic stem cells differentially regulate long-term hematopoietic output.* Proc Natl Acad Sci U S A, 2010. **107**(32): p. 14235-40.

248. Han, Y.C., et al., *microRNA-29a induces aberrant self-renewal capacity in hematopoietic progenitors, biased myeloid development, and acute myeloid leukemia.* J Exp Med, 2010. **207**(3): p. 475-89.

249. Hu, W., et al., *miR-29a maintains mouse hematopoietic stem cell self-renewal by regulating Dnmt3a.* Blood, 2015. **125**(14): p. 2206-16.

250. Fazi, F., et al., *A minicircuitry comprised of microRNA-223 and transcription factors NFI-A and C/EBPalpha regulates human granulopoiesis.* Cell, 2005. **123**(5): p. 819-31.

251. Johnnidis, J.B., et al., *Regulation of progenitor cell proliferation and granulocyte function by microRNA-223.* Nature, 2008. **451**(7182): p. 1125-9.

252. Velu, C.S., A.M. Baktula, and H.L. Grimes, *Gfi1 regulates miR-21 and miR-196b to control myelopoiesis.* Blood, 2009. **113**(19): p. 4720-8.

253. Androulidaki, A., et al., *The kinase Akt1 controls macrophage response to lipopolysaccharide by regulating microRNAs.* Immunity, 2009. **31**(2): p. 220-31.

254. Alsaleh, G., et al., *Bruton's tyrosine kinase is involved in miR-346-related regulation of IL-18 release by lipopolysaccharide-activated rheumatoid fibroblast-like synoviocytes.* J Immunol, 2009. **182**(8): p. 5088-97.

255. El Gazzar, M. and C.E. McCall, *MicroRNAs distinguish translational from transcriptional silencing during endotoxin tolerance.* J Biol Chem, 2010. **285**(27): p. 20940-51.

256. O'Neill, L.A., F.J. Sheedy, and C.E. McCoy, *MicroRNAs: the fine-tuners of Toll-like receptor signalling.* Nat Rev Immunol, 2011. **11**(3): p. 163-75.

257. Mehta, A. and D. Baltimore, *MicroRNAs as regulatory elements in immune system logic.* Nat Rev Immunol, 2016. **16**(5): p. 279-94.

258. Cremer, T.J., et al., *MiR-155 induction by F. novicida but not the virulent F. tularensis results in SHIP down-regulation and enhanced pro-inflammatory cytokine response.* PLoS One, 2009. **4**(12): p. e8508.

259. O'Connell, R.M., et al., *Inositol phosphatase SHIP1 is a primary target of miR-155.* Proc Natl Acad Sci U S A, 2009. **106**(17): p. 7113-8.

260. Wang, P., et al., *Inducible microRNA-155 feedback promotes type I IFN signaling in antiviral innate immunity by targeting suppressor of cytokine signaling 1.* J Immunol, 2010. **185**(10): p. 6226-33.

261. Bala, S., et al., *Up-regulation of microRNA-155 in macrophages contributes to increased tumor necrosis factor {alpha} (TNF{alpha}) production via increased mRNA half-life in alcoholic liver disease.* J Biol Chem, 2011. **286**(2): p. 1436-44.

262. Ceppi, M., et al., *MicroRNA-155 modulates the interleukin-1 signaling pathway in activated human monocyte-derived dendritic cells.* Proc Natl Acad Sci U S A, 2009. **106**(8): p. 2735-40.

263. Hsin, J.P., et al., *The effect of cellular context on miR-155-mediated gene regulation in four major immune cell types.* Nat Immunol, 2018. **19**(10): p. 1137-1145.

264. Taganov, K.D., et al., *NF-kappaB-dependent induction of microRNA miR-146, an inhibitor targeted to signaling proteins of innate immune responses.* Proc Natl Acad Sci U S A, 2006. **103**(33): p. 12481-6.

265. Hou, J., et al., *MicroRNA-146a feedback inhibits RIG-I-dependent Type I IFN production in macrophages by targeting TRAF6, IRAK1, and IRAK2.* J Immunol, 2009. **183**(3): p. 2150-8.

266. Sheedy, F.J., et al., *Negative regulation of TLR4 via targeting of the proinflammatory tumor suppressor PDCD4 by the microRNA miR-21.* Nat Immunol, 2010. **11**(2): p. 141-7.

267. Yang, H.S., et al., *The transformation suppressor Pdcd4 is a novel eukaryotic translation initiation factor 4A binding protein that inhibits translation.* Mol Cell Biol, 2003. **23**(1): p. 26-37.

268. Loh, P.G., et al., *Structural basis for translational inhibition by the tumour suppressor Pdcd4.* EMBO J, 2009. **28**(3): p. 274-85.

269. McCoy, C.E., et al., *IL-10 inhibits miR-155 induction by toll-like receptors.* J Biol Chem, 2010. **285**(27): p. 20492-8.

270. Eis, P.S., et al., *Accumulation of miR-155 and BIC RNA in human B cell lymphomas.* Proc Natl Acad Sci U S A, 2005. **102**(10): p. 3627-32.

271. Costinean, S., et al., *Pre-B cell proliferation and lymphoblastic leukemia/high-grade lymphoma in E(mu)-miR155 transgenic mice.* Proc Natl Acad Sci U S A, 2006. **103**(18): p. 7024-9.

272. Clurman, B.E. and W.S. Hayward, *Multiple proto-oncogene activations in avian leukosis virus-induced lymphomas: evidence for stage-specific events.* Mol Cell Biol, 1989. **9**(6): p. 2657-64.

273. Tam, W., D. Ben-Yehuda, and W.S. Hayward, *bic, a novel gene activated by proviral insertions in avian leukosis virus-induced lymphomas, is likely to function through its noncoding RNA.* Mol Cell Biol, 1997. **17**(3): p. 1490-502.

274. Tam, W., *Identification and characterization of human BIC, a gene on chromosome 21 that encodes a noncoding RNA.* Gene, 2001. **274**(1-2): p. 157-67.

275. Heimberg, A.M., et al., *MicroRNAs and the advent of vertebrate morphological complexity.* Proc Natl Acad Sci U S A, 2008. **105**(8): p. 2946-50.

276. Sethupathy, P., et al., *Human microRNA-155 on chromosome 21 differentially interacts with its polymorphic target in the AGTR1 3' untranslated region: a mechanism for functional single-nucleotide polymorphisms related to phenotypes.* Am J Hum Genet, 2007. **81**(2): p. 405-13.

277. Elton, T.S., et al., *Regulation of the MIR155 host gene in physiological and pathological processes.* Gene, 2013. **532**(1): p. 1-12.

278. Zhou, H., et al., *miR-155 and its star-form partner miR-155* cooperatively regulate type I interferon production by human plasmacytoid dendritic cells.* Blood, 2010. **116**(26): p. 5885-94.

279. Zheng, L., et al., *MicroRNA-155 regulates angiotensin II type 1 receptor expression and phenotypic differentiation in vascular adventitial fibroblasts.* Biochem Biophys Res Commun, 2010. **400**(4): p. 483-8.

280. Lagos-Quintana, M., et al., *Identification of tissue-specific microRNAs from mouse.* Curr Biol, 2002. **12**(9): p. 735-9.

281. O'Connell, R.M., et al., *Sustained expression of microRNA-155 in hematopoietic stem cells causes a myeloproliferative disorder.* J Exp Med, 2008. **205**(3): p. 585-94.

282. Georgantas, R.W., 3rd, et al., *CD34+ hematopoietic stem-progenitor cell microRNA expression and function: a circuit diagram of differentiation control.* Proc Natl Acad Sci U S A, 2007. **104**(8): p. 2750-5.

283. Masaki, S., et al., *Expression patterns of microRNAs 155 and 451 during normal human erythropoiesis.* Biochem Biophys Res Commun, 2007. **364**(3): p. 509-14.

284. Rodriguez, A., et al., *Requirement of bic/microRNA-155 for normal immune function.* Science, 2007. **316**(5824): p. 608-11.

285. Vigorito, E., et al., *microRNA-155 regulates the generation of immunoglobulin class-switched plasma cells.* Immunity, 2007. **27**(6): p. 847-59.

286. Thai, T.H., et al., *Regulation of the germinal center response by microRNA-155.* Science, 2007. **316**(5824): p. 604-8.

287. Dance, A., *Mouse miRNA library to open.* Nature, 2008. **454**(7202): p. 264.

288. Hu, Y.L., et al., *HOXA9 regulates miR-155 in hematopoietic cells.* Nucleic Acids Res, 2010. **38**(16): p. 5472-8.

289. Manning, B.D. and A. Toker, *AKT/PKB Signaling: Navigating the Network.* Cell, 2017. **169**(3): p. 381-405.

290. Kane, L.P., et al., *Induction of NF-kappaB by the Akt/PKB kinase.* Curr Biol, 1999. **9**(11): p. 601-4.

291. Fukao, T., et al., *PI3K-mediated negative feedback regulation of IL-12 production in DCs.* Nat Immunol, 2002. **3**(9): p. 875-81.

292. Guha, M. and N. Mackman, *The phosphatidylinositol 3-kinase-Akt pathway limits lipopolysaccharide activation of signaling pathways and expression of inflammatory mediators in human monocytic cells.* J Biol Chem, 2002. **277**(35): p. 32124-32.

293. Cheung, S.T., et al., *Interleukin-10 inhibits lipopolysaccharide induced miR-155 precursor stability and maturation.* PLoS One, 2013. **8**(8): p. e71336.

294. Lu, L.F., et al., *Foxp3-dependent microRNA155 confers competitive fitness to regulatory T cells by targeting SOCS1 protein.* Immunity, 2009. **30**(1): p. 80-91.

295. Nazari-Jahantigh, M., et al., *MicroRNA-155 promotes atherosclerosis by repressing Bcl6 in macrophages.* J Clin Invest, 2012. **122**(11): p. 4190-202.

296. Piccinini, A.M. and K.S. Midwood, *Endogenous control of immunity against infection: tenascin-C regulates TLR4-mediated inflammation via microRNA-155.* Cell Rep, 2012. **2**(4): p. 914-26.

297. Louafi, F., R.T. Martinez-Nunez, and T. Sanchez-Elsner, *MicroRNA-155 targets SMAD2 and modulates the response of macrophages to transforming growth factor-{beta}.* J Biol Chem, 2010. **285**(53): p. 41328-36.

298. Kim, H., *The transcription factor MafB promotes anti-inflammatory M2 polarization and cholesterol efflux in macrophages.* Sci Rep, 2017. **7**(1): p. 7591.

299. He, M., et al., *MicroRNA-155 regulates inflammatory cytokine production in tumor-associated macrophages via targeting C/EBPbeta.* Cell Mol Immunol, 2009. **6**(5): p. 343-52.

300. Tang, B., et al., *Identification of MyD88 as a novel target of miR-155, involved in negative regulation of Helicobacter pylori-induced inflammation.* FEBS Lett, 2010. **584**(8): p. 1481-6.

301. Huang, R.S., et al., *MicroRNA-155 silencing enhances inflammatory response and lipid uptake in oxidized low-density lipoprotein-stimulated human THP-1 macrophages.* J Investig Med, 2010. **58**(8): p. 961-7.

302. Costinean, S., et al., *Src homology 2 domain-containing inositol-5-phosphatase and CCAAT enhancer-binding protein beta are targeted by miR-155 in B cells of Emicro-MiR-155 transgenic mice.* Blood, 2009. **114**(7): p. 1374-82.

303. Lu, D., et al., *The miR-155-PU.1 axis acts on Pax5 to enable efficient terminal B cell differentiation.* J Exp Med, 2014. **211**(11): p. 2183-98.

304. Alivernini, S., et al., *MicroRNA-155 influences B-cell function through PU.1 in rheumatoid arthritis.* Nat Commun, 2016. **7**: p. 12970.

305. Kurowska-Stolarska, M., et al., *MicroRNA-155 as a proinflammatory regulator in clinical and experimental arthritis.* Proc Natl Acad Sci U S A, 2011. **108**(27): p. 11193-8.

306. Bluml, S., et al., *Essential role of microRNA-155 in the pathogenesis of autoimmune arthritis in mice.* Arthritis Rheum, 2011. **63**(5): p. 1281-8.

307. O'Connell, R.M., et al., *MicroRNA-155 promotes autoimmune inflammation by enhancing inflammatory T cell development.* Immunity, 2010. **33**(4): p. 607-19.

308. Leng, R.X., et al., *Role of microRNA-155 in autoimmunity.* Cytokine Growth Factor Rev, 2011. **22**(3): p. 141-7.

309. Stanczyk, J., et al., *Altered expression of MicroRNA in synovial fibroblasts and synovial tissue in rheumatoid arthritis.* Arthritis Rheum, 2008. **58**(4): p. 1001-9.

310. Skeoch, S. and I.N. Bruce, *Atherosclerosis in rheumatoid arthritis: is it all about inflammation?* Nat Rev Rheumatol, 2015. **11**(7): p. 390-400.

311. Junker, A., et al., *MicroRNA profiling of multiple sclerosis lesions identifies modulators of the regulatory protein CD47.* Brain, 2009. **132**(Pt 12): p. 3342-52.

312. Leiss, H., et al., *MicroRNA 155-deficiency leads to decreased autoantibody levels and reduced severity of nephritis and pneumonitis in pristane-induced lupus.* PLoS One, 2017. **12**(7): p. e0181015.

313. Xin, Q., et al., *miR-155 Deficiency Ameliorates Autoimmune Inflammation of Systemic Lupus Erythematosus by Targeting S1pr1 in Faslpr/lpr Mice.* J Immunol, 2015. **194**(11): p. 5437-45.

314. Takagi, T., et al., *Increased expression of microRNA in the inflamed colonic mucosa of patients with active ulcerative colitis.* J Gastroenterol Hepatol, 2010. **25 Suppl 1**: p. S129-33.

315. Prinz, C. and D. Weber, *MicroRNA (miR) dysregulation during Helicobacter pylori-induced gastric inflammation and cancer development: critical importance of miR-155.* Oncotarget, 2020. **11**(10): p. 894-904.

316. Zhang, C.M., J. Zhao, and H.Y. Deng, *MiR-155 promotes proliferation of human breast cancer MCF-7 cells through targeting tumor protein 53-induced nuclear protein 1.* J Biomed Sci, 2013. **20**: p. 79.

317. Kim, S., et al., *microRNA-155 positively regulates glucose metabolism via PIK3R1-FOXO3a-cMYC axis in breast cancer.* Oncogene, 2018. **37**(22): p. 2982-2991.

318. Volinia, S., et al., *A microRNA expression signature of human solid tumors defines cancer gene targets.* Proc Natl Acad Sci U S A, 2006. **103**(7): p. 2257-61.

319. Yanaihara, N., et al., *Unique microRNA molecular profiles in lung cancer diagnosis and prognosis.* Cancer Cell, 2006. **9**(3): p. 189-98.

320. Eissa, M.G. and C.M. Artlett, *The MicroRNA miR-155 Is Essential in Fibrosis.* Noncoding RNA, 2019. **5**(1).

321. Wu, X., et al., *miR-155 inhibits the formation of hypertrophic scar fibroblasts by targeting HIF-1alpha via PI3K/AKT pathway.* J Mol Histol, 2018. **49**(4): p. 377-387.

322. Gatto, G., et al., *Epstein-Barr virus latent membrane protein 1 trans-activates miR-155 transcription through the NF-kappaB pathway.* Nucleic Acids Res, 2008. **36**(20): p. 6608-19.

323. Thompson, R.C., I. Vardinogiannis, and T.D. Gilmore, *Identification of an NF-kappaB p50/p65-responsive site in the human MIR155HG promoter.* BMC Mol Biol, 2013. **14**: p. 24.

324. Tili, E., et al., *Resveratrol decreases the levels of miR-155 by upregulating miR-663, a microRNA targeting JunB and JunD.* Carcinogenesis, 2010. **31**(9): p. 1561-6.

325. Zhao, H., et al., *Transforming Growth Factor beta1/Smad4 Signaling Affects Osteoclast Differentiation via Regulation of miR-155 Expression.* Mol Cells, 2017. **40**(3): p. 211-221.

326. Kong, W., et al., *MicroRNA-155 is regulated by the transforming growth factor beta/Smad pathway and contributes to epithelial cell plasticity by targeting RhoA.* Mol Cell Biol, 2008. **28**(22): p. 6773-84.

327. Zhang, X., et al., *The ATM kinase induces microRNA biogenesis in the DNA damage response.* Mol Cell, 2011. **41**(4): p. 371-83.

328. Ruggiero, T., et al., *LPS induces KH-type splicing regulatory protein-dependent processing of microRNA-155 precursors in macrophages.* FASEB J, 2009. **23**(9): p. 2898-908.

329. Bhattacharyya, S., et al., *Regulation of miR-155 biogenesis in cystic fibrosis lung epithelial cells: antagonistic role of two mRNA-destabilizing proteins, KSRP and TTP.* Biochem Biophys Res Commun, 2013. **433**(4): p. 484-8.

330. Das, S., et al., *Hzf Determines cell survival upon genotoxic stress by modulating p53 transactivation.* Cell, 2007. **130**(4): p. 624-37.

331. Neilsen, P.M., et al., *Mutant p53 drives invasion in breast tumors through up-regulation of miR-155.* Oncogene, 2013. **32**(24): p. 2992-3000.

332. Chen, T., A.M. Brownawell, and I.G. Macara, *Nucleocytoplasmic shuttling of JAZ, a new cargo protein for exportin-5.* Mol Cell Biol, 2004. **24**(15): p. 6608-19.

333. Lam, S.S., et al., *A novel p70 S6 kinase-microRNA biogenesis axis mediates multicellular spheroid formation in ovarian cancer progression.* Oncotarget, 2016. **7**(25): p. 38064-38077.

334. Wynn, T.A., A. Chawla, and J.W. Pollard, *Macrophage biology in development, homeostasis and disease.* Nature, 2013. **496**(7446): p. 445-55.

335. Epelman, S., et al., *Embryonic and adult-derived resident cardiac macrophages are maintained through distinct mechanisms at steady state and during inflammation.* Immunity, 2014. **40**(1): p. 91-104.

336. Gordon, S. and A. Pluddemann, *Tissue macrophages: heterogeneity and functions.* BMC Biol, 2017. **15**(1): p. 53.

337. Taylor, P.R., et al., *Macrophage receptors and immune recognition.* Annu Rev Immunol, 2005. **23**: p. 901-44.

338. Geissmann, F., S. Jung, and D.R. Littman, *Blood monocytes consist of two principal subsets with distinct migratory properties.* Immunity, 2003. **19**(1): p. 71-82.

339. Jakubzick, C., et al., *Minimal differentiation of classical monocytes as they survey steady-state tissues and transport antigen to lymph nodes.* Immunity, 2013. **39**(3): p. 599-610.

340. Ziegler-Heitbrock, L., *The CD14+ CD16+ blood monocytes: their role in infection and inflammation.* J Leukoc Biol, 2007. **81**(3): p. 584-92.

341. Carlin, L.M., et al., *Nr4a1-dependent Ly6C(low) monocytes monitor endothelial cells and orchestrate their disposal.* Cell, 2013. **153**(2): p. 362-75.

342. Mosser, D.M. and J.P. Edwards, *Exploring the full spectrum of macrophage activation.* Nat Rev Immunol, 2008. **8**(12): p. 958-69.

343. Paolicelli, R.C., et al., *Synaptic pruning by microglia is necessary for normal brain development.* Science, 2011. **333**(6048): p. 1456-8.

344. Schafer, D.P., et al., *Microglia sculpt postnatal neural circuits in an activity and complement-dependent manner.* Neuron, 2012. **74**(4): p. 691-705.

345. Chow, A., et al., *CD169(+) macrophages provide a niche promoting erythropoiesis under homeostasis and stress.* Nat Med, 2013. **19**(4): p. 429-36.

346. Kohyama, M., et al., *Role for Spi-C in the development of red pulp macrophages and splenic iron homeostasis.* Nature, 2009. **457**(7227): p. 318-21.

347. Murray, P.J., et al., *Macrophage activation and polarization: nomenclature and experimental guidelines.* Immunity, 2014. **41**(1): p. 14-20.

348. Murray, P.J. and T.A. Wynn, *Protective and pathogenic functions of macrophage subsets.* Nat Rev Immunol, 2011. **11**(11): p. 723-37.

349. Sindrilaru, A., et al., *An unrestrained proinflammatory M1 macrophage population induced by iron impairs wound healing in humans and mice.* J Clin Invest, 2011. **121**(3): p. 985-97.

350. Krausgruber, T., et al., *IRF5 promotes inflammatory macrophage polarization and TH1-TH17 responses.* Nat Immunol, 2011. **12**(3): p. 231-8.

351. Qian, B.Z. and J.W. Pollard, *Macrophage diversity enhances tumor progression and metastasis.* Cell, 2010. **141**(1): p. 39-51.

352. Udalova, I.A., A. Mantovani, and M. Feldmann, *Macrophage heterogeneity in the context of rheumatoid arthritis.* Nat Rev Rheumatol, 2016. **12**(8): p. 472-85.

353. Wynn, T.A. and K.M. Vannella, *Macrophages in Tissue Repair, Regeneration, and Fibrosis.* Immunity, 2016. **44**(3): p. 450-462.

354. Lavin, Y., et al., *Tissue-resident macrophage enhancer landscapes are shaped by the local microenvironment.* Cell, 2014. **159**(6): p. 1312-26.

355. Okabe, Y. and R. Medzhitov, *Tissue-specific signals control reversible program of localization and functional polarization of macrophages.* Cell, 2014. **157**(4): p. 832-44.

356. Piccinini, A.M., et al., *Distinct microenvironmental cues stimulate divergent TLR4-mediated signaling pathways in macrophages.* Sci Signal, 2016. **9**(443): p. ra86.

357. Hynes, R.O., *The extracellular matrix: not just pretty fibrils.* Science, 2009. **326**(5957): p. 1216-9.

358. Frantz, C., K.M. Stewart, and V.M. Weaver, *The extracellular matrix at a glance.* J Cell Sci, 2010. **123**(Pt 24): p. 4195-200.

359. Sorokin, L., *The impact of the extracellular matrix on inflammation.* Nat Rev Immunol, 2010. **10**(10): p. 712-23.

360. Agrawal, S., et al., *Dystroglycan is selectively cleaved at the parenchymal basement membrane at sites of leukocyte extravasation in experimental autoimmune encephalomyelitis.* J Exp Med, 2006. **203**(4): p. 1007-19.

361. Leask, A. and D.J. Abraham, *TGF-beta signaling and the fibrotic response.* FASEB J, 2004. **18**(7): p. 816-27.

362. Mouw, J.K., et al., *Tissue mechanics modulate microRNA-dependent PTEN expression to regulate malignant progression.* Nat Med, 2014. **20**(4): p. 360-7.

363. Banzhaf-Strathmann, J. and D. Edbauer, *Good guy or bad guy: the opposing roles of microRNA 125b in cancer.* Cell Commun Signal, 2014. **12**: p. 30.

364. Gerson, K.D., et al., *Integrin beta4 regulates SPARC protein to promote invasion.* J Biol Chem, 2012. **287**(13): p. 9835-44.

365. Goh, F.G., et al., *Transcriptional regulation of the endogenous danger signal tenascin-C: a novel autocrine loop in inflammation.* J Immunol, 2010. **184**(5): p. 2655-62.

366. Kuriyama, N., et al., *Tenascin-C: a novel mediator of hepatic ischemia and reperfusion injury.* Hepatology, 2011. **54**(6): p. 2125-36.

367. Patel, L., et al., *Tenascin-C induces inflammatory mediators and matrix degradation in osteoarthritic cartilage.* BMC Musculoskelet Disord, 2011. **12**: p. 164.

368. Liu, R., et al., *Tenascin-C produced by oxidized LDL-stimulated macrophages increases foam cell formation through Toll-like receptor-4.* Mol Cells, 2012. **34**(1): p. 35-41.

369. Machino-Ohtsuka, T., et al., *Tenascin-C aggravates autoimmune myocarditis via dendritic cell activation and Th17 cell differentiation.* J Am Heart Assoc, 2014. **3**(6): p. e001052.

370. Bhattacharyya, S., et al., *Tenascin-C drives persistence of organ fibrosis.* Nat Commun, 2016. **7**: p. 11703.

371. Kanayama, M., et al., *Alpha9 integrin and its ligands constitute critical joint microenvironments for development of autoimmune arthritis.* J Immunol, 2009. **182**(12): p. 8015-25.

372. Kanayama, M., et al., *alpha9beta1 integrin-mediated signaling serves as an intrinsic regulator of pathogenic Th17 cell generation.* J Immunol, 2011. **187**(11): p. 5851-64.

373. Asano, T., et al., *alpha9beta1 integrin acts as a critical intrinsic regulator of human rheumatoid arthritis.* Rheumatology (Oxford), 2014. **53**(3): p. 415-24.

374. Midwood, K.S., et al., *Tenascin-C at a glance.* J Cell Sci, 2016. **129**(23): p. 4321-4327.

375. Chiquet-Ehrismann, R., *Tenascins.* Int J Biochem Cell Biol, 2004. **36**(6): p. 986-90.

376. Chiquet-Ehrismann, R. and M. Chiquet, *Tenascins: regulation and putative functions during pathological stress.* J Pathol, 2003. **200**(4): p. 488-99.

377. Chiquet-Ehrismann, R. and R.P. Tucker, *Connective tissues: signalling by tenascins.* Int J Biochem Cell Biol, 2004. **36**(6): p. 1085-9.

378. Valcourt, U., et al., *Tenascin-X: beyond the architectural function.* Cell Adh Migr, 2015. **9**(1-2): p. 154-65.

379. Petersen, J.W. and J.Y. Douglas, *Tenascin-X, collagen, and Ehlers-Danlos syndrome: tenascin-X gene defects can protect against adverse cardiovascular events.* Med Hypotheses, 2013. **81**(3): p. 443-7.

380. Anlar, B. and A. Gunel-Ozcan, *Tenascin-R: role in the central nervous system.* Int J Biochem Cell Biol, 2012. **44**(9): p. 1385-9.

381. Xu, J.C., et al., *The extracellular matrix glycoprotein tenascin-R regulates neurogenesis during development and in the adult dentate gyrus of mice.* J Cell Sci, 2014. **127**(Pt 3): p. 641-52.

382. Martina, E., R. Chiquet-Ehrismann, and F. Brellier, *Tenascin-W: an extracellular matrix protein associated with osteogenesis and cancer.* Int J Biochem Cell Biol, 2010. **42**(9): p. 1412-5.

383. Martina, E., et al., *Tenascin-W is a specific marker of glioma-associated blood vessels and stimulates angiogenesis in vitro.* FASEB J, 2010. **24**(3): p. 778-87.

384. Tucker, R.P. and M. Degen, *The Expression and Possible Functions of Tenascin-W During Development and Disease.* Front Cell Dev Biol, 2019. **7**: p. 53.

385. Bourdon, M.A., et al., *Human glioma-mesenchymal extracellular matrix antigen defined by monoclonal antibody.* Cancer Res, 1983. **43**(6): p. 2796-805.

386. Chiquet, M. and D.M. Fambrough, *Chick myotendinous antigen. II. A novel extracellular glycoprotein complex consisting of large disulfide-linked subunits.* J Cell Biol, 1984. **98**(6): p. 1937-46.

387. Grumet, M., et al., *Cytotactin, an extracellular matrix protein of neural and non-neural tissues that mediates glia-neuron interaction.* Proc Natl Acad Sci U S A, 1985. **82**(23): p. 8075-9.

388. Kruse, J., et al., *The J1 glycoprotein--a novel nervous system cell adhesion molecule of the L2/HNK-1 family.* Nature, 1985. **316**(6024): p. 146-8.

389. Midwood, K.S. and G. Orend, *The role of tenascin-C in tissue injury and tumorigenesis.* J Cell Commun Signal, 2009. **3**(3-4): p. 287-310.

390. Gulcher, J.R., et al., *Chromosomal localization of the human hexabrachion (tenascin) gene and evidence for recent reduplication within the gene.* Genomics, 1990. **6**(4): p. 616-22.

391. Rocchi, M., et al., *Assignment of the gene for human tenascin to the region q32-q34 of chromosome 9.* Hum Genet, 1991. **86**(6): p. 621-3.

392. Giblin, S.P. and K.S. Midwood, *Tenascin-C: Form versus function.* Cell Adh Migr, 2015. **9**(1-2): p. 48-82.

393. Orend, G. and R. Chiquet-Ehrismann, *Tenascin-C induced signaling in cancer.* Cancer Lett, 2006. **244**(2): p. 143-63.

394. Sriramarao, P. and M.A. Bourdon, *A novel tenascin type III repeat is part of a complex of tenascin mRNA alternative splices.* Nucleic Acids Res, 1993. **21**(1): p. 163-8.

395. Latijnhouwers, M.A., et al., *Expression of tenascin-C splice variants by human skin cells.* Arch Dermatol Res, 2000. **292**(9): p. 446-54.

396. Chiovaro, F., R. Chiquet-Ehrismann, and M. Chiquet, *Transcriptional regulation of tenascin genes.* Cell Adh Migr, 2015. **9**(1-2): p. 34-47.

397. Jones, F.S., et al., *Prx1 controls vascular smooth muscle cell proliferation and tenascin-C expression and is upregulated with Prx2 in pulmonary vascular disease.* Circ Res, 2001. **89**(2): p. 131-8.

398. Jones, F.S., et al., *Activation of the cytotactin promoter by the homeobox-containing gene Evx-1.* Proc Natl Acad Sci U S A, 1992. **89**(6): p. 2091-5.

399. Maqbool, A., et al., *Interleukin-1 has opposing effects on connective tissue growth factor and tenascin-C expression in human cardiac fibroblasts.* Matrix Biol, 2013. **32**(3-4): p. 208-14.

400. Chevillard, G., et al., *Identification of interleukin-1beta regulated genes in uterine smooth muscle cells.* Reproduction, 2007. **134**(6): p. 811-22.

401. Gratchev, A., et al., *Interleukin-4 and dexamethasone counterregulate extracellular matrix remodelling and phagocytosis in type-2 macrophages.* Scand J Immunol, 2005. **61**(1): p. 10-7.

402. Jinnin, M., et al., *Upregulation of tenascin-C expression by IL-13 in human dermal fibroblasts via the phosphoinositide 3-kinase/Akt and the protein kinase C signaling pathways.* J Invest Dermatol, 2006. **126**(3): p. 551-60.

403. Xu, X., et al., *Transforming growth factor-beta in stem cells and tissue homeostasis.* Bone Res, 2018. **6**: p. 2.

404. Scherberich, A., et al., *Tenascin-W is found in malignant mammary tumors, promotes alpha8 integrin-dependent motility and requires p38MAPK activity for BMP-2 and TNF-alpha induced expression in vitro.* Oncogene, 2005. **24**(9): p. 1525-32.

405. Dobbertin, A., et al., *Analysis of combinatorial variability reveals selective accumulation of the fibronectin type III domains B and D of tenascin-C in injured brain.* Exp Neurol, 2010. **225**(1): p. 60-73.

406. Jinnin, M., et al., *Tenascin-C upregulation by transforming growth factor-beta in human dermal fibroblasts involves Smad3, Sp1, and Ets1.* Oncogene, 2004. **23**(9): p. 1656-67.

407. Ekblom, M., et al., *Downregulation of tenascin expression by glucocorticoids in bone marrow stromal cells and in fibroblasts.* J Cell Biol, 1993. **123**(4): p. 1037-45.

408. Trottier, M.D., et al., *Natural glucocorticoids induce expansion of all developmental stages of murine bone marrow granulocytes without inhibiting function.* Proc Natl Acad Sci U S A, 2008. **105**(6): p. 2028-33.

409. Oppong, E., N. Flink, and A.C. Cato, *Molecular mechanisms of glucocorticoid action in mast cells.* Mol Cell Endocrinol, 2013. **380**(1-2): p. 119-26.

410. Tavazoie, S.F., et al., *Endogenous human microRNAs that suppress breast cancer metastasis.* Nature, 2008. **451**(7175): p. 147-52.

411. Zhu, H., et al., *FC-99 reduces macrophage tenascin-C expression by upregulating miRNA-494 in arthritis.* Int Immunopharmacol, 2020. **79**: p. 106105.

412. Gulcher, J.R., et al., *An alternatively spliced region of the human hexabrachion contains a repeat of potential N-glycosylation sites.* Proc Natl Acad Sci U S A, 1989. **86**(5): p. 1588-92.

413. Steentoft, C., et al., *Precision mapping of the human O-GalNAc glycoproteome through SimpleCell technology.* EMBO J, 2013. **32**(10): p. 1478-88.

414. Schwenzer, A., et al., *Identification of an immunodominant peptide from citrullinated tenascin-C as a major target for autoantibodies in rheumatoid arthritis.* Ann Rheum Dis, 2016. **75**(10): p. 1876-83.

415. Sano, K., et al., *Changes in glycosylation of vitronectin modulate multimerization and collagen binding during liver regeneration.* Glycobiology, 2007. **17**(7): p. 784-94.

416. Jones, G.E., R.G. Arumugham, and M.L. Tanzer, *Fibronectin glycosylation modulates fibroblast adhesion and spreading.* J Cell Biol, 1986. **103**(5): p. 1663-70.

417. Kasbaoui, L., et al., *Differences in glycosylation state of fibronectin from two rat colon carcinoma cell lines in relation to tumoral progressiveness.* Cancer Res, 1989. **49**(19): p. 5317-22.

418. Siri, A., et al., *Different susceptibility of small and large human tenascin-C isoforms to degradation by matrix metalloproteinases.* J Biol Chem, 1995. **270**(15): p. 8650-4.

419. Saito, Y., et al., *A peptide derived from tenascin-C induces beta1 integrin activation through syndecan-4.* J Biol Chem, 2007. **282**(48): p. 34929-37.

420. Tucker, R.P. and S.E. McKay, *The expression of tenascin by neural crest cells and glia.* Development, 1991. **112**(4): p. 1031-9.

421. Wehrle, B. and M. Chiquet, *Tenascin is accumulated along developing peripheral nerves and allows neurite outgrowth in vitro.* Development, 1990. **110**(2): p. 401-15.

422. Chiquet, M. and D.M. Fambrough, *Chick myotendinous antigen. I. A monoclonal antibody as a marker for tendon and muscle morphogenesis.* J Cell Biol, 1984. **98**(6): p. 1926-36.

423. Inaguma, Y., et al., *Epithelial induction of stromal tenascin in the mouse mammary gland: from embryogenesis to carcinogenesis.* Dev Biol, 1988. **128**(2): p. 245-55.

424. Chiquet-Ehrismann, R., et al., *Tenascin: an extracellular matrix protein involved in tissue interactions during fetal development and oncogenesis.* Cell, 1986. **47**(1): p. 131-9.

425. Aufderheide, E., R. Chiquet-Ehrismann, and P. Ekblom, *Epithelial-mesenchymal interactions in the developing kidney lead to expression of tenascin in the mesenchyme.* J Cell Biol, 1987. **105**(1): p. 599-608.

426. Koch, M., et al., *Epithelial synthesis of tenascin at tips of growing bronchi and graded accumulation in basement membrane and mesenchyme.* Exp Cell Res, 1991. **194**(2): p. 297-300.

427. Fluck, M., V. Tunc-Civelek, and M. Chiquet, *Rapid and reciprocal regulation of tenascin-C and tenascin-Y expression by loading of skeletal muscle.* J Cell Sci, 2000. **113 (Pt 20)**: p. 3583-91.

428. Chiquet-Ehrismann, R., et al., *Tenascins in stem cell niches.* Matrix Biol, 2014. **37**: p. 112-23.

429. Saga, Y., et al., *Mice develop normally without tenascin.* Genes Dev, 1992. **6**(10): p. 1821-31.

430. Forsberg, E., et al., *Skin wounds and severed nerves heal normally in mice lacking tenascin-C.* Proc Natl Acad Sci U S A, 1996. **93**(13): p. 6594-9.

431. Fukamauchi, F., et al., *Abnormal behavior and neurotransmissions of tenascin gene knockout mouse.* Biochem Biophys Res Commun, 1996. **221**(1): p. 151-6.

432. Fukamauchi, F. and M. Kusakabe, *Preprotachykinin A and cholecystokinin mRNAs in tenascin-gene knockout mouse brain.* Neuropeptides, 1997. **31**(2): p. 199-201.

433. Tamaoki, M., et al., *Tenascin-C regulates recruitment of myofibroblasts during tissue repair after myocardial injury.* Am J Pathol, 2005. **167**(1): p. 71-80.

434. Nishioka, T., et al., *Tenascin-C may aggravate left ventricular remodeling and function after myocardial infarction in mice.* Am J Physiol Heart Circ Physiol, 2010. **298**(3): p. H1072-8.

435. Tanaka, K., et al., *Tenascin-C regulates angiogenesis in tumor through the regulation of vascular endothelial growth factor expression.* Int J Cancer, 2004. **108**(1): p. 31-40.

436. Midwood, K.S., et al., *Advances in tenascin-C biology.* Cell Mol Life Sci, 2011. **68**(19): p. 3175-99.

437. Swindle, C.S., et al., *Epidermal growth factor (EGF)-like repeats of human tenascin-C as ligands for EGF receptor.* J Cell Biol, 2001. **154**(2): p. 459-68.

438. Iyer, A.K., et al., *Tenascin cytotactin epidermal growth factor-like repeat binds epidermal growth factor receptor with low affinity.* J Cell Physiol, 2007. **211**(3): p. 748-58.

439. Tucker, R.P. and R. Chiquet-Ehrismann, *Tenascin-C: Its functions as an integrin ligand.* Int J Biochem Cell Biol, 2015. **65**: p. 165-8.

440. Yoshida, T., T. Akatsuka, and K. Imanaka-Yoshida, *Tenascin-C and integrins in cancer.* Cell Adh Migr, 2015. **9**(1-2): p. 96-104.

441. Zuliani-Alvarez, L., et al., *Mapping tenascin-C interaction with toll-like receptor 4 reveals a new subset of endogenous inflammatory triggers.* Nat Commun, 2017. **8**(1): p. 1595.

442. Adamsky, K., et al., *Glial tumor cell adhesion is mediated by binding of the FNIII domain of receptor protein tyrosine phosphatase beta (RPTPbeta) to tenascin C.* Oncogene, 2001. **20**(5): p. 609-18.

443. Milev, P., et al., *The fibrinogen-like globe of tenascin-C mediates its interactions with neurocan and phosphacan/protein-tyrosine phosphatase-zeta/beta.* J Biol Chem, 1997. **272**(24): p. 15501-9.

444. Chung, C.Y., L. Zardi, and H.P. Erickson, *Binding of tenascin-C to soluble fibronectin and matrix fibrils.* J Biol Chem, 1995. **270**(48): p. 29012-7.

445. Vaughan, L., et al., *Tenascin-contactin/F11 interactions: a clue for a developmental role?* Perspect Dev Neurobiol, 1994. **2**(1): p. 43-52.

446. Rigato, F., et al., *Tenascin-C promotes neurite outgrowth of embryonic hippocampal neurons through the alternatively spliced fibronectin type III BD domains via activation of the cell adhesion molecule F3/contactin.* J Neurosci, 2002. **22**(15): p. 6596-609.

447. Fischer, D., et al., *A single heparin binding region within the fibrinogen-like domain is functional in chick tenascin-C.* J Biol Chem, 1995. **270**(7): p. 3378-84.

448. Weber, P., et al., *Tenascin-C binds heparin by its fibronectin type III domain five.* J Biol Chem, 1995. **270**(9): p. 4619-23.

449. Chung, C.Y. and H.P. Erickson, *Cell surface annexin II is a high affinity receptor for the alternatively spliced segment of tenascin-C.* J Cell Biol, 1994. **126**(2): p. 539-48.

450. De Laporte, L., et al., *Tenascin C promiscuously binds growth factors via its fifth fibronectin type III-like domain.* PLoS One, 2013. **8**(4): p. e62076.

451. Chiquet-Ehrismann, R., et al., *Tenascin interferes with fibronectin action.* Cell, 1988. **53**(3): p. 383-90.

452. Huang, W., et al., *Interference of tenascin-C with syndecan-4 binding to fibronectin blocks cell adhesion and stimulates tumor cell proliferation.* Cancer Res, 2001. **61**(23): p. 8586-94.

453. Orend, G., et al., *Tenascin-C blocks cell-cycle progression of anchorage-dependent fibroblasts on fibronectin through inhibition of syndecan-4.* Oncogene, 2003. **22**(25): p. 3917-26.

454. Day, J.M., et al., *Alternative splicing in the aggrecan G3 domain influences binding interactions with tenascin-C and other extracellular matrix proteins.* J Biol Chem, 2004. **279**(13): p. 12511-8.

455. Hauzenberger, D., et al., *Tenascin-C inhibits beta1 integrin-dependent T lymphocyte adhesion to fibronectin through the binding of its fnIII 1-5 repeats to fibronectin.* Eur J Immunol, 1999. **29**(5): p. 1435-47.

456. Shimojo, N., et al., *Tenascin-C may accelerate cardiac fibrosis by activating macrophages via the integrin alphaVbeta3/nuclear factor-kappaB/interleukin-6 axis.* Hypertension, 2015. **66**(4): p. 757-66.

457. Yokoyama, K., et al., *Identification of amino acid sequences in fibrinogen gamma -chain and tenascin C C-terminal domains critical for binding to integrin alpha vbeta 3.* J Biol Chem, 2000. **275**(22): p. 16891-8.

458. Schenk, S., R. Chiquet-Ehrismann, and E.J. Battegay, *The fibrinogen globe of tenascin-C promotes basic fibroblast growth factor-induced endothelial cell elongation.* Mol Biol Cell, 1999. **10**(9): p. 2933-43.

459. Martino, M.M., et al., *Growth factors engineered for super-affinity to the extracellular matrix enhance tissue healing.* Science, 2014. **343**(6173): p. 885-8.

460. Jones, P.L., J. Crack, and M. Rabinovitch, *Regulation of tenascin-C, a vascular smooth muscle cell survival factor that interacts with the alpha v beta 3 integrin to promote epidermal growth factor receptor phosphorylation and growth.* J Cell Biol, 1997. **139**(1): p. 279-93.

461. Ishigaki, T., et al., *Tenascin-C enhances crosstalk signaling of integrin alphavbeta3/PDGFR-beta complex by SRC recruitment promoting PDGF-induced proliferation and migration in smooth muscle cells.* J Cell Physiol, 2011. **226**(10): p. 2617-24.

462. Benbow, J.H., et al., *Diet-Induced Obesity Enhances Progression of Hepatocellular Carcinoma through Tenascin-C/Toll-Like Receptor 4 Signaling.* Am J Pathol, 2016. **186**(1): p. 145-58.

463. Ruhmann, M., et al., *Endogenous activation of adaptive immunity: tenascin-C drives interleukin-17 synthesis in murine arthritic joint disease.* Arthritis Rheum, 2012. **64**(7): p. 2179-90.

464. Maqbool, A., et al., *Tenascin C upregulates interleukin-6 expression in human cardiac myofibroblasts via toll-like receptor 4.* World J Cardiol, 2016. **8**(5): p. 340-50.

465. Lowy, C.M. and T. Oskarsson, *Tenascin C in metastasis: A view from the invasive front.* Cell Adh Migr, 2015. **9**(1-2): p. 112-24.

466. Steitz, A.M., et al., *Tumor-associated macrophages promote ovarian cancer cell migration by secreting transforming growth factor beta induced (TGFBI) and tenascin C.* Cell Death Dis, 2020. **11**(4): p. 249.

467. Hesse, J., et al., *CD73-derived adenosine and tenascin-C control cytokine production by epicardium-derived cells formed after myocardial infarction.* FASEB J, 2017. **31**(7): p. 3040-3053.

468. van den Berg, W.B. and P. Miossec, *IL-17 as a future therapeutic target for rheumatoid arthritis.* Nat Rev Rheumatol, 2009. **5**(10): p. 549-53.

469. De Wever, O., et al., *Tenascin-C and SF/HGF produced by myofibroblasts in vitro provide convergent pro-invasive signals to human colon cancer cells through RhoA and Rac.* FASEB J, 2004. **18**(9): p. 1016-8.

470. Matsuda, A., et al., *Corneal wound healing in tenascin knockout mouse.* Invest Ophthalmol Vis Sci, 1999. **40**(6): p. 1071-80.

471. Sumioka, T., et al., *Impaired cornea wound healing in a tenascin C-deficient mouse model.* Lab Invest, 2013. **93**(2): p. 207-17.

472. Carey, W.A., et al., *Tenascin-C deficiency attenuates TGF-ss-mediated fibrosis following murine lung injury.* Am J Physiol Lung Cell Mol Physiol, 2010. **299**(6): p. L785-93.

473. Jachetti, E., et al., *Tenascin-C Protects Cancer Stem-like Cells from Immune Surveillance by Arresting T-cell Activation.* Cancer Res, 2015. **75**(10): p. 2095-108.

474. Puente Navazo, M.D., D. Valmori, and C. Ruegg, *The alternatively spliced domain TnFnIII A1A2 of the extracellular matrix protein tenascin-C suppresses activation-induced T lymphocyte proliferation and cytokine production.* J Immunol, 2001. **167**(11): p. 6431-40.

475. Loike, J.D., et al., *Blockade of alpha 5 beta 1 integrins reverses the inhibitory effect of tenascin on chemotaxis of human monocytes and polymorphonuclear leukocytes through three-dimensional gels of extracellular matrix proteins.* J Immunol, 2001. **166**(12): p. 7534-42.

476. Schenk, S., et al., *Tenascin-C in serum: a questionable tumor marker.* Int J Cancer, 1995. **61**(4): p. 443-9.

477. Kaarteenaho-Wiik, R., et al., *Tenascin expression and distribution in pleural inflammatory and fibrotic diseases.* J Histochem Cytochem, 2000. **48**(9): p. 1257-68.

478. Paallysaho, T., et al., *Cellular fibronectin and tenascin in an orbital nylon prosthesis removed because of infection caused by Staphylococcus aureus.* Graefes Arch Clin Exp Ophthalmol, 1993. **231**(2): p. 61-5.

479. Seluanov, A., A. Vaidya, and V. Gorbunova, *Establishing primary adult fibroblast cultures from rodents.* J Vis Exp, 2010(44).

480. Gagnon, K.T., et al., *Analysis of nuclear RNA interference in human cells by subcellular fractionation and Argonaute loading.* Nat Protoc, 2014. **9**(9): p. 2045-60.

481. Gagliardi, M. and M.R. Matarazzo, *RIP: RNA Immunoprecipitation.* Methods Mol Biol, 2016. **1480**: p. 73-86.

482. Bustin, S.A., et al., *The MIQE guidelines: minimum information for publication of quantitative real-time PCR experiments.* Clin Chem, 2009. **55**(4): p. 611-22.

483. Brooks, S.A. and P.J. Blackshear, *Tristetraprolin (TTP): interactions with mRNA and proteins, and current thoughts on mechanisms of action.* Biochim Biophys Acta, 2013. **1829**(6-7): p. 666-79.

484. Taylor, G.A., et al., *A pathogenetic role for TNF alpha in the syndrome of cachexia, arthritis, and autoimmunity resulting from tristetraprolin (TTP) deficiency.* Immunity, 1996. **4**(5): p. 445-54.

485. Carballo, E., W.S. Lai, and P.J. Blackshear, *Feedback inhibition of macrophage tumor necrosis factor-alpha production by tristetraprolin.* Science, 1998. **281**(5379): p. 1001-5.

486. Zhao, W., et al., *Tristetraprolin regulates interleukin-6 expression through p38 MAPK-dependent affinity changes with mRNA 3' untranslated region.* J Interferon Cytokine Res, 2011. **31**(8): p. 629-37.

487. Stoecklin, G., et al., *Genome-wide analysis identifies interleukin-10 mRNA as target of tristetraprolin.* J Biol Chem, 2008. **283**(17): p. 11689-99.

488. Ma, F., et al., *MicroRNA-466l upregulates IL-10 expression in TLR-triggered macrophages by antagonizing RNA-binding protein tristetraprolin-mediated IL-10 mRNA degradation.* J Immunol, 2010. **184**(11): p. 6053-9.

489. Guo, J., et al., *MiRNA-29c regulates the expression of inflammatory cytokines in diabetic nephropathy by targeting tristetraprolin.* Sci Rep, 2017. **7**(1): p. 2314.

490. Liu, J., et al., *Tristetraprolin expression and microRNA-mediated regulation during simian immunodeficiency virus infection of the central nervous system.* Mol Brain, 2013. **6**: p. 40.

491. Yuan, H., et al., *SUMO1 modification of KHSRP regulates tumorigenesis by preventing the TL-G-Rich miRNA biogenesis.* Mol Cancer, 2017. **16**(1): p. 157.

492. Chen, Y.L., et al., *Transcriptional regulation of tristetraprolin by NF-kappaB signaling in LPS-stimulated macrophages.* Mol Biol Rep, 2013. **40**(4): p. 2867-77.

493. Tchen, C.R., et al., *The stability of tristetraprolin mRNA is regulated by mitogen-activated protein kinase p38 and by tristetraprolin itself.* J Biol Chem, 2004. **279**(31): p. 32393-400.

494. Brooks, S.A., J.E. Connolly, and W.F. Rigby, *The role of mRNA turnover in the regulation of tristetraprolin expression: evidence for an extracellular signal-regulated kinase-specific, AU-rich element-dependent, autoregulatory pathway.* J Immunol, 2004. **172**(12): p. 7263-71.

495. Gebeshuber, C.A., K. Zatloukal, and J. Martinez, *miR-29a suppresses tristetraprolin, which is a regulator of epithelial polarity and metastasis.* EMBO Rep, 2009. **10**(4): p. 400-5.

496. Al-Ahmadi, W., et al., *miR-29a inhibition normalizes HuR over-expression and aberrant AU-rich mRNA stability in invasive cancer.* J Pathol, 2013. **230**(1): p. 28-38.

497. Pfeiffer, J.R. and S.A. Brooks, *Cullin 4B is recruited to tristetraprolin-containing messenger ribonucleoproteins and regulates TNF-alpha mRNA polysome loading.* J Immunol, 2012. **188**(4): p. 1828-39.

498. Qi, M.Y., et al., *AU-rich-element-dependent translation repression requires the cooperation of tristetraprolin and RCK/P54.* Mol Cell Biol, 2012. **32**(5): p. 913-28.

499. Tiedje, C., et al., *The p38/MK2-driven exchange between tristetraprolin and HuR regulates AU-rich element-dependent translation.* PLoS Genet, 2012. **8**(9): p. e1002977.

500. Pfeiffer, J.R., et al., *CARHSP1 is required for effective tumor necrosis factor alpha mRNA stabilization and localizes to processing bodies and exosomes.* Mol Cell Biol, 2011. **31**(2): p. 277-86.

501. Linker, K., et al., *Involvement of KSRP in the post-transcriptional regulation of human iNOS expression-complex interplay of KSRP with TTP and HuR.* Nucleic Acids Res, 2005. **33**(15): p. 4813-27.

502. Fechir, M., et al., *Tristetraprolin regulates the expression of the human inducible nitric-oxide synthase gene.* Mol Pharmacol, 2005. **67**(6): p. 2148-61.

503. Sedlyarov, V., et al., *Tristetraprolin binding site atlas in the macrophage transcriptome reveals a switch for inflammation resolution.* Mol Syst Biol, 2016. **12**(5): p. 868.

504. Su, Y.L., et al., *Tristetraprolin inhibits poly(A)-tail synthesis in nuclear mRNA that contains AU-rich elements by interacting with poly(A)-binding protein nuclear 1.* PLoS One, 2012. **7**(7): p. e41313.

505. Barrios-Garcia, T., et al., *Nuclear tristetraprolin acts as a corepressor of multiple steroid nuclear receptors in breast cancer cells.* Mol Genet Metab Rep, 2016. **7**: p. 20-6.

506. Liang, J., et al., *RNA-destabilizing factor tristetraprolin negatively regulates NF-kappaB signaling.* J Biol Chem, 2009. **284**(43): p. 29383-90.

507. Xu, L., et al., *Tristetraprolin induces cell cycle arrest in breast tumor cells through targeting AP-1/c-Jun and NF-kappaB pathway.* Oncotarget, 2015. **6**(39): p. 41679-91.

508. Tiedje, C., et al., *The RNA-binding protein TTP is a global post-transcriptional regulator of feedback control in inflammation.* Nucleic Acids Res, 2016. **44**(15): p. 7418-40.

509. Hasegawa, M., et al., *Expression of large tenascin-C splice variants in synovial fluid of patients with rheumatoid arthritis.* J Orthop Res, 2007. **25**(5): p. 563-8.

510. Schenk, S., et al., *Tenascin-C in serum: an acute-phase protein or a carcinoma marker?* Int J Cancer, 1995. **60**(1): p. 145.

511. Fujimoto, M., et al., *Epidermal growth factor-like repeats of tenascin-C-induced constriction of cerebral arteries via activation of epidermal growth factor receptors in rats.* Brain Res, 2016. **1642**: p. 436-444.

512. Midwood, K.S., et al., *Coregulation of fibronectin signaling and matrix contraction by tenascin-C and syndecan-4.* Mol Biol Cell, 2004. **15**(12): p. 5670-7.

513. Derr, L.B., et al., *The expression of tenascin-C with the AD1 variable repeat in embryonic tissues, cell lines and tumors in various vertebrate species.* Differentiation, 1997. **62**(2): p. 71-82.

514. Ricard-Blum, S., *The collagen family.* Cold Spring Harb Perspect Biol, 2011. **3**(1): p. a004978.

515. To, W.S. and K.S. Midwood, *Plasma and cellular fibronectin: distinct and independent functions during tissue repair.* Fibrogenesis Tissue Repair, 2011. **4**: p. 21.

516. Pankov, R. and K.M. Yamada, *Fibronectin at a glance.* J Cell Sci, 2002. **115**(Pt 20): p. 3861-3.

517. To, W.S. and K.S. Midwood, *Identification of novel and distinct binding sites within tenascin-C for soluble and fibrillar fibronectin.* J Biol Chem, 2011. **286**(17): p. 14881-91.

518. Radwanska, A., et al., *Counterbalancing anti-adhesive effects of Tenascin-C through fibronectin expression in endothelial cells.* Sci Rep, 2017. **7**(1): p. 12762.

519. Giblin, S.P., A. Schwenzer, and K.S. Midwood, *Alternative splicing controls cell lineage-specific responses to endogenous innate immune triggers within the extracellular matrix.* Matrix Biol, 2020.

520. Simoes, F.C., et al., *Macrophages directly contribute collagen to scar formation during zebrafish heart regeneration and mouse heart repair.* Nat Commun, 2020. **11**(1): p. 600.

521. Afik, R., et al., *Tumor macrophages are pivotal constructors of tumor collagenous matrix.* J Exp Med, 2016. **213**(11): p. 2315-2331.

522. Chang, M.Y., et al., *Monocyte-to-macrophage differentiation: synthesis and secretion of a complex extracellular matrix.* J Biol Chem, 2012. **287**(17): p. 14122-35.

523. Etich, J., et al., *Gene Expression Profiling of the Extracellular Matrix Signature in Macrophages of Different Activation Status: Relevance for Skin Wound Healing.* Int J Mol Sci, 2019. **20**(20).

524. Chiquet, M., et al., *Isolation of chick tenascin variants and fragments. A C-terminal heparin-binding fragment produced by cleavage of the extra domain from the largest subunit splicing variant.* Eur J Biochem, 1991. **199**(2): p. 379-88.

525. Villa-Diaz, L.G., et al., *Analysis of the factors that limit the ability of feeder cells to maintain the undifferentiated state of human embryonic stem cells.* Stem Cells Dev, 2009. **18**(4): p. 641-51.

526. Soteriou, D., et al., *Comparative proteomic analysis of supportive and unsupportive extracellular matrix substrates for human embryonic stem cell maintenance.* J Biol Chem, 2013. **288**(26): p. 18716-31.

527. Chung, C.Y. and H.P. Erickson, *Glycosaminoglycans modulate fibronectin matrix assembly and are essential for matrix incorporation of tenascin-C.* J Cell Sci, 1997. **110 (Pt 12)**: p. 1413-9.

528. Ramos, D.M., et al., *Tenascin-C matrix assembly in oral squamous cell carcinoma.* Int J Cancer, 1998. **75**(5): p. 680-7.

529. Borsi, L., et al., *Cell-cycle dependent alternative splicing of the tenascin primary transcript.* Cell Adhes Commun, 1994. **1**(4): p. 307-17.

530. Parekh, K., et al., *Tenascin-C, over expressed in lung cancer down regulates effector functions of tumor infiltrating lymphocytes.* Lung Cancer, 2005. **47**(1): p. 17-29.

531. Mercado, M.L., et al., *Neurite outgrowth by the alternatively spliced region of human tenascin-C is mediated by neuronal alpha7beta1 integrin.* J Neurosci, 2004. **24**(1): p. 238-47.

532. Antonov, A.S., et al., *alphaVbeta3 integrin regulates macrophage inflammatory responses via PI3 kinase/Akt-dependent NF-kappaB activation.* J Cell Physiol, 2011. **226**(2): p. 469-76.

533. Kumanogoh, A. and H. Kikutani, *Immunological functions of the neuropilins and plexins as receptors for semaphorins.* Nat Rev Immunol, 2013. **13**(11): p. 802-14.

534. Tordjman, R., et al., *A neuronal receptor, neuropilin-1, is essential for the initiation of the primary immune response.* Nat Immunol, 2002. **3**(5): p. 477-82.

535. Dai, X., et al., *A novel role for myeloid cell-specific neuropilin 1 in mitigating sepsis.* FASEB J, 2017. **31**(7): p. 2881-2892.

536. Cantuti-Castelvetri, L., et al., *Neuropilin-1 facilitates SARS-CoV-2 cell entry and infectivity.* Science, 2020.

537. Daly, J.L., et al., *Neuropilin-1 is a host factor for SARS-CoV-2 infection.* Science, 2020.

538. Solovjov, D.A., E. Pluskota, and E.F. Plow, *Distinct roles for the alpha and beta subunits in the functions of integrin alphaMbeta2.* J Biol Chem, 2005. **280**(2): p. 1336-45.

539. Hynes, R.O., *Integrins: bidirectional, allosteric signaling machines.* Cell, 2002. **110**(6): p. 673-87.

540. Ling, G.S., et al., *Integrin CD11b positively regulates TLR4-induced signalling pathways in dendritic cells but not in macrophages.* Nat Commun, 2014. **5**: p. 3039.

541. Yao, X., et al., *Leukadherin-1-Mediated Activation of CD11b Inhibits LPS-Induced Pro-inflammatory Response in Macrophages and Protects Mice Against Endotoxic Shock by Blocking LPS-TLR4 Interaction.* Front Immunol, 2019. **10**: p. 215.

542. Zhou, H., et al., *Antagonism of Integrin CD11b Affords Protection against Endotoxin Shock and Polymicrobial Sepsis via Attenuation of HMGB1 Nucleocytoplasmic Translocation and Extracellular Release.* J Immunol, 2018. **200**(5): p. 1771-1780.

543. Zhou, H., et al., *CD11b/CD18 (Mac-1) is a novel surface receptor for extracellular double-stranded RNA to mediate cellular inflammatory responses.* J Immunol, 2013. **190**(1): p. 115-25.

544. Bruder, D., et al., *Neuropilin-1: a surface marker of regulatory T cells.* Eur J Immunol, 2004. **34**(3): p. 623-630.

545. Glinka, Y. and G.J. Prud'homme, *Neuropilin-1 is a receptor for transforming growth factor beta-1, activates its latent form, and promotes regulatory T cell activity.* J Leukoc Biol, 2008. **84**(1): p. 302-10.

546. Prud'homme, G.J. and Y. Glinka, *Neuropilins are multifunctional coreceptors involved in tumor initiation, growth, metastasis and immunity.* Oncotarget, 2012. **3**(9): p. 921-39.

547. Soker, S., et al., *Neuropilin-1 is expressed by endothelial and tumor cells as an isoform-specific receptor for vascular endothelial growth factor.* Cell, 1998. **92**(6): p. 735-45.

548. Ji, J.D., K.H. Park-Min, and L.B. Ivashkiv, *Expression and function of semaphorin 3A and its receptors in human monocyte-derived macrophages.* Hum Immunol, 2009. **70**(4): p. 211-7.

549. Oussa, N.A., et al., *VEGF Requires the Receptor NRP-1 To Inhibit Lipopolysaccharide-Dependent Dendritic Cell Maturation.* J Immunol, 2016. **197**(10): p. 3927-3935.

550. Ehirchiou, D., et al., *CD11b facilitates the development of peripheral tolerance by suppressing Th17 differentiation.* J Exp Med, 2007. **204**(7): p. 1519-24.

551. Khan, S.Q., et al., *A Small Molecule beta2 Integrin Agonist Improves Chronic Kidney Allograft Survival by Reducing Leukocyte Recruitment and Accompanying Vasculopathy.* Front Med (Lausanne), 2014. **1**: p. 45.

552. Maiguel, D., et al., *Small molecule-mediated activation of the integrin CD11b/CD18 reduces inflammatory disease.* Sci Signal, 2011. **4**(189): p. ra57.

553. Varga, G., et al., *Active MAC-1 (CD11b/CD18) on DCs inhibits full T-cell activation.* Blood, 2007. **109**(2): p. 661-9.

554. Fossati-Jimack, L., et al., *Phagocytosis is the main CR3-mediated function affected by the lupus-associated variant of CD11b in human myeloid cells.* PLoS One, 2013. **8**(2): p. e57082.

555. Wolf, D., et al., *A ligand-specific blockade of the integrin Mac-1 selectively targets pathologic inflammation while maintaining protective host-defense.* Nat Commun, 2018. **9**(1): p. 525.

556. Gao, H.M., et al., *HMGB1 acts on microglia Mac1 to mediate chronic neuroinflammation that drives progressive neurodegeneration.* J Neurosci, 2011. **31**(3): p. 1081-92.

557. Zhang, D., et al., *Microglial MAC1 receptor and PI3K are essential in mediating beta-amyloid peptide-induced microglial activation and subsequent neurotoxicity.* J Neuroinflammation, 2011. **8**(1): p. 3.

558. Han, C., et al., *Integrin CD11b negatively regulates TLR-triggered inflammatory responses by activating Syk and promoting degradation of MyD88 and TRIF via Cbl-b.* Nat Immunol, 2010. **11**(8): p. 734-42.

559. Altieri, D.C., J. Plescia, and E.F. Plow, *The structural motif glycine 190-valine 202 of the fibrinogen gamma chain interacts with CD11b/CD18 integrin (alpha M beta 2, Mac-1) and promotes leukocyte adhesion.* J Biol Chem, 1993. **268**(3): p. 1847-53.

560. Altieri, D.C., et al., *A unique recognition site mediates the interaction of fibrinogen with the leukocyte integrin Mac-1 (CD11b/CD18).* J Biol Chem, 1990. **265**(21): p. 12119-22.

561. Ugarova, T.P., et al., *Identification of a novel recognition sequence for integrin alphaM beta2 within the gamma-chain of fibrinogen.* J Biol Chem, 1998. **273**(35): p. 22519-27.

562. Roy, S., et al., *Multifaceted Role of Neuropilins in the Immune System: Potential Targets for Immunotherapy.* Front Immunol, 2017. **8**: p. 1228.

563. Moutal, A., et al., *SARS-CoV-2 Spike protein co-opts VEGF-A/Neuropilin-1 receptor signaling to induce analgesia.* PAIN, 2020. **Articles in Press**.

564. Valdembri, D., et al., *Neuropilin-1/GIPC1 signaling regulates alpha5beta1 integrin traffic and function in endothelial cells.* PLoS Biol, 2009. **7**(1): p. e25.

565. Murga, M., O. Fernandez-Capetillo, and G. Tosato, *Neuropilin-1 regulates attachment in human endothelial cells independently of vascular endothelial growth factor receptor-2.* Blood, 2005. **105**(5): p. 1992-9.

566. Robinson, S.D., et al., *Alphav beta3 integrin limits the contribution of neuropilin-1 to vascular endothelial growth factor-induced angiogenesis.* J Biol Chem, 2009. **284**(49): p. 33966-81.

567. Ellison, T.S., et al., *Suppression of beta3-integrin in mice triggers a neuropilin-1-dependent change in focal adhesion remodelling that can be targeted to block pathological angiogenesis.* Dis Model Mech, 2015. **8**(9): p. 1105-19.

568. Lepelletier, Y., et al., *Immunosuppressive role of semaphorin-3A on T cell proliferation is mediated by inhibition of actin cytoskeleton reorganization.* Eur J Immunol, 2006. **36**(7): p. 1782-93.

569. Fantin, A., et al., *NRP1 Regulates CDC42 Activation to Promote Filopodia Formation in Endothelial Tip Cells.* Cell Rep, 2015. **11**(10): p. 1577-90.

570. Midwood, K.S. and J.E. Schwarzbauer, *Tenascin-C modulates matrix contraction via focal adhesion kinase- and Rho-mediated signaling pathways.* Mol Biol Cell, 2002. **13**(10): p. 3601-13.

571. Guo, H.F. and C.W. Vander Kooi, *Neuropilin Functions as an Essential Cell Surface Receptor.* J Biol Chem, 2015. **290**(49): p. 29120-6.

572. Ellis, L.M., *The role of neuropilins in cancer.* Mol Cancer Ther, 2006. **5**(5): p. 1099-107.

573. Yakovlev, S., et al., *Interaction of fibrin(ogen) with leukocyte receptor alpha M beta 2 (Mac-1): further characterization and identification of a novel binding region within the central domain of the fibrinogen gamma-module.* Biochemistry, 2005. **44**(2): p. 617-26.

574. Ustinov, V.A. and E.F. Plow, *Identity of the amino acid residues involved in C3bi binding to the I-domain supports a mosaic model to explain the broad ligand repertoire of integrin alpha M beta 2.* Biochemistry, 2005. **44**(11): p. 4357-64.

575. Lishko, V.K., et al., *Multiple binding sites in fibrinogen for integrin alphaMbeta2 (Mac-1).* J Biol Chem, 2004. **279**(43): p. 44897-906.

576. Morgan, J., et al., *Structural basis of the leukocyte integrin Mac-1 I-domain interactions with the platelet glycoprotein Ib.* Blood Adv, 2019. **3**(9): p. 1450-1459.

577. Nong, Y., et al., *Tenascin-C expression is associated with poor prognosis in hepatocellular carcinoma (HCC) patients and the inflammatory cytokine TNF-alpha-induced TNC expression promotes migration in HCC cells.* Am J Cancer Res, 2015. **5**(2): p. 782-91.

578. Scott, E.A. and D.L. Elbert, *Mass spectrometric mapping of fibrinogen conformations at poly(ethylene terephthalate) interfaces.* Biomaterials, 2007. **28**(27): p. 3904-17.

579. Zhou, L., et al., *Differential ligand binding specificities of recombinant CD11b/CD18 integrin I-domain.* J Biol Chem, 1994. **269**(25): p. 17075-9.

580. Curreli, S., et al., *Polysialylated neuropilin-2 is expressed on the surface of human dendritic cells and modulates dendritic cell-T lymphocyte interactions.* J Biol Chem, 2007. **282**(42): p. 30346-56.

581. Kim, Y.J., et al., *Co-targeting of EGF receptor and neuropilin-1 overcomes cetuximab resistance in pancreatic ductal adenocarcinoma with integrin beta1-driven Src-Akt bypass signaling.* Oncogene, 2017. **36**(18): p. 2543-2552.

582. Kalliolias, G.D. and L.B. Ivashkiv, *TNF biology, pathogenic mechanisms and emerging therapeutic strategies.* Nat Rev Rheumatol, 2016. **12**(1): p. 49-62.

583. Kawasaki, T. and T. Kawai, *Toll-like receptor signaling pathways.* Front Immunol, 2014. **5**: p. 461.

584. Nakoshi, Y., et al., *Regulation of tenascin-C expression by tumor necrosis factor-alpha in cultured human osteoarthritis chondrocytes.* J Rheumatol, 2008. **35**(1): p. 147-52.

585. Gais, P., et al., *TRIF signaling stimulates translation of TNF-alpha mRNA via prolonged activation of MK2.* J Immunol, 2010. **184**(10): p. 5842-8.

586. Kotlyarov, A., et al., *MAPKAP kinase 2 is essential for LPS-induced TNF-alpha biosynthesis.* Nat Cell Biol, 1999. **1**(2): p. 94-7.

587. Hong, S., et al., *Signaling by p38 MAPK stimulates nuclear localization of the microprocessor component p68 for processing of selected primary microRNAs.* Sci Signal, 2013. **6**(266): p. ra16.

588. Fukuda, T., et al., *DEAD-box RNA helicase subunits of the Drosha complex are required for processing of rRNA and a subset of microRNAs.* Nat Cell Biol, 2007. **9**(5): p. 604-11.

589. Page, T.H., et al., *Raised circulating tenascin-C in rheumatoid arthritis.* Arthritis Res Ther, 2012. **14**(6): p. R260.

590. Hendaoui, I., et al., *Tenascin-C is required for normal Wnt/beta-catenin signaling in the whisker follicle stem cell niche.* Matrix Biol, 2014. **40**: p. 46-53.

591. Calabro, N.E., et al., *Thrombospondin-2 regulates extracellular matrix production, LOX levels, and cross-linking via downregulation of miR-29.* Matrix Biol, 2019. **82**: p. 71-85.

592. Flick, M.J., et al., *Leukocyte engagement of fibrin(ogen) via the integrin receptor alphaMbeta2/Mac-1 is critical for host inflammatory response in vivo*. J Clin Invest, 2004. **113**(11): p. 1596-606.

593. Cao, C., et al., *A specific role of integrin Mac-1 in accelerated macrophage efflux to the lymphatics.* Blood, 2005. **106**(9): p. 3234-41.

594. Jaumouille, V., A.X. Cartagena-Rivera, and C.M. Waterman, *Coupling of beta2 integrins to actin by a mechanosensitive molecular clutch drives complement receptor-mediated phagocytosis.* Nat Cell Biol, 2019. **21**(11): p. 1357-1369.

595. !!! INVALID CITATION !!! [52, 53].

596. He, S., et al., *EWS-FLI1-mediated tenascin-C expression promotes tumour progression by targeting MALAT1 through integrin alpha5beta1-mediated YAP activation in Ewing sarcoma.* Br J Cancer, 2019. **121**(11): p. 922-933.

597. Sun, Z., et al., *Tenascin-C Promotes Tumor Cell Migration and Metastasis through Integrin alpha9beta1-Mediated YAP Inhibition.* Cancer Res, 2018. **78**(4): p. 950-961.

598. Grun, D., G. Adhikary, and R.L. Eckert, *NRP-1 interacts with GIPC1 and alpha6/beta4-integrins to increase YAP1/Np63alpha-dependent epidermal cancer stem cell survival.* Oncogene, 2018. **37**(34): p. 4711-4722.

599. Huang, J., et al., *MiR-155 is upregulated in patients with active tuberculosis and inhibits apoptosis of monocytes by targeting FOXO3.* Mol Med Rep, 2015. **12**(5): p. 7102-8.

Appendix

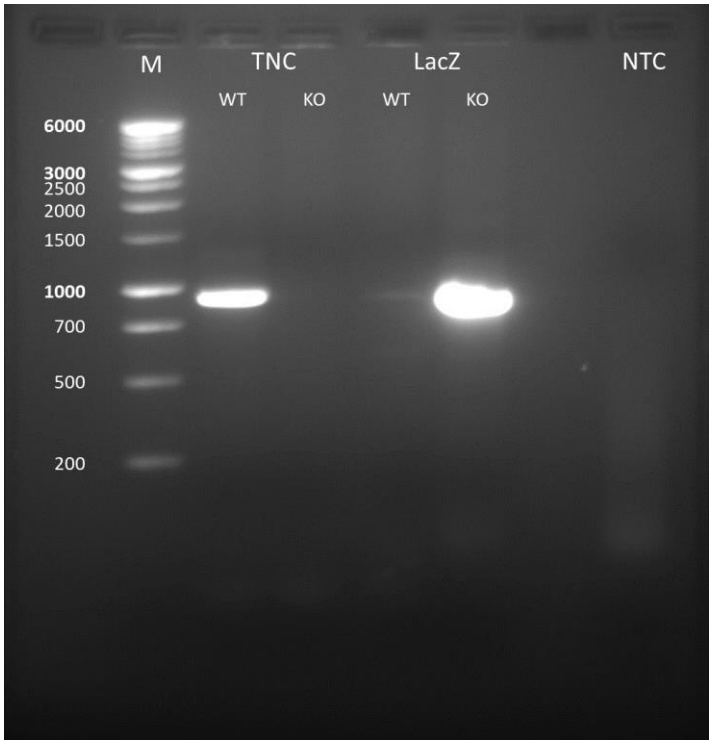
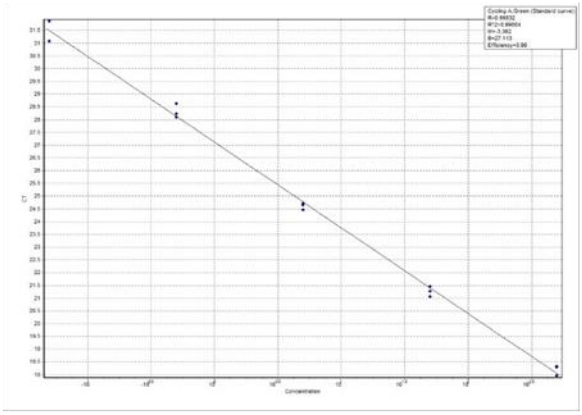


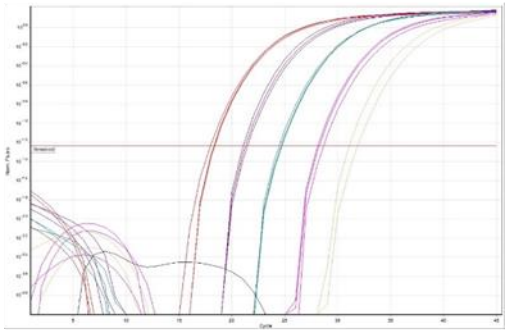
Figure 7.1 Mouse genotype was confirmed by PCR.

Mice were confirmed to be *tnc+/+* or *tnc-/-* by performing PCR on genomic DNA extracted from tail biopsies (representative gel).

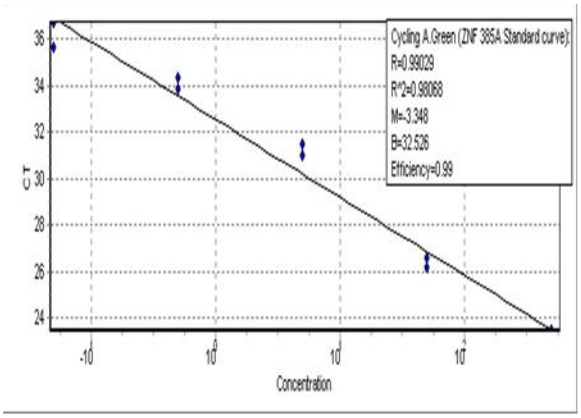
Samples were amplified by PCR and run on 1% w/v agarose gel stained with ethidium bromide.

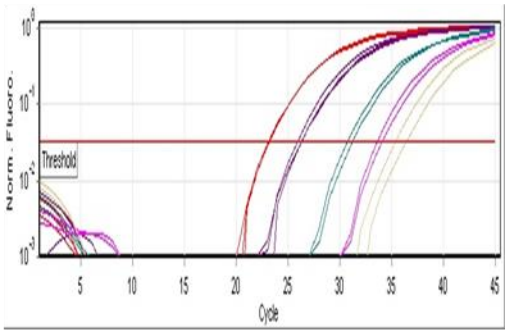
KH-SRP



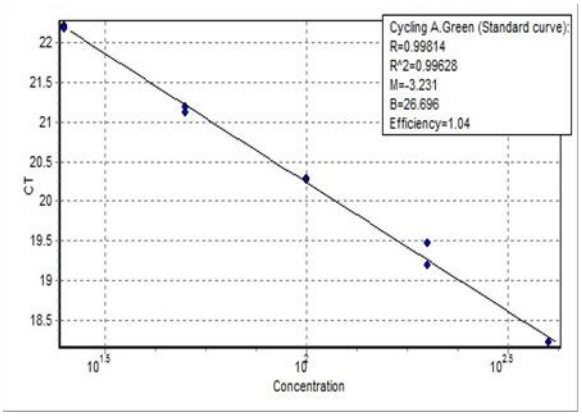


ZNF-385A





7S-RNA1



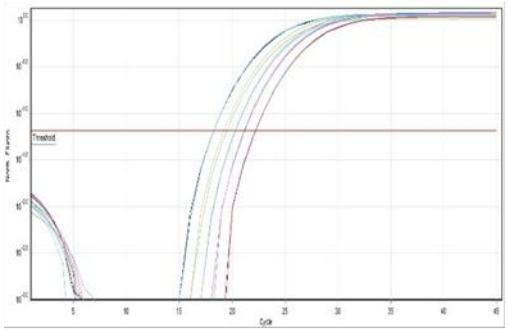
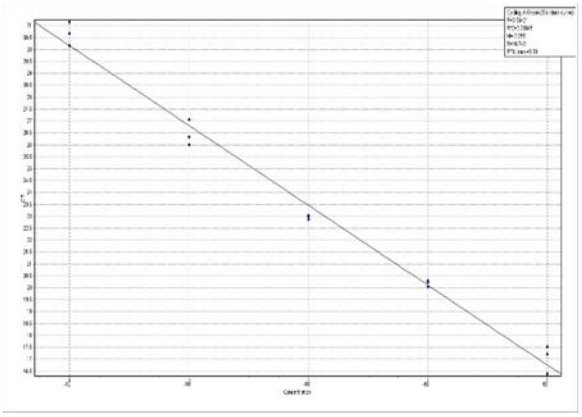
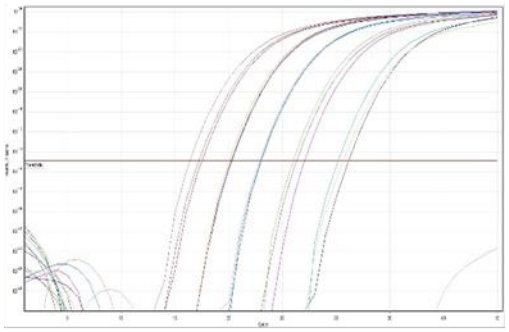


Figure 7.2 Amplification efficiency of primers.

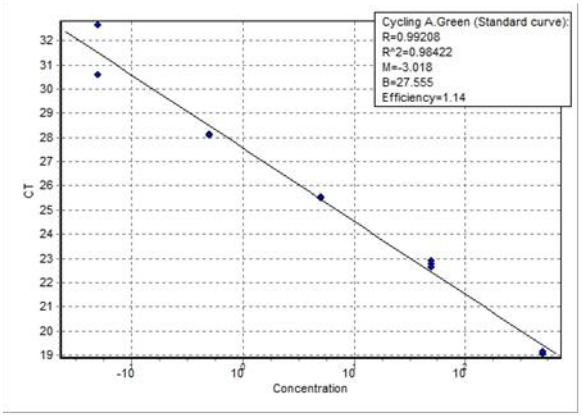
Continued on next page.

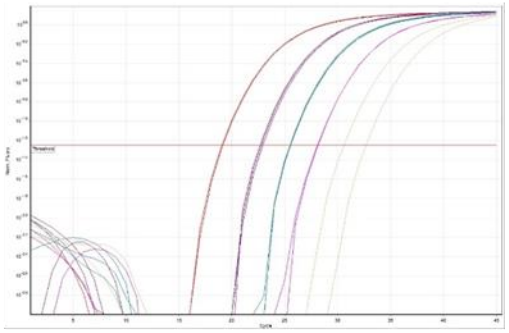
Unsp pri-mir-155



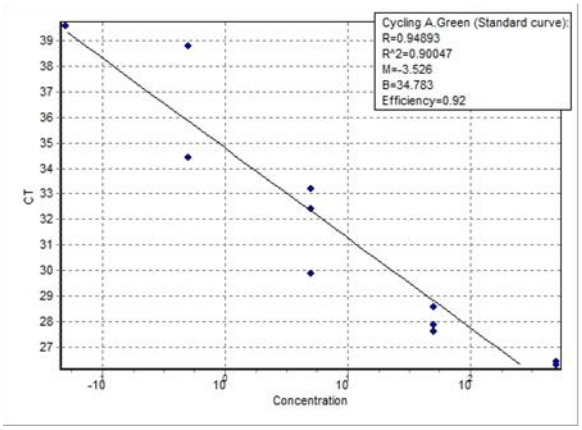


TTP





ZNF346



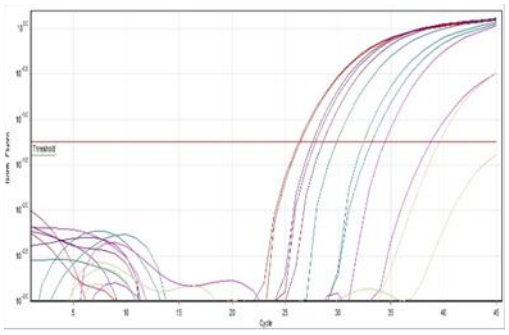


Figure 7.3 Amplification efficiency of primers.

Primers were tested for amplification efficiency by generating standard curves from ten-fold serial dilutions of cDNA samples.

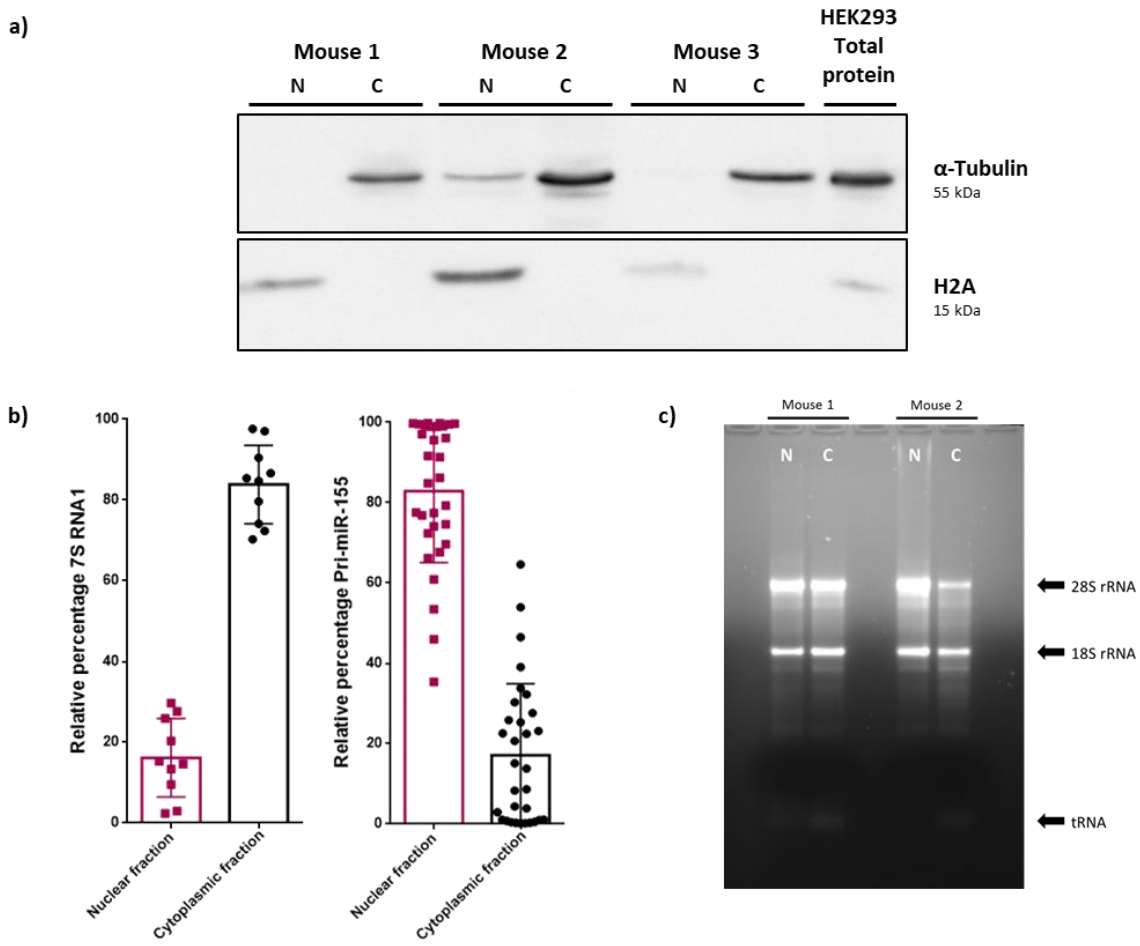


Figure 7.4 Quality of nuclear and cytoplasmic fractionation from BMDMs.

a) Proteins from cytoplasmic and nuclear fractions were extracted from the phenol-chloroform layer, after TRIzol RNA extraction. 10 μg of the extracts were run on a 12% SDS-page and tested for the presence of nuclear-specific protein Histone 2A (H2A ~15kDa) and cytoplasmic-specific protein α-Tubulin (~55kDa).

b) RNA from cytoplasmic and nuclear fraction from tnc+/+ and tnc-/- BMDMs was isolated and retro-transcribed. Expression of small cytoplasmic RNA (7S RNA1) and pri-miR-155 were measured by qPCR and normalised to HPRT1 expression. Data are represented as mean relative percentage of the transcript in the nuclear and cytoplasmic fractions ± SD; 7S RNA1 n=10, pri-miR-155 n= 31.

c) 1 μg of nuclear and cytoplasmic RNA from BMDMs was run on 1% w/v agarose gel stained with ethidium bromide.

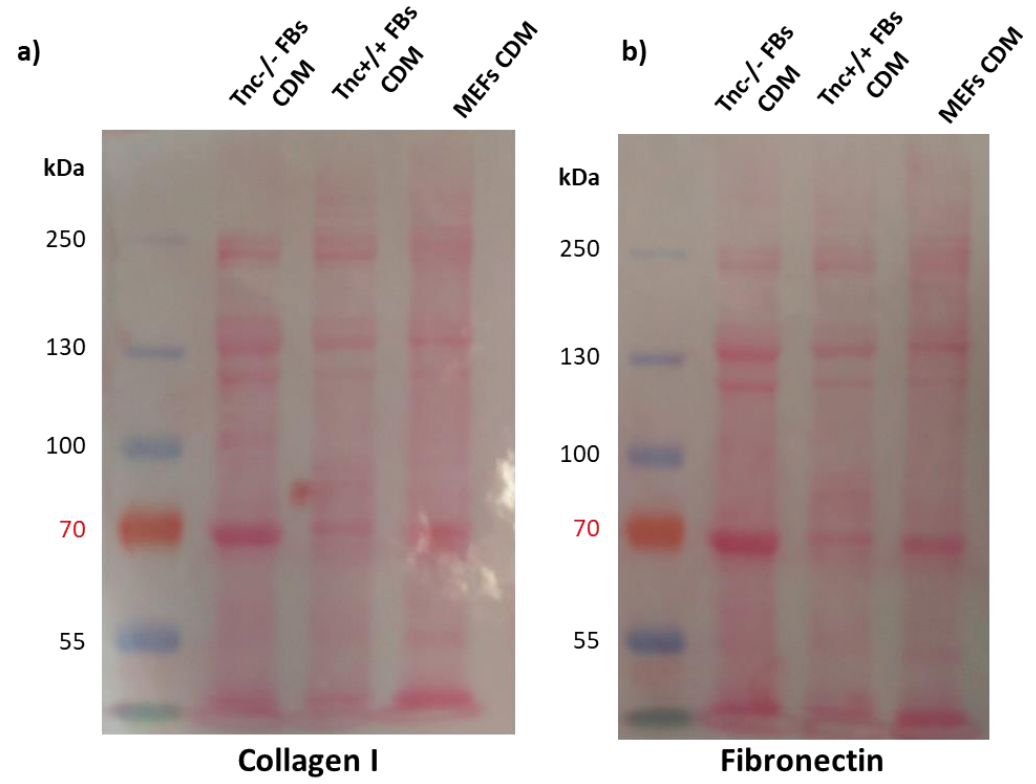


Figure 7.5 Ponceau S staining of nitrocellulose membranes before western blot.
Loading of wild type and tnc-/- FBs and MEFs decellularised CDM lysates were checked by Ponceau S staining before incubating with antibodies. The antibodies used for each membrane are reported under each membrane picture.

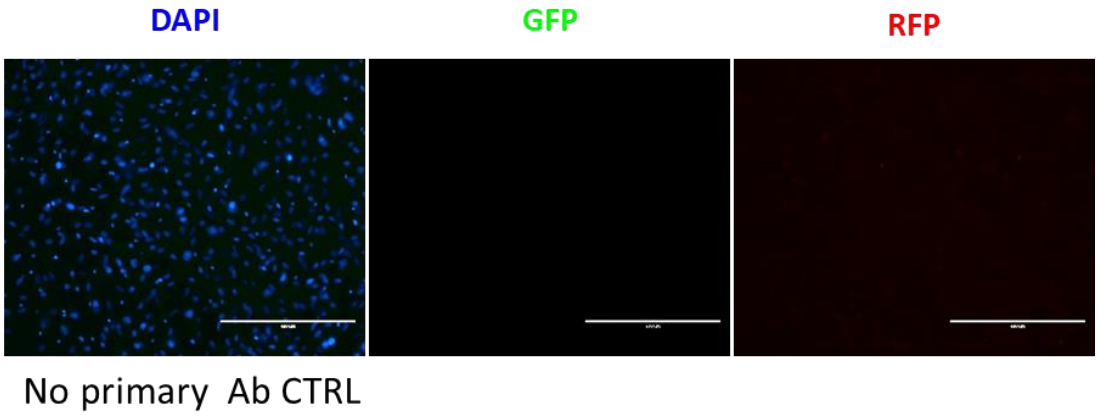


Figure 7.6 No primary antibody control for CDMs immunofluorescence.
Skin FBs from *wild type* (WT) and *tnc-/-* mice and MEFs were cultured for 10 days in complete media supplemented with 50 µg/ml L-Ascorbic acid, before de-cellularisation. Representative images showing no aspecific secondary antibodies binding in no primary antibody control samples. DAPI staining of genomic DNA (blue) was used to mark the nuclei. Scale bar, 400µm.

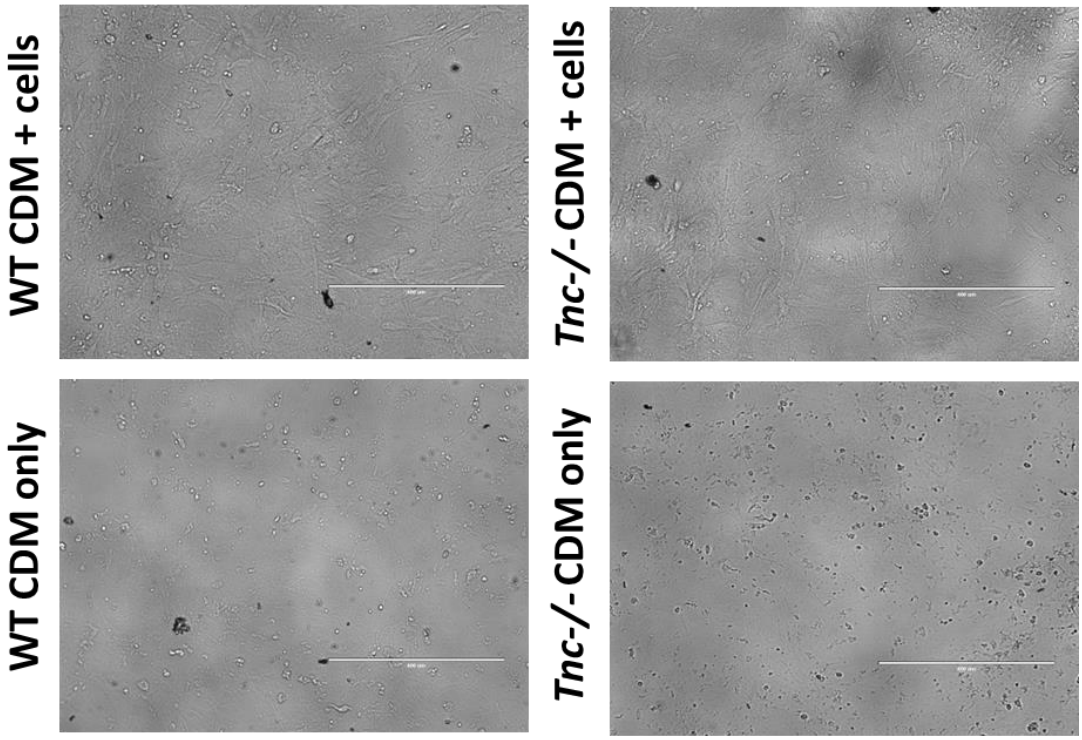


Figure 7.7 Decellularisation of CDMs.
CDMs originated by either wild type or tnc-/- skin FBs, before (top panels) or after decellularisation (bottom panels). Phase-contrast microscopy, magnification 10X.